UC Berkeley
UC Berkeley Electronic Theses and Dissertations

Title
Parameter variation and scenario analysis in impact assessments of emerging energy technologies

Permalink
https://escholarship.org/uc/item/5t5354vn

Author
Breunig, Hanna Marie

Publication Date
2015

Peer reviewed|Thesis/dissertation

eScholarship.org Powered by the California Digital Library
University of California

Parameter variation and scenario analysis in impact assessments of emerging energy technologies

By

Hanna Marie Breunig

A dissertation submitted in partial satisfaction of the

requirements for the degree of

Doctor of Philosophy

in

Engineering - Civil and Environmental Engineering

in the

Graduate Division

of the

University of California, Berkeley

Committee in charge:

Professor Ashok Gadgil, Co-Chair

Professor Thomas E. McKone, Co-Chair

Professor Arpad Horvath

Professor John D. Radke

Spring 2015

Abstract

Parameter variation and scenario analysis in impact assessments of emerging energy technologies

by

Hanna Marie Breunig

Doctor of Philosophy in Civil and Environmental Engineering

University of California, Berkeley

Professor Ashok Gadgil, Co-Chair

Professor Thomas E. McKone, Co-Chair

There is a global need for energy technologies that reduce the adverse impacts of societal progress and that address today's challenges without creating tomorrow's problems. Life cycle impact assessment (LCIA) can support technology developers in achieving these prerequisites of sustainability by providing a systems perspective. However, modeling the early-stage scale up and impacts of technology systems may lead to unreliable or incomplete results due to a lack of representative technical, spatial, and temporal data. The goal of this dissertation is to support the acceleration of clean energy technology development by providing information about the regional variation of impacts and benefits resulting from plausible deployment scenarios. Three emerging energy technologies are selected as case studies: (1) brine management for carbon dioxide sequestration; (2) carbon dioxide capture, utilization, and sequestration; (3) stationary fuel cells for combined heat and power in commercial buildings. In all three case studies, priority areas are identified where more reliable data and models are necessary for reducing uncertainty, and vital information is revealed on how impacts vary spatially and temporally. Importantly, moving away from default technology and waste management hierarchies as a source of data fosters goal-driven systems thinking which in turn leads to the discovery of technology improvement potentials.

Case Study 1: Brine Management for Geologic Carbon Sequestration

Large-scale deployment of carbon dioxide (CO_2) capture and sequestration (CCS) has the potential to reduce global CO_2 emissions, but this technology faces social, economic, and environmental challenges that must be managed early in the technology readiness cycle. Carbon capture technology is water-, energy-, and capital-intensive and proposed geologic carbon sequestration (GCS) storage options, if conducted in pressure-constrained formations, may generate large volumes of extracted brine that require costly disposal. Brine management is a poorly understood life-cycle phase of CCS and has either been ignored or simplified in LCA of CCS. In Chapter Two of this dissertation, brine management is evaluated in three locations of the United States (US) to assess whether recovered heat, water, and minerals can turn the brine into a resource.

Before an LCA of brine management for GCS could be conducted, the matrix of possible value chains had to be reduced to a manageable number. Technical feasibility and cost-effectiveness were used as metrics in a new approach to determine which values chains for brine management should be assessed in future LCA (Breunig et al., 2013; Breunig et al., 2014). Climate and aquifer parameters varied between the three regions and strongly affected technical feasibility. The levelized net present value (NPV) of extracted brine ranged from −$50 (a cost) to +$10 (a revenue) per tonne of CO_2 injected (mt-CO_2) for a CO_2 point source equivalent to emissions from a 1000 MW coal-fired power plant (CFPP), compared to CCS NPV ranging from −$40 to −$70 per mt-CO_2. Upper bound scenarios reflect assumed advancements in current treatment technologies and a favorable market and regulation landscape for brine products and disposal. A regionally appropriate management strategy may be able to treat the extracted brine as a source of revenue, energy, and water.

Case Study 2: CO_2 Utilization and Sequestration

Carbon dioxide utilization is a strategy for redirecting CO_2 emissions from point-sources to beneficial applications that result in either effective storage or significant delay of emission. Like brine management, likely future value chains for CO_2 utilization are poorly defined. In Chapter Three of this dissertation, the role that CO_2 utilization can play in creating an industry for CO_2 capture and sequestration (CCS) over the next 50 years is examined.

Chapter Three presents a method for performing temporally and spatially-explicit life-cycle modeling to quantify the long-range climate implications of scenario projections through which captured CO_2 at coal fired power plants (CFPP) is directed to industrial applications. This method required the modeling of future economic sectors like the coal, gas, methanol, and hydrogen industries. In this top-down approach, national and regional markets dictated which value chains would be subsequently assessed using LCA. This approach was selected over a bottom-up approach since the captured CO_2 composition was assumed to be spatially homogeneous. A bottom-up approach, where NPV was used to determine the most likely future value chain, was necessary in the brine management assessment (Chapter Two) because the brine composition varied from site to site.

It was found that CO_2 utilization could reach 0.4 to 1.4 $GtCO_2/y$ by 2065 and reduce cumulative greenhouse gas (GHG) emissions by 2 to 17 $GtCO_2eq$ if started in 2020. Enhanced gas recovery accounts for a majority of the possible CO_2 consumption (62 to 76%), followed by urea production (4 to 11%), fly ash mineralization (4 to 10%), enhanced coal bed methane recovery (9 to 11%), enhanced oil recovery (5% to 9%), and methanol production (1 to 3%). These findings confirm the disparity between the GHG reduction that CO_2 utilization can provide, and the reduction needed to slow climate change. However, it was found that regionally deployable CO_2 utilization applications could provide a near term solution for 26 of the largest CFPP in the US.

Case Study 3: Fuel Cell Systems for CHP

Proton exchange membrane (PEM) fuel cells, which rely on thin polymers as their electrolytes, could play an important role in distributed generation and backup power in the United States (Lipman et al., 2004; Feroldi and Basualdo, 2012). Decision-makers, particularly those involved in writing government support and tax policies, use total cost of ownership (TCO) and emissions analyses to compare alternative distributed generation technologies. Externalities ranging from global warming to disease burden caused by air pollution have been called the "hidden costs" of energy technologies because they are often ignored in total cost of ownership analyses (NRC2010). This research seeks to integrate these hidden costs into the TCO for PEM fuel cells.

In order to assess PEM fuel cells as an emerging technology for CHP applications, a life-cycle model was needed that could integrate data specific to the targeted buildings and regions identified by fuel cell developers. Chapter Four of this dissertation provides the first spatially-explicit approach for completing and matching localized inventory and impact assessment of the operation phase of PEM fuel cell systems for stationary CHP applications (Wei et al., 2014). As a case study, the GHG and human health implications of adopting PEM fuel cell systems in large hospitals and small hotels in Phoenix (AZ), Chicago, (IL), New York City (NY), Houston (TX), Minneapolis (MN), and San Diego (CA) were assessed.

Environmental and human health impacts of the adoption of FCS varied widely among locations due to differences in building- and fuel-cell-operation, nearby population, and the regional conditions affecting the transport and transformation of pollutants. All six cities experienced a positive net health benefit from adopting FCS in small hotels and large hospitals. Certain cities did not, however, realize a positive climate benefit from FCS adoption; this includes Phoenix and San Diego. The largest annual benefit from city-wide deployment occurred in New York City and Chicago, valued at $31.8 million and $29.2 million, respectively. In a scenario where FCS only provided heat for water heating, and not space heating, FCS would not provide carbon savings to large hospitals in Phoenix, NYC, Houston, or San Diego or to small hotels in Phoenix. FCS will provide the greatest monetary benefit from avoided health damages in regions where there are poorly controled NOx and SOx emissions from energy sources like fuel-oil-powered boilers and power plants. Disparate results from a model run using only national-average data revealed that spatially-explicit anaylsis was essential for detecting variations in impacts at the city-level.

Conclusions

Understanding the risks of emerging energy technology adoption requires spatially- and temporally-resolved impact assessments. The ability of technologies like fuel cells to reduce GHG and CAP emissions will depend on where and when they are deployed. This has implications for policy makers who are trying to determine the most appropriate tax or subsidy schemes for a new technology. Spatially- and temporally-explicit life cycle assessment can be achieved by building scenarios of future technology deployment and scale-up in different regions of the globe. In a changing and heterogeneous world, the longevity and robustness of a result is just as important as the result itself. This dissertation determined that scenario analysis and parameter variation are useful in situations where uncertainty is a concern but not readily measurable.

Several methodological challenges had to be addressed in order to capture spatial and temporal variation in the three assessments included in this dissertation. First, the value chain of technologies that are not well-defined or understood must be researched, designed, and assessed using available lab-scale or comparable-technology data. This is a challenging step as alternative value chains may have widely different economic and environmental consequences or benefits over different spatial and temporal scales. As demonstrated in Chapters Two and Three, it is possible to use both top-down and bottom-up approaches for modeling future value chains for brine and CO_2 utilization and disposal, which are a part of the larger CO_2 capture and sequestration life cycle. Both approaches allow identification of novel pathways that convert the waste streams into resource streams. Importantly, moving away from default technology and waste management hierarchies as a source of data fosters goal-driven systems thinking which in turn leads to the discovery of technology improvement potentials.

Secondly, conditions for both the reference scenario and the scenarios in which new technologies are introduced must be selected in a defensible and consistent manner. Trying to estimate plausible conditions for future economic sectors is not simple, especially in the energy sector where elements like natural-gas and petroleum prices are sensitive to political and regulatory actions. Organization like the Energy Information Agency (EIA) provided detailed information on the future of energy markets. The same level of detail was not as available for other markets in the United States. Uncertainty in developing market scenarios can be partially managed by systematically varying sets of parameters that represent an uncertain assumption.

Thirdly, spatially-specific inventory must be matched to spatially-specific impact assessment. Chapter Four presents an approach for obtaining site-dependent inventory for the operation phase of a PEM fuel cell system. This inventory was matched to a county-level impact assessment. Data availability, emission factors for city- or county-specific electricity grids in particular, created challenges when matching the spatial scale of the inventory to the spatial scale of the impact assessment. However, when the spatial scales were successfully matched at the county-level for Phoenix and Minneapolis, the variability between the resulting emission factors and those estimated at the state and NERC region was not significantly different from the variability originating from modeling choices.

Dedication

This dissertation is dedicated to my mother and father, Jenny and Harold Smith. You taught me to love learning and to never stop exploring. This dissertation was shaped as much by you as it was by world events and scientific advances.

I would also like to dedicate this work to my husband, Kevin Breunig, for his unwavering support and companionship during these challenging years.

Table of Contents

Abstract 1

Dedication i

Dissertation Organization iii

Acknowledgements iv

Chapter 1: Introduction 1
- 1.1 Emerging energy technology assessment 2
- 1.2 Life cycle assessment 3
- 1.3 Uncertainty analysis in LCA 4
- 1.4 Localized inventory and impact assessments 6
- 1.5 Localized technology management 8
- 1.6 Improvement potential 9
- 1.7 Case studies 10
- 1.8 References 13

Chapter 2: Regional Evaluation of Brine Management for Geologic Carbon Sequestration 16

Chapter 3: Assessment of Carbon Dioxide Utilization as a Carbon Management Strategy for Coal-Fired Power Plants 40

Chapter 4**:** Spatially-explicit life-cycle impact assessment approach for stationary proton exchange membrane fuel cell systems in the United States. 54

Appendices 92

Dissertation Organization

Chapter One discusses the need for spatial and temporal sensitivity in impact assessments of early-stage energy technologies. It also introduces the three technologies used as case studies in this dissertation. Chapters Two, Three, and Four present new methods for incorporating spatial and temporal variation to improve the relevance of impact assessment in energy technology analysis. Chapter Two is dedicated to brine management, Chapter Three is dedicated to carbon dioxide (CO_2) utilization, and Chapter Four is dedicated to stationary proton exchange membrane (PEM) fuel cell systems for combined heat and power (CHP) applications. Each chapter concludes with a summary of findings and recommendations for future research. A set of appendixes with supporting data and methods follows Chapter Four.

Acknowledgements

I would like to thank my committee for their support throughout my graduate education. Thanks go to Ashok Gadgil for opening the door to research at the Lawrence Berkeley National Laboratory. His graduate student meetings gave my years at Berkeley some continuity and taught me a great deal about professional development. Thanks go to John Radke for giving me the most constructive research meetings. I always felt like a colleague when I met with him. Thanks go to Arpad Horvath for introducing me to systems thinking and for his excellent course on LCA. Thanks go to James Hunt for teaching the best class I took during my Master's program.

Huge thanks go to Shelley Okimoto, Natasha Nelson, Cynthia Task, Olivia Salazar, Mark Stacey, Linda M. Von Hoene, and Sabrina Soracco for getting me from start to finish. Also, for keeping the loneliness at bay and letting me kvetch, I would like to thank Yang-Seon Kim, Caroline Delare, Chandni Navalkha, Katherine Hamilton, The Gadgil Lab @ UC Berkeley (thanks for graduating with me Case Van Genuchten!), and the Emerging Technology Analysis Team @ LBNL.

Special thanks to the Breunig, Burdick, Böer, Lyverse, and Young west coast families for adopting me during my graduate career.

Finally, I would not be where I am today without Tom McKone. He taught me how to think big picture in the fields of energy science and public health, reminded me of my own strengths, advocated for me, helped me present my research to a European audience, introduced me to leading scientists at conferences, shared his stories, and enthusiastically worked with me on the Schmidt MacArthur Fellowship. I am honored to be one of his last PhD students.

Chapter 2: Brine Management
I would like to acknowledge the contributions of Jens Birkholzer, Curtis Oldenburg, Philip Price, Tom McKone, Roger Sathre, Andrea Borgia, and Yasmina El Hasnaoui to this research. These scientists provided valuable advice and revisions. I would like to thank Yasmina for dedicating five months to gathering inventory data for this research and for a follow-up study.

Chapter 3: Carbon Dioxide Utilization
I would like to acknowledge the contributions of Tom McKone and Meriem Kassite to this research. Tom provided many hours of guidance while Meriem dedicated five months of work gathering inventory data for this research. I would like to thank Roger Sathre for his support and invaluable insight.

Chapter 4: Fuel Cell Systems
I would like to acknowledge the contributions of Max Wei, Tom McKone, and Ahmad Mayyas. Each of these scientists provided valuable guidance and revisions. Special thanks goes to Max for his commitment to our bi-monthly meetings.

Acknowledgements cont.

Funding:
I am very grateful for the funding support that was provided by:

- The Laboratory Directed Research and Development funding at the Lawrence Berkeley National Laboratory, which is operated for the U.S. Department of Energy under Contract Grant No. DE-AC02-05CH11231.

- The U.S. Department of Energy, Office of Energy Efficiency and Renewable Energy (EERE) Fuel Cells Technologies Office (FCTO) funding at the Lawrence Berkeley National Laboratory under Contract No. DE-AC02-05CH11231.

- The STAR Fellowship Assistance Agreement No. 91766101-0 awarded by the U.S. Environmental Protection Agency.

- The Robert B. Rothschild, Jr. Memorial Fellowship

- The A.J. and Catherine Orselli Fund

- The University of California, Berkeley Graduate Division Travel Grant

- The Joseph A. Dias Scholarship Fund

Chapter 1: Introduction

This chapter introduces the key concepts and themes explored in this dissertation.

Mitigating energy-related impacts like climate change and human health damages requires a rapid and strategic integration of low-emission technologies in all economic sectors. Emerging energy technologies (EET) must be cost-effective, reliable, and achieve competitive emissions reductions despite heterogeneous and dynamic real-world conditions. A life-cycle approach has proven useful for estimating the resource consumption and emission burdens, and associated impacts, of scenarios where lab-scale technologies are deployed at large scales, but not without limitations (Section 1.1). Standardized life cycle impact assessment (LCIA) methodology was intended for the auditing of end-point economic activity with little to no spatial differentiation (Section 1.2). As such, standardized methods produce results that do not account for the context-dependency of economic activity, emission and consumption rates, and impacts. Developing methods that incorporate uncertainty due to spatial and temporal variations in a technology's performance and impacts make LCIA more relevant to research and development (R&D) scientists, to policymakers, and to prospective adopters of EET.

This dissertation explores ways in which parameter variation and scenario analysis can incorporate data uncertainty into LCIA. Three emerging energy technologies are selected as case studies: (1) brine management for carbon dioxide sequestration; (2) carbon dioxide capture, utilization, and sequestration; (3) stationary fuel cells for combined heat and power in commercial buildings. Insights from this work reveal how LCIA can be applied at the local level in scenario analyses of EET to provide more reliable information to decision makers. The term "local" is used, rather than the term "site-specific", because the objective of this study is not to assess operating sites, but to develop the capacity of LCIA to incorporate uncertainty and variability in local conditions. Furthermore, the case studies demonstrate ways in which methodological limitations of LCIA can be overcome. Limitations addressed include:

- Life cycle inventory and impact assessment methods do not capture spatial heterogeneity (Section 1.4) and temporal dynamics.
- Economic activity in the life-cycle of a technology and process (the value chain) varies at the local level, but is typically modeled as context-independent in LCIA methodology (Section 1.5).
- LCIA typically measures the potential for creating negative impacts, but not the potential for creating positive impacts or co-benefits (Section 1.6).

Chapters Two and Three present approaches for managing uncertainty regarding the future management of technologies in different locations. These Chapters also take a waste-to-resources perspective to identify opportunities for creating value from life-cycle waste streams. In Chapter Three, scenario analysis is used to incorporate the effect of temporal uncertainty on the avoided cumulative radiative forcing (CRF) of CO_2 utilization scale up. Chapter Four presents an approach for localizing emission factors that determine the mass of emissions resulting from a unit of economic activity and for localizing characterization factors that convert emissions to impacts.

1.1 Emerging energy technology assessment

The increasing demand for energy, coupled with the need for sustainable energy production, has led to the development of a number of emerging energy technologies (EET) in the transportation, building, and energy sectors. Sustainable energy production goes beyond using renewable energy resources or reducing greenhouse gas (GHG) emissions. It protects water resources, reduces impacts to human health, and avoids the transfer of emission burdens from the energy sector to other economic sectors. Emerging technologies must also be cost-effective and provide energy security. These stipulations are a tall order for any technology and early life-cycle assessments (LCA) have identified tradeoffs that are likely to occur with the adoption of technologies like biofuels (McKone et al., 2011), wind power (Arvesen and Hertwich, 2012), and electric vehicles (Scown et al., 2013). Life-cycle assessment offers a systematic approach for evaluating the human health and environmental impacts of products and processes (methodology is discussed in detail in Section 1.2). Life cycle assessment has proven useful for providing a holistic understanding of EET and for identifying sources of impacts (Masanet et al., 2013). The challenge for analysts is to try to advise decision-makers in a manner that drives action without causing lock-in of suboptimal technologies and policies.[1] This can only be achieved if the impacts of alternative EET can be compared. However, there is still a risk that the burden of some alternatives may transfer to ecosystems and populations that are not accounted for in economic and environmental life-cycle analysis.

The impacts of investing in emerging energy technologies must be assessed, but this is challenging for several reasons. For one, LCA is a data intensive process and field data is unavailable or limited for lab-scale technologies, meaning that data must be extrapolated from experimental data or approximated from comparable technologies. Available data may not represent the technology's performance at industrial or commercial scales, over long timespans, or at different locations.

Furthermore, scientists must develop scenarios for future conditions with and without a deployed technology using today's data. Predicting future conditions is impossible, and some unexpected impacts will occur. For example, the oxygenate MTBE that was blended with gasoline to improve air quality ultimately required costly cleanup efforts after it leaked from underground storage tanks and contaminated drinking water aquifers. Conversely, if co-benefits are identified early on, they could improve the rate of technology adoption. As an example, the reduction of health impacts due to carbon monoxide exposures was an undervalued benefit of the catalytic converter. Even baseline scenario conditions for the energy sector may be difficult to predict. Fossil fuel prices are notoriously difficult to predict beyond a few years because they are sensitive to unpredictable market forces like technology advancements and war.

Analysts are capital and time limited, and frequently chose metrics that are of greatest interest to their funding stakeholders (Masanet et al., 2013). A large number of impacts can be determined through LCA, but it is difficult to know which impacts to include and at what spatial or temporal scale. In some cases, the appropriate metric requires new methodology for characterizing burdens at sub-national spatial scales or over long range time scales. Overcoming

[1] This lock-in is of particular concern for emerging technologies like carbon dioxide capture and sequestration that require substantial infrastructure and capital for their deployment.

methodological challenges, like the development of representative metrics, is essential for improving the robustness of early-stage impact assessment.

Finally, assessment tools that do not achieve appropriate spatial and temporal granularity will mask local burdens in aggregated results. In a recent article, Hellweg and Canals highlighted "enhancing regional detail and accuracy" as one of the most important opportunities for making LCA "more relevant for producers and consumers alike". This is because life-cycle phases are often site-specific and have spatially heterogeneous impacts due to variations in ecosystems and population sensitivities. However, acquiring spatial data is not always possible, and decision must be made on how to manage incomplete or low quality spatial data.

1.2 Life cycle assessment

In an LCA, the value chain of a product or process, which includes the supply chain, fabrication, operation/use, and disposal phases, is assessed to help decision-makers identify and target key contributors to impact categories, like the loss of biodiversity, global warming, and human disease burden.

The International Organization for Standardization (ISO) published a four-step framework for conducting LCA (ISO, 2006). The goal and scope of the LCA are defined in the first step, as is the system boundary. Defining the system boundaries of a study cannot be done without a clear understanding of what the LCA is trying to achieve. Is the goal of the study to identify sources of greenhouse gas (GHG) emissions in the supply chain to help a company reduce its emissions and receive carbon credits? Or, perhaps, the goal of the LCA is to understand the marginal change in GHG emissions that occurs when the product is used in place of a conventional product that delivers the same service. The first goal would require an attributional LCA while the second goal would require a consequential LCA. In an attributional LCA, the entire value chain of the product or process is included in the system boundary. In a consequential LCA, only the marginal change in impacts is quantified; therefore, phases of the value chain that are the same for two products being compared would not be included in the system boundary.

An inventory of energy and material consumption (inputs) and emissions (outputs) is developed for each life-cycle phase in the second step. Large databases have been developed to assist with collecting inventory data for some life cycles. For example, the inputs and outputs associated with the value chains of numerous transportation technologies can be acquired by using The Greenhouse Gases, Regulated Emissions, and Energy Use Transportation (GREET) model, developed by the Argonne National Laboratory. This step can be tedious for products and processes that do not have well characterized life-cycle phases, since inventory data must be approximated from similar technologies or gathered in the field.

The third step of an LCA is to convert input and outputs into impacts. Inventory data is converted to impact categories using characterization factors (CF) (Pennington et al., 2004). To facilitate comparisons, a reference chemical is often used for each type of impact to measure a specific contribution to that impact. Other chemicals that contribute to the impact category are converted into equivalencies of the reference chemical. For example, carbon dioxide (CO_2) is the representative chemical for global warming potential (GWP), an impact category that measures

the potential for a gas to trap a certain amount of heat in the atmosphere. Carbon dioxide has a CF of one since GWP is the ratio of the radiative forcing caused by a gas to that of the reference gas. Methane has a GWP CF of 24 when calculated over a time horizon of 100 years, meaning that one kg of CH_4 has the potential to cause the same radiative forcing as 24 kg of CO_2 over 100 years. A majority of LCA identify a set of impact factors that are relevant to their specific goals, rather than try to quantify all LCA impacts. Care should be taken when choosing impacts to include as critical information can be lost through the exclusion of impact categories that are incorrectly assumed to be negligible.

Finally, the last step of an LCA is to interpret the findings through an improvement analysis. How directly an LCA is able to guide decision-making depends on the goals and scope of the study, and the reliability of the analysis (due to uncertainty and other knowledge gaps). The utility of LCA has been expanded from product analyses to organizational and company analyses, consumer lifestyle LCA, regional/country LCA, and prospective analyses of emerging technologies (Hellweg and Canals, 2014). The inherent uncertainty in a prospective LCA that attempts to model a technology deployment scenario will be much larger than the uncertainty in a product LCA that explores the value chain of an established product. Given the uncertainty in all LCA, this approach should be valued for its ability to improve understanding rather than its ability to point to definite solutions. This four step approach is known as process-based LCA.

An alternative LCA approach is Economic Input-Output (EIO) analysis. This approach quantifies the impacts of the supply chain (not the use or disposal phases) using the entire economy as a system boundary. The supply chain is modeled as a matrix of changes in economic activity that results from producing a dollars' worth of product. With this method, the economic activity required to produce one million dollars' worth of steel could be included in an LCA. The impacts attributed to each economic activity are inventoried and summed; this can be done using Input-Output models like the Economic Input-Output Life-Cycle Assessment (EIO-LCA) model developed at Carnegie Mellon University.

A hybrid LCA uses process-based LCA for the primary supply chain phases, and the use and the disposal phases, and uses EIO LCA for the less significant upstream phases (Williams et al., 2009). The hybrid LCA provides the detail of process-based LCA and the comprehensiveness of EIO LCA. It attempts to reduce types of uncertainty that challenges process-based LCA and EIO-LCA. For example, in process-based LCA cutoff issues can happen if non-negligible life cycle phases are excluded due to system boundary decisions. Williams et al. (2009) state that EIO methods "typically" have higher geographic and temporal uncertainties, but process-based LCA also have significant uncertainty if inventory data is gathered from databases that are (1) infrequently undated or (2) provide data at a spatial level that is not appropriate for the study. Both methods, and therefore hybrid LCA as well, are still challenged by uncertainty introduced by data collection limitations.

1.3 Uncertainty analysis in LCA

Uncertainty is a feature of research that occurs when a quantified value and an actual value differ due to a lack of knowledge. Technical, methodological, and epistemological uncertainty limit knowledge and enter LCA through data, choices, and relationships (Finnveden et al., 2010).

Several classifications of uncertainty are summarized in Heijungs and Huijibregts (2004), and reveal the lack of consensus on how uncertainty is thought about and approached in the LCA community. As a decision support tool, it is essential that LCA results are presented in a manner that speaks to the possibility and nature of uncertainty and variations. Uncertainty analysis techniques are critical for helping decision-makers makes sense and responsibly apply the results of an LCA in their work.

In theory, variations in data due to spatial heterogeneity or temporal dynamics do not cause uncertainty if they are characterized (Lloyd and Ries, 2007). However, it is very difficult and capital intensive to account for spatial variations and impossible to predict temporal dynamics in practice. This explains why LCA case studies generally use national averages and historical data in their inventories and why their results quickly become irrelevant as time move on and as decision-makers from unrepresented locations ask the same questions, necessitating further LCA on the same topic. Even more problematic is the possibility that LCA results are inappropriately used because the implications of using averages are ignored or poorly communicated.

Uncertainty management practices are generally categorized as scientific, social/constructive/legal, and statistical categories (Finnveden et al., 2010). Scientific practices focus on doing more research to improve the quality of data and to develop more refined and robust models. The social-focused approach is to gather knowledge from members of the field through activities like workshops and panels to develop a consensus on uncertainties. Statistical practices incorporate uncertainty into a study in an attempt to gain knowledge and possibly reduce uncertainty; this distinguishes it from the first two categories which focus on removing or reducing uncertainty, not incorporating it.

Both parameter variation and scenario analysis are classified as statistical practices for uncertainty management by Finnveden et al. In parameter variation, models are run using high and low parameter values to understand the consequences of variation. This method can be used like a sensitivity analysis if the distribution of parameter values is difficult to determine due to limited data. Sampling methods like Monte Carlo simulations can identify the effect of parameter distributions on results *if* the uncertainty of the parameters can be specified by a probability distribution. Many times, there are not sufficient data to develop a distribution that can accurately express uncertainty. And, since this is a capital intensive step, Huijibregts (2001) suggest only performing stochastic (such as Monte Carlo) modeling for parameters that are first identified as significant in a sensitivity analysis step.

In scenario analysis, models are run using data, choices and relationships that are consistent with a defined scenario and the results are compared to the results of a reference or baseline scenario (Spielmann et al. 2005). A review of scenario development in life cycle analysis can be found in Pesonen et al. (1988) Scenario analysis creates a context for results, allowing decision-makers to understand the longevity and robustness of the LCA conclusions.

Alternative methods for managing spatial and temporal variations have been discussed in the current LCA literature. For example, the lack of specific information about processes in a value chain can be addressed by (1) using hybrid-LCA to model gaps in processes with input-output models like EIO-LCA or (2) by using data from analogs [REFs??]. Data quality indicators can be

used when technological, temporal, or geographically representative data is missing to give a sense of the reliability of results (Weidema, 1998). In some cases, it is challenging to know how well a similar technology and its infrastructure may represent the system being evaluated. While methods are available for adjusting data using an uncertainty factor (Huijibregts, 2001), it may be safer to provide a qualitative discussion on the lack of data and uncertainty in the paper, so as not to give the impression that the uncertainty can be fully quantified.

Uncertainty analysis and treatment in LCA continues to be an important area of development despite over a decade of research specifically focused on educating the LCA community about the effects of uncertainty. This problem partially stems from the fact that the standardized ISO methodology guiding LCA research and LCA software development lacks guidance on how to manage uncertainty. Heijungs and Huijibregts (2004) point to a lack of knowledge in the LCA community on uncertainty analysis techniques, a lack of data on input uncertainty, and lack of software for dealing with and visualizing uncertainty as three reasons why uncertainty analysis remained unused as of 2004. The goal of their review was to provide a survey of uncertainty theory and treatment to build consensus in the LCA community on best management practices. They predicted that uncertainty management would become a standard practice in LCA case studies and "no longer be restricted to academic exploratory work, like PhD-theses". Six years later, Finnveden et al. (2010) discuss the progress that has been made in uncertainty management, but concluded that the "area of uncertainty in LCA need[s] further attention and development" because uncertainties are "often not considered in LCA studies". Since software for managing and visualizing uncertainty, ranging from geographic information systems (GIS) to R software, have become abundant and accessible, it could be concluded that improved knowledge and/or consensus in the LCA community on uncertainty management[2], and a more data on input uncertainty is needed.

1.4 Localized inventory and impact assessments

Spatial data necessary for conducting regional-, local-, or even site-specific LCA includes information on the value chain, the inputs and outputs from the value chain, and characterization factors that model how emissions and resource consumption will impact populations and ecosystems. This leads into a related challenge: new approaches and models are required to regionalize inventory analysis and impact assessment. Progress has been made for some impacts. For example, Azevedo et al. (2013) developed spatially explicit characterization factors (CF) of phosphorus causing eutrophication for life cycle impact assessment (LCIA), applicable for streams and lakes in Europe. The authors found that variation in CF was mainly due to differences in freshwater types and fate factors of phosphorus in rivers.

Assessments have used varying methods to match spatial inventory to spatial impact assessment. Mutel et al. (2011) proposed a framework for regionalizing LCA in which the spatial scale of an LCA is set to minimize the loss of information due to aggregation. The authors introduce a method for using geographic information science to generate auto-correlation optimized characterization factor (CF) maps; the method was demonstrated using electricity generation in

[2] Heijungs and Huijibregts (2004) point out that this is a problem in the "uncertainty community" itself, and not just the LCA community.

the United States as a case study. An auto-correlation optimized map aggregates spatial units with similar CF in order to match the scale of a map to the scale of processes influencing CF. This method was useful for revealing regional hotspots where the energy sector had a significantly large negative effect on the environment. A concern is that results can be skewed by inaccurate geospatial data, incomplete data sets, and the way in which continuous data is represented by discrete spatial units. The authors propose drawing ring buffers around point objects in inventories with questionable spatial quality. These buffers are built to improve the likelihood of capturing the actual location of activities assessed in the LCA.

This dissertation did not use the Mutel et al. (2011) method since the focus was on scenario analysis; future specific geospatial boundaries and coordinates were not available. A localized LCA of fuel cell deployment for CHP in cities in the US required an inventory of ground-level emissions at the site of operation, and stack emissions at power plants where electricity was offset. This required data on local fuel consumption in buildings and emission factors for city specific electricity consumption. Neither dataset was available, so new approaches were developed to generate this critical data. Emissions were converted into human health damages (morbidity and mortality) and environmental impacts (global warming potential, visibility impairment, damages to crop and timber) by modifying a county-level air quality assessment model called the Air Pollution Emissions Experiments and Policy (APEEP) analysis model, discussed in detail in Chapter 4.

1.4.1 Spatial differentiation in LCA

The lack of spatial differentiation in standardized LCA methodology has been an issue since LCA was first used as an environmental tool (Potting and Hauschild, 2006). In many analyses, part of the LC inventory is regionally specific, while the rest of the data is taken from databases using national or global averages. This hybridization mirrors the hybridization of process and EIO-LCA methodology, only the methods used to merge spatial scales are not always transparent, making meta-analysis difficult. Three categories for spatial differentiation were defined in Potting (2000) and Hauschild and Potting (2005):

Site-generic: no spatial differentiation is performed. A site-generic LCA is a study that has not taken location into account when modeling value chains or when choosing characterization factors. LCA software packages commonly used by analysts, like Gabi and SimaPro, are useful for reducing the extensive data and time requirements necessary for performing an LCA, but these tools do not provide the user with the flexibility to adjust spatial resolution, which is typically set at the global scale (Mutel and Hellweg, 2009).

Site-dependent: some spatial differentiation is performed. In these studies inventory data is not collected at specific locations where processes may occur, but at larger spatial scales, such as regions or countries. The receiving population and environment may be defined at a high spatial resolution, but not at the local level. A frequent problem with this type of study is that the spatial resolution for the inventory and impact analysis may simply reflect the scale of available data and not the scale that is appropriate for the study. Databases may provide information collected from national surveys that are presented as nation-wide averages, and characterization factors are developed based on field data that was collected from *somewhere*.

Site-specific: detailed spatial differentiation at the source level. Emissions and impacts are modeled at a local level. In 2006, Potting and Hauschild largely dismissed site-specific LCA as being "unrealistic" due to data challenges and because "LCA is normally not focused on the local impacts". They suggest that site-specific characterization of a "few central processes" may be useful, and that local information could support step four of the LCA, the improvement analysis.

1.5 Localized technology management

In this dissertation, an approach was developed for modeling the waste management life cycles of EETs in a way that accounts for both spatial heterogeneity and undetermined future management decisions. This approach deviates from the tradition waste management hierarchy (Figure 1), by developing decision trees to represent possible future management pathways.

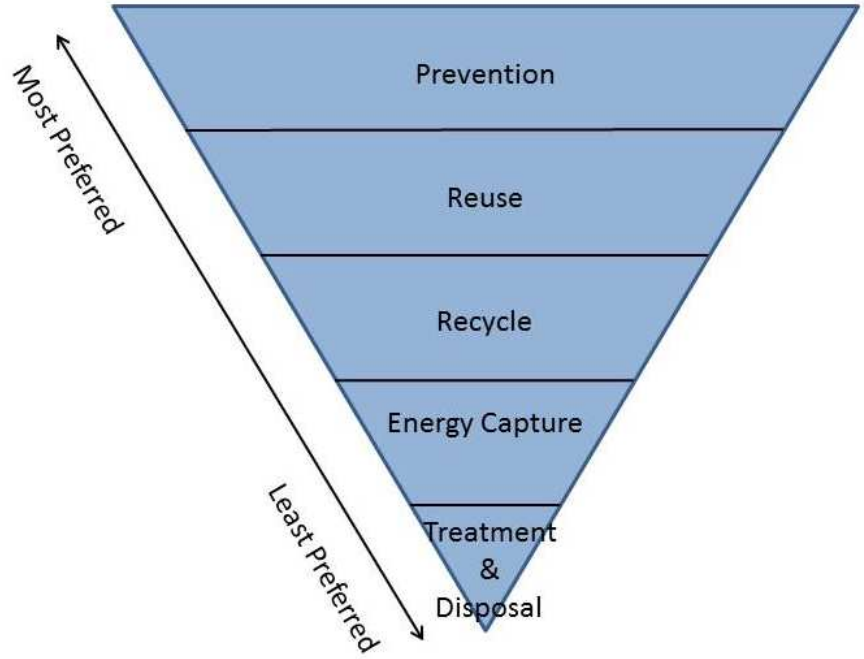


Figure 1. Non-hazardous waste management hierarchy. Arrows rank management steps from most to least preferred solutions to waste according to the United States Environmental Protection Agency. Preference is given to steps that reduce the consumption of raw materials and avoid landfilling.

Literature review and systems analysis were used to identify: (1) conventional and emerging utilization, treatment, storage, and disposal technologies, (2) marketable chemical and physical aspects of the waste, and (3) synergistic elements of decisions. This information was useful for designing decision trees that could maximize co-benefits. For example, a technology that captured heat from geologic brine was placed early in a management pathway. The decision tree was modeled using a set of equations for each decision node (management step) and by identifying the range in parameters where a decision was technically feasible. In the previous example, the temperature range needed for heat recovery was determined for the decision node that denotes whether heat recovery would be included in brine management. A set of spatially-

specific feasible decisions were acquired when the characteristics of a potential deployment site were applied to the model. A net present analysis was then performed to determine a final set of local management pathways. The output of this approach was a reduced number of life cycle value chains that were selected in a process that increases confidence of their future adoption. This output can be provided to an LCA analyst to (1) broaden the system boundary of the LCA, allowing the LCA to take on a value-adding role, to (2) incorporate context-dependency, and to (3) manage uncertainty regarding future technology management.

By using this approach, it was determined that the life-cycle of brine management is highly context-dependent, as the cost of management is spatially heterogeneous. Expanding the system boundaries to include the most feasible management pathways created a platform for identifying opportunities for positive development (the term positive development is discussed further in Section 1.3).

When this method was applied to CO_2 management, it was determined that the regional markets and CO_2 storage capacity were the most important parameters influencing the probability of future adoption.

Trying to estimate plausible conditions for future economic sectors is not simple, especially in the energy sector where elements like natural gas and petroleum prices are sensitive to political and regulatory actions. Organizations like the Energy Information Agency (EIA) provide detailed information on the future of energy markets. The same level of detail was not as readily available for other markets in the United States. Instead of trying to forecast future conditions, parameters characterizing the future were modeled as ranges in Chapter Three, and not as specific values. These ranges were built based on conservative, business as usual, moderate, and optimistic assumptions. Predicting how coupled energy markets may transition over several decades is complicated and outside the focus of this study. Instead, the set of assumptions defining future scenarios were clearly described to allow the results of this analysis to be compared in a future meta-analysis.

1.6 Improvement potential

The solution space for possible future value chains for an emerging technology must be reduced to a manageable size without missing opportunities for creating value. One key way that value can be created is by identifying co-benefits. The value chain of technologies that are not well-defined or understood must be researched, designed, and assessed using available lab-scale or comparable-technology-at-scale data. This is a challenging step as alternative value chains may have widely different economic and environmental consequences or benefits over different spatial and temporal scales. As demonstrated in Chapters Two and Three, it is possible to use both top down and bottom up approaches for modeling future value chains for brine and CO_2 utilization and disposal, which are a part of the larger carbon dioxide capture and sequestration life cycle. Both approaches allowed the identification of novel pathways that converted the waste streams into resource streams.

Janis Birkeland describes this objective as “positive development” in her discussion on restructuring businesses to add-value to society:

> "… sustainable development frameworks and tools have only measured negative (or less negative) impacts. Therefore, developers and designers have had little information or incentives for generating net positive environmental and social outcomes. PD [positive development] is based on the recognition that society, nature and cities are complex systems requiring not only closed-loop engineering and manufacturing, but open systems design that generates virtuous cycles throughout society."

Hellweg and Canals also note this objective, stating that "…widen[ing] the system boundaries beyond waste treatment and recycling to cover integrated resource management…" will help decision-makers to not "…miss improvement potentials through waste prevention and recycle-friendly product design."

Geologic brine can be treated as a feedstock for heat, desalinated water, and minerals, as well as a source of water for applications that only require low-grade water, such as algae production. With so many applications, it is difficult to know what value chains should be compared in an LCA. Chapter two introduces a method for identifying feasible and cost-effective brine management processes, called Brine Utilization Sequences (BUS), for any location that could then be assessed using LCA. This required the use of regional geologic-, market-, and climate-data, and the review of state regulations.

1.7 Case studies

1.7.1 Brine management for geologic carbon sequestration

Large scale deployment of carbon dioxide (CO_2) capture and sequestration (CCS) has the potential to significantly reduce global CO_2 emissions, but this technology faces social, economic, and environmental challenges that must be managed early on technology readiness cycle. Carbon capture technology is water-, energy-, and capital-intensive and proposed geologic carbon sequestration (GCS) storage options, if conducted in pressure-constrained formations, may generate large volumes of extracted brine that require costly disposal. Brine management is a poorly understood life cycle phase of CCS and has either been ignored or simplified in LCA of CCS. Most environmental assessments leave brine and CO_2 management out of the system boundary to avoid modeling this uncertain component (Marx et al., 2011; Schreiber et al., 2012; Corsten et al., 2013). The few assessments that do address brine or CO_2 management do not look at the full range of possible utilization and sequestration options (Buscheck et al., 2012; Benetto et al., 2004; Khoo and Tan, 2006). The assessments fail to capture the range of impacts resulting from plausible future life cycle processes. Not knowing the carbon mitigation potential of the full life cycle is a serious problem for a technology as water-, energy-, and capital-intensive as CO_2 capture. In addition, assuming a common management option, such as enhanced oil recovery, is better than leaving out CO_2 management all together, but it reduces the potential for identifying profitable or low-impact matches between deployment sites and management decision. In Chapter Two of this dissertation, brine management is evaluated in three locations of the United States (US) to assess whether recovered heat, water, and minerals can turn the brine into a resource.

Before an LCA of brine management for geologic carbon sequestration could be conducted, the matrix of possible value chains had to be reduced to a manageable number. Technical feasibility and cost-effectiveness were used as metrics in a new approach to determine which values chains for brine management should be assessed in future LCA (Breunig et al. 2013; Breunig et al. 2014).

Climate and aquifer parameters varied between the three regions and strongly affected technical feasibility. The levelized net present value (NPV) of extracted brine ranged from −$50 (a cost) to +$10 (a revenue) per ton of CO_2 injected (mt-CO_2) for a CO_2 point source equivalent to emissions from a 1000 MW coal-fired power plant (CFPP), compared to CCS NPV ranging from −$40 to −$70 per mt-CO_2. Upper bound scenarios reflect assumed advancements in current treatment technologies and a favorable market and regulation landscape for brine products and disposal. A regionally appropriate management strategy may be able to treat the extracted brine as a source of revenue, energy, and water.

1.7.2 CO_2 utilization and sequestration

Carbon dioxide utilization and sequestration (CCUS) is a strategy for redirecting CO_2 emissions from point-sources to beneficial applications that result the effective storage or significant delay of emissions. Like brine management, likely future value chains for CO_2 utilization are poorly defined. CO_2 utilization may be able to create an industry for CO_2 capture and sequestration (CCS) over the next 50 years if it can lower the cost of CCS. However, CCUS must be examined to ensure that greenhouse gas (GHG) emissions are not transferred from the energy sector to other industries.

Chapter Three of this dissertation presents a method for performing temporally and spatially explicit life-cycle modeling to quantify the long-range climate implications of scenario projections through which captured CO_2 at coal fired power plants (CFPP) is directed to industrial applications. This method required the modeling of future economic sectors like the coal, gas, methanol, and hydrogen industries. In this top down approach, national and regional markets for CO_2 are characterized out to 2065 to determine the CO_2 mitigation that different CCUS value chains could achieve given moderate or aggressive market penetration. This approach was chosen over a bottom up approach since the captured CO_2 composition was assumed to be spatially homogeneous. A bottom up approach, where NPV is used to determine site-specific future value chains, was necessary in the brine management assessment (Chapter Two) because the brine composition varied from site to site. Value chains with the greatest potential to direct captured CO_2 to markets were then assessed using a hybrid LCA approach. Temporal and spatial models supported this LCA to quantify the cumulative radiative forcing and to determine where captured CO_2 would be transported over time.

CO_2 utilization could reach 0.4 to 1.4 GtCO_2/y by 2065 and reduce cumulative greenhouse gas emissions by 2 to 17 Gt CO_2eq if started in 2020. Enhanced gas recovery accounts for a majority of the possible CO_2 consumption (62 to 76%), followed by urea production (4 to 11%), fly ash mineralization (4 to 10%), enhanced coal bed methane recovery (9 to 11%), enhanced oil recovery (5% to 9%), and methanol production (1 to 3%). These findings confirm the disparity between the greenhouse gas (GHG) reduction that CO_2 utilization can provide, and the reduction

needed to slow climate change. However, it was found that regionally deployable CO_2 utilization applications could provide a near term solution for 26 of the largest CFPP in the US.

1.7.3 Fuel cell systems for combined heat and power

Proton exchange membrane (PEM) fuel cells, which rely on thin polymers as their electrolytes, could play an important role in distributed generation and backup power in the United States (Lipman et al., 2004; Feroldi and Basualdo, 2012). They are characterized by their fast start-up and rapid response to dynamic electricity loads, and by their high power density of ~0.7 W/cm^2 (Mehta and Cooper, 2003). Low temperature PEM fuel cells operate at temperatures less than 90°C. Fuel cells are often thought of as low-carbon, low-criteria-air-pollutant (CAP) technologies because they convert hydrogen to electricity without combustion. However, no study has proven that PEM fuel cells are competitive with current and future energy supply systems from an emissions perspective. Without a supportive hydrogen industry in the United States (US), PEM fuel cells will need equipment onsite to synthesize hydrogen from natural gas. This equipment has non-negligible emissions associated with it. Decision-makers, particularly those involved in writing government support and tax policies, use total cost of ownership (TCO) and emissions analyses to compare alternative distributed generation technologies. Externalities ranging from global warming to mortalities caused by air pollution have been called the "hidden costs" of energy technologies because they are often ignored in total cost of ownership analyses (NRC2010). This research seeks to integrate these hidden costs into the TCO for PEM fuel cells.

In order to assess PEM fuel cells as an emerging technology for CHP applications, a life cycle model was needed that could integrate data specific to the targeted buildings and regions identified by fuel cell developers. Chapter Four of this dissertation provides the first approach for completing and matching localized inventory and impact assessment of the operation phase of PEM fuel cell systems for stationary CHP applications (Wei et al., 2014). As a case study, the greenhouse gas and human health implications of adopting PEM fuel cell systems in large hospitals and small hotels in Phoenix (AZ), Chicago, (IL), New York City (NY), Houston (TX), Minneapolis (MN), and San Diego (CA) were assessed.

Environmental and human health impacts of the adoption of FCS varied widely between locations due to differences in building and fuel cell operation, nearby population, and regional conditions affecting the transport and transformation of pollutants. All six cities experienced a positive net benefit from adopting FCS in small hotels and large hospitals. Certain cities did not, however, realize a positive climate benefit from FCS adoption; this includes Phoenix and San Diego. The largest benefit from city-wide deployment occurred in New York City and Chicago, valued at $31.8 million and $29.2 million over one year, respectively. These values represent the monetized value of the marginal change in criteria air pollutant emissions (NO_X, SO_2, $PM_{2.5}$, PM_{10}) and greenhouse gas emissions (CO_2, CH_4, N_2O). In a scenario where FCS only provided heat for water heating, and not space heating, FCS would not provide carbon savings to large hospitals in Phoenix, NYC, Houston, or San Diego or to small hotels in Phoenix. FCS will

provide the greatest monetary benefit from avoided health damages in regions where there are poorly controled NOx and SOx emissions from energy sources like fuel-oil-powered boilers and power plants.

1.8 References

McKone, T.E.; Nazaroff, W.W.; Berck, P.; Auffhammer, M.; Lipman, T.l Torn, M.S.; Masanet, E., Lobscheild, A.; Santero, N.; Mishra, U.; Barrett, A.; Bomberg, M.; Fingerman, K.; Scown, C.; Strogen, B.; Horvath, A. Grand Challenges for Life-Cycle Assessment of Biofuels. *Environ. Sci. Technol.* **2011.** *45*. 1751-1756.

Arvesen A.; Hertwich E. G. Assessing the life cycle environmental impacts of wind power: a review of present knowledge and research needs. *Renew. Sustain. Energy Rev.* **2012**. *16.* 5994–6006.

Scown, C. D.; Taptich, M.; Horvath, A.; McKone, T. E. Nazaroff, W. W. Achieving deep cuts in the carbon intensity of U.S. automobile transportation by 2050: Complementary roles for electricity and biofuels. *Environ. Sci. Technol*. **2013**. *47*. 9044-9052.

Masanet, E.; Chang, Y.; Gopal, A. R.; Larsen, P.; Morrow, W. R.; Sathre, R.; Shehabi, A. Zhai, P. Life-cycle assessment of electric power systems. *Annu. Rev. Environ. Resour*. **2013**. *38*. 107-36.

Hellweg, S.; Canals, L. M. Emerging approaches, challenges and opportunities in life cycle assessment. *Science*. **2014**. *344*. 1109-1113.

International Organization for Standardization (ISO),The New International Standards for Life Cycle Assessment: ISO 14040 and ISO 14044 (ISO, Geneva,Switzerland, 2006).

The Greenhouse Gases, Regulated Emissions, and Energy Use in Transportation (GREET) Model, 1.8c; Argonne, IL, Accessed 2014; http://www.transportation.anl.gov/modeling_simulation/GREET/

Pennington, D. W.; Potting, J.; Finnveden, G.; Lindeijer, E.; Jolliet, O.; Rydberg, T.; Rebitzer, G. Life cycle assessment Part 2: Current impact assessment practices. *Environmental International*. **2004**. *30*, 721-739.

Economic Input-Output Life Cycle Assessment (EIO-LCA) US 2002 (428) model. Carnegie Mellon University Green Design Institute: Pittsburgh, PA, 2010; http://www.eiolca.net/

Williams, E. D.; Weber, C. L.; Hawkins, T. R. Hybrid Framework for Managing Uncertainty in Life Cycle Inventories. *Journal of Industrial Ecology* **2009,** *13* (6).

Guinee, J.B.; Heijungs, R.; Huppes, G.; Zamagni, A.; Masoni, P. et al. Life cycle assessment: past, present, and future. *Environ. Sci. Technol.* **2011**. *45*. 90-96.

Finnveden, G.; Hauschild, M. Z.; Ekvall, T.; Guinee, J.; Heijungs, R.; Hellweg, S.; Koehler, A.; Pennington, D.; Suh, S. Recent developments in Life Cycle Assessment. *Journal of Env. Management*. **2009**. *91*. 1-21/

Heijungs, R., Huijbregts, M.A.J. A review of approaches to treat uncertainties in LCA. In: Pahl-Wostl, C., Schmidt, S., Rizzoli, A.E., Jakeman, A.J. (Eds), Complexity and Integrated Resources Management, Transactions of the 2nd Biennial Meeting of the International Environmental Modelling and Software Society, June **2004**, *vol. 1*. iEMSs, pp. 332–339.

Lloyd, S.M., Ries, R. Characterizing, propagating, and analyzing uncertainty in life-cycle assessment: a survey of quantitative approaches. *J. Indust. Ecol*. **2007**. *11* (1), 161–179.

Spielmann, M., Scholz, R.W., Tietje, O., de Haan, P. Scenario modelling in prospective LCA of transport systems. Application of formative scenario analysis. *Int. J. Life Cycle Assess*. **2005**. *10*, 325–335.

Pesonen, H-L.; Ekvall, T.; Fleischer, G.; Huppes, G.; Jahn, C. et al. Framework for scenario development in LCA. *Int. J. of Life Cycle Assess*. **2000**. *5*, 21-30.

Weidema B.P. Multi-user test of the data quality matrix for product life cycle inventory data. *Int. J. LCA*. **1988**. *5*, 259-265.

Huijbregts, M.A.J., Norris, G., Bretz, R., Ciroth, A., Maurice, B., von Bahr, B., Weidema, B.P., de Beaufort, A.S.H., Framework for modelling data uncertainty in life cycle inventories. *Int. J. Life Cycle Assess*. **2001**. *6*, 127–132.

Azevedo, L. B.; Henderson, A. D.; Zelm, R.; Jolliet, O.; Huijbrets, M. A. J. Assessing the importance of spatial variability versus model choices in life cycle impact assessment: the case of freshwater eutrophication in Europe. *Environ. Sci. Technol.* **2013**, *47*, 13565-13570.

Mutel, C. L.; Pfister, S.; Hellweg, S. GIS-based regionalized life cycle assessment: how big is small enough? Methodology and case study of electricity generation. *Environ. Sci. Technol*. **2011**. *46*. 1096-1103.

Mutel, C. L.; Hellweg, S. Regionalized life cycle assessment: computational methodology and application to inventory databases. *Environ. Sci. Technol*. **2009**. *43*. 5797-5803.

Potting, J. (2000): Spatial differentiation in life cycle impact assessment. A framework and site-dependent factors to assess acidification and human exposure. Ph.D.-thesis. Utrecht University, The Netherlands.

Potting J.; Hauschild, M. (2005): Background for spatial differentiation in life cycle impact assessment – The EDIP2003 methodology. Environmental project no. 996, Danish Environmental Protection Agency, Copenhagen.

Potting, J.; Hauschild, M. Z. Spatial differentiation in life cycle impact assessment: A decade of method development to increase the environmental realism of LCIA. *Int. J. LCA*. **2006**, *11*, 11-13.

Wastes –non-hazardous waste-municipal solid waste. U.S. Environmental Protection Agency. Accessed March 10, 2015. http://www.epa.gov/waste/nonhaz/municipal/hierarchy.htm

Chapter 7: Business opportunities through positive development; In: A new dynamic effective business in a circular economy; Janis Birkeland; Ellen MacArthur Foundation. Pp. 90.

Marx, J.; Schreiber, A.; Zapp, P.; Haines, M.; Hake, J.-Fr.; Gale, J. Environmental evaluation of CCS using Life Cycle Assessment - a synthesis report. *Energy Procedia*. **2011**. *4*. 2448-2456.

Schreiber, A.; Zapp, P.; Marx, J. Meta-analysis of life cycle assessment studies on electricity generation with carbon capture and storage. *Journal of Industrial Ecology*. **2012**. *16*. 5155-5168.

Corsten, M.; Ramirez, A.; Shen, L.; Koornneef, J.; Faaij, A. Environmental impact assessment of CCS chains – Lessons learned and limitations from LCA literature. *International Journal of Greenhouse Gas Control*. **2013**. *13*. 59-71.

Buscheck, T.A.; Sun, Y.; Chen, M.; Hao, Y.; Wolery, T.J.; Bourcier, W.L.; Court, B.; Celia, M.A.; Friedmann, S.J.; Aines, R.D. Active CO_2 reservoir management for carbon storage: analysis of operational strategies to relieve pressure buildup and improve injectivity. *International Journal of Greenhouse Gas Control*. **2012**. *6*. 230–245.

Benetto, E.; Popovici, E.-C.; Rousseaux, P.; Blondin, J. Life cycle assessment of fossil CO_2 emissions reduction scenarios in coal-biomass based electricity production. *Energy Conversion and Management*. **2004**. *45*. 3053-3074.

Khoo, H. H.; Tan, R. B. H. Life cycle investigation of CO_2 recovery and sequestration. *Environ. Sci. Technol*. **2006**. *40*. 4016-4024.

Regional evaluation of brine management for geologic carbon sequestration. Breunig, Hanna; Birkholzer, Jens; Borgia, Andrea; Oldenburg, Curtis; Price, Phillip; McKone, Thomas. *International Journal of Greenhouse Gas Control*. **2013**. *14*. 39-48.

Assessment of brine management for geologic carbon sequestration. Breunig, Hanna; Birkholzer, Jens; Borgia, Andrea; Oldenburg, Curtis; Price, Phillip; McKone, Thomas. *Lawrence Berkeley National Laboratory Report*, LBNL-6361E, April 2014.

A Total Cost of Ownership Model for Low Temperature PEM Fuel Cells in Combined Heat and Power and Backup Power Applications. Wei, Max; Lipman, Timothy; Mayyas, Ahmad; Chien, Joshua; Chan Shuk Han; Breunig, Hanna; Stadler, Michael; McKone, Thomas; Beattie, Paul; Chong, Patricia; Collela, Whitney; James, Brian. *Lawrence Berkeley National Laboratory Report.* LBNL-6772E, October 2014.

Chapter 2: Regional Evaluation of Brine Management for Geologic Carbon Sequestration

Adapted with permissions from: Jens Birkholzer, Curtis Oldenburg, Philip Price, Thomas McKone, and Andrea Borgia.

Copyright 2013 International Journal of Greenhouse Gas Control.

Copyright 2013 Lawrence Berkeley National Laboratory.

2.1 Introduction

Carbon dioxide (CO_2) capture and sequestration (CCS) is designed to prevent anthropogenic CO_2 from entering the atmosphere. Geologic carbon sequestration (GCS) is the injection of CO_2 into geologic formations such as sedimentary basins (Gale, 2004; Holloway, 2005). The large storage capacities of saline aquifers within sedimentary basins in the United States (US) make them a promising choice for GCS. Unfortunately, because the pore space in saline aquifers is already filled with brine, the injection of large quantities of CO_2 can lead to widespread and lasting pressure perturbation in the subsurface (Birkholzer et al., 2012; Nicot, 2008). Potential impacts related to elevated formation pressure include: (1) caprock fracturing and fault reactivation, and (2) pressure-driven leakage of CO_2 and brine (Rutqvist et al., 2008). One developing technique for mitigating pressure concerns is GCS with brine extraction, whereby CO_2 is injected into a saline formation and resident brine is brought to the surface through extraction wells to direct CO_2 plume flow and to manage formation pressure (Bergmo et al., 2011; Birkholzer et al., 2012; Buscheck, et al., 2012).

While brine extraction is not required and may not be necessary for most GCS sites, it is useful to explore methods for reducing disposal costs for sites where pressure constraints require that brine be extracted. (Buscheck et al., 2012) provide a qualitative overview of potentially viable options including: desalination; saline water for cooling towers; makeup water for enhanced oil recovery (EOR) systems; and geothermal energy production. Various industries provide evidence that brine-sourced heat, minerals, and water are marketable products that present an opportunity for considering the brine as a resource in certain regions of the country (Ahmed et al., 2001; Aines et al., 2011; Buscheck et al., 2011; Frick et al., 2010; Harto and Veil, 2011; Sullivan et al., 2011; Veil et al., 2004). Aside from desalination, there is currently no method for exploring the feasibility, cost, or benefit of brine management for GCS (Bourcier et al., 2011).

Our objective is to develop a spatially resolved method for quantifying the costs and environmental impacts of brine management. We assume that the GCS projects studied require extraction of brine at an extraction ratio of one (i.e., volume of CO_2 injected equals volume of brine extracted). Our cost estimates start after brine has been brought to the surface; we do not account for the infrastructure and energy cost for extracting brine. Brine management may have one disposal step, or it may involve a brine use sequence (BUS) of treatment and disposal steps. Our study is unique in that it: (1) evaluates several usages that have yet to be applied to brine management for GCS, in particular mineral harvesting, fish aquaculture, and algae biodiesel production; (2) develops a method for organizing a BUS; (3) calculates the feasibility, levelized net present value (NPV), resource production, and land footprint of BUSs in three regions of the

US. Each treatment, use, and disposal option introduced in this report requires further detailed assessments, but this report is a starting point and lays the groundwork for future life cycle assessments (LCA) of brine management. LCA is an important tool for quantifying environmental impacts related to life cycle stages of a product or process and has yet to be completed for brine management.



Figure 1: Map of three saline aquifers in different regions of the US (areas in grey). Climate data used to analyze each region were taken from locations shown in red (Department of Energy 2012; Gulf Coast Carbon Center 2003).

Disposal processes included in this report are: (1) discharge to the ocean, (2) evaporation ponds, (3) deep well injection and (4) use of brine for road deicing. Usages included in this paper are: (1) geothermal energy, (2) desalination, (3) salt, boron, magnesium, calcium, and potassium harvesting, (4) algae pond recharge, and (5) aquaculture pond recharge. We include these options because they can be monetarily quantified using available regional data.

A BUS that creates value from the brine may help pay back part of the water-, energy-, and monetary (capital and operating) cost of brine extraction and CCS.

2.2 Methodology

2.2.1 Regional Sequestration Scenarios

The system boundary of our assessment begins once brine is brought to the surface and ends once components of the brine are sold or sent off site for treatment, injected underground, discharged into surface water bodies, or evaporated. We selected three saline aquifers from different regions of the US to encompass some of the variation in parameters relevant to the feasibility and economics of brine disposal: (1) the southern Mt. Simon Sandstone Formation (Mt. Simon) in the Illinois Basin, IL; (2) the Vedder Formation (Vedder) in the San Joaquin Basin, CA; and (3) the Jasper Formation (Jasper) in the eastern Texas Gulf Basin, TX (Figure 1). These aquifers were selected for their prominent role in GCS research, for their close proximity to CO_2 sources which makes them prospective sequestration sites, and for the large quantity of available data characterizing them (see Appendix A1, Section S1).

One tonne of CO_2 injected (mt-CO_2) is the functional unit of our assessment. We assumed a 1:1 volume displacement of pore water per volume of CO_2 injected and a density of supercritical CO_2 of 500 g/L. From these assumptions, we calculated that 2 m3/mt-CO_2 of brine are extracted. Lower brine production rates will occur if formation-water extraction is conducted at extraction rates less than 1:1 or if the density of CO_2 is higher than 500 g/L.

Our scenarios evaluated one 1000MWe coal-fired power plant (CFPP) as the CO_2 point source per brine formation, and assumed capture and storage of 90% of CO_2 emissions for 30 years. We further postulated that the energy penalty (EP) arising from the carbon capture process increased initial emissions by 24%, resulting in an annual injection of 8.9 million mt-CO_2 and a brine extraction of ~2000 m3/h (~13 million gallons per day (GPD)) (Zenz House et al., 2009). Although our selected EP is optimistic relative to current technology, we believe that carbon capture technology will improve over time. In addition, our conservative formation-water displacement ratio favors realistic extraction scenarios. The formations chosen have the capacity to hold CO_2 from multiple CCS projects and we discuss challenges that may come with upscaling our results to multiple GCS projects later in the paper.

A cost effective BUS would maximize NPV by: (1) optimizing resource production and synergies between BUS stages, (2) reducing the total volume of brine requiring disposal, and (3) choosing BUS options that take advantage of current on and offsite infrastructure. A generic non-site-specific BUS would include: extraction of energy, extraction of freshwater from cooled brine, direct use of brine, extraction of minerals from concentrated brine, and disposal (Fig. 2). Algae production and fish production are stages that could either use the extracted brine itself, the extracted energy, or desalinated brine; these stages could act in parallel or in series with additional BUS stages. Treatment, use, and disposal stages were modeled using the equations and assumptions described in Section 2.2. Aquifer- and region-specific inputs were collected and used to generate site-specific BUS scenarios. We assumed the entire volume of extracted brine was sent through a BUS unless our assumed feasibility limits for parameters like total land footprint and maximum transportation distances would be violated. In these instances, we modeled the BUS so that a feasible fraction of brine was sent through the BUS and the remaining fraction of brine was sent through an alternative BUS.

We carried out a regionally specific literature review for each brine management option to explore the use and maturity of current practices in the US, technical limitations and results of previous environmental impact assessments (Appendix A1, Section S2). We analyzed the construction and in-use-phase costs (Table 1, Table 2). We used calendar-year 2010 mineral markets to determine sale prices and potential demands for brine resources. Data were collected to calculate ranges in NPV, land footprint, and resource production for individual management stages applied to brines from different saline aquifers (Department of Energy, 2012; Ventyx, 2012). Ranges were given for some parameters to signify heterogeneity or uncertainty in the system. Site-generic costs and values were used when site-specific data were unavailable.

2.2.2 Brine Management Options

2.2.2.1 Energy Production

Geothermal energy production is a mature technology that has a low carbon footprint and is a growing industry in the US. If energy production was included in a BUS, we assumed it was performed at extraction and the captured energy was used onsite (Fig. 2). The feasibility of this BUS option is dependent on there being a demand for heat onsite. The NPV of combined heat and power (CHP) generation using a binary cycle and heat exchangers was calculated and compared to the NPV of heat generation for brines with average temperature above 90°C (Table 2) (Lund, 2010). Heat and power savings reflect assumed annual load hours and auxiliary electricity requirements for pumping and re-cooling (Table 2) (Frick et al., 2010). NPV was calculated using:

$$NPV/(mt\text{-}CO_2) = (\text{Capital Cost}) + (\text{Heat Savings}) + (\text{Power Savings}) + (\text{O\&M Cost}) + (\text{Land Cost}) \quad (1)$$

where potential thermal [$MJ_{th}/mt\text{-}CO_2$] and electrical energy [$kWh/mt\text{-}CO_2$] production ranges were used to determine high and low revenue [$\$/mt\text{-}CO_2$] assuming current regional energy prices. Costs were adapted from (Lund 2010), assuming a 30-year life time and 8% interest rate; operations and maintenance (O&M) were assumed to be 10% of capital costs. Land costs used in this study are listed in Table 1.

Synergies between geothermal energy production, GCS, and other BUS options could improve joint feasibility:

- Sequestered CO_2 would maintain formation pressures and thus brine production rates. This would greatly reduce the energy demand and water withdrawal typical of enhanced geothermal systems (EGS) which recharge geothermal reservoirs by injecting water.
- Energy production could provide a low carbon source of electricity or heat to the CO_2 source or to subsequent BUS stages
- Energy capture removes the necessity for a cooling stage prior to desalination

2.2.2.2 Freshwater Water Production

Numerous technologies are available for treating high salinity water. Membrane treatment is one mature technology used by water utilities and other industries throughout the US. Reverse osmosis (RO) desalination is typically used to treat seawater (around 35 g/L), but we assumed RO was feasible for saline groundwater with TDS less than 90 g/L at low recovery rates and in water scarce regions (Aines et al., 2011; Bourcier et al., 2011). This assumption may be optimistic given current RO membrane technology, but we assumed the technology will improve over time. Additional filtration or chemical pre-treatment stages can improve the performance of current RO membranes by removing silica and minerals that cause scale.

Desalination treatment would come after heat capture if the two stages were included in a BUS (Fig. 2). NPV was calculated using:

$$NPV/(mt\text{-}CO_2) = (Capital\ Cost) + (Water\ Savings) + (O\&M\ Cost) \quad (2)$$

where water savings occur either on-site, or through the sale of water off-site (Maulbetsch and DiFilippo, 2006). Capital, operation, and maintenance costs were adapted from (Bourcier, et al. 2011) given our assumed freshwater production rate (dependent on volume of extracted water) and our assumed maximum freshwater recovery fraction (function of TDS concentration).

Synergies between freshwater production, GCS, and other BUS options could improve joint feasibility:

- GCS with brine extraction could reduce competition between future CCS projects and future brackish water desalination projects (Udo de Haes et al., 2004)
- Desalination could provide a source of freshwater for cooling towers or to subsequent BUS stages
- Desalination would generate a concentrated stream of brine. This would reduce the land footprint of evaporation ponds for mineral harvesting or for disposal
- The volume of brine requiring disposal would be reduced

2.2.2.3 Mineral Production

We assumed harvesting of salt NaCl, magnesium Mg, boron for boric acid B_2CO_3, potassium for potash K_2O, and calcium for gypsum $Ca(SO_4)*2(H_2O)$ would incorporate evaporation ponds and a salt electrolysis treatment similar to the process used to treat concentrated water from the Great Salt Lake in Utah (Ahmed et al., 2003; Thayer and Neelameggham, 2001; Tripp, 2009). These compounds were selected due to maturity in harvesting technology, and higher current market values (Angulo, 2011; Bueno, 2011; Jasinski, 2011; Jeppesen et al., 2009; Kostick, 2011). Mineral harvesting could occur directly after extraction, or it could occur after geothermal energy and freshwater are harvested from the brine (Fig. 2). The mass mineral production was estimated from brine concentration ranges (Gulf Coast Carbon Center, 2003; Kharaka and Hanor, 2003; USGS, 2002). NPV was calculated using:

$$NPV/(mt\text{-}CO_2) = (\text{Capital Cost}) + (\text{Mineral Revenue}) + (\text{O\&M Electrolysis Stage Cost}) + (\text{Land Cost}) \quad (3)$$

where the revenue is a function of the brine composition and current compound market value. Cost for evaporation ponds is composed of land and construction costs, and is directly proportional to pond SA (Table 2; SI, Section 3) (Jeppesen et al., 2009).
While it is possible to capture rare earth elements (REE) from extracted brine, little to no data were available on the presence of recoverable REE in our three saline aquifers.

Synergies between mineral production, GCS, and other BUS options could improve joint feasibility:

- Potassium could be used as fertilizers for algae ponds or for local agriculture
- Salt could be used for road de-icing if brine cannot be applied to roads
- Evaporation and mineral production would substantially reduce the volume of brine requiring disposal

2.2.2.4 Algae Biodiesel Production

Algae biodiesel is an emerging technology, and renewed interest in algae biodiesel has led to an increase in research of species that can grow in nutrient-supplemented saline waters (Borowitzka and Moheimani, 2010; Pate et al., 2011; Singh et al., 2011). Brine could supply algae ponds directly after extraction, or after geothermal energy and/or freshwater are harvested (Fig. 2). Algae reach their highest production rates in climates with high solar incidence and high temperatures. Pond purging is necessary to maintain optimal salinity concentrations; a BUS with algae production must include a stage that manages pond wastewater (Appendix A1, Section S3). Productivity and lipid content achievable during the months of operation at the three sites were adapted from previous regional studies (Borowitzka and Moheimani, 2010; Pate et al., 2011). Regional algae productivity [L lipid/(ha-yr)] values were compared to those estimated by (Borowitzka and Moheimani, 2010) (Table 2). Algae reach their highest production rates in climates with high solar incidence and high temperatures. NPV was calculated using:

$$NPV/(mt\text{-}CO_2) = (\text{Capital Cost}) + (\text{Lipids Revenue}) + (\text{Operation Cost}) + (\text{Land Cost}) \quad (4)$$

where revenue from lipid production was estimated using the current sale price of lipids. The value of selling byproduct algal biomass was not included in this calculation due to our assumption that biomass sales would yield little revenue.

Synergies between algae production, GCS, and other BUS options could improve joint feasibility:

- Bio-diesel and/or biogas from the anaerobic digestion of bio-solids could be used at the CO_2 point source or in other BUS stages
- Captured CO_2 could supply the algae ponds with a pure source of carbon and reduce the volume of CO_2 injected into the aquifer (and thus the volume of extracted brine)
- Seasonal evaporation could reduce the volume of brine requiring final disposal

2.2.2.5 Fish Production

Brine could recharge fish ponds directly after extraction if the water composition is acceptable for aquaculture. Since most brines are not suitable and require costly pre-treatment, geothermal energy and/or desalinated brine could be used to support fish ponds instead (Kharaka and Hanor, 2003; Zheng et al., 2009). Current practice shows that 0.24 TJ_{th}/yr is required for producing one tonne of fish, like tilapia, in aquaculture ponds and that tilapia growth diminishes when pond water drops below 30 °C (Boyd and Lund, 2003). This heating requirement can be partly met by insulation of the aquaculture pond in warmer seasons. The additional mass of fish that could be raised and harvested using geothermal heat captured from the brine was calculated using:

$$M_{fish} = (e_{th} * \Delta Q_{th})/(0.24 * 1e6\ MJ/TJ) \quad (5)$$

where [$*\Delta Q_{th}$] is heat flow [kJ/h], and it was assumed that heat production has an efficiency (e_{th}) of 40%. NPV was calculated using:

$$NPV/(mt\text{-}CO_2) = (\text{Capital Cost}) + (\text{Fish Revenue}) + (\text{Pond Operation Cost}) + (\text{Land Cost}) \quad (6)$$

where the SA of the ponds depended on fish production (Appendix A1, Section S3) and where the cost was adapted from a previous study that assumed a 30-year life time and an interest rate of 8% (Boyd and Lund, 2003; Lund, 2010). Production would have to be seasonal in Illinois unless the ponds were indoors. A disposal stage that manages organic wastes and concentrated salts must follow in a BUS that includes fish production. The value of tilapia was included in this study as a reference; it does not imply that the CFPP will reap the value of the tilapia without paying for fish cultivation.

Synergies between algae production, GCS, and other BUS options could improve joint feasibility:

- Anaerobic digestion of bio-solids could provide a small source of energy
- Seasonal evaporation could reduce the volume of brine requiring final disposal

2.2.2.6 Disposal

A BUS can include multiple stages of treatment prior to disposal, or it could include only disposal stages (Fig. 2). In effect, brine management inevitably becomes waste management despite the potential for resource harvesting.

Saline water bodies and treatment facility within 50 miles were considered potential disposal sites. Only the Jasper is within 50 miles of a saline water body, the Gulf of Mexico. Site selection for brine discharge into the ocean must meet local regulations and this may require a local source of low salinity water for dilution (Khan et al., 2009; Voutchkov, 2011). The sale of brine for road de-icing was a possible application in Illinois; this option was treated as both a use and a disposal stage for winter months (Table 2) (Mitchell et al., 2004; ND Department of Health, 2009; Ripley, 2011). Evaporation ponds and deep well injection were feasible options at all three sites, although ponds were seasonal in Illinois. Off-site disposal of brine by truck cost \$0.3-1.6/mt-CO_2-mile; disposal using newly constructed pipelines had a NPV of -\$0.1-0.2/mt-CO_2-mile. The NPV and feasibility of pipeline disposal is discussed in Appendix A1, Section 4.

Cost ranges for brine disposal were adapted from regional produced water management assessments and were used to calculate NPV assuming a 30-year life time and 8% interest rate (Table 2) (Clark and Veil, 2009; Puder and Veil, 2006). These values were multiplied by the fraction of brine remaining for disposal at the end of a BUS. When converted to our functional unit, costs incurred by the oil and gas industry equaled \$0.1-100/mt-CO_2 assuming the entire volume of water was sent for disposal (Veil et al., 2004).

We predict that finding cost effective disposal options that have large capacities and low environmental footprints will continue to be a significant challenge of brine management. Disposal options may change over time if brine sink capacities are reached by CCS projects in a region.

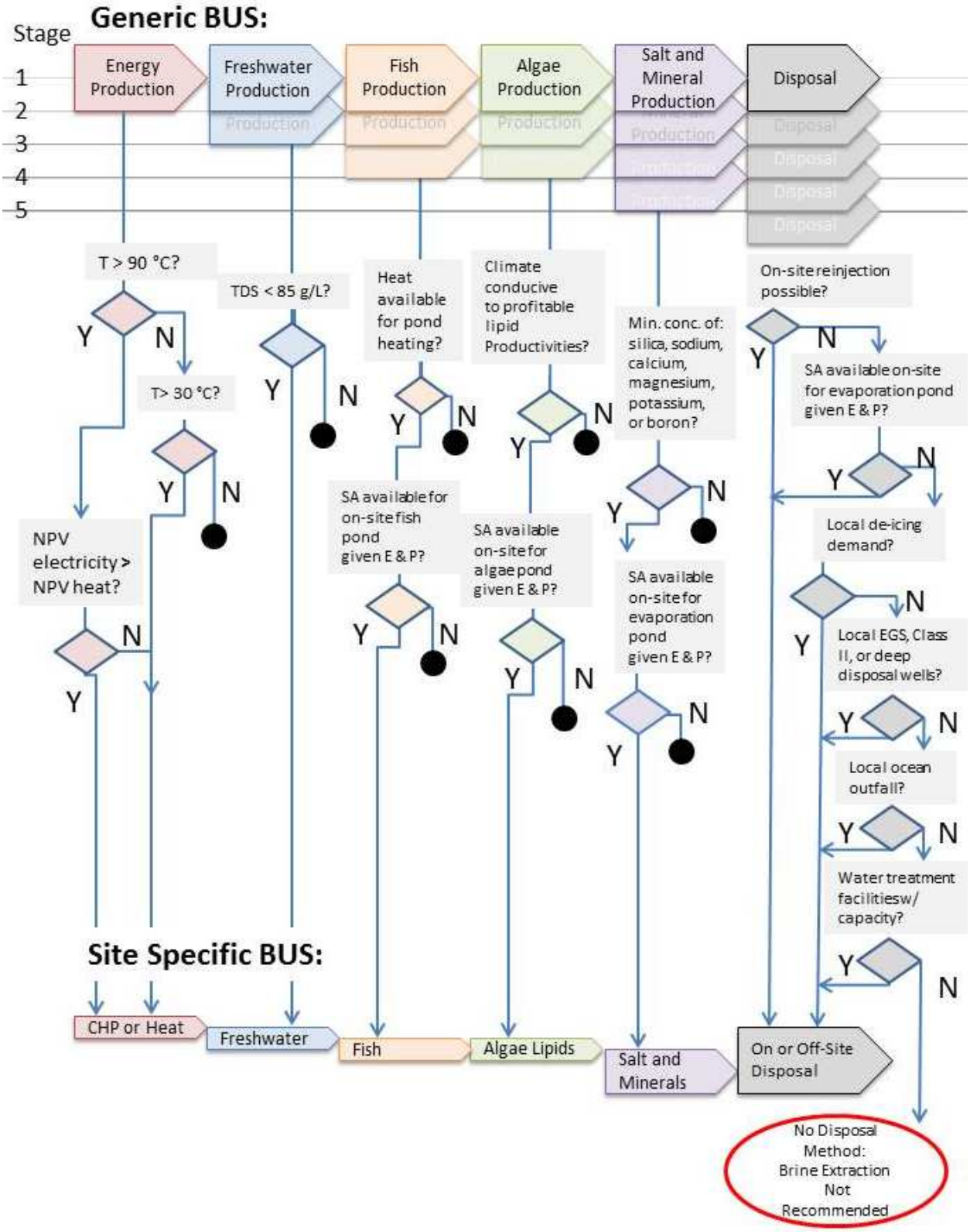


Figure 2: System Diagram. This diagram shows on- and off-site resource harvesting, treatment and disposal stages included in the study. Inputs include parameters like brine temperature (T), brine TDS, treatment net present value (NPV) and surface area (SA) requirements calculated from evaporation (E) or precipitation (P) data. Combined heat and power (CHP) is the generation of electricity as well as heat.

Table 1: Regionally variable inputs and assumptions. Percent of 2010 US domestic mineral production that could be met by the maximum production from one brine management project are listed in italics (%). NA stands for not applicable. *Did not find sufficient US production data for boric acid.

Region	**Southwest**		**South**		**Midwest**		
Formation	**Vedder**		**Jasper**		**Mt. Simon**		
Energy Production Inputs and Assumptions							Frick et al. (2010)
North American Electric Reliability Corporation Grid Region	WECC		TRE		SERC		
Cost Electricity [¢/kWh]	13.0		9.3		9.1		
Cost Natural Gas [¢/kWh]	3.0		3.2		2.9		
Heat Recovery Only							
Assumed Temperature (low, high) [°C]	(50, 90)		(50, 80)		(50, 90)		
Heat and Power Generation (Binary Cycle)							
Assumed T Low [°C]	(90, 150)		NA		(90, 150)		
Freshwater Production Inputs and Assumptions							Bourcier et al. (2011)
Assumed Percent Recovery [%]	50		10		NA		
Assumed Cost Reverse Osmosis [$/$m^3$ permeate]	0.32		0.81		NA		
Mineral Production Inputs and Assumptions	*% US domestic production 2010*						GCCC (2003) and
Annual Average Evaporation-Precip [m]	1.6		0.2		0.2		USGS (2002)
Days of Operation for Ponds	365		365		183		
Concentration Boron* (low, high) [mg/L]	(3, 91)		(53, 60)		(0, 500)		
Concentration Sodium (low, high) [mg/L]	(500, 10400)	*1*	(6250, 35200)	*3.6*	(24569, 44295)	*4.5*	
Concentration Potassium (low, high) [mg/L]	(0.5, 100)	*0.4*	(100, 225)	*0.8*	(200, 393)	*1.4*	
Concentration Magnesium (low, high) [mg/L]	(4, 44)	*0.3*	(37, 453)	*3.3*	(1287, 1713)	*12.6*	
Concentration Calcium (low, high) [mg/L]	(10, 147)	*0.1*	(169, 2150)	*0.9*	(4292, 9023)	*3.8*	Mitchell et al. (2004) and
Value Brine for Road De-icing [$/mt]	0		0		35		Ripley (2011)
Algae Production Inputs and Assumptions							Borowitzka and
Assumed Algae Productivity (warm days) [g/(m^2*d)]	30		20		30		Moheimani (2010) and
Assumed Algae Lipid Content (low, high) [% dry wt]	40		(30, 40)		(30, 40)		Pate et al. (2011)
Days of Operation for Ponds	365		365		183		
Disposal Inputs and Assumptions [$/mt-$CO_2$-injected]							Khan et al. (2009)
Dilution Factors for Ocean Discharge (low,high) [%]	NA		(0, 0.37)		NA		Clark and Veil (2009)
Surface Discharge Cost (low, high)	(-0.1, -1.0)		NA		NA		Veil et al. (2004) and
Evaporation Pond for Disposal Cost (low, high)	(-0.1, -1.0)		(-0.1, -1.0)		(-0.1, -1.0)		Purder and Veil (2006) an
Disposal Wells (low, high)	(-0.6, -33)		(-0.6, -33)		(-0.6, -33)		Clark and Veil (2009) and
Offsite Commercial Treatment (low, high)	(-2-13)		(-2-13)		(-13,-53)		Harto and Veil (2011)
Landfill	(-13)						
Transportation of Brine Through Pipeline	(-0.1, -0.2)		(-0.1, -0.2)		(-0.1, -0.2)		

Table 2: Inputs and assumptions that are not regionally specific.

Energy Production Inputs and Assumptions		**Source**
Heat Recovery Only		Frick et al. (2010)
T_ambient [°C]	20	Lund (2010)
Desired T_Pond [°C]	35	
Assumed Heating System Efficiency [%]	40	
Assumed Thermal Load Hours [h/yr]	7000	
Construction & Maintenance [$/kW yr]	19.6	
Heat and Power Generation		
Assumed Binary Cycle Efficiency [%]	10	
Assumed Binary Cycle Load Hours [h/yr]	6529	
Binary Cycle T_exit [°C]	77	
Heat Recovery T_ enter [°C]	70	
Assumed Auxiliary Power for Recooling [kWh/MWth]	20	
Assumed Percent of Power Capacity Used for Pumps [%]	10	
Construction & Maintenance [$/kW yr]	63.4	
Freshwater Production Inputs and Assumptions		Maulbetsch and DiFilippo (2006)
Value Desalinated Water [$/m^3]	0.42	
Value Reclaimed Water [$/m^3]	0.58	
Value Water in Arid Regions [$/m^3]	1.45	
Mineral Production Inputs and Assumptions		
Assumed Evaporation Pan Factor	0.69	Ahmed et al. (2003)
Assumed Height Pond [m]	0.03	
Cost Salt Production [$/L]	1.92	Jeppesen et al. (2009)
Value Boric Acid [$/mt]	360	Angulo (2011)
Value Salt in Brine [$/mt]	8	Bueno (2011)
Value Potash [$/mt]	600	USGS (2011)
Value Magnesium [$/mt]	3200	USGS (2011)
Value Crude Gypsum [$/mt]	6.5	USGS (2011)
Algae Production Inputs and Assumptions		
Value Algae Lipids [$/L]	0.69	Borowitzka and Moheimani (2010) and Pate et al. (2011)
Assumed Height Pond [m]	0.3	
Fish Production Inputs and Assumptions		Boyd and Lund (2003)
Assumed Energy for Tilapia [TJ/(yr*mt-fish)]	0.24	
Assumed Height Pond [m]	0.7	
Sale Price Tilapia [$/mt-tilapia]	2200	
Construction & Maintenance [$/kW yr]	19.6	Lund (2010)
Land Footprint Inputs and Assumptions		
Geothermal Land Footprint (low, high) [km^2/TWh]	(18,74)	Evans et al. (2009)
Road and Buildings (R&B) SA for Algae Ponds [%SA]	30	
R&B SA for Evaporation Disposal Ponds [%SA]	20	
Price Arid, Semi-arid, Desert Land (low, high) [$/acre]	(200, 2000)	

2.3 Results

2.3.1 NPV

Potential NPV was maximized using our BUS method after we generated a list of viable treatment and disposal options for each site; these results represent the High Scenarios shown in Figure 3. Alternative scenarios were explored for each location (Figure 3). Results were levelized over a 30 year period and are given per tonne CO_2 injected.
For brine from the Vedder, (1) capturing geothermal heat, (2) sending brine to supply algae ponds, and (3) disposing of brine in evaporation ponds resulted in the largest NPV, ranging from +$1 to +$2. This range reflects variations in potential heat capture, in the price of land and disposal, and in potential algae productivity. A BUS with a higher probability of being implemented in the near future and which includes: (1) capturing geothermal heat, (2) desalinating brine and selling the freshwater, and (3) paying to have the concentrated brine transported 50 miles to disposal wells, would result in a NPV of -$33 to +$1. This large range is due to the varying cost of deep well disposal. The Vedder has TDS below 40,000 mg/L and could become a valuable source of water for agriculture in the San Joaquin Valley (Udo de Haes et al., 2004). Direst disposal of brine into evaporation ponds and landfills within 25 miles represents a Low Scenario and could reach -$13.

The largest potential NPV or High Scenario, ranging from -$10 to +$4, for Jasper brine management resulted from: (1) capturing geothermal heat for fish ponds, (2) desalinating brine and selling the freshwater, (3) harvesting salt, boron, potash, gypsum, magnesium, and (4) paying to have the brine transported 25 miles to a disposal site and diluted in the Gulf of Mexico. NPV was affected by variations in potential heat and mineral capture, in the price of land, and in waste discharge costs which include permit, transportation, and dilution. Available land near Houston, TX is limited and water is not scarce (Ventyx, 2012); a more feasible BUS would exclude desalination and mineral harvesting steps (requiring over 80 km2 of land) and would result in a NPV of -$0.3 to $0.3. Shallow reinjection of brine 50 miles from the CFPP near freshwater resources could reach -$18.

The largest potential NPV, ranging from $1 to +$13, for Mt. Simon brine management in warm months results from (1) capturing geothermal heat for fish ponds, (2) harvesting salt, boron, potash, gypsum, magnesium, and (3) discharging wastes into evaporation ponds 25 miles away via trucks. This range would drop to -$7 to +$2 if magnesium is not harvested and sold. In the winter, use of extracted water for geothermal heat onsite and then as a road anti-icing solution could reach $3/mt-$CO_2$, assuming 50% of the brine could be used for road deicing within a 100 mile radius and that the remaining 50% is transported 25 miles to a deep well disposal site (the cost of land for evaporation ponds would still be incurred during winter months). Seasons with low road anti-icing demand could lead to significant losses for a GCS project that did not invest in a backup winter BUS (-$35). At the upper range of disposal costs, sending the brine for commercial treatment and subsequent surface disposal in Illinois could double the cost of CCS (-$53). We assumed this option would not be feasible in the near future, but we included it to show how costly brine disposal can be.

Net present value of brine management ranged from -$50 (a cost) to +$10 (a revenue) per tonne of CO_2 injected (mt-CO_2) for a CO_2 point source equivalent to one 1000MW CFPP.

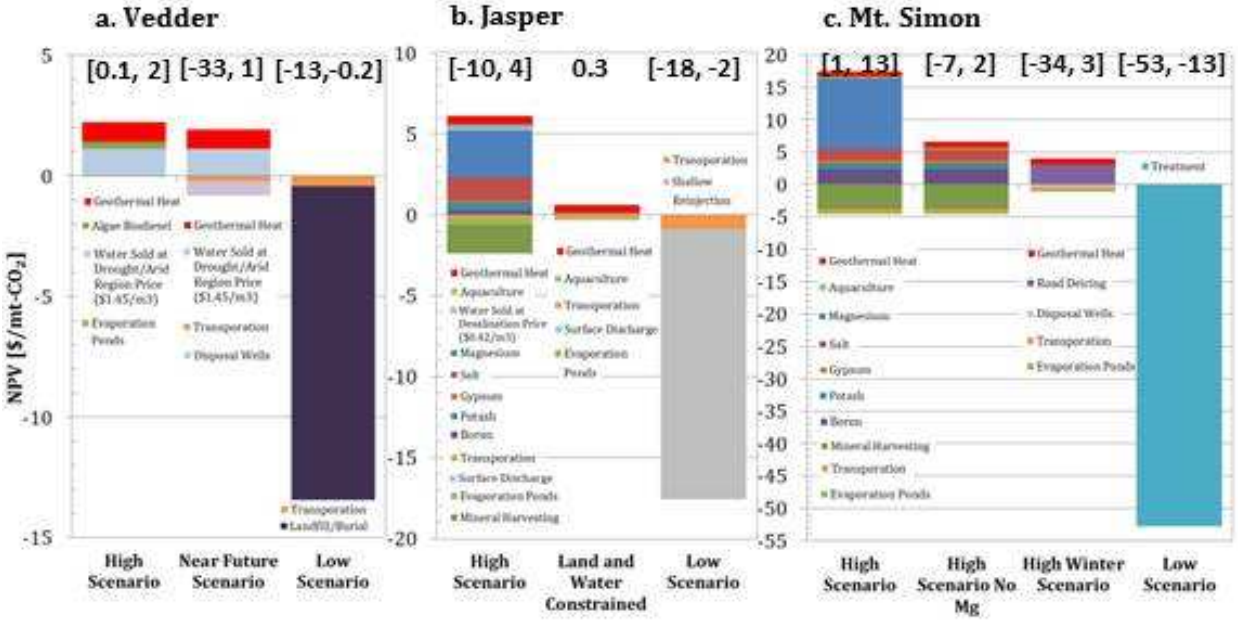


Figure 3: Net Present Value (NPV) for alternative BUS scenarios in three saline aquifers. Each scenario's BUS stages are listed in the column. Cumulative NPV is listed in bold at the top of each scenario's column.

2.3.2 Resource Production

Maximum production of magnesium, potash, gypsum, or salt using brine from one CCS project in any of the three formations resulted in annual quantities less than 5% of US domestic production (Table 1). Exceptions include magnesium from the Mt. Simon, where high concentrations resulted in maximum productions equivalent to 13% of 2010 US production. Total US imports for 2007 reached nearly 400,000 mt-tilapia, while ~9000 mt-tilapia were produced domestically in the US (Harvey 2012). Desalination of extracted brine at maximum TDS could produce 25 million liters per day of freshwater from the Vedder and 5 million liters per day from the Jasper. Ponds supplied with the average geothermal heat captured from the Mt. Simon, Jasper, or Vedder could produce 8, 6, or 14 mt-tilapia respectively; pond systems supplied with desalinated brine from the Vedder or Jasper could produce 3000 or 4000 mt-tilapia respectively, but we assumed these ponds were not feasible due to land, energy, and freshwater requirements (Appendix A1, Section S3). Annual US rock salt sales have fluctuated around 18 million tonnes the last 5 years. Salt produced from Mt. Simon sourced brine during four winter months in Illinois could supply 5% of US winter demand for road de-icing rock salt. These values are for one CCS project. In order for CCS to make a measurable impact in climate mitigation, many CCS projects will be needed, and market thresholds and excessive land use may hinder the application of some BUS options in certain regions of the country.

2.3.3 Environmental Impacts

Peer reviewed environmental impact assessments were found for many BUS options, including: geothermal systems, desalination systems, algae biodiesel production, magnesium harvesting, fish aquaculture, and ocean discharge of brine (Appendix A1, Section S2). Opportunities for mitigating local, regional, and global environmental impacts associated with each brine management option, and with the CO_2 source itself, may be recognized through careful allocation of energy, water, and material supply and demand across a BUS. Using Vedder brine as an example, a geothermal system needing ~0.1 m3/mt-CO_2 of low salinity water could supply an average of 1 kWh/mt-CO_2 of electricity to a desalination system requiring ~4 kWh/mt-CO_2 of electricity and producing fresh water at an average of 1 m3/mt-CO_2. Impacts attributed to the construction of buildings and roads could be allocated between the two systems, reducing their individual contributions. The potential for these synergies at different GCS sites will be evaluated in a future study.

Evaporation system land footprint ranged from 5 km^2 in southern California to 90 km^2 in eastern Texas. Total land footprint increased when geothermal systems (<1 km^2), algae (<10 km^2), or fish ponds (<0.1 km^2) were included (Appendix A1, Section S3). Additional land for brine storage tanks may be required in scenarios where the load hours of BUS steps differ significantly. Substantial land alterations may lead to indirect land use changes, negatively impacting local ecosystems.

2.3.4 Sensitivity Analysis

A sensitivity analysis was performed for energy and freshwater production to gain insight on how the NPV of these brine treatment options vary between and within saline aquifers (Fig. 4-5). We determined that the NPV of energy production is sensitive to brine temperature, regional electricity costs, and energy capture efficiencies (Fig. 4). Electricity generation is more expensive than heat generation at temperatures found in the three saline formations due to lower conversion efficiencies and higher auxiliary energy demands (Evans et al., 2009). Regardless, CCS projects may choose to generate electricity, or capture energy after some cooling of the brine if they cannot find adequate demand for heat.

The NPV of freshwater production is also sensitive to technology efficiencies, as well as TDS concentration and regional water rates. As seen in Figure 5, revenue can be obtained from desalinating brine from both the Jasper and Vedder formations if the water is sold at a high rate. Temporally dynamic variables, like changing market prices and market responses to new domestic sources of products like magnesium, are a major source of uncertainty. The effects of fluctuations in resource market prices on BUS utility were not quantified, as this was beyond the scope of our current study. In addition, implementation of emerging technologies like algae biodiesel depends on political, social, and economic forces that are difficult to predict and that add uncertainty to any future-looking study.

We explored brine management in the context of pressure management for GCS projects. As such, we chose an injection:extraction ratio of 1:1 to avoid reservoir pressure build-up. The extraction ratio required to control pressure rise may be less than a 1:1 ratio due to site specific geologic conditions that are outside the scope of this study. Certain aspects of our economic

assessment would scale linearly with brine extraction volume due to the sequential nature of our method. For example, desalination reduces the volume of brine entering later BUS stages like evaporation ponds (Appendix A1, Figure S1). We predict that other aspects of our economic assessment will show non-linear behavior at low brine volumes, capital costs for geothermal facilities for example. Exploring these non-linearities will be an important topic for a future study.

Inconsistencies and limitations of available regional data are another source of uncertainty (Appendix A1, Section S5). For example, well data without sufficient depth information in the Mt. Simon were excluded from the study. These values gave higher TDS concentrations and thus higher potential mineral recovery ($18 vs $13/mt-$CO_2$-eq) for the Mt. Simon High Scenario.

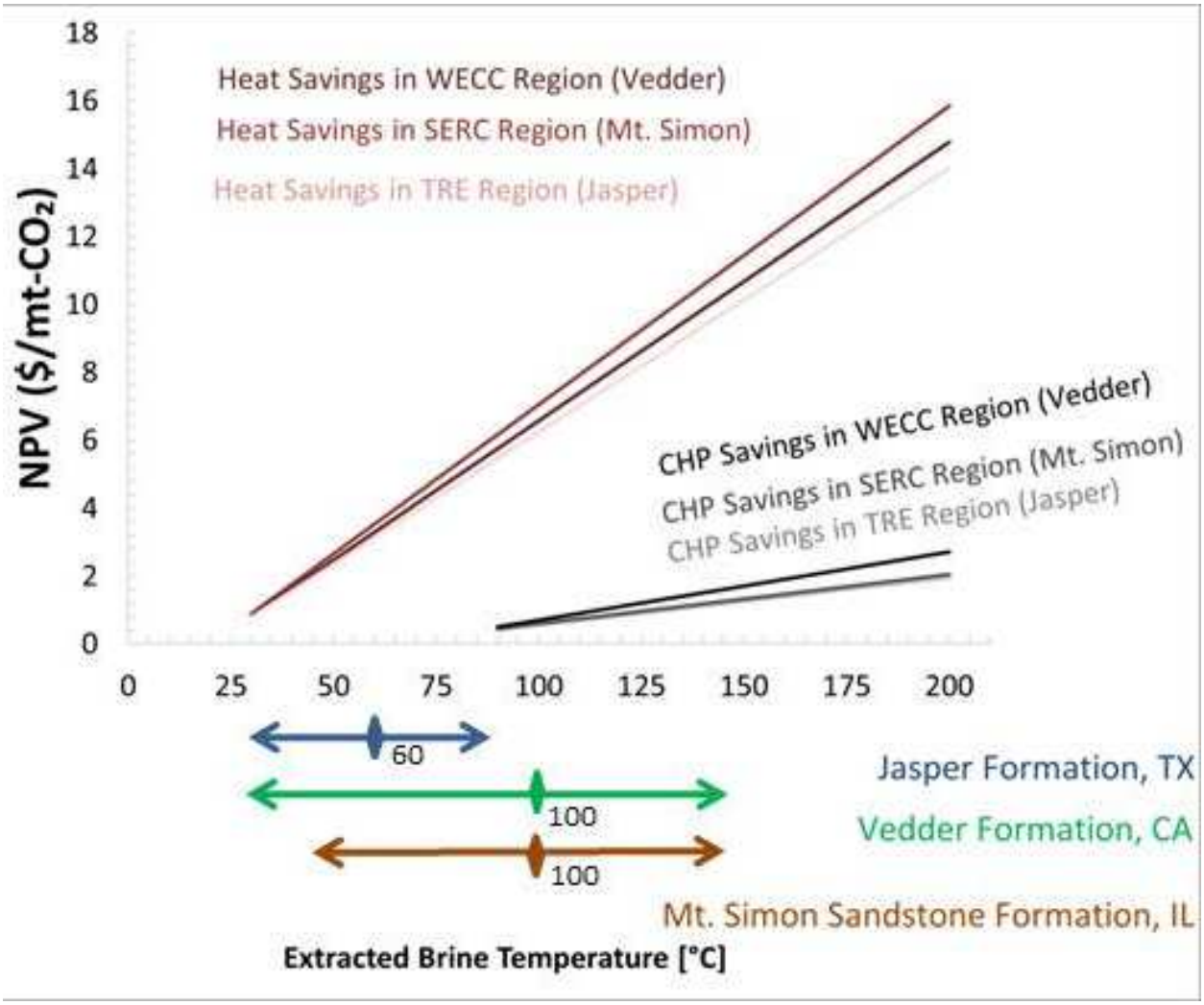


Figure 4: Parameter variation analysis for energy production. Geothermal energy can be used for (1) heating aquaculture ponds if brine T is above 30 °C, and (2) combined heat and power (CHP) if brine T is above 90 °C. Temperature ranges for saline aquifers are shown as solid arrows below graph. Representative aquifer temperatures are marked as diamonds on the solid arrows.

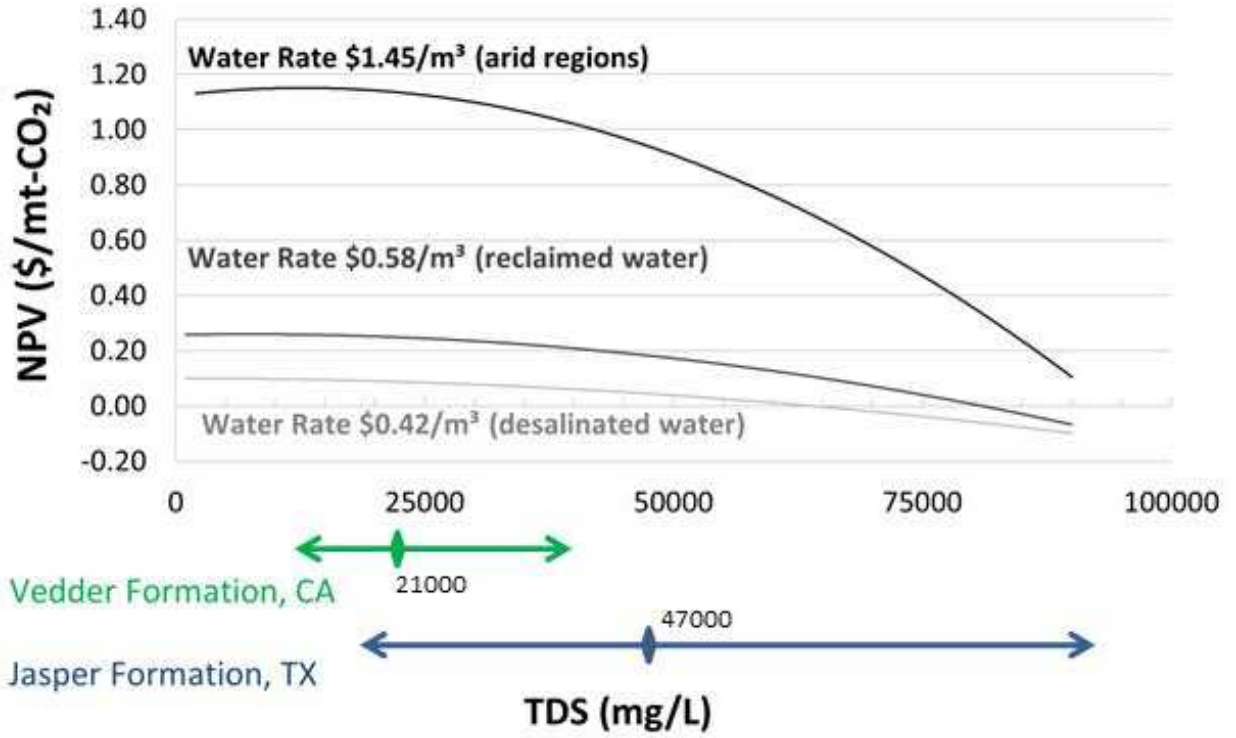


Figure 5: Parameter variation analysis for freshwater production. The NPV of desalinated water was plotted as a function of TDS in extracted brine and regional water rates. The current RO membrane technological limit was used as an upper bound (~90,000 mg/L). TDS ranges for saline aquifers are shown as solid arrows below graph. Representative aquifer TDS concentrations are marked as diamonds on the solid arrows. The TDS concentrations found in the southern Mt. Simon Sandstone Formation are much higher than the technological limit and were not included.

2.3.5 Perspective on Brine Extraction for GCS and Produced Water from Oil and Gas

A natural question is: if brine can be economically valuable under certain circumstances, then why has it not been used as such by the oil and gas industry? Unlike select GCS sites, where brine is extracted to reduce formation pressure, large quantities of brine (produced water) are unavoidably co-produced by the oil and gas industry as fields mature (Clark and Veil, 2009). After oil and gas are separated out of the water, (Ahmadun et al., 2009) the most common method of disposal for onshore sites is re-injection back into the reservoir; most offshore sites discharge the water into the ocean.

Likely answers to the question posed include:

(1) there is no need to keep the brine out of the oil and gas reservoir, making reinjection an obvious option (Stewart, 2006)
(2) there is a desire to maintain reservoir pressure to enhance oil and gas recovery which makes reinjection useful
(3) lack of familiarity with water, mineral, and aquaculture markets and technologies (Stewart, 2006)
(4) removal of soluble organics, gases, carcinogenic production contaminants, and unpredictable production rates greatly increase the cost and difficulty of brine management options (Ahmadun et al., 2009; Mondal and Wickramasinghe, 2008; Veil et al., 2004)
(5) their interest in taking on the responsibility of produced water management may fluctuate with the price of fossil fuels (Puder and Veil, 2006).

That being said, economic and environmental reuse of produced water through wetlands, irrigation, desalination, as water for cooling towers, for dust and fire control, and for enhanced oil and gas recovery is an active area of study (Finnveden et al., 2009; Mondal and Wickramasinghe, 2008; Stewart, 2006; Veil et al., 2004; Zamagni et al., 2012). For example, Devon Energy Corporation has treated produced water from the Barnett Shale in Texas to freshwater quality for reuse in hydro-fracking wells since 2005 (Earles and Halog, 2011). The volume treated in the Barnett Shale project is smaller than the total volume of brine modeled in this study (~10%), but Devon Energy Corporation has other projects exploring treatment, transportation, disposal, and storage of volumes of produced water on the same order of magnitude as our study. In 2010, a project in Oman started using reed beds to treat the equivalent volume of produced water modeled in our report; local applications for the treated water are being explored.

In GCS sites with pressure constraints, reinjection of the brine back into the same reservoir is not practical, hence the need to consider brine management. Despite the large role that GCS could play in US carbon emissions mitigation, the cost of GCS and brine management will inhibit national adoption unless methods are found to lower costs or until a substantial carbon tax incentivizes CCS adoption by large CO_2 stationary sources (Fischbeck et al., 2012).

2.4 Discussion and Conclusions

Multiple BUSs provided positive NPV for each site. These scenarios were sensitive to market prices for energy and water, fluctuations in brine temperature and chemistry, and relied on the assumption that related technologies would mature by the time of implementation. As a result, BUSs that provided revenue under optimal conditions did not show robustness under less optimal market and technological conditions. In addition, the BUS that can maximize NPV for one CCS project may not be feasible for multiple CCS projects in the same region due to limitations in land availability, brine disposal capacities, climate, and potential market thresholds. Brine management at each site had the potential to reach very negative NPV when the strictest regional disposal regulations were included (Fig. 3). Reducing the volume of waste brine will be imperative for improving the feasibility of disposal options in all regions evaluated. There is a risk that certain local, regional, and global environmental impacts will be introduced by brine management options. Although we used our method to generate BUS scenarios that maximize NPV in this study, our method can also be used to generate BUS scenarios that minimize environmental impacts.

The method developed in this study captures a high level of spatial heterogeneity in climate, market, and aquifer data. As a result, we were able to characterize prospective regional constraints and opportunities for cost effective local environmental management of large brine waste streams associated with large-scale GCS projects. Assessment of brine management should be integrated into a GCS project as early as site selection to avoid or manage challenges that may act as barriers to CCS deployment. We predict that rising water scarcity and progressive regulatory changes regarding GCS brine transportation and disposal will be key driving-forces for increasing the feasibility of brine management.

Additional data for the three case study aquifers, calculations for land footprint and pipeline economics, a literature review of related environmental assessments and a data quality assessment can be found in Sections 1-5.

2.5 References

Ahmadun, F. l.-R.; Pendashteh, A.; Abdullah, C.; Biak, D. R. A.; Madaeni, S. S.; Abidin, Z. Z., Review of technologies for oil and gas produced water treatment. Journal of Hazardous Materials 2009, 170, 530-551.

Ahmed, M.; Arakel, A.; Hoey, D.; Coleman, M., Integrated power, water and salt generation: a discussion paper. Desalination 2001, 134, 37-45.

Ahmed, M.; Arakel, A.; Hoey, D.; Thumarukudy, M. R.; Goosen, M. F. A.; Al-Haddabi, M.; Al-Belushi, A., Feasibility of salt production from inland RO desalination plant reject brine: a case study. Desalination 2003, 109-117.

Aines, R. D.; Wolery, T. J.; Bourcier, W. L.; Wolfe, T.; Hausmann, C., Fresh water generation from aquifer-pressured carbon storage: feasibility of treating saline formation waters. Energy Procedia 2011, 4, 2269-2276.

Angulo, M. A. Boron; Mineral Commodity Summaries; USGS: 2011.

Bergmo, P. E. S.; Grimstad, A.-A.; Lindeberg, E., Simultaneous CO_2 injection and water production to optimise aquifer storage capacity. International Journal of Greenhouse Gas Control 2011, 5, 555-564.

Birkholzer, J. T.; Cihan, A.; Zhou, Q., Impact-driven pressure management via targeted brine extraction-Conceptual studies of CO_2 storage in saline formations. International Journal of Greenhouse Gas Control 2012, 7, 168-180.

Borowitzka, M. A.; Moheimani, N. R., Sustainable biofuels from algae. Mitigation and Adaptation Strategy for Global Change 2010.

Bourcier, W. L.; Wolery, T. J.; Haussmann, C.; Buscheck, T. A.; Aines, R. D., A preliminary cost and engineering estimate for desalinating produced formation water associated with carbon dioxide capture and storage. International Journal of Greenhouse Gas Control 2011, 1319-1328.

Boyd, T. L.; Lund, J. W., Geothermal heating of greenhouses and aquaculture facilities. In International Geothermal Conference, Reykjavik, Iceland, 2003.

Bueno, B. Salt and ash: The industry faces slow growth due to increasing imports; 21239; IBISWorld: 2011.

Buscheck, T. A.; Sun, Y.; Chen, M.; Hao, Y.; Wolery, T. J.; Bourcier, W. L.; Court, B.; Celia, M. A.; Friedmann, S. J.; Aines, R. D., Active CO_2 reservoir management for carbon storage: Analysis of operational strategies to relieve pressure buildup and improve injectivity. International Journal of Greenhouse Gas Control 2012, 6, 230-245.

Buscheck, T. A.; Sun, Y.; Hao, Y.; Wolery, T. J.; Bourcier, W.; Tompson, A. F. B.; Jones, E. D.; Friedmann, S. J.; Aines, R. D., Combining Brine Extraction, Desalination, and Residual-Brine Reinjection with CO_2 Storage in Saline Formations: Implications for Pressure Management, Capacity, and Risk Mitigation. 10th International Conferance on Greenhouse Gas Control Technologies, GHFT-10. Energy Procedia 2011, 4, 4283-4290.

Clark, C. E.; Veil, J. A. Produced Water Volumes and Management Practices in the United States; National Energy Technology Laboratory: Argonne National Laboratory for the U.S. Department of Energy, Office of Fossil Energy, 2009.

Department of Energy, National Carbon Sequestration Database and Geographic Information System In Technologies: Carbon Sequestration, NETL: 2012.

Earles, M. J.; Halog, A., Consequential life cycle assessment: a review. International Journal of Greenhouse Gas Control 2011, 16, 445-453.

Evans, A.; Strezov, V.; Evans, T. J., Assessment of sustainability indicators for renewable energy technologies. Renewable and Sustainable Energy Reviews 2009, 13, 1082-1088.

Finnveden, G.; Hauschild, M. Z.; Ekvall, T.; Guinee, J.; Heijungs, R.; Hellweg, S.; Koehler, A.; Pennington, D.; Suh, S., Recent developments in life cycle assessment. Journal of Environmental Management 2009, 91, 1-21.

Fischbeck, P. S.; Gerard, D.; Mccoy, S. T., Sensitivity analysis of the build decision for carbon capture and sequestration projects. Greenhouse Gases Science and Technology 2012, 2, 35-45.

Frick, S.; Kaltschmitt, M.; Schroder, G., Life cycle assessment of geothermal binary power plants using enhanced low-temperature reservoirs. Energy 2010, 35, 2281-2294.

Gale, J., Geological storage of CO_2: What we know, where are the gaps, and what more needs to be done. Energy Conversion and Management 2004, 29 (9-10), 1329-1338.

Gulf Coast Carbon Center, Brine-Formation Database. Horvorka, S. D., Ed. Bureau of Economic Geology and Jackson School of Geosciences: 2003.

Harto, C. B.; Veil, J. A. Management of Water Extracted from Carbon Sequestration Projects; 2011.

Harvey, D. Aquaculture Data; US tilapia imports, value by selected sources. http://www.ers.usda.gov/Data/Aquaculture/TilapiaImportsValue.htm.

Holloway, S., Underground sequestration of carbon dioxide- a viable greenhouse gas mitigation option. Energy 2005, 30, 2318-2333.

Jasinski, S. M. Potash; Mineral Commodity Summaries; USGS: 2011.

Jeppesen, T.; Shu, L.; Keir, G.; Jegatheesan, V., Metal recovery from reverse osmosis concentrate. Journal of Cleaner Production 2009, 703-707.

Khan, S. J.; Murchland, D.; Rhodes, M.; Waite, T. D., Management of Concentrated Waste Streams from High-Pressure Membrane Water Treatment Systems. Environmental Science and Technology 2009, 39, 367-415.

Kharaka, Y. K.; Hanor, J. S. Deep Fluids in the Continents: I. Sedimentary Basins; 2003; pp 499-540.

Kostick, D. S. Salt; Mineral Commodity Summaries; USGS: 2011.

Lund, J. W., Direct Utilization of Geothermal Energy. Energies 2010, 1443-1471.

Maulbetsch, J. S.; DiFilippo, M. N. Cost and value of water use at combined-cycle power plants; California Energy Commission: 2006.

Mitchell, G. F.; Hunt, C. L.; Richardson, W., Prediction of Brine Application for Pretreatment and Anti-Icing. Journal of the Transportation Research Board 2004, 129-136.

Mondal, S.; Wickramasinghe, S. R., Produced water treatment by nanofiltration and reverse osmosis membranes. Journal of Membrane Science 2008, 322, 162-170.

ND Department of Health Guidelines for the Use of Oilfield Salt Brines for Dust and Ice Control; North Dakota Department of Health: 2009.

Nicot, J. P., Evaluation of large-scale CO_2 storage on freshwater sections of aquifers: An example from the Texas Gulf Coast Basin. International Journal of Greenhouse Gas Control 2008, 2, 582-593.

Pate, R.; Klise, G.; Wu, B., Resource demand implications for US algae biofuels production scale-up. Applied Energy 2011, 88, 3377-3388.

Puder, M. G.; Veil, J. A. Offsite commercial disposal of oil and gas exploration and production waste: availability, options, and costs; Argonne National Laboratory, 2006.

Ripley, K. Smooth road ahead: A rise in local funding and a new bill will lead to steady growth; Report 23411b; IBISWorld: 2011; pp 1-34.

Rutqvist, J.; Birkholzer, J. T.; Tsang, C.-F., Coupled reservoir-geomechanical analysis of the potential for tensile and shear failure associated with CO_2 injection in multilayered reservoir-caprock systems. International Journal of Rock Mechanics & Mining Sciences 2008, 45, 132-143.

Singh, A.; Nigam, P. S.; Murphy, J. D., Renewable fuels from algae: An answer to debatable land based fuels. Bioresource Technology 2011, 102, 10-16.

Stewart, D. R., Developing a New Water Resource from Produced Water. In 13th International Petroleum Environmental Conference, National San Antonio, TX, 2006.

Sullivan, E. J.; Chu, S.; Pawer, R. J., Effects of Concentrate Disposal and Energy Recovery on Costs for Treatment of Water Produced During Geologic Sequestration. In Tenth Annual Conference on Carbon Capture & Sequestration, Pittsburgh, Pennsylvania, 2011.

Thayer, R. I.; Neelameggham, R., Improving the Electrolytic Process for magnesium Production. Journal of Management 2001, 15-17.

Tripp, T. G., Production of magnesium from Great Salt Lake, Utah USA. Natural Resources and Environmental Issues 2009, 15 (1: Saline Lakes Around the World: Unique Systems with Unique Values), 54-61.

U.S.G.S., Produced Waters Database. Management, C. E. D., Ed. 2002.

Udo de Haes, H. A.; Heijungs, R.; Suh, S.; Huppes, G., Three strategies to overcome the limitations of life-cycle assessment. Journal of Industrial Ecology 2004, 8, 19-32.

Veil, J. A.; Puder, M. G.; Elcock, D.; Redweik, R. J. J. A white paper describing produced water from production of crude oil, natural gas, and coal bed methane; US DOE, NETL: 2004.

Ventyx, Velocity Suite Mapping Module. Ventyx, Ed. Atlanta, 2012.

Voutchkov, N., Overview of seawater concentrate disposal alternatives. Desalination 2011, 205-219.

Zamagni, A.; Guinee, J.; Heijungs, R.; Masoni, P.; Raggi, A., Lights and shadows in consequential LCA. International Journal of Life Cycle Assessment 2012, 17, 904-918.

Zenz House, K.; Harvey, C. F.; Aziz, M. J.; Schrag, D. P., The energy penalty of post-combustion CO_2 capture & storage and its implications for retrofitting the U.S. installed base. Energy & Environmental Science 2009, 2, 193-205.

Zheng, L.; Apps, J. A.; Zhang, Y.; Xu, T.; Birkholzer, J. T., On mobilization of lead and arsenic in groundwater in response to CO_2 leakage from deep geological storage. Chemical Geology 2009, 268, 281-297.

Chapter 3: Assessment of Carbon Dioxide Utilization as a Carbon Management Strategy for Coal-Fired Power Plants

3.1 Introduction

Carbon dioxide capture and sequestration (CCS) is a currently deployable technology that can provide immediate reductions in CO_2 emissions from point-sources such as coal-fired power plants (CFPP). Despite evidence that delays in large-scale greenhouse gas (GHG) emissions reductions will make it increasingly difficult to avoid dangerous temperature rises, the scale-up of supporting infrastructure for CCS remains mostly unrealized in the United States (US).[1-2] None of the most promising geologic storage sites are online due to both a lack of financial commitment from power plants and a lack of regulations mandating CO_2 sequestration.[3] Consequently, there is an urgent need for alternative means of large-scale CO_2 storage. Unlike sequestration, where CO_2 is regarded as a financially and legally costly waste, CO_2 utilization manages captured CO_2 as a commodity. In addition to being a source of carbon, CO_2 has physical properties that make it marketable for a range of uses. The carbon mitigation potential of a CO_2 utilization application depends on how the CO_2 is captured, transported, and used to produce a product, and on the product life cycle.[4] The reduction in radiative forcing that could be realized through national adoption of CO_2 utilization also depends on the rate of carbon capture adoption, and on the growth and size of both CO_2 and product markets.[5] Presently, the scale up of CO_2 utilization has not been explored. In this analysis, we develop utilization adoption scenarios using a market assessment approach and compare scenario outcomes using life cycle assessment. Our research seeks to promote strategic growth in national CO_2 consumption and sequestration by understanding the carbon mitigation potential for current and emerging CO_2 utilization applications in the US.

Carbon dioxide utilization is often disregarded as a solution to climate change because global industrial CO_2 consumption is estimated to be 115[5] million tonnes (Mt) CO_2/y, while the US electric power sector emits 2 gigatonnes (Gt) CO_2/y alone.[6] This consumption estimate was derived from steady-state market assessments of large industrial applications. However, reviews of the status of research and development in CCS and utilization reveal that there are a number of applications for CO_2 that are deployable in the near future.[5,7-11] Emerging industrial and technology applications include enhanced gas recovery, coal bed methane recovery,[5,7] grid-scale compressed air energy storage (CAES),[8] enhanced photosynthesis and algae biofuel production,[9] and the production of dimethyl ether (DME), organic and inorganic carbonate, olefins, and polymers.[10-12] Centi et al and Song et al include emerging applications in their estimates of possible global CO_2 consumption by assessing stoichiometric equations. They estimate that the yearly market for CO_2 could reach 1-10 Gt if CO_2 is used as the carbon feedstock for all synthetic liquid fuel, organic chemical and material production.

The objective of this study is to characterize the spatial and temporal CO_2 emission profiles of emerging economic activities that could utilize or sequester CO_2 in the US. We quantify these profiles for scenarios where CFPP built after 2020 are co-located with saline aquifer sequestration projects, and CFPP built prior to 2020 are retrofitted based on the demand for CO_2 from CO_2 utilizing economic activity. We use a market-based analysis to determine the number

of retrofitted CFPP that could direct their CO_2 to markets that demand CO_2. We use life cycle assessment (LCA) to quantify the cumulative radiative forcing (CRF) that could be avoided by 2065 for three CO_2 utilization adoption scenarios. Finally, we conduct a geographic information system (GIS)-based spatial analysis to identify regional barriers.

This paper focuses on the potential for emerging and mature utilization applications to reduce GHG emissions. To our knowledge, this is the first paper to develop an approach for quantifying the potential of CO_2 utilization from power plants as a carbon mitigation strategy. The advantage of our approach is that it provides a methodology for comparing policy decisions at different temporal and spatial scales. The disadvantage of our approach is that our upper-bound scenario, which provides a context for our results, is dependent on market production projections that require a higher data quality than is currently available. Despite this limitation, our analysis provides the most comprehensive characterization of scale up scenarios for CO_2 utilization applications to date.

3.2 Methods

3.2.1 Applications

Current and emerging uses of CO_2 were selected for this analysis based on (1) the stability and growth of their production output in the United States, (2) a non-zero residence time for the captured/utilized CO_2, (3) data availability for modeling the CO_2 utilization process and life cycle, and (4) the potential for demand to reach at least one Mt of CO_2 annually by 2065 (details are discussed in Section 1 of Appendix A2). One Mt is roughly a quarter of the CO_2 that could be captured at a medium sized (400 MW) CFPP with today's CCS technology. These selection criteria led to the exclusion of a number of applications, including carbonated beverage-, dry ice-, CO_2 fire extinguisher-, olefin-, organic carbonate-, dimethyl ether-, algae biodiesel-, and decaffeinated coffee-production, and of compressed air energy storage with CO_2 buffering, inert gas welding, refrigeration, and enhanced photosynthesis (Section 2 of Appendix A2). However, we included nine of these applications in our sensitivity analysis. The selection criteria led to the inclusion of the six applications discussed in this paper: EOR, enhanced gas recovery (EGR), enhanced coal bed methane recovery (ECBM), urea synthesis, methanol synthesis, and fly ash mineralization. The production of inorganic carbonates through the mineralization of fly ash is a lab-scale technology that uses CO_2 to convert waste ash into calcium and magnesium carbonate, chemically fixing CO_2 in the process.

3.2.2 Market Potentials

Market potentials for products derived from CO_2 utilization applications were modeled by projecting future product demand in the US from 2020 out to 2065. A recent overview of carbon capture technology found 2020 to be a feasible starting data for carbon capture at CFPP.[1] With full recognition of uncertainty about changes in CO_2 emissions over long time periods, we selected a mid-range time-horizon of 45 years for our evaluation. We believe this is an appropriate time-horizon because alternative manufacturing processes typically take between 10 and 50 years to reach full economic potential. Because of uncertainty about long-range market projections and about year-to year fluctuations in fossil-fuel-sensitive markets, we carried out sensitivity analysis by sampling from likely value ranges in key parameters including starting production volumes. We used the most recent available production volumes as starting points for current markets, and obtained starting production volumes for emerging technologies based on estimates in the literature (Section S3 of Appendix A2).

3.2.3 Technology Diffusion Scenarios

Three CCS diffusion scenarios presented by Sathre and Masanet (2012) provide our bounding estimates for captured CO_2 supply: (1) a business as usual scenario (BAU) without CCS; (2) an upper-bound scenario where 75% of CFPP built before 2010 and retired after 2040 are gradually retrofitted with CCS by 2100, and where all new CFPP built after 2020 perform CCS; and (3) a more conservative scenario where only new CFPP built after 2020 perform CCS.[13] In this analysis CCS refers to the use of monoethanolamine-based carbon capture with the subsequent geologic sequestration of CO_2 in saline aquifers.

Based on variation of assumptions, we developed upper-bound, moderate, and conservative technology diffusion scenarios to generate a set of alternative time profiles for the annual mass of CO_2 that could be directed to CO_2 utilization. In the upper-bound scenario, the total economic potential of CO_2 utilization for each application is reached by 2020. For the moderate scenario, our goal was to develop a scenario that arises from the constraints of our present-day world. Our assumptions were therefore based on what expert opinion offers as the 90th percentile upper confidence limit of what is possible (the conservative scenario targeted at the 50th percentile, assuming CCS is adopted at CFPP). Scenario differences in the rate and upper limits on technology diffusion for each CO_2 application are included in Table 1 and discussed in Section S4 of Appendix A2. Due to data limitations, an engineering cost analysis was outside the scope of this study. As a result we did not quantify the full economic potential of CO_2 utilization applications based on detailed product values.

Table 1. Percent of product markets met by CO_2 utilization applications, increasing from 2020 to 2065, in the conservative, moderate, and upper-bound scenarios. *The values for mineralization represent the percent of available fly ash in the United States.

CO2 utilization application	conservative	moderate	upper-bound
enhanced oil recovery (EOR)	1% to 15%	10% to 50%	100%
enhanced gas recovery (EGR)	1% to 1.5%	1 to 3%	10%
enhanced coalbed methane recovery (ECBM)	1% to 1.5%	1 to 3%	10%
urea synthesis	1% to 5%	1% to 10%	100%
methanol synthesis	1% to 5%	1% to 10%	100%
fly ash mineralization*	1% to 10%	1 to 20%	100%

3.2.4 Life Cycle Assessment

We used a consequential life cycle assessment (C-LCA) approach to quantify energy use and emissions from life cycle stages associated with each CO_2 utilization application. Consequential LCA allowed us to determine *marginal* changes in CO_2 emissions that result if current processes are replaced with processes that use captured CO_2 (Figure S1 of Appendix A2).

Life cycle stages associated with captured CO_2 production include: coal mining and transportation, the construction and operation of CFPP, the construction and operation of CO_2 capture equipment, and the transportation and storage of CO_2. These stages are modeled using the method described by Sathre and Masanet (2012).[13] Further details on the LCA methodology used in this study can be found in Section S1 of Appendix A2.

3.2.5 Temporal and Spatial Analysis

We used the method developed by Sathre and Masanet (2012) to quantify cumulative radiative forcing (CRF) in units of $MW \cdot s/m^2$ to account for the time-dependence of climate impacts.[13] Cumulative radiative forcing represents the energy accumulated or removed from the earth's energy balance over a specified time step.

For comparison and evaluation, we converted annual GHG emissions time profiles for CO_2 utilization life-cycle scenarios into CO_2 equivalents (CO_2e) emissions. We used an atmospheric decay function to determine the mass of CO_2 in the atmosphere over time (cumulative GHG

emissions) (*Equation S17*). To convert these mass time profiles into concentration time profiles, we used the molecular mass of air, 28.95 $gmol^{-1}$, and the mass of the atmosphere, 5.148 x 10^{21} g.[14] We then converted concentration profiles to radiative forcing (*Equation S18)*. To estimate CRF for each year in a time profile we integrated the time-dependent radiative forcing (F_{CO2}) over that period using one-second time steps. This method is described in Zetterberg (1993) and was updated in the IPCC 1997 report (Section S5 of Appendix A2).[15-16]

Maps were generated in ArcGIS for specific years from 2020 to 2065 to show changes in the spatial distribution of CCS adoption and geologic CO_2 utilization. Feasible transportation distances of 50 and 155 miles (used in the LCA) were plotted around all power plant locations.[17] These spatial buffers allowed us to identify power plants that are near gas, oil, and unmineable coal bed formations suitable for CO_2 utilization. The CO_2 storage capacity of each geologic formation was modeled using average storage estimates from the United States Carbon Utilization and Storage Atlas, Fourth Edition.[18] We assumed that retrofitted power plants inject CO_2 at a constant rate until 75% of the formation's storage capacity is reached. At that time, power plants would then redirect their CO_2 to the next available option within 155 miles.

We developed a spreadsheet model to estimate the year and order in which CO_2 capture adoption occurred at CFPPs. Power plants were ranked based on their nameplate capacities and their predicted retirement dates, with the largest power plants adopting CO_2 capture first. A plant was retrofitted when its annual mass of captured CO_2 increased the CO_2 supply curve to match the growing demand curves for CO_2 (Section S6 of Appendix A2).

3.3 Results

Based on the compilation of simulations described above, the annual mass of captured CO_2 diverted to various utilization applications reaches estimated levels of 910, 240, 110 Mt/y for the upper-bound, moderate, and conservative scenarios (Figure 1a). When the constraints of carbon capture adoption are introduced, as seen in Figure 1b, the upper-bound mass is limited by the rate of CCS deployment in the first 28 years of the 45-year evaluation period and by the projected rate of power plant retirements and energy efficiency improvements at power plants in the last 15 years of the evaluation period. As a result, the cumulative mass of CO_2 redirected towards CO_2 utilization is 19% less than the estimated market potential for CO_2 consumption in the upper-bound scenario. This indicates that the upper-bound on CO_2 demand from emerging utilization markets could surpass the supply of captured CO_2 from CFPP out to 2045. In all scenarios, enhanced gas recovery accounts for a majority of the cumulative captured CO_2 consumption (62 to 76%), followed by urea production (4 to 11%), fly ash mineralization (4 to 10%), enhanced coal bed methane recovery (9 to 11%), enhanced oil recovery (5% to 9%), and methanol production (1 to 3%) (Figures S6).

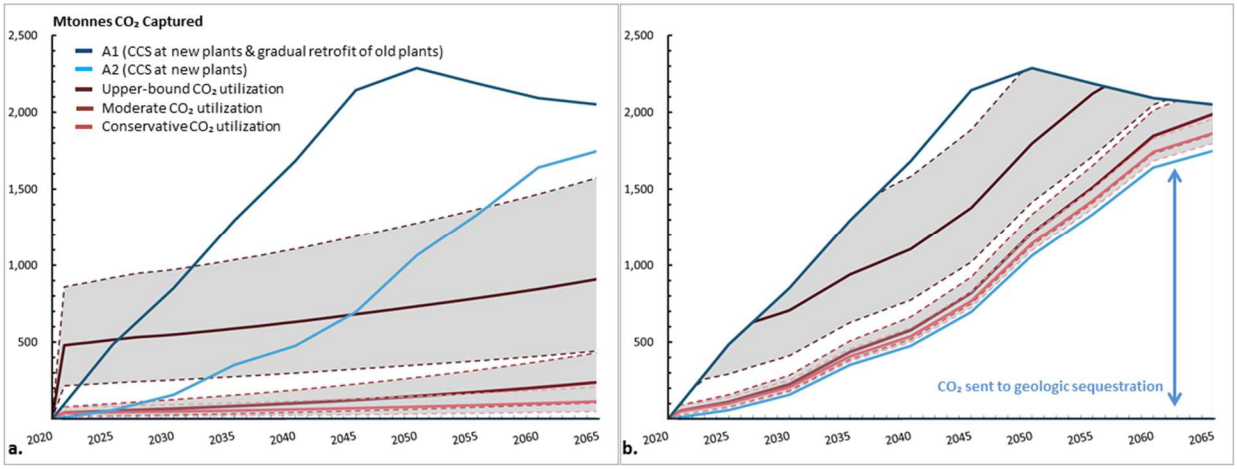


Figure 1. Time profiles of the captured CO_2 that could be supplied to utilization or sequestration options. (a) Shows the demand (red) for captured CO_2 vs. the supply (blue) of captured CO_2 from CCS deployment scenarios A1 and A2. (b) In our scenarios, CO_2 captured at new power plants is sent to geologic sequestration (light blue). CO_2 from older power plants is captured and utilized at a capacity determined by CO_2 market demand scenarios (red) and by feasible carbon capture technology diffusion (dark blue). Upper and lower dashed lines represent high and low CO_2-to-product conversion factors, respectively.

The mass of product that could be produced from a specific power plant with carbon capture can be estimated given a power plant's initial CO_2 emissions, the CO_2 capture efficiency and energy penalty, and the utilization technology's efficiency (Figure S2 and S3). Figure 2 illustrates the results of the C-LCA for six applications that convert one $MtCO_2$ into product (9.8 Mbarrels crude oil; 43.9 Mft^3 natural gas; 17.9 Mft^3 coalbed methane; 0.38 Mt methanol; 0.91 Mt urea; 2.2 Mt mineralized fly ash). Urea production using captured CO_2 and renewably-sourced hydrogen provides the greatest reduction in life cycle GHG emissions per tonne of utilized CO_2 (0.7 tCO_2 avoided per tonne of captured CO_2). For urea and methanol synthesis, the release of captured CO_2 over the product life cycle led to a 28% and 49% decrease in the avoided GHG emissions, respectively. Improving the conversion efficiency of CO_2 to product through technology

advancements or CO_2 recycling during manufacturing could mitigate these losses. No avoided GHG emissions were allocated to EOR or ECBM because it was assumed that these processes would not directly displace other production methods. Enhanced oil-, gas-, and coalbed-methane-recovery and fly ash mineralization provide CO_2 storage on geologic time scales and were therefore assumed to fully contain CO_2 during the 45 year evaluation time period. The significance of this assumption is explored in our sensitivity analysis (Table S3).

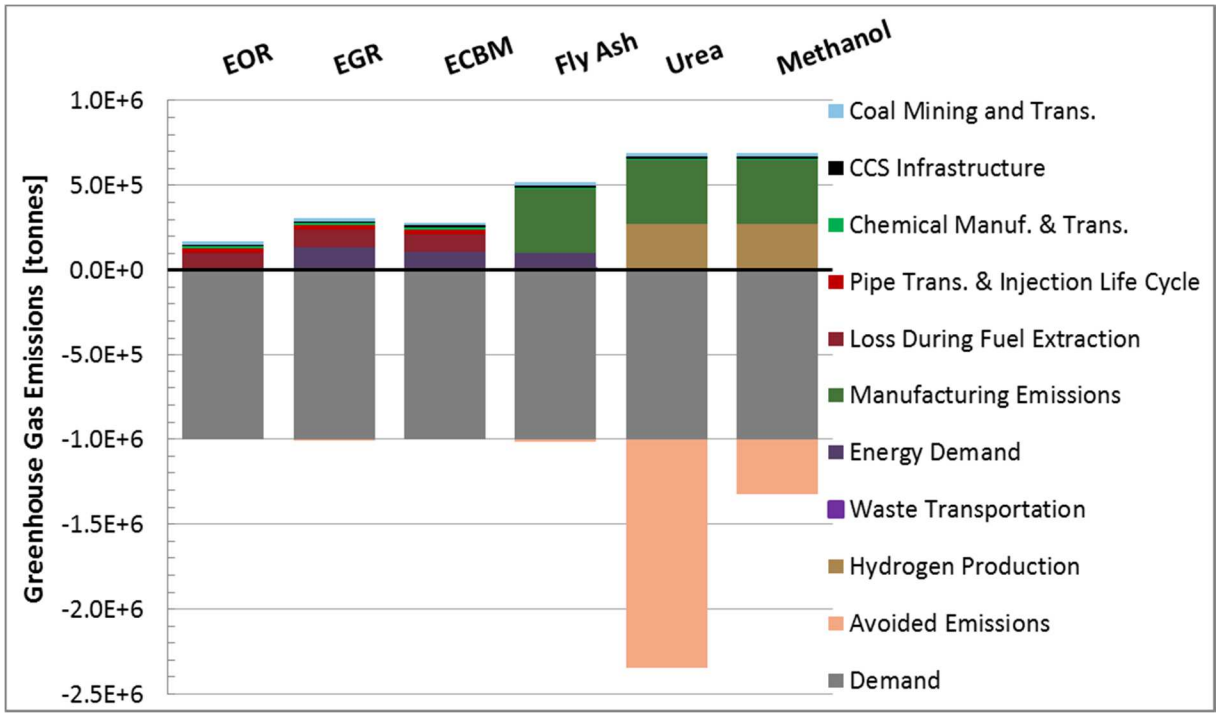


Figure 2. Marginal GHG emissions for CO_2 utilization applications shown for one million tonnes of utilized CO_2. Negative emissions are not emitted into the atmosphere.

Our forecasts indicate that by 2065, the cumulative supply of CO_2 to utilization applications can reach 25.4, 5.6, and 3.2 Gt for the upper-bound, moderate, and conservative scenarios; the cumulative net reduction in GHG emissions can reach 17.3, 3.7, and 2.1 $GtCO_2e$, respectively. For comparison, Pacala and Socolow (2004) have estimated that CCS could provide at least one stabilization wedge (one wedge decreases GHG emissions by 0.02 GtC each year [0.07 $GtCO_2$]) to avoid 25 GtC (92 $GtCO_2$) over 50 years.[20]

The resulting marginal change in the atmospheric mass of GHG emissions is shown in Figure3a. In our moderate scenario for CO_2 utilization, the cumulative reduction in mass reaches 2 Gt in 2065, equivalent to taking twenty-three 400 MW or eight 1000 MW CFPP offline in 2020. Compared to a scenario with only geologic sequestration at new power plants, scenarios with upper, moderate, or conservative CO_2 utilization could further reduce the atmospheric mass of GHG emissions by 59%, 14%, or 8% and cumulative radiative forcing (CRF) by 104%, 18%, or 11% (Figure 3a,b). The rate of carbon mitigation slows in the upper-bound scenario, reflecting the decrease in captured CO_2 production from CFPP. The upper-bound scenario maintained a higher avoided CRF than the stabilization wedge and CCS adoption at new power plants through the 45 year study period, because the early avoided emissions contributed radiative forcing long after their point of emission (Figure 3b). When we assume that the time profiles of avoided GHG

emissions from our upper-bound scenario and from the wedge continue at the same rate after 2065, the avoided CRF of our upper-bound scenario exceeds the stabilization wedge before falling behind the wedge in 2070.

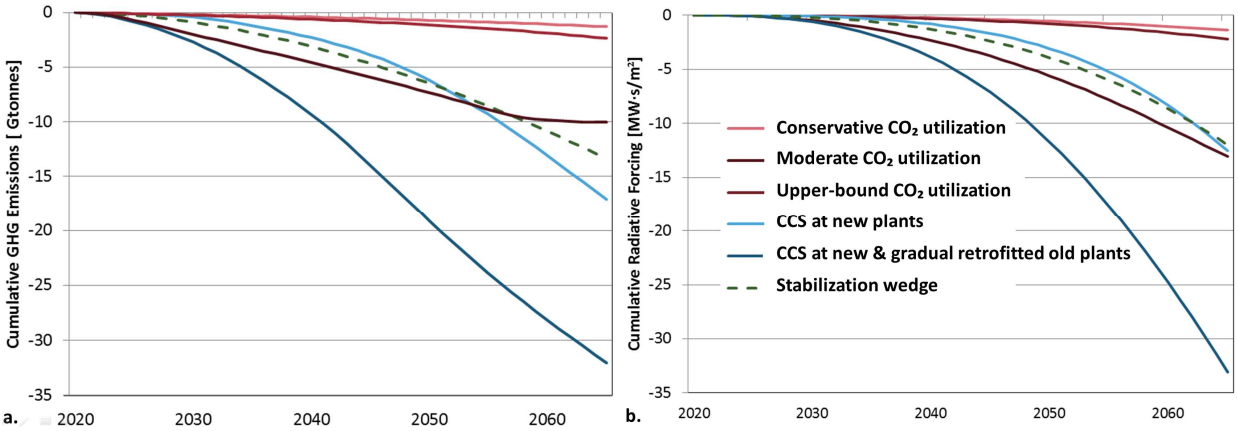


Figure 3. Marginal change in (a) cumulative GHG emissions [Gt CO_2e] and (b) cumulative radiative forcing [MW s/m^2] from a BAU case (zero on the y-axis).

3.3.1 Spatial Analysis

If CO_2 utilization experiences conservative or moderate growth, there would be enough demand for CO_2 to retrofit ten or twenty-six of the largest CFPP in the US by 2065, respectively (Figure S7). These values rose to 108 and 169 CFPP, when we retrofitted power plants based on age and not nameplate capacity (Figure S8). Figure 4 shows that most of the twenty-six largest CFPP are located in the North and Southeast. Oil fields suitable for storing CO_2 are found throughout the US, while suitable gas fields are clustered in the Northeast and unmineable coalbeds are spread throughout the Southern, Central, and Western US. Three of the twenty-six largest US CFPP are more than 155 miles from available formations. One of these plants, a 740 MW CFPP in North Carolina, exceeded the storage capacity of its nearby formations in 2048. In the absence of a national CO_2 transportation network, the proximity of oil, gas, and coalbed formations will limit the number power plants that can transport CO_2 for use in these formations. In addition, states have unique permitting processes for pipeline transportation. In our moderate scenario, seven power plants would face delays if they were unable to build interstate long-distance pipelines.

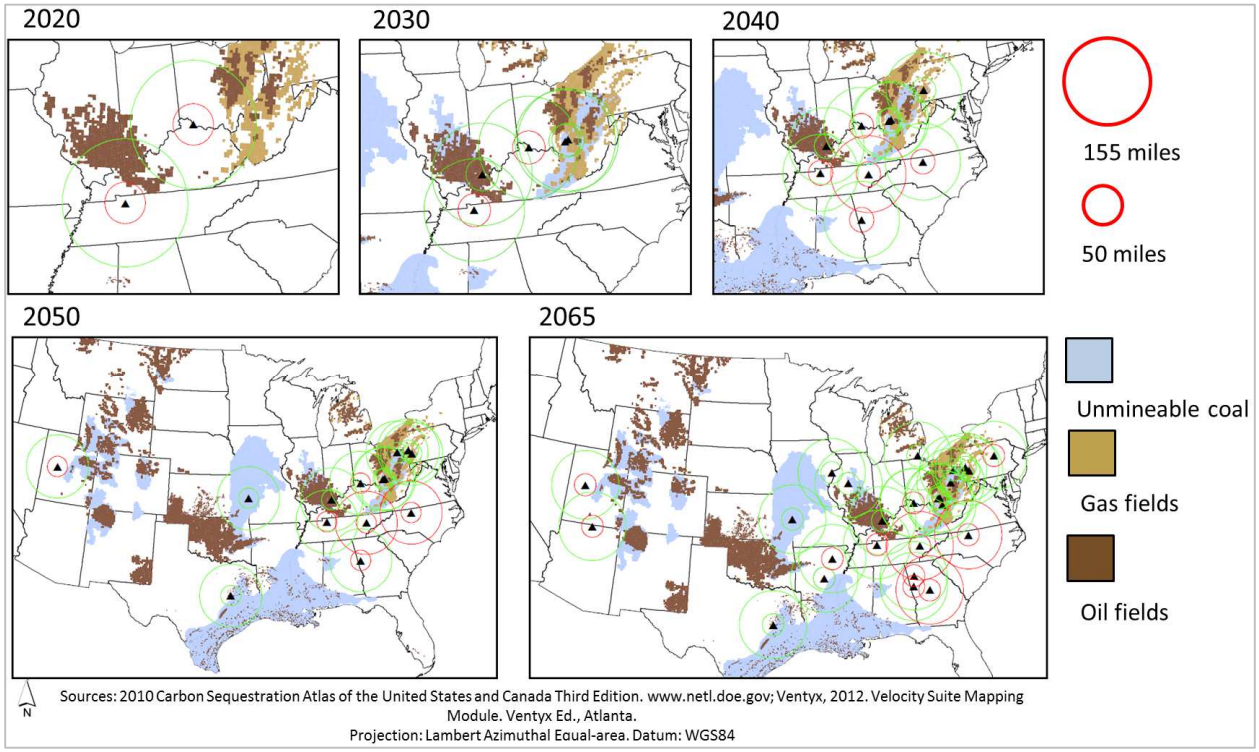


Figure 4. Maps of the spatial distribution of CO_2 supply from 2020 (2 plant) to 2065 (26 plants). CFPP with a nameplate capacity >=15 MW and built before 2020 are retrofitted. Larger CFPP are retrofitted first to match the CO_2 demand of the moderate scenario. A red circle indicates that oil or gas production regions are not within a feasible transportation distance from the power plant.

3.3.2 Sensitivity Analysis

In order to confront the challenges of forecasting how emerging utilization technologies will perform at scale, we performed a sensitivity analysis to evaluate how uncertainty in key variables impacts estimated performance metrics (Section S7 of Appendix A2). The large range in estimated product yields from CO_2 applications had the largest impact on results (Table S3). Low and high CO_2-to-product conversion factors changed the avoided CRF for the moderate scenario by -52% and +69%, respectively. The year in which utilization applications were deployed also plays a key role in carbon mitigation. Delaying the deployment of enhanced gas recovery from 2020 to 2050 resulted in more than a 20% reduction in the avoided CRF for all three CO_2 utilization scenarios. The addition of small-scale applications had a negligible effect on the CRF. Interestingly, dimethyl ether and algae biodiesel synthesis from captured CO_2 were two applications that had large potential market growth, but resulted in negligible life cycle carbon savings. The results of this analysis indicate that technology development will play a significant role in shaping the competitive advantage that CO_2 utilization processes have over current production methods with the same functional output but without CO_2 utilization.

3.4 Discussion

This research contributes the first temporally explicit life cycle assessment of CO_2 utilization options. We use market analysis, technology diffusion scenarios, and spatial assessment to define the bounds for our results. Seventeen CO_2 utilization applications were assessed using this approach. Of the applications that had net negative life cycle GHG emissions, enhanced oil recovery, enhanced gas recovery, enhanced coalbed methane recovery, methanol synthesis, urea synthesis, and fly ash mineralization accounted for at least 1% of the total demand for CO_2. By 2065, total demand grew to 110 Mt/y in our conservative scenario and to 910 Mt/y in our upper-bound scenario. This range is comparable to current estimates for global CO_2 consumption. Enhanced gas recovery accounted for a majority of cumulative CO_2 consumption. Infrastructure and market constraints in our scenarios limited the contribution of emerging technologies to CO_2 sequestration; however, we do assume renewably-sourced hydrogen will be available for methanol and urea production.

The results of our LCA and sensitivity analysis indicate that losses of CO_2 during fossil fuel extraction can greatly reduce the carbon mitigation potential of EOR, EGR, and ECBM as CO_2 utilization applications. Improvements to CO_2-fuel separation, CO_2 recycling, and fugitive emission reduction at oil and gas fields can lower these losses. Methanol synthesis, urea synthesis, and fly ash mineralization for CO_2 utilization offer modest carbon savings. Improving CO_2-to-product conversion efficiencies and reducing energy consumption for hydrogen production and fly ash mineralization will improve these savings.

Our results show that CO_2 utilization has the potential to reduce cumulative GHG emissions by 17 $GtCO_2eq$ and the atmospheric mass of GHG emissions by 10 $GtCO_2$ by 2065 if started in 2020. Unfortunately, this is only 3% of the GHG reductions roughly needed to stabilize atmospheric CO_2 at 500 ppm. Previous studies focus on the large gap between the CO_2 emissions of power plants and the potential CO_2 demand of utilization. However, since CCS is expected to diffuse slowly across the US, regional development of CO_2 markets could provide a near term solution for early adopters.

This research highlights critical areas for future market and engineering cost analyses to investigate. Large power plants that adopt carbon capture must be paired with CO_2 utilization and sequestration options that provide storage for decades and are not prone to fluctuations in availability. While enhanced oil and gas recovery has the potential to utilize and sequester CO_2 at large scales, demand for oil and gas is prone to fluctuations. Competition for oil and gas formations and low fossil fuel demand periods may drive CFPP to either retire early or adopt alternative methods of CO_2 utilization and sequestration. At a local level, the adjacency of 20 of the largest CFPP with oil and gas fields will likely enable the cheap production of fossil fuels through enhanced recovery. It should be noted that this may create a conflict for the next generation of power plants wishing to adopt CO_2 utilization, since CO_2 is in direct competition with natural gas as a feedstock for the production of urea and methanol.

Other interesting relationships appeared when we assessed small-scale CO_2 applications. Alternative fuels such as algae biodiesel and dimethyl ether that could be produced through CO_2 utilization may not be able to compete with petroleum products in the transportation sector if oil

produced from EOR is cheap. Similarly, CO_2 may not be able to compete with EOR-sourced petrochemicals as a feedstock for the synthesis of polymers and olefins. Our analysis suggests that using CO_2 for urea production would displace conventional manufacturing methods that use natural gas and that are a large source of CO_2 for consumer products and chemical industries; this may decreasing competition between captured CO_2 and industry-sourced CO_2.

Understanding the significance of these relationships requires further market and engineering cost analyses to characterize the effect of policy on the cost-competitiveness of CO_2 utilization with current and alternative methods of product production. Nevertheless, the use of spatially and temporally explicit life cycle assessment in CO_2 utilization research is essential for supporting decision-making at local and national scales.

4. References

(1) Hazeldine, R.S. Carbon Capture and Storage: How green can black be? Science, **2009**, 325, 1647-1652.

(2) Herzog, H.J. Scaling up carbon dioxide capture and storage: From megatons to gigatons. Energy Econ. **2011**, 33, 597–604.

(3) Szulczewski, M.L.; MacMinn, C.W.; Herzog, H.J.; Juanes, R. Lifetime of carbon capture and storage as a climate-change mitigation technology. Proc. Natl. Acad. Sci. **2012**, 109, 5185–5189.

(4) Von der assen, N.; Jung, J.; Bardow, A. Life-cycle assessment of carbon dioxide capture and utilization: avoiding the pitfalls. Energy Environ. Sci. **2013**, 6, 2721-2734.

(5) Chapter 7: Mineral carbonation and industrial uses of carbon dioxide, by Marco Mazzotti; IPCC special report on carbon dioxide capture and storage; Intergovernmental Panel on Climate Change, **2005**; https://www.ipcc.ch/pdf/special-reports/srccs/srccs_chapter7.pdf.

(6) Emissions of greenhouse gases in the United States 2009; Report no. DOE/EIA-0573; US Energy Information Administration, **2009**; http://www.eia.gov/ (accessed February 12, 2014).

(7) Song, C. Global challenges and strategies for control, conversion and utilization of CO_2 for sustainable development involving energy, catalysis, adsorption and chemical processing. Catal. Today. **2006**, 115, 2–32.

(8) Oldenburg, C. M.; Pan, L. Utilization of CO_2 as cushion gas for porous media compressed air energy storage. Greenhouse Gas Sci. Technol. **2013**, 3, 124–135.

(9) Hunt, A.; Sin, E.; Marriott, R.; Clark, J.; Generation, Capture, and Utilization of Industrial Carbon Dioxide. ChemSusChem. **2010**, 3, 306-322.

(10) Olah, G.A.; Prakash, G.K.S.; Goeppert, A. Anthropogenic Chemical Carbon Cycle for a Sustainable Future. J. Am. Chem. Soc. **2011**, 133, 12881–12898.

(11) Centi, G.; Perathoner, S. Opportunities and prospects in the chemical recycling of carbon dioxide to fuels. Catalysts Today. **2009**, 148, 191-205.

(12) Markewitz, P.; Kuckshinrichs, W.; Leitner, W.; Linssen, J.; Zapp, P. et al. Worldwide innovations in the development of carbon capture technologies and the utilization of CO_2. Energy Environ. Sci. **2012**, 5, 7281-7305.

(13) Sathre, R.; Masanet, E. Long-Term Energy and Climate Implications of Carbon Capture and Storage Deployment Strategies in the US Coal-Fired Electricity Fleet. Environ. Sci. Technol. **2012**, 46, 9768–9776.

(14) Trenberth, K.E.; Smith, L. The Mass of the Atmosphere: A Constraint on Global Analyses. J. Clim. **2005**, 18, 864–875.

(15) Zetterburg L. A method for assessing the expected climatic effects from emission scenarios using the quantity radiative forcing; Swedish Environmental Research Institute, Stockholm, **1993**.

(16) An Introduction to Simple Climate Models Used in the IPCC. Second Assessment Report; IPCC Technical Paper II, Intergovernmental Panel on Climate Change, **1997**; http://www.ipcc.ch (accessed 02/13/2012).

(17) Ventyx, **2012**. Velocity Suite Mapping Module. Ventyx Ed., Atlanta.

(18) Carbon Storage NATCARB; www.netl.doe.gov (accessed July **2013**).

(19) The United States Carbon Utilization and Storage Atlas, Fourth Edition. National Energy Technology Laboratory. **2012**.

(20) Pacala, S.; Socolaw, R. Stabilization wedges: solving the climate problem for the next 50 years with current technologies. Science. **2004**, 305, 968-972.

Chapter 4: Spatially-explicit life-cycle impact assessment approach for stationary proton exchange membrane fuel cell systems in the United States.

Adapted with permission from:

A Total Cost of Ownership Model for Low Temperature PEM Fuel Cells in Combined Heat and Power and Backup Power Applications. Wei, Max; Lipman, Timothy; Mayyas, Ahmad; Chien, Joshua; Chan Shuk Han; Breunig, Hanna; Stadler, Michael; McKone, Thomas; Beattie, Paul; Chong, Patricia; Collela, Whitney; James, Brian. *Lawrence Berkeley National Laboratory Report.* LBNL-6772E, October 2014.

The goal of this dissertation is to support the acceleration of clean energy technology development by providing information about the regional variation of impacts and benefits resulting from plausible deployment scenarios. In this chapter, an approach and supporting model are developed to estimate the climate change and human health damages that may result from the adoption of proton exchange membrane (PEM) fuel cell systems (FCS) in commercial buildings in urban areas of the United States. The model was developed as part of a total cost of ownership (TCO) analysis of PEM fuel cells in combined heat and power (CHP) applications. The versatility of this approach, and the model supporting it, allows it to be applied in TCO of other technologies intended to be used for combined heat and power applications in commercial buildings in the United States.

4.1 Introduction

4.1.1 Fuel Cells as an Emerging Technology

Proton exchange membrane (PEM) fuel cells, which rely on thin polymers as their electrolytes, could play an important role in distributed generation and backup power in the United States (Lipman et al., 2004; Feroldi and Basualdo, 2012). They are characterized by their fast start-up and rapid response to dynamic electricity loads, and by their high power density of ~0.7 W/cm^2 (Mehta and Cooper, 2003). Low temperature PEM fuel cells operate at temperatures less than 90°C. Fuel cells are often thought of as low-carbon, low-criteria-air-pollutant (CAP) technologies because they convert hydrogen to electricity without combustion. However, no study has proven that PEM fuel cells are competitive with current and future energy supply systems from an emissions perspective. Without a supportive hydrogen industry in the United States (US), PEM fuel cells will need equipment onsite to synthesize hydrogen from natural gas. This equipment has non-negligible emissions associated with it. Decision-makers, particularly those involved in writing government support and tax policies, use total cost of ownership (TCO) and emissions analyses to compare alternative distributed generation technologies. Externalities ranging from global warming to mortalities caused by air pollution have been called the "hidden costs" of energy technologies because they are often ignored in total cost of ownership analyses (NRC2010). This research seeks to integrate these hidden costs into the TCO for PEM fuel cells.

A number of papers have performed partial or complete life cycle assessments (LCA) of fuel cell technologies for transportation. Baratto and Diwekar used a life-cycle approach to determine the potential human health and environmental benefit of using solid oxide fuel cells (SOFC) in

heavy-duty trucks that typically use idling diesel engines for non-propulsion applications. A majority of CO_2 life-cycle emissions (92.2%) were attributed to the operation phase of the fuel cell. Non-negligible emissions of oxides of nitrogen (NO_X), carbon monoxide (CO), course particulate matter (PM_{10}), volatile organic compounds (VOC), and oxides of sulfur (SO_X) were produced from manufacturing and from the diesel and system life cycle phases. The subscript on PM indicates the greatest particle diameter in micrometers that is captured in the particle measurement. Despite these emission, the study determined that fuel cell-based auxiliary power units (APUs) would generate lower emissions of major air pollutants (reductions from 64% to 99%) when they replaced idling diesel engines.

Elgowainy et al. used the Greenhouse Gas, Regulated Emissions, and Energy Use in Transportation (GREET) model, developed by Argonne National Laboratory, to conduct an LCA of the fuel-cycle for stationary phosphoric acid fuel cells and molten carbonite fuel cells in a hypothetical hospital, large office building, and warehouse in Chicago and Los Angeles. Their study found that buildings using fuel cells for combined heat and power (CHP) or for combined heat, hydrogen, and power (CHHP) contributed less CO, PM_{10}, and NO_X emissions than buildings using natural gas-fired internal combustion and the California-grid electricity mix. The ability of the fuel cells to produce a carbon offset varied depending on the carbon intensity of the displaced generation systems and on the energy efficiency of the fuel cells.

In order to assess PEM fuel cells as an emerging technology for CHP applications, a life cycle model must be capable of integrating data specific to the targeted buildings and regions identified by fuel cell developers. This dissertation provides the first spatially-explicit approach for completing an inventory and impact assessment of the operation phase of PEM fuel cell systems for stationary CHP applications. A supporting excel model was developed to quantify the environmental and human health damages caused by PEM fuel cell systems in commercial buildings. The model incorporates: (1) regional electricity grid emissions, (2) city-specific building-energy consumption and load data, and (3) county-specific benefit-of-abatement factors that determine the environmental and human health benefits of avoiding marginal emissions emitted at ground and smoke stake heights. Fuel cells displace grid-based electricity and some fraction of heating demand fuel, as specified by the user of the model. Externalities to be valued include morbidity, mortality, impaired visibility, recreational disruptions, material damages, agricultural and timber damages, and global warming.

The model accepts inputs from databases on building power and heat consumption, and on power generators that are updated every few years. This flexibility allows the model to be updated as electricity grids and buildings change. The model currently uses fuel consumption and emission factors from 2010. Both electricity grids and PEM fuel cell systems are expected to get cleaner over time; the emission factors (tonnes of pollutant per kWh generated) from these systems were adjusted in a sensitivity analysis to understand how the PEM fuel cell technology may compete as a clean technology in the future.

As a case study, the greenhouse gas and human health implications of adopting PEM fuel cell systems in large hospitals and small hotels in Phoenix (AZ), Chicago, (IL), New York City (NY), Houston (TX), Minneapolis (MN), and San Diego (CA) were assessed. These buildings

and cities were chosen because their building heat and power load shapes and the regional electricity and natural gas markets were favorable for fuel cell operation (Wei et al., 2014).

4.1.2 Background

4.1.2.1 Fuel Cell Systems

A fuel cell system consists of the cell stack assembly and the balance of plant (BOP) (Mehta and Cooper, 2003). The cell stack assembly consists of several membrane-electrode assemblies (MEA) comprised of multiple layers of a catalyst coated membrane (CCM), a gas diffusion layer (GDL), bi-polar plates (BPP), an end plate, gaskets, and an MEA frame/seal. The balance of plant is divided into six subsystems (Wei et al., 2014): fuel, air, coolant and humidification, power, controls & meters, and miscellaneous.

4.1.2.2 Electrical Emission Factors

4.1.2.2.1 Marginal emission factors

Electricity from fuel cells would displace energy and associated emissions from local electricity grids, comprised of conventional and renewable generators. Over long periods of time (on the order of decades), a large reduction in demand for grid electricity due to wide-spread fuel cell adoption may lead to the retirement of conventional generators. In this study, only short-term displacement is considered; it is measured using regional marginal emission factors (MEFs). Marginal emission factors measure the GHG and CAP emissions from the last generators to be deployed to meet grid demand. It is difficult to know exactly which generators are operating at the margin, but the set of generators that are deployed to meet electricity demand during high demand periods (commonly called peaker plants) in different regions of the US have been estimated using dispatch models and historical regressions.

Peaker plants are typically the most expensive or dirtiest plants to operate, such as natural gas-turbines and older coal- and natural gas-fired power plants, and are often operated on the margin. This means that they are not operated unless changes in demand warrant their use. Nuclear power plants would not typically be operated on the margin since they are run near continuously. Siler-Evans et al. developed a method for calculating MEFs for eight North American Electric Reliability Corporation (NERC) regions in the US using historical data from the EPA Continuous Emissions Monitoring System (CEMS). CEMS provides hourly data on CO_2, SO_2, and NOx emissions up to the year 2011 from fossil-fueled generators with a nameplate capacity greater than or equal to 25 MW. These regions are on the same spatial scale as power control areas, which estimate the control area over which power plants provide energy to consumers. This study is “the first systematic calculation of MEFs for the US electricity system”, but it is only an estimate since the MEFs do not include imports and exports of energy, or data on nuclear-, renewable-, or small generators. This method was applied in a separate study quantifying the health, environmental, and climate benefits attributed to displaced emissions from wind and solar adoption in Emissions and Generation Resource Integrated Database (eGRID) sub-regions (Siler-Evans et al., 2013). Marginal Emission Factors for all eGRID

regions and seasons are available at http://cedmcenter.org/tools-for-cedm/marginal-emissions-factors-repository/.

Average emission factors (AEF) are commonly used in LCA to determine emissions from electricity grids because they are readily available at regional and state levels. These factors are calculated by dividing the annual emissions of a pollutant by the annual electricity generation from electricity generating units (EGUs) aggregated over a specified spatial area (e.g. state, region, nation).

In this dissertation, MEFs for greenhouse gases GHG (CO_2, CH_4, and N_2O), NOx, and SO_2 were taken from Siler-Evans et al. Unfortunately, a set of marginal emission factors for direct particulate matter emissions (PM_{10} and $PM_{2.5}$) were not identified. However, since a significant fraction of PM from electricity generation comes from reactions of SO_2 and NOx in the atmosphere, having a MEF of zero for direct PM is reasonable as an initial estimate.

4.1.2.2.2 City versus NERC spatial scale

The MEF used in this dissertation are aggregated by North American Electric Reliability Corporation (NERC) region. The NERC is an electric reliability organization (ERO) that was formed to provide coordination support as power companies began to connect and trade generation resources. Buildings receive their electricity from local electric companies that own shares of specific power generators and have set import and export contracts with nearby companies. When a building requires power, it receives it from different generators depending on the time of day, week, and year. Therefore, it is difficult to know exactly which generators are being operated at a given time. Aggregating the data from generators in a large region where generation trading is focused provides a useful estimate when more spatially resolved data is limited. Enough data was available at the NERC regional scale for Siler-Evans et al to develop a set of monthly MEFs.

To understand the uncertainty introduced by this scale discrepancy, local average emission factors were estimated for the cities of Phoenix and Minneapolis. These cities were selected because detailed information on power plant ownership, generation rates, and imports and exports was available on company websites and from a GIS database operated by Ventyx (2012). As an alternative treatment for displaced electricity emissions, local average annual emissions factors (L-AEF) were estimated for these electricity grids (Appendix A2).

4.1.2.3 Marginal Benefit of Abatement:

The benefit of reducing emissions through FCS adoption can be monetized using marginal benefit of abatement (MBA) conversion factors. These factors estimate the damage that a unit of emitted pollutant will cause if released in a specific location ($/tonne), thus explaining their alternative name “damage factors”. The potential damage from a pollutant emission from a given source is estimated by multiplying the mass of emitted pollutant by the MBA factor.

The most widely referenced approaches, presented in Fann et al., Muller and Mendelson, and the National Research Council (NRC2010), estimate the economic costs of human health and

environmental impacts associated with pollutant sources in the United States (Figure 1). In each approach, atmospheric chemistry models and transportation models are used to estimate downwind primary and secondary pollution doses from an original spike or plume of pollutant. For example, SO_2 forms $PM_{2.5}$ (sulfate), and NO is converted to NO_2, which reacts with VOC to form ozone (O_3) and $PM_{2.5}$ (nitrate). Exposure is estimated from a database of receptor populations (humans, materials, crops, timber etc.). Concentration-response (CR) models are then used to convert exposure to damages. This data is paired with economic models to convert impacts like morbidity, mortality, visibility impairment, reduced recreation, lower agricultural and timber yields, and material degradation to dollar values. In all studies, the cost of human health impacts dominated the damages attributed to criteria air pollutants, and these health impacts were largely a result of primary and secondary $PM_{2.5}$.

Brown et al. collected the average MBA factors from each study and found that the monetized damages range from \$1500 to \$80,000 per tonne SO_2, \$370 to \$15,000 per tonne NOx, \$2700 to\$33,000 per tonne $PM_{2.5}$, and \$440 to \$1800 per tonne PM_{10} (Figure 1). Values are given using units of 2005 USD/tonne-pollutant.

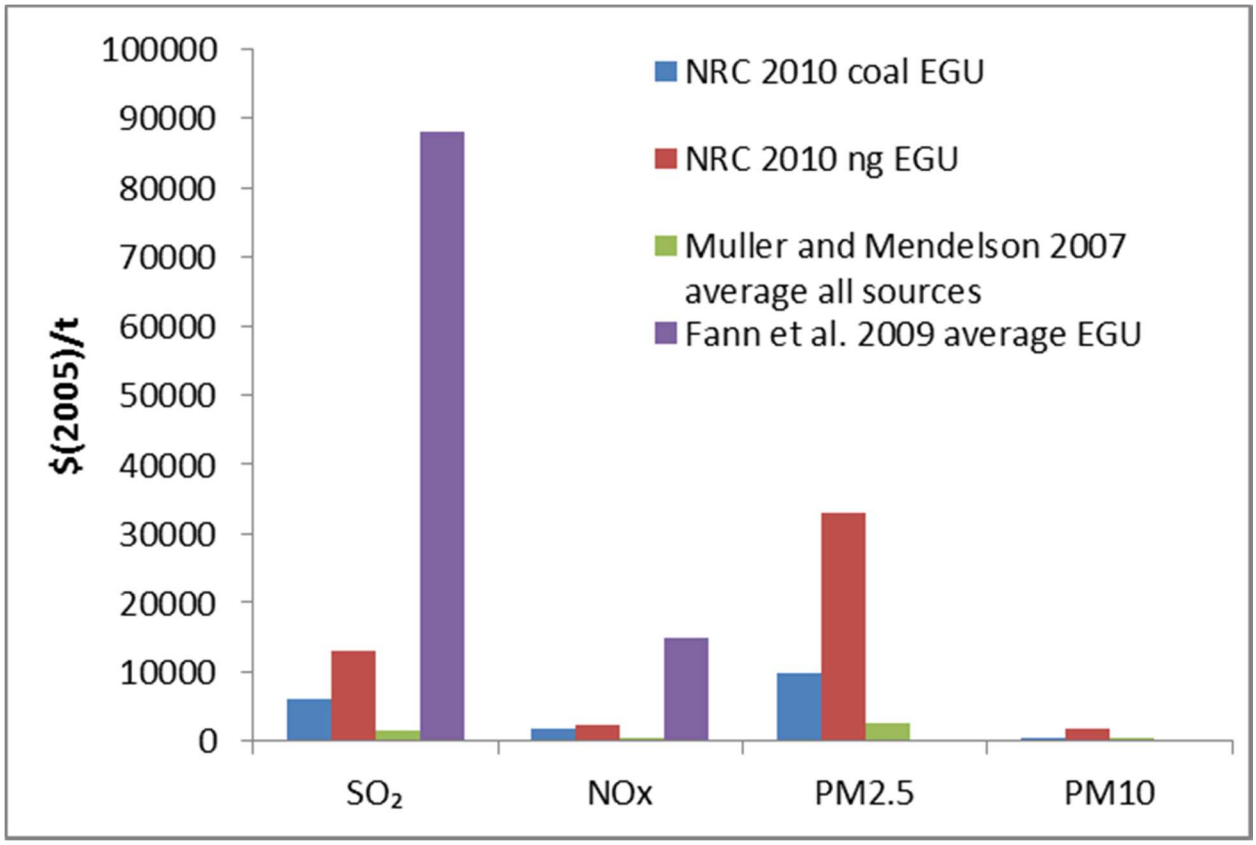


Figure 1. Marginal Benefit of Abatement factors based on three approaches (Brown et al. 2010).

Variations in the MBA factors result from differences in study scope, model decisions, and assumptions, including differences in: (1) the CR function used to estimate mortalities from $PM_{2.5}$ exposure; (2) whether urban or rural areas were modeled separately; (3) the atmospheric model; (4) the type of pollutant sources included; (5) the value of a statistical life (VSL).

(1) The Muller and Mendelson and NRC studies use the CR function developed in Pope et al., while Fann et al. uses the function presented in Laden et al.

(2) Muller and Mendelson modeled urban and rural areas separately.

(3) The values in Figure 1 are grouped based on fuel type, however, the NRC and Fann et al. (represented by the "present analysis" category) studies only consider electrical generation units (EGUs), while the Muller and Mendelson study considers all emission sources.

(4) Both the NRC and Muller and Mendelson studies use the Air Pollution Emission Experiments and Policy Analysis Model (APEEP) model to relate emissions to concentration changes. Fann et al. uses the Community Multiscale Air Quality Response Surface Model (CMAQ).

(5) The value of a statistical life is an economic estimate of individuals' willingness to pay (WTP) to reduce their risk of death (OECD, 2014). In a recent report by the OECD, a VSL of $3 million 2005USD was suggested for studies estimating the costs of emissions from road transportation. MBA factors from the Muller and Mendelson study are significantly lower than those determined in other studies. This difference is largely due to the fact that the VSL used in Muller and Mendelson of $6 million (2000USD) was not applied uniformly, but was differentiated based upon age. The NRC study set their VSL at $6 million and applied it uniformly. The VSL used in Fann et al. is $5.5 million 2000USD, but was adjusted to $6.4 million 2006USD using the EPA standard inflators.[3]

The approach in Fann et al. is currently the default approach used by the US Environmental Protection Agency (EPA). The EPA has continued to update their estimated values, referred to as "benefit per ton estimates" using a computer program called BenMAP. When Fann et al. was undertaken, the EPA was using a VSL estimated based on their estimate that the VSL ranged from $1 million to $10 million 2000USD. Values are now updated for both currency year and income growth using a VSL determined based on 26 VSL studies of $4.8 million 1990USD (APPENDIX A5). The income growth adjustment accounts for the fact that peoples WTP changes as they become wealthier; income growth adjustments are determined by health endpoint groups.

Variation in the MBA factor reflects the challenge of tracking pollution and determining impacts in near and distant populations. This is an important area of research since the stringency of policies curtailing emissions is set based on the level of marginal damages expected (Fann et al.).

[3] A typo in Fann et al. states that the VSL used was $6.2 million. This typo was corrected in a personal correspondence with Charlie Fulcher of the EPA on March 5, 2014.

4.1.2.3.1 APEEP

In this dissertation, a set of MBA factors are calculated using the Air Pollution Emission Experiments and Policy Analysis Model (APEEP). APEEP is designed to calculate and monetize human health and environmental damages associated with SO_2, VOC, NO_X, ammonia (NH_3), fine particulate $PM_{2.5}$, and course particulate PM_{10} emissions from power plants (Muller and Mendelsohn, 2007). Damages include morbidity, mortality, reduced air visibility, and damages to crop and timber yields.

The APEEP model generates data at the county level. To get this data, the authors had to establish a baseline level of damage using pollution levels in 2002. One additional metric ton of pollutant from a specific source was introduced and the change in national damages was measured. This process was repeated for each pollutant at ~10,000 sources, generating a set of marginal damages. Damages factors were calculated for effective emission heights: "ground level: (less than 250 meters off the ground), medium smoke stack sources (<500 m), and tall smoke stack sources (>500 m). Concentration-response (CR) models were used to convert exposure to damages. This data was paired with economic models to convert morbidity, mortality, visibility impairment, reduced recreation, lower agricultural and timber yields, and material degradation to dollar values.

In this dissertation, human health impacts determined using the APEEP model are monetized using a VSL of $6 million and are adjusted using a discount rate of three percent. The approach presented in Muller and Mendelson is chosen for two reasons. First, there is a great deal of uncertainty regarding MBA factors, and the approach presented in Muller and Mendelson provided the most conservative estimates of the cost of CAP emissions. Secondly, detailed county-level data sets and modeling instructions for APEEP were provided by Thomas McKone of the Lawrence Berkeley National Laboratory. Errors and uncertainty can be introduced into a study by using a "blackbox" modeling platform that limits the user's interactions to simply input and output queries. Having access to the datasets used in the APEEP modeling equations limited this uncertainty.

4.2 Methodology:
4.2.1 Life-Cycle Scope

The life-cycle of a fuel cell system used for CHP applications includes pre-manufacturing, manufacturing, operation and maintenance, and end-of-life phases. Energy and material inventories were developed for several sizes of PEM fuel cell systems for a TCO model in Wei et al. (2014). The PEM fuel cell systems were sized to operate in CHP applications ranging from 1 to 1000 kilowatts-electricity (kWe) over a lifespan of 15 years. Wei et al. estimate that over 90% of both GHG and CAP emissions from the FCS life cycle are attributed to the operation phase. This dissertation presents the complimentary approach and model developed to understand how the placement of PEM fuel cell systems into buildings in the US would displace greenhouse gas (GHG) and criteria air pollutant (CAP) emissions from heating systems and electricity grids. Unlike an attributional LCA, which calculates the impacts attributed to a product or process's entire life cycle, a consequential LCA is used to calculate the marginal change in impacts caused by the life cycle as it displaces established economic activities that provide the same services.

The scope of this life-cycle component is therefore limited to components of the operation phase of PEM fuel cell systems (Figure 2). The contributions of installation and maintenance of the FCS to emissions are assumed to be negligible. Previous LCAs have shown that the upstream life-cycle phases of natural gas, petroleum, and coal production contribute non-negligable CO_2, SOx, and NOx emissions (Jermello et al,; Burnham et al.,). The error of excluding emissions attributed to upstream stages like infrastructure and fuel production varies depending on whether coal is mined using underground or surface techniques, whether natural gas is produced from shale or conventional gas seams, and whether petroleum is produced from crude or oil sand reservoirs. An important future study would identify the sources of heating fuels for commercial buildings in each city and the sources of fuels for electricity generation in each region to understand the upstream consequences of switching from conventional heat and power to fuel cell systems. The goal of this dissertation is to tease out variations in impacts directly associated with spatial heterogeneity and, since fuel production data was not readily available at the city level, this life cycle phase was not included.

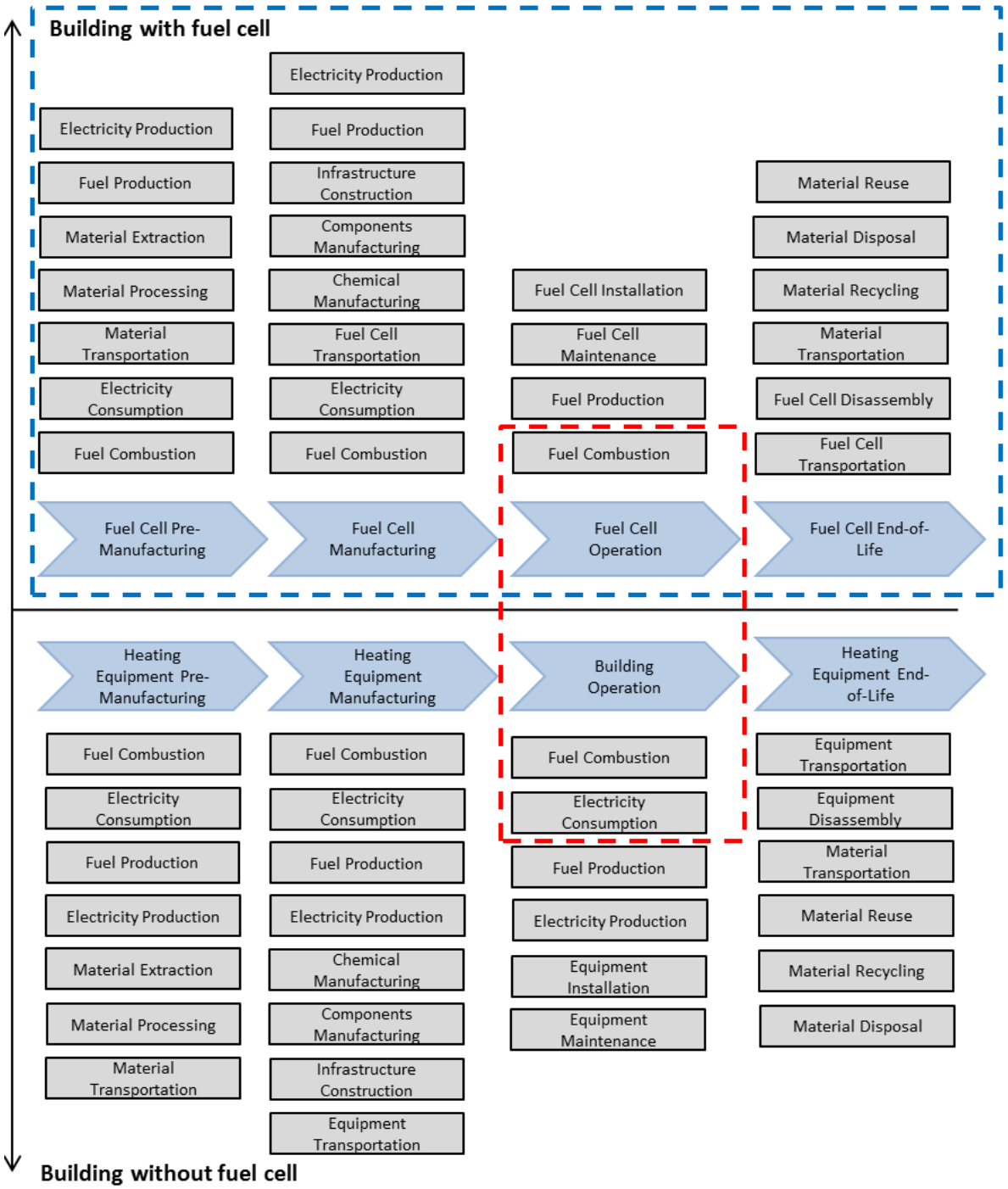


Figure 2. Scope of the life cycle inventory assessment in Wei et al. (blue box) and of the life cycle approach and model in this dissertation (red box). Fuel production includes: fuel extraction, processing, and transportation. Electricity consumption refers to the combustion or use of fuels at the power plant for electricity generation.

4.2.2 Life Cycle Inventory Modeling

The annual consumption of electricity and heating fuels are estimated by region using the 2003 Commercial Buildings Energy Consumption Survey (CBECS) database (for more information about CBECS, see: http://www.eia.gov/consumption/commercial). Annual power and heat provision supplied by a FCS to a specific building type are taken from Wei et al. (Table 1 and Table 2) and coupled with data from CBECS to determine the avoided consumption of grid-electricity, natural gas, propane, fuel oils, and district heating. The FCS are sized to effectively meet the needs of the building using power and heat load-shape data generated by DER-CAM. Four 250 kW FCS are needed to meet power requirements in one large hospital, while one 50kW FCS could feasibly supply energy needs in one small hotel. Electricity and fuel consumption are converted to mass of emissions using emission factors (EF).

Table 1. Power and heat provision scenarios for large hospitals in seven cities. Values are in kWh.

1 MW FC system- Hospital							
	Phx	Mnpls	Chicago	NYC	Miami	San Diego	Houston
P	8111893.92	6702691.52	7116573.68	6989153.12	NA	2079694.00	8251068.00
Hs	2688992.92	3632798.42	3466709.50	4101952.33	NA	528840.67	2811567.83
Hw	139578.50	229907.00	215320.67	209528.75	NA	75516.00	150697.92

Table 2. Power and heat provision scenarios for small hotels in seven cities. Values are in kWh.

50 kW FC system- Small Hotel							
	Phx	Mnpls	Chicago	NYC	Miami	San Diego	Houston
P	366962.78	331553.02	331959.34	302332.84	NA	NA	347820.30
Hs	23307.31	174742.97	135869.02	135869.00	NA	NA	0.00
Hw	76953.57	127112.48	118971.08	116075.40	NA	NA	83071.00

4.2.2.1 Emissions from Fuel Cells

Direct emission factors (EF) for CO_2, CH_4, N_2O, CO, NO_X, SO_X, PM_{10} and VOC reported in recent literature on fuel cells provide emissions intensities in tonne per kWh units (Table 3). The value for CO_2 is an average derived from Colella et al. and the Fuel Cell Fundamentals book. All other values are taken from Colella et al. The total mass of emissions emitted from the fuel cell over a year is calculated by multiplying each EF by the power (P) provided by the fuel cell.

Table 3. Fuel cell emission factors in metric ton per kWh (Colella et al., ; Fuel Cell Fundamentals,).

Emission in g/kWh	Value
CO_2	543
NO_x	0.0069
SO_x	Neglible
PM_{10}	Neglible
VOC	Neglible
CH_4	0.51
CO	0.017
N_2O	0.06

4.2.2.2 Emissions from Buildings

Emission factors used in the baseline scenario are listed in Table 4. CO_2, CH_4, and N_2O emissions for natural gas (HHV from 975 to 1100 Btu/scf), propane, and middle distillate fuel oils are taken from Appendix H of the 2011 EPA guide on reporting emissions, instructions to Form EIA-1605, revised in 2014. PM_{10}, $PM_{2.5}$, NO_X, and SO_X emissions for fuel oils are taken from Table 1.3-1 and 1.3-4 of an EPA report, AP42 External Combustion Sources on fuel oil combustion, Section 1.3. PM_{10}, NO_X, and SO_X emissions for natural gas are taken from Table 1.4-1 and 1.4-2 of the same report, Section 1.4 on natural gas combustion. Space heating equipment efficiency is assumed to be 80% (100% in model runs discussed in Appendix A3, Section 4).

The emissions of NO_X, SO_X, and PM from propane are set to zero. District heating is assumed to be a product of natural gas combustion, however, the power and heat from this natural gas is not counted as a displaced emission because it is assumed that it would occur regardless of fuel cell adoption. The effect of this assumption on results is explored in the sensitivity analysis (Section 3.3).

Table 4. Regional marginal emission factors for electricity and emission factors for heating fuels. CO_2 represents CO_2eq for the electricity sector. An explanation of the variable codes is provided in Appendix A3.

Emission Factors	CO2	CH4	N2O	NOx	SOx	PM10	PM2.5
Fuel Cell							
	EF_f1	EF_f2	EF_f3	EF_f4	EF_f5	EF_f6	EF_f7
	543.00	0.56	0.07	0.01	0	0	0
Natural Gas							
	EF_ng1	EF_ng2	EF_ng3	EF_ng4	EF_ng5	EF_ng6	EF_ng7
	181.05	0.02	3.41E-04	0.15	9.21E-04	0.01	0
Fuel Oil							
	EF_o1	EF_o2	EF_o3	EF_o4	EF_o5	EF_o6	EF_o7
	249.60	0.01	0.01	0.34	1.73	0.09	0.05
Propane							
	EF_p1	EF_p2	EF_p3	EF_p4	EF_p5	EF_p6	EF_p7
	209.71	6.82E-06	6.82E-06	0	0	0	0
District Heating							
	EF_dh1	EF_dh2	EF_dh3	EF_dh4	EF_dh5	EF_dh6	EF_dh7
	0	0	0	0	0	0	0
Electricity							
	EF_e1	EF_e2	EF_e3	EF_e4	EF_e5	EF_e6	EF_e7
Minneapolis	834.29	0	0	1.09	2.11	0	0
Phoenix	486.13	0	0	0.32	0.18	0	0
Chicago	731.00	0	0	0.94	3.29	0	0
San Diego	486.13	0	0	0.32	0.18	0	0
NYC	489.00	0	0	0.32	0.55	0	0
Houston	526.60	0	0	0.32	0.40	0	0
National	609.00	0	0	0.66	1.32	0	0

4.2.2.3 Original Fuel Consumption in Commercial Buildings

Table 5. Table of constants.

E_{Total}	Total energy consumption
E_E	Electricity consumption
E_{NG}	Natural gas consumption
E_{FO}	Fuel oil consumption
E_W	Energy to water heating end use
E_S	Energy to space heating end use
E_C	Energy to cooling end use
E_{DH}	District heating consumption
E_P	Propane consumption

Buildings are characterized by size, primary use, and location. The two commercial building types examined are large hospitals (>=200,000 sq. ft floor space), and small hotels (<50 sq. ft floor space); these building types are chosen because their power and heating loads and local energy markets allowed for cost-effective operation of the fuel cell (Wei et al., 2014). Floor space size divisions are chosen to match the size breaks used in Wei et al., which took building sizes from the National Renewable Energy Laboratory (NREL) study described in Deru et al.

Data on energy and fuel consumption (electricity, natural gas, and fuel oil) are taken from the 2003 Commercial Buildings Energy Consumption Survey (CBECS, 2014) database. Data can be queried at http://buildingsdatabook.eren.doe.gov/CBECS.aspx.

The reported annual energy consumption by regional and building type was frequently larger than the sum of the reported energy consumption by electricity, natural gas, and fuel oils:

$$E_{Total} > E_E + E_{NG} + E_{FO} \qquad \textit{Equation 1}$$

This is because E_{Total} includes energy provided by district heating (E_{DH}) and propane (E_P). Unfortunately, CBECS does not list exact values for these two categories. To fill this data gap, the energy from district heating is estimated from an EIA report that gave district heating per building per region (EIA, accessed 2014). Values are scaled to 2013 using a scaling ratio of total floorspace in 2013 divided by total floorspace in 1999 for commercial buildings (82.9/67 in Gft^3). CBECS values are scaled to 2013 using a scaling ratio of total floorspace in 2013 divided by total floorspace in 2003 for commercial buildings (82.9/71.7 in Gft^3). CBECS data is scaled from population-region to city-scale using the following scaling ratio: 2010_Population_City/2010_Population_Region.

The 2010 populations for cities, states, and regions are taken from 2010 census data. Population-regions divide the nation into nine segments (Figure 3). The cities included in this study are located in six different segments: Pacific; Mountain; West South Central; West North Central; East North Central; Mid-Atlantic.

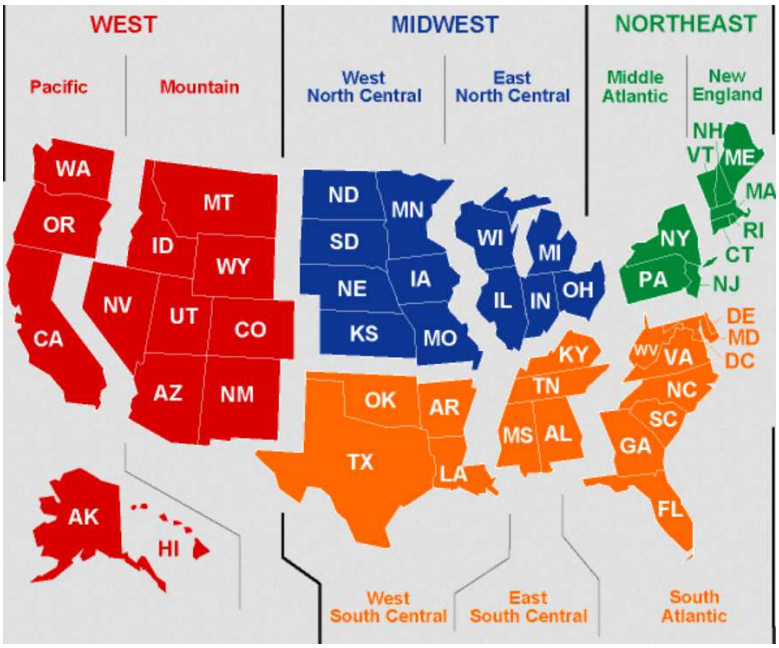


Figure 3. Nine census divisions used as population-regions in CBECS (figure acquired from http://buildingsdatabook.eren.doe.gov/CBECS.aspx).

Values for district heating are compared to (E_{Total} - E_E - E_{NG} - E_{FO}), and the minimum value is used in this study. The minimum value is chosen to avoid exceeding E_{Total} and as a conservative estimate since the emissions associated with district heating are set to zero in the baseline scenario. Then, the remaining total energy consumed in the building is allocated to propane so that:

$$E_{Total} - E_E - E_{NG} - E_{FO} - E_{DH} = E_P \qquad \textit{Equation 2}$$

4.2.2.4 Original Fuel End use in Commercial Buildings

An allocation scheme is developed to match fuel consumption to end use for each building and region.

a. Initially, it is assumed that 90% of energy provided by natural gas (E_{NG}) is used for water heating (E_W) and space heating (E_S). [This seems a very reasonable assumption based on data from California http://energyalmanac.ca.gov/naturalgas/residential_use.html -- and because CA is a mild climate for space heating]
b. It is assumed that 100% of energy from district heating and fuel oils (E_{DH} and E_{FO}) are used for heating.
c. The remaining fraction of heating is assumed to be met with electricity so that:
$$E_{W+} E_{S-} 0.9*E_{NG} - E_{FO} - E_{DH} = E_E \qquad \textit{Equation 3}$$

i. Electrical energy consumed by the building is allocated to lighting, computer, and other purely electrical end uses. In cases where there is not enough electrical energy to also meet Equation 3 (Minneapolis Large Office), it is assumed that propane (E_P) is used for heating.
d. The fraction of natural gas supplied to heating, assumed in step (a) above, is reduced in cases where 90% of E_{NG} exceeds the buildings water and space heating demands ($E_{W+} E_S$).
e. It is assumed that all cooling is met with electricity.

This approach provides values for the annual average consumption of natural gas, electricity, fuel oil, district heat, and propane for cooling, water heating, and space heating. The fraction of heat provided by each of the different fuel types is shown in Figure 4 for large hospitals and in Figure 5 for small hotels. Natural gas is the dominant heating fuel in the US in both large hospitals and small hotels. District heating and fuel oils are commonly used heating fuels in large hospitals. Following natural gas, electricity is used in small hotels to power a significant portion of heating equipment. It is important to note that these fractions are not representative at the building level, but at the city level. Most likely, one fuel would be used to heat a building during regular demand periods. The fractions for large hotels, small offices, and large offices are included in Table A1 of Appendix A3. Fractions allocating heat to space or water heating can be determined using this method, but are not used since more detailed building load shape data were available in Wei et al.

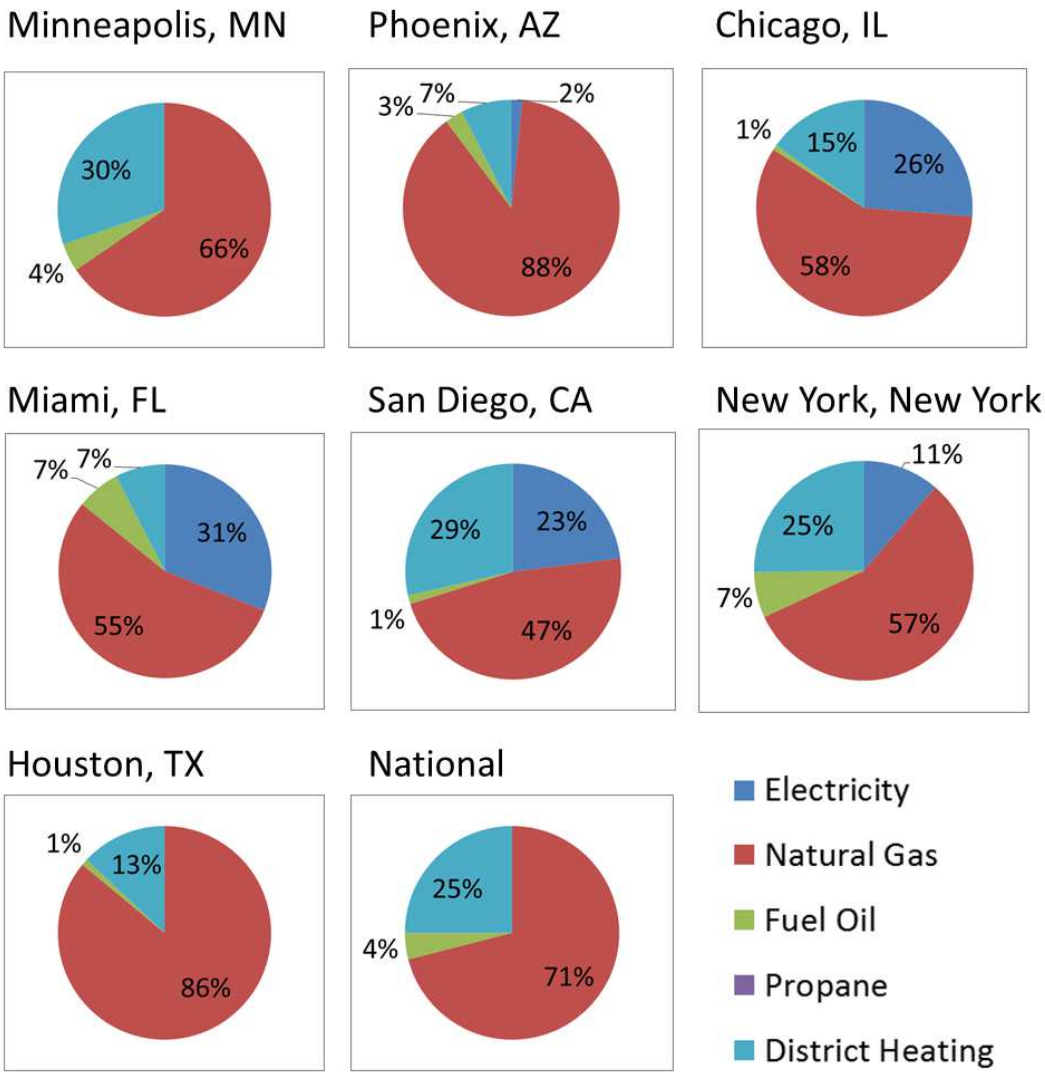


Figure 4. Percentage of heating in large hospitals met by specific heating fuel.

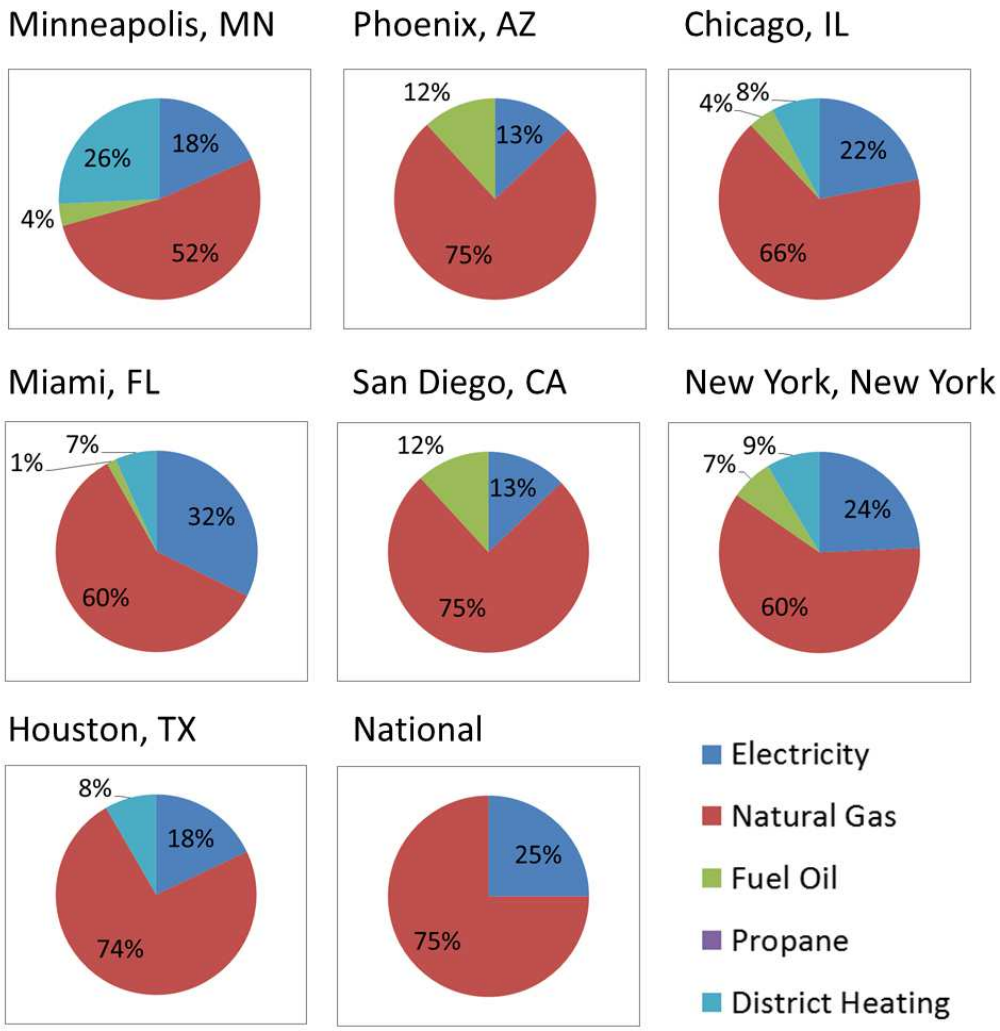


Figure 5. Percentage of heating in small hotels met by specific heating fuel.

4.2.2.5 Emissions from Electricity Grid

Stationary fuel cells could provide electricity and heat to commercial buildings in different cities in the United States. Electricity from fuel cells would displace energy and emissions from local electricity grids, comprised of fossil-fueled and renewably-fueled generators. Over long periods of time (on the order of decades), a large reduction in demand for grid electricity may lead to the retirement of conventional generators. Only short-term displacement is considered in this study. Regional marginal emission factors (MEF) are used to measure the avoided CO_2, SO_2, and NOx, emissions from displaced marginal generators, listed in Table 4 (Siler-Evans et al.). Background on these MEF is provided in Section 4.1.2.

4.2.3 Life Cycle Impact Assessment

Emissions from the fuel cells and the heating equipment in the buildings are modeled as ground-level emissions and are converted to net damages using APEEP county-specific ground-level conversion factors (Table 6) (see Section 4.1.3 for further details on this model). Emissions from the electricity grid are modeled using effective stack-height conversion factors (Table 7).

Table 6. Ground-level marginal benefit of abatement in dollars per ton (2000 dollar values). VSL of 6 million dollars.

State	County	Ammonia (NH3)	Particulate Matte PM2.5	Nitrogen Oxides (Nox)	Sulfur Dioxide (SO2)	Volatile Organic Compounds (VOC)	Particulate Matter PM10
Arizona	Maricopa County	2205	11035	2333	4448	1156	1677
Minnesota	Hennepin County	27427	28905	6870	12628	3327	7688
Illinois	Cook County	337926	70039	766	9516	7298	10236
New York	New York County	30703	117234	5666	27346	12201	16973
Texas	Harris County	5410	26793	3644	11845	2724	3170
California	San Diego County	54444	40880	197	33139	4392	7432

Table 7. Effective stack-height-level marginal benefit of abatement in dollars per ton (2000 dollar values). Points sources with height >250 m and <500 m. VSL of 6 million dollars.

State	NH3	PM2.5	Nox	SO2	VOC	PM10
Arizona	919	1615	606	1521	277	281
Minnesota	1699	2791	975	3071	405	512
Illinois	9665	4934	880	3375	619	727
New York	7386	8232	479	3462	963	1214
Texas	764	2228	819	1500	339	356
California	6038	4968	399	3461	648	1013

Greenhouse gases including CO_2, CH_4, and N_2O are converted to CO_{2eq} using 100 year global warming potential (GWP) factors of 1, 21, and 310, respectively (IPCC, 2007). Then, emissions are monetized by assuming a social cost of carbon (SCC) of \$44/tCO_{2eq}. Suggested values for the social cost of carbon, provided by the Interagency Working Group on Social Cost of Carbon, United States Government, range from \$5 to \$55/tCO_2 for use in regulatory analysis. An

intermediate value of $37/tCO$_2$ (USD 2007) for 2015 is selected and adjusted for inflation to get ~$44/tCO$_2$.

Finally, the total benefit of adopting FCS at the city-level is calculated by multiplying the number of buildings estimated to be in the specific size range for hospitals and hotels by the per-building benefit from GHG, indirect CAP, and direct CAP. These three values are calculated using the equations listed in Section 2.4 and APENDIX A3. The number of buildings per building type in a specific city is estimated from CBECS data. Building numbers are scaled from population-region to city-scale using a scaling ratio: 2010_Population_City/2010_Population_Region.

The 2010 populations for cities, states, and regions are taken from the 2010 census data.

4.2.4 National Average

The model is rerun using representative data for the average US grid and the average large hospital and small hotel to assess the importance of using spatially-explicit data, as opposed to national averages. Data used in the model to represent the national average can be found in Tables 8-10.

Table 8. Average national marginal benefit of abatement ($/ton) (2000 USD) queried from APEEP model. VSL of $6 million dollars.

Source	Ammonia (NH3)	Particulate Matter PM2.5	Nitrogen Oxides (Nox)	Sulfur Dioxide (SO2)	Volatile Organic Compounds (VOC)	Particulate Matter PM10
Ground	8053	7226	761	3626	754	1072
Stack (>250 & <500)	3933	3775	656	2702	499	563

Table 9. Average Annual US GRID emission factors (kg/MWh) (eGRID2012 2009 Data; Siler-Evans et al.).

	NOX	SO2	CO2	CH4	N2O
Average US Grid EF	0.65	1.47	562.67	0.01	0.01
Average US Grid MEF	0.66	1.32	609.00		

Values in Tables 8 and 9 combine to give a national factor of $0.007/kWh for SO_2 and $0.001/kWh for NOx, giving a total factor of $0.008/kWh. In other words, generating one kWh in the US causes 0.8 cents worth of damages on average. These values are compared to those calculated in Machol et al. 2013 in the sensitivity analysis.

Using the method described in Section 2.2.2.2, it was determined that the average large hospital supplies its heating demand with the following mix of fuels: 71% natural gas, 4% fuel oil, and 25% district heating. The average small hotel supplies its heating demand with the following mix of fuels: 75% natural gas and 25% electricity.

Table 10. Average national building fuel use.

Building Type	Sample Size	# Buildings Represented	Floorspace [sq ft]	Fuel Use [BBTU/yr]				End Use [BBTU/yr]		
				Electricity	Natural Gas	Fuel Oil	Major Fuels	Heating	Cooling	Water Heating
Large Hospitals	179	2,543	1,438,250,171	131,391	148,136	8,113	367,931	144,377	28,691	64,534
Small Hotels	28	10,902	280,291,450	161,715	9,427	0	25,599	3,695	1,795	8,902

4.2.5 Sensitivity Analysis

Fuel cells will be introduced into dynamic regional energy systems that are governed by local, state, and national policies and energy markets (see Chapter 1). In this analysis, the sensitivity of CO_2, CH_4, and N_2O, and criteria air pollutants NO_X, SO_2, PM_{10}, and $PM_{2.5}$ emission offsets to changes in fuel cell efficiency, heat provision, and emission rates, and to changes in electricity grid emission rates are explored. A time step of one year is used.

The social cost of carbon (P_{CO2}), emission factors (EF) from electricity grids, heating fuels, and fuel cells, and the heat provided by the fuel cell (Hs and Hw) are varied to assess the effectiveness of fuel cells to abate greenhouse gases ($\$_{GWP}$) in dynamic energy systems. (Equation 4).

$$\$_{GWP}=(P_{CO2})*[(CO2_{elec}+CO2_{fuel}-CO2_{fcell})+ (CH4_{elec}+CH4_{fuel}-CH4_{fcell})*21+(N2O_{elec}+N2O_{fuel}-N2O_{fcell})*310]$$

Equation 4

where P_{CO2} is the cost of carbon [$/t$CO_2$]. Global warming potential conversion factors for CH_4 and N_2O are 21 CO_2eq/CH_4 and 310 CO_2eq/N_2O, respectively.

To assess the effectiveness of fuel cells to abate direct onsite fuel emissions ($\$_{onsite}$), the marginal benefit of abatement conversion factors (D), emission factors, and fuel cell heat provision are varied (Equation 5).

$$\$_{Onsite} = (CO2_{fuel}-CO2_{fcell})*D_{G1}+ (CH4_{fuel}-CH4_{fcell})*D_{G2}+(N2O_{fuel}-N2O_{fcell})*D_{G3}+ (NOx_{fuel}-NOx_{fcell})*D_{G4}+(SOx_{fuel}-SOx_{fcell})*D_{G5}+ (PM10_{fuel}-PM10_{fcell})*D_{G6}+(PM2.5_{fuel}-PM2.5_{fcell})*D_{G7}$$

Equation 5

where D is the damage factor, or marginal benefit of abatement, for one tonne of a specific pollutant [$/t] at the ground level (subscript "G"), at the regional level (subscript "R") or at the county level (subscript "L").

As seen in Equation 6, the marginal benefit of abating electricity grid emissions ($\$_{indirect}$) is proportional to the marginal benefit of abating electricity (D_{elec}) in $/kWh. Primary PM_{10} and $PM_{2.5}$ from electricity generators are not included in the baseline scenario because a complete set of marginal primary PM emission factors were not identified. While it is understood that the majority of damages occur to secondary PM emissions, the significance of excluding indirect primary PM emissions is assessed in the sensitivity analysis. This is achieved by calculating the marginal benefit of abatement using a set of average PM emission factors and then adding this dollar value to the baseline estimate.

$$\$_{Indirect} = P*D_{elec}$$ *Equation 6*

4.3 Results

4.3.1 Monetized environmental and human health impacts

The following results are for a scenario where FCS provide power, space heating and water heating at the annual generation rates determined in Wei et al. (Table 11). Impacts are grouped into three categories: (1) avoided global warming potential; (2) avoided damages due to direct emissions of CAPs; (3) avoided damages due to indirect emissions of CAPs. All six cities would experience a positive net benefit from adopting FCS in small hotels and large hospitals. Phoenix and San Diego would not, however, realize a positive climate benefit from FCS adoption. The primary contributor to benefits varied by building and location, with indirect CAP emissions dominating benefits in places like Chicago and San Diego, and direct CAP emissions dominating in places like New York City. Greenhouse gas emissions and indirect CAP emissions had comparable contributions in Minneapolis and Houston. The largest annual benefit from city-wide deployment occurred in New York City and Chicago, valued at $31.8 million and $29.2 million, respectively.

Table 11. Monetized marginal environmental and human health impacts of FCS operation scenarios.

City	Building Type	Estimated # Buildings	Electricity [kWh/y]	Space Heating [kWh/y]	Water Heating [kWh/y]	GWP Damages ($44/tCO2) [$/building]	Direct Avoided CAP Damages [$/building]	Indirect Avoided CAP Damages [$/building]	Total Avoided Damages [$/city]
Minneapolis									
	Hospital	9	6702692	3632798	229907	$ 104,477	$ 13,894	$ 105,903	$ 2,018,467
	Small Hotels	96	331553	174743	127112	$ 7,551	$ 1,008	$ 6,097	$ 1,407,011
Phoenix									
	Hospital	23	8111894	2688993	139579	$ (3,521)	$ 3,355	$ 7,352	$ 165,267
	Small Hotels	206	366963	23307	76954	$ (195)	$ 279	$ 342	$ 87,906
New York City									
	Hospital	325	6989153	4101952	209529	$ 13,318	$ 40,642	$ 31,507	$ 27,776,813
	Small Hotels	249	302333	135869	116075	$ 1,947	$ 2,399	$ 1,532	$ 1,463,540
Chicago									
	Hospital	90	7116574	3466709	215321	$ 102,314	$ 2,639	$ 201,040	$ 27,539,376
	Small Hotels	266	331959	135869	118971	$ 5,942	$ 531	$ 9,662	$ 4,291,817
San Diego									
	Hospital	22	2079694	528841	75516	$ (1,994)	$ 838	$ 3,044	$ 41,554
	Small Hotels		NA	NA	NA				
Houston									
	Hospital	69	8251068	2811568	150698	$ 9,249	$ 4,267	$ 13,523	$ 1,865,653
	Small Hotels	163	347820	0	83071	$ 261	$ 62	$ 595	$ 149,480

In Figures 6-8, the national result for a specific building type differs by city as a result of differences in the fuel cell's power and heat provision only.

Avoided GHG emissions were lower for all scenarios except Minneapolis and Chicago when spatial data was used in the model. This indicates that most of the regional grids studied had lower GHG emissions than the average US grid. FCS did not provide carbon savings to large hospitals or small hotels in Phoenix or San Diego (Figure 6). Conversely, large carbon savings occurred in Minneapolis and Chicago.

The adoption of FCS resulted in reduced direct CAP damages in all six cities, with noticeable benefits in Minneapolis and New York City (Figure 7). Avoided damages for hospitals in New York City and Minneapolis were much higher when spatial data was used due to high ground-level MBA factors and high space heating requirements. Direct damages in the San Diego scenario for hospitals were low regardless of whether national or spatial data were used, at $451 and $838, respectively. This is because the power and heat provision possible from fuel cells in large hospitals in San Diego were over 70% less than the amount supplied in other cities.

Both MBA factors and avoided building fuel emissions significantly influenced results. For example, the average small hotel in Chicago uses heating oil while the average small hotel in the nation does not. In Chicago, avoided damages from direct SO_2 emissions were 100x higher when spatial data was used in the small hotel scenario due to higher SO_2 emission from heating oil and a higher city-specific MBA factor for SO_2. On the other hand, direct SO_2 emissions from large hospitals were lower when modeled with Chicago data, but the higher city-specific MBA factor for SO_2 led to comparable model results of $2639 and $2783 for city and national.

Finally, avoided damages due to indirect CAP emissions (from avoided grid electricity generation) were lower for all scenarios except Minneapolis and Chicago when spatial data was used in the model (Figure 8). Surprisingly, the avoided damages associated with FCS adoption in NYC scenario were low. This can be explained by the fact that the marginal emission factors in the NPCC NERC region for NOx and SO_2 are lower than the national average, and the MBA factors for NOx and SO_2 were lower and higher than the national average, respectively. This resulted in a lower damage factor ($/kWh) for NYC than for the national average.

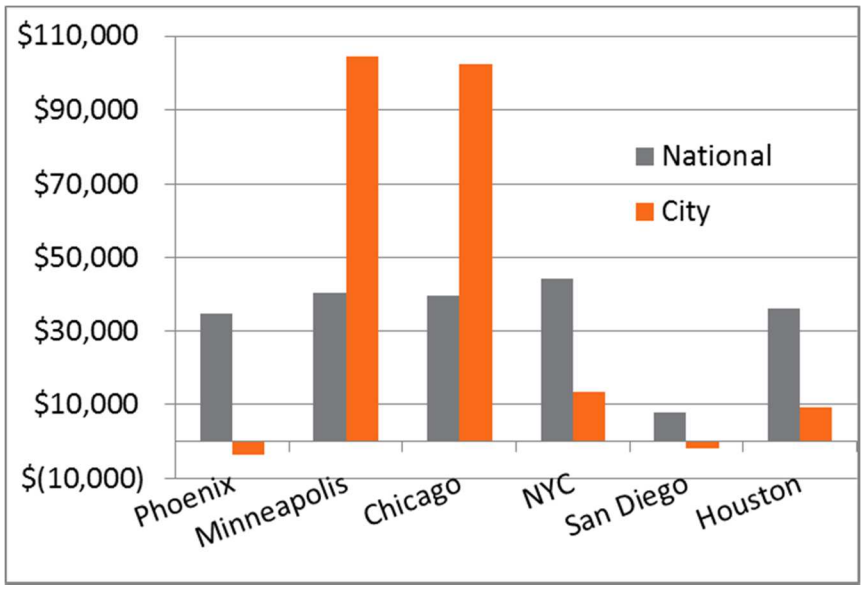


Figure 6a. Comparison of avoided GWP damages results for large hospitals using spatial or US average data.

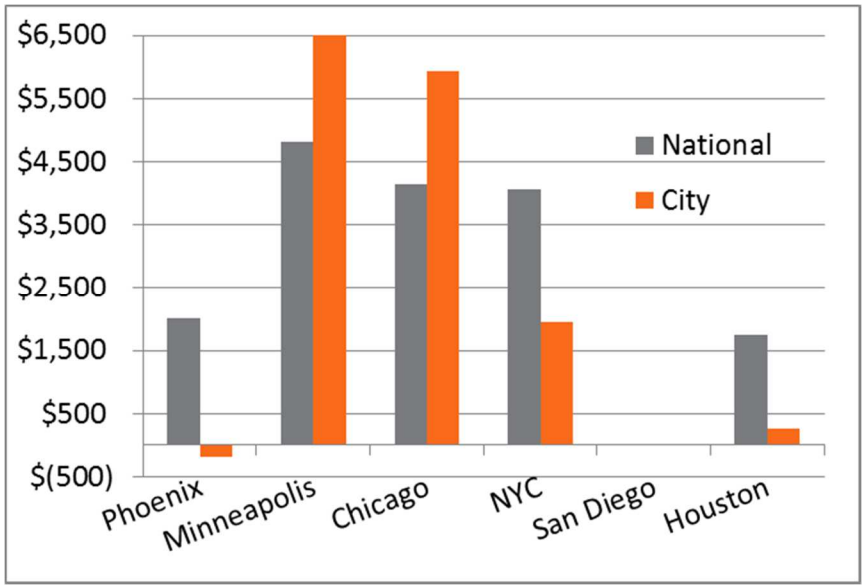


Figure 6b. Comparison of avoided GWP damages results for small hotel using spatial or US average data.

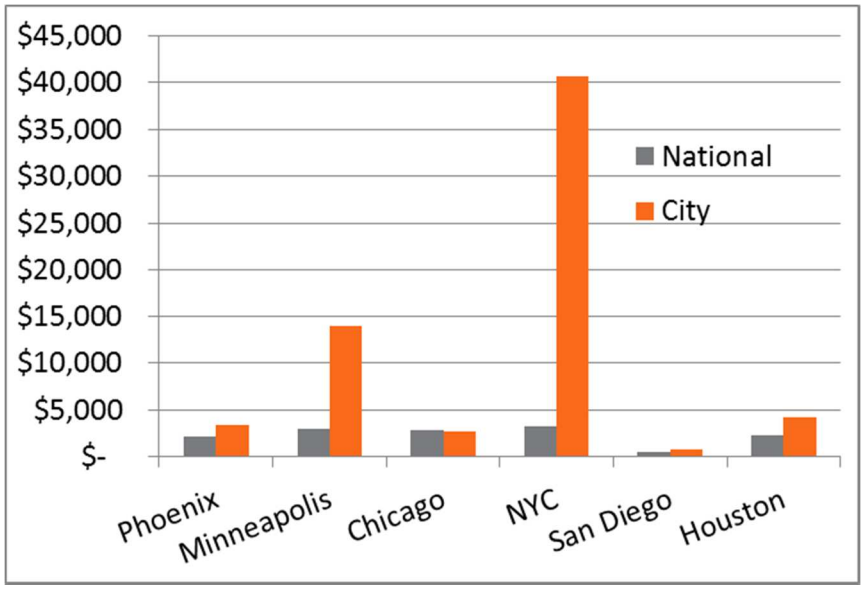


Figure 7a. Comparison of avoided direct CAP damages results for large hospitals using spatial or US average data.

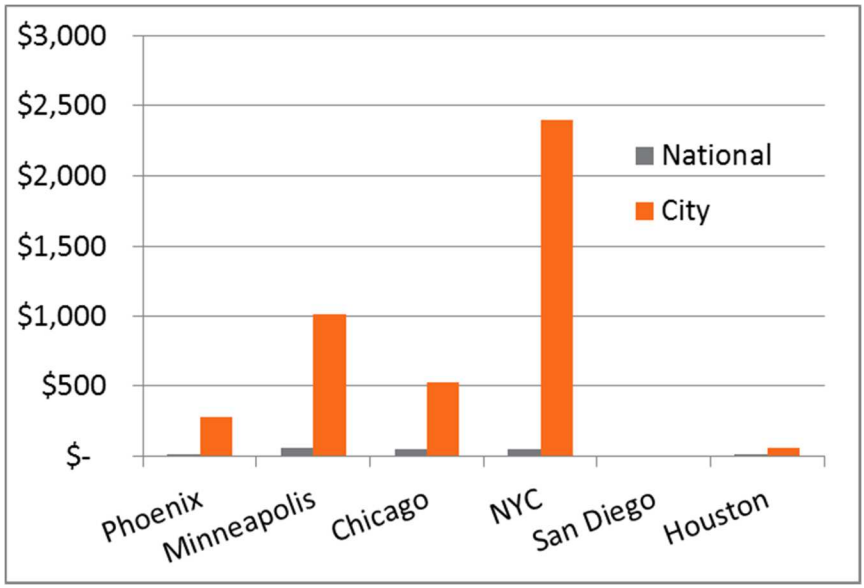


Figure 7b. Comparison of avoided direct CAP damages results for small hotels using spatial or US average data.

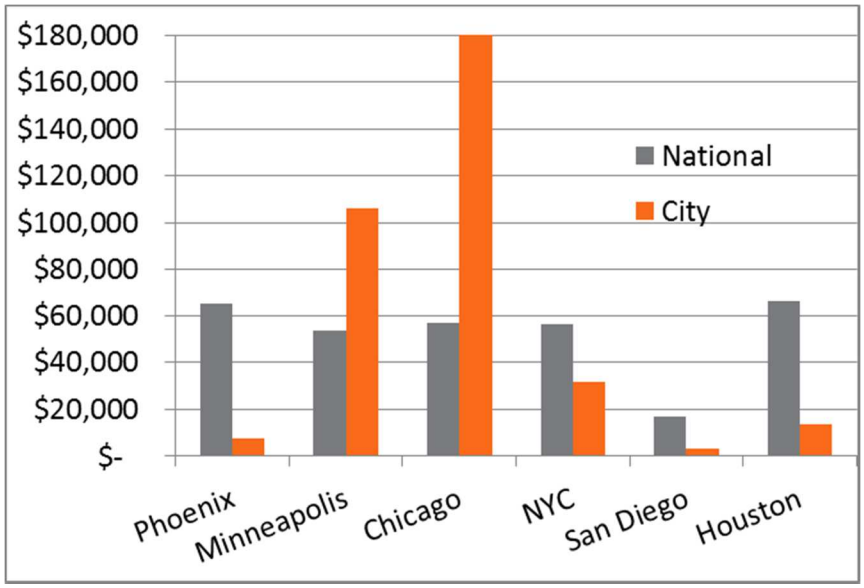


Figure 8a. Comparison of avoided indirect CAP damages results for large hospitals using spatial or US average data.

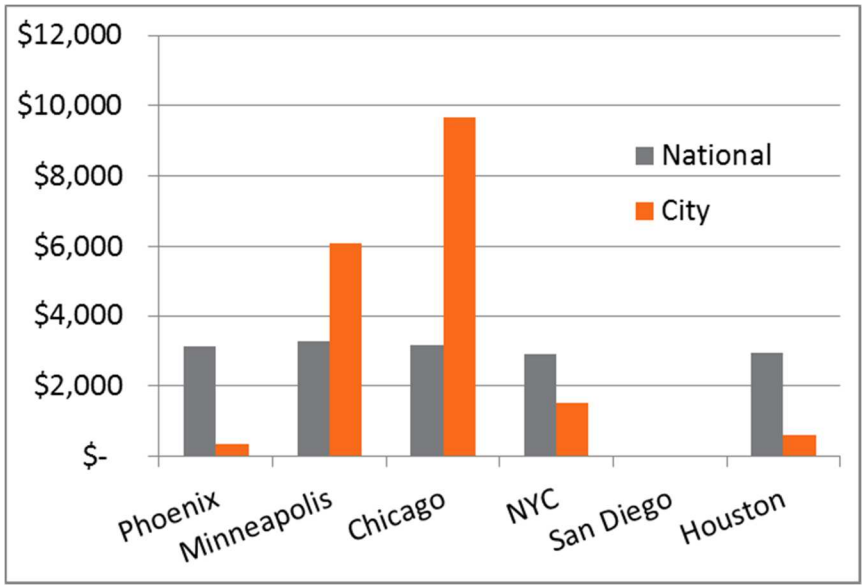


Figure 8b. Comparison of avoided indirect CAP damages results for small hotels using spatial or US average data.

4.3.2 Results of Sensitivity Analysis

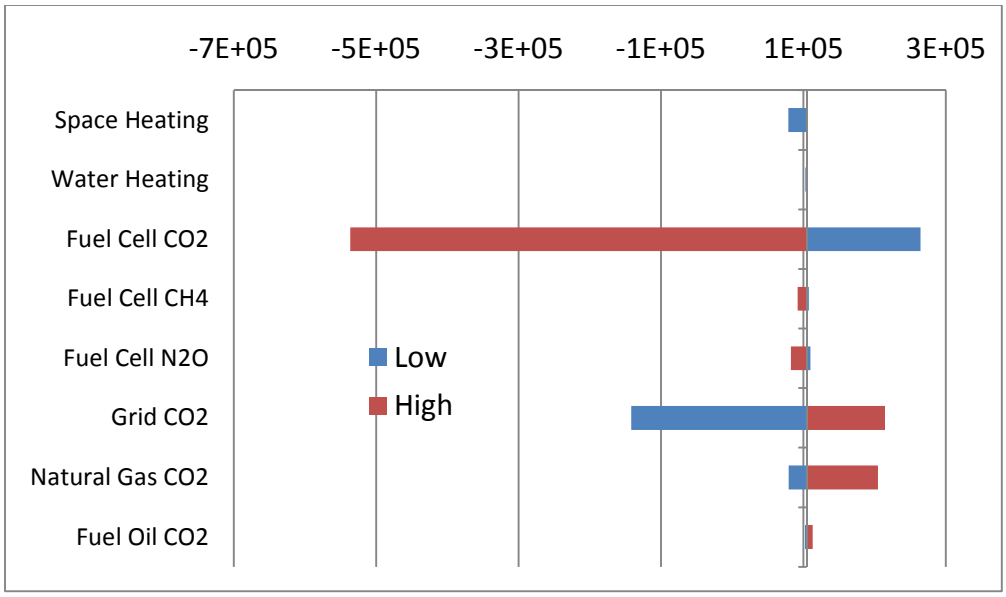
Results for Phoenix and Minneapolis are a good representation of the range of impacts from fuel cell adoption scenarios studied in this analysis. In this section, the sensitivity of results for Phoenix and Minneapolis to changes in key parameters is discussed.

In the following figures, all parameters used to calculate the monetized result are varied using either value ranges found in literature, or best estimates of ranges as discussed in the following sections. Parameters are listed along the side of the figure while the monetized value of the result is shown above the figure as the x-axis. High and low values for a parameter changed the monetized result, and this change is represented by the colored bars in the figure. The origin on the x-axis represents the point where a fuel cell system has a zero monetized impact. In other words, its emissions create the same level of damages as the reference system.

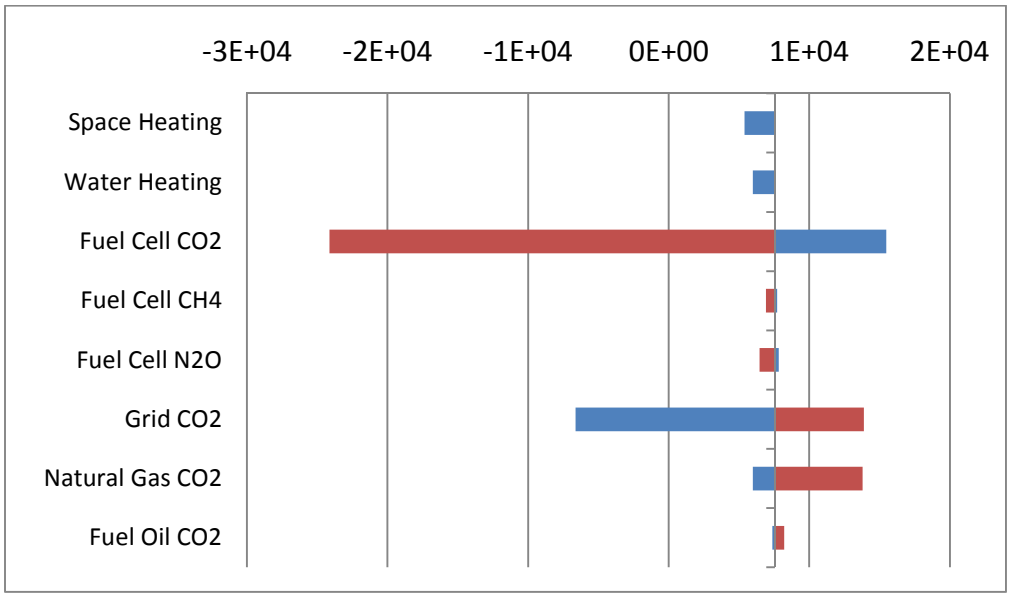
Greenhouse gas and CAP emission factors from regional electricity grids, building energy systems, and fuel cells, and the energy supplied by the fuel cell to heating were varied to explore the effect of future changes in building and power emissions intensities, and fuel cell technology improvements. The lowest and highest US county-specific ground level MBA factors for NOx, SOx, PM_{10} and $PM_{2.5}$ were used the model to approximate the impact of increasing population and changes in atmospheric conditions on results.

The monetized value from marginal GHG emission in Minneapolis and Phoenix was most sensitive to the CO_2 emission from (1) fuel cells, (2) natural gas powered heating equipment, and (3) regional electricity grids (Figure 10a-d). In Minneapolis, the monetized value in large hospitals was zero when the electricity grid CO_{2eq} emission factor dropped to 475 g/kWh, a value 43% less than the 2011 marginal emission factor. In Phoenix, the value became negative when the electricity grid CO_{2eq} emission factor dropped below 494 g/kWh. This value is 2% higher than the 2011 marginal emission factor used in the baseline analysis, explaining why FCS deployed in Phoenix would not receive carbon credits.

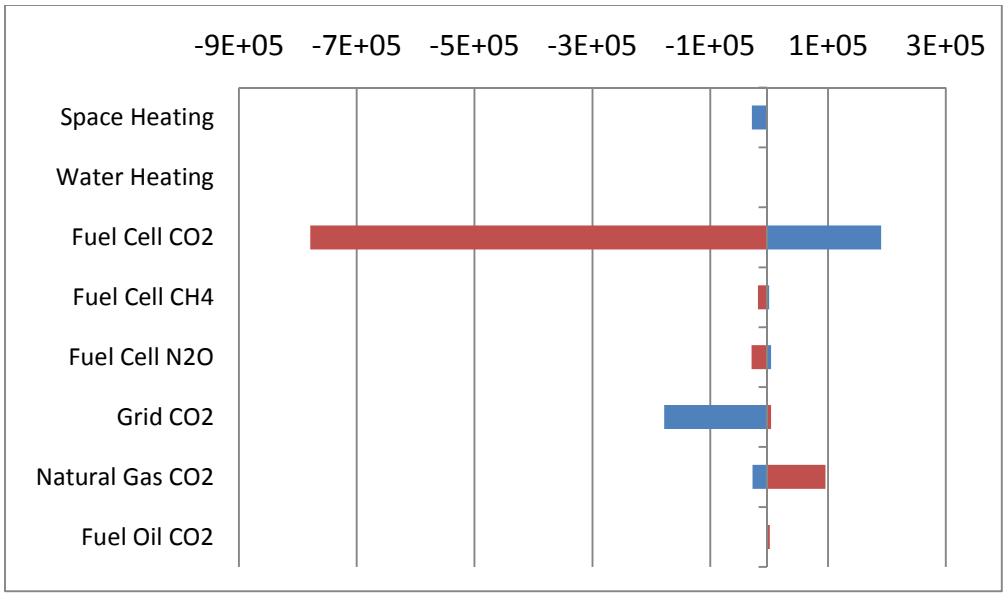
The monetized value from direct marginal CAP emission in Minneapolis and Phoenix was most sensitive to: (1) the SO_2 emissions from fuel oil powered heating equipment, (2) NOx emissions from natural gas powered heating equipment, (3) the ground-level MBA of NOx, and (4) the ground-level MBA of SO_2 (Figure 11 a-d). FCS will provide the greatest monetary benefit from avoided health damages in regions where there are poorly controled NOx emissions from natural gas and SOx emissions from heating oils. Furthermore, FCS must achieve lower emissions in counties where population is growing to maintain health benefits.



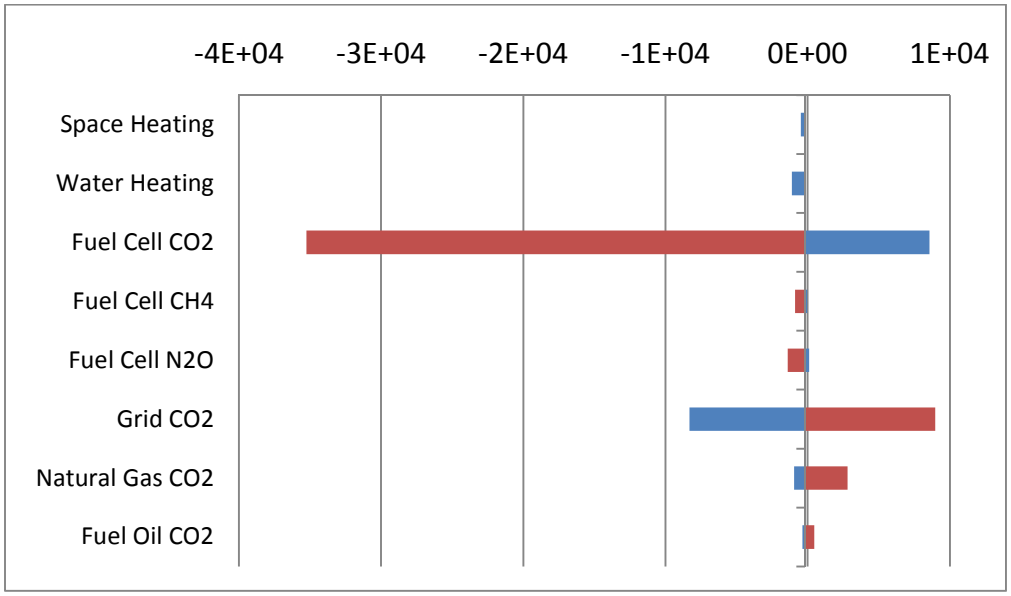
a. Monetized value of marginal GHG emissions from large hospitals in Minneapolis.



b. Monetized value of marginal GHG emissions from small hotels in Minneapolis.

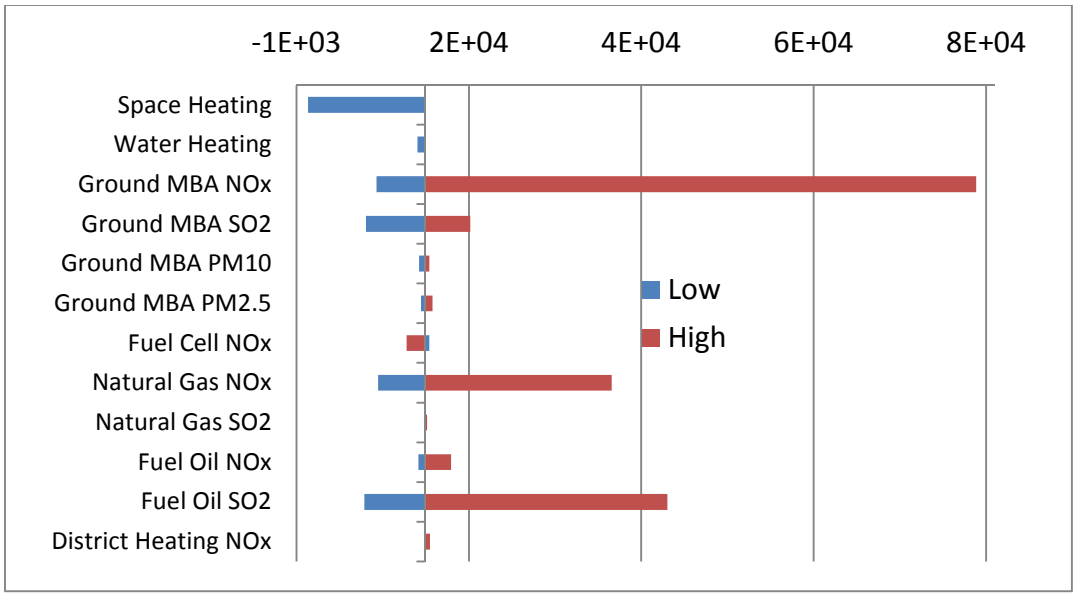


c. Monetized value of avoided GHG emissions from large hospitals in Phoenix.

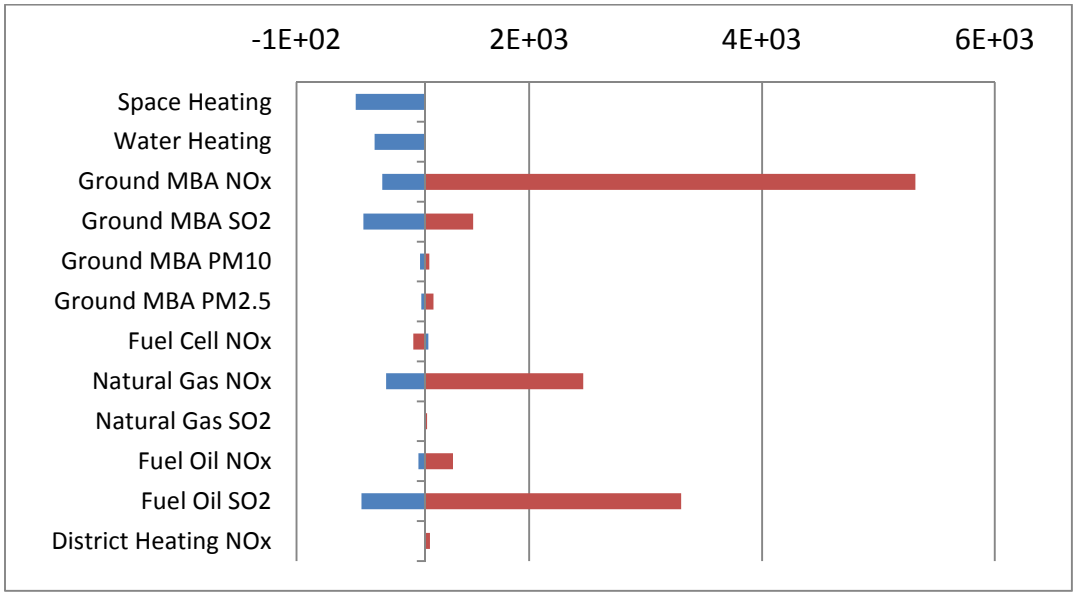


d. Monetized value of avoided GHG emissions from small hotels in Phoenix.

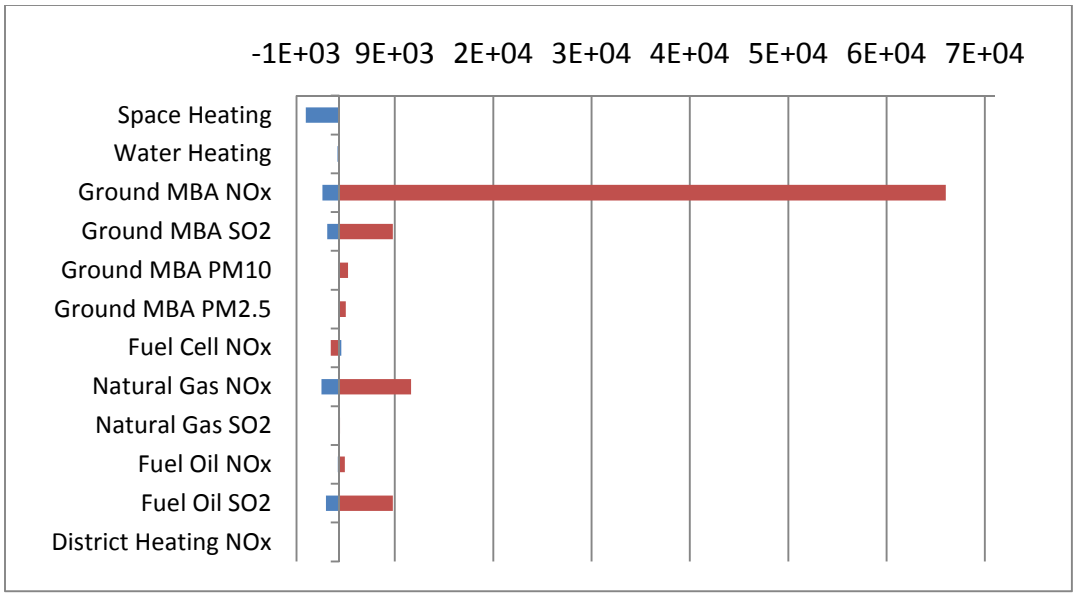
Figure 9. A-D. Tornado plots showing sensitivities of monetized value of marginal GHG emissions from scenarios run in Minneapolis and Phoenix. See previous discussion for guidance on how to read these plots.



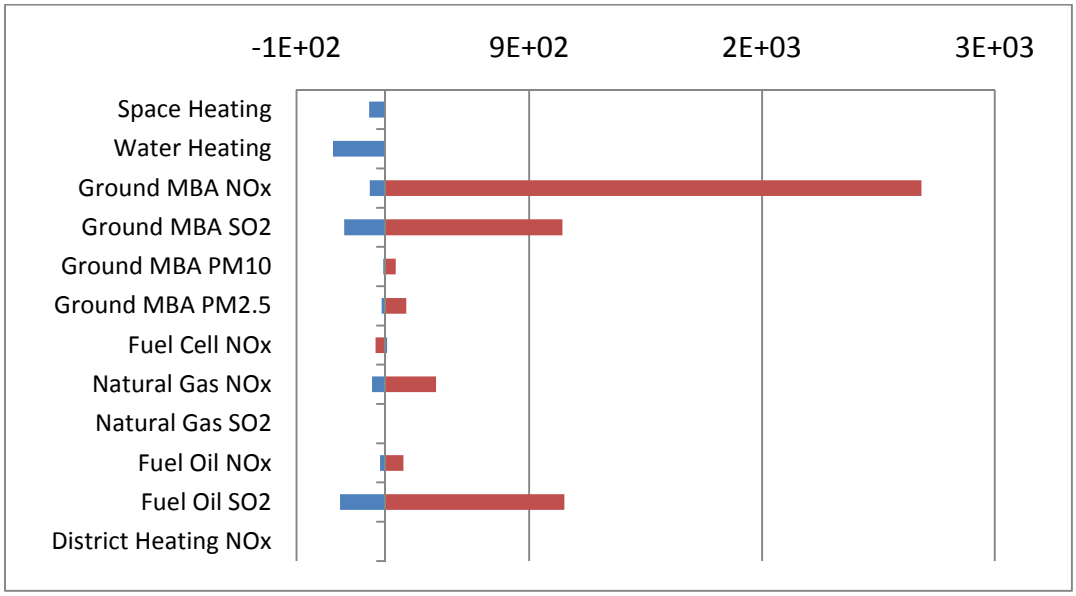
a. Monetized value of avoided direct CAP emissions from large hospitals in Minneapolis.



b. Monetized value of avoided direct CAP emissions from small hotels in Minneapolis.



c. Monetized value of avoided direct CAP emissions from large hospitals in Phoenix.



d. Monetized value of avoided direct CAP emissions from small hotels in Phoenix.

Figure 10. A-D. Tornado plots showing sensitivities of monetized value of marginal direct CAP emissions from scenarios run in Minneapolis and Phoenix. See previous discussion for guidance on how to read these plots.

4.3.2.1 Dynamic Electricity Grid

Carbon emissions for electricity generators in the Midwest Reliability Organization (MRO) NERC region ranged from 0 - 1208 gCO_2/kWh, 0 – 0.51 gCH_4/kWh, and 0 – 0.07 gN_2O/kWh (Cai et al.). Upper bound values resulted in 104%, 3%, and 6% increase in the dollar value that was calculated when 2011 marginal CO_2 emission factors from Siler-Evans et al. were used. The dollar value was negative when the electricity grid CO_{2eq} emission factor dropped below 475 g/kWh, which is 43% less than the 2011 marginal emission factor. Emission factors for the electricity generators in the Western Electricity Coordinating Council (WECC) NERC region ranged from 0 - 1035 gCO_2/kWh, 0 – 0.55 gCH_4/kWh, and 0 – 0.074 gN_2O/kWh. Upper bound values resulted in 6993%, 113%, and 292% increase in the dollar value, respectively. The dollar value was negative when the electricity grid CO_{2eq} emission factor was less than 494 g/kWh. This value is 2% more than the 2011 marginal emission factor used the analysis, explaining why the FCS in Phoenix did not receive carbon credits.

Ground-level damage factors for NOx, SOx, PM_{10} and $PM_{2.5}$ vary from 68 - 141,038 $\$/tNO_X$, 743 – 36,669 $\$/tSO_X$, 203 – 22,116 $\$/tPM_{10}$, and 844 - 141,038 $\$/tPM_{2.5}$ in the United States according to Muller and Mendelson (given in $2014 for a VSL of 6 million). For NOx emissions, the change in the dollar value ranged from -39% to 449% in Minneapolis and from -51% to 1844% in Phoenix. For SO_X, PM_{10} and $PM_{2.5}$, the changes ranged from -50 to 39%, -5 to 4%, and -3 to 7%, respectively in Minneapolis and from -37 to 144%, -4 to 26%, and -3 to 19%, respectively, in Phoenix. These results indicate that FCS must further reduce emissions in counties where population is growing to maintain health benefits.

4.3.2.2 Fuel Cell Technology Improvement

There is a great deal of discrepancy in the literature regarding fuel cell emission factors. Fuel cell emission factors were varied from 0 to 500% of base case values, and found the GWP benefit of FCS in Minneapolis hospitals became negative when fuel cell CO_2, CH_4, and N_2O emission factors were greater than 902.21, 17.62, and 1.22 g/kWh, respectively. The benefit was negative for FCS in hospitals in Phoenix when fuel cell CO_2, CH_4, and N_2O emission factors were greater than 535.12, 0.14, and 0.04 g/kWh, respectively.

Changing the fuel cell NOx emission factor from 0 to 500% of the base case value 0.0069 g/kWh caused the benefit in Minneapolis to change from 4% to -14% of its base value, and from 6% to -25% in Phoenix. The benefit in Minneapolis and Phoenix dropped by 26% and 101% when the FCS did not provide energy for space heating.

4.3.2.3 Dynamic Building Emissions

Changing the NOx emission factors for natural gas and heating oil from 0 to 500% caused the dollar value in Minneapolis to change from -38% to 150% and from -6 to 22%, respectively. Changing the SOx emission factor for heating oil over the same range resulted in a -52% to 207% change in the dollar value. Varying the emission factors for other pollutants resulted in <20% change in the dollar value. When the emissions of district heating were modeled using

100 to 500% of natural gas's emission factor for NOx, the dollar value changed from 17% to 87% of the base value. Similar ranges were found in the dollar value change for Phoenix.

These results indicate that FCS will provide the greatest monetary benefit from avoided health damages in regions where there are poorly controled NOx emissions from natural gas and NOx and SOx emissions from heating oils.

4.3.2.4 Marginal Benefit of Abatement Factors

The marginal benefit of abatement factor for Minneapolis rose to 0.022 $/kWh when the baseline value for electricity damage factors ($/kWh) were appended with an average estimate of EF for $PM_{2.5}$ from the GREET model. The benefit from avoided indirect emissions increased by 39% when this appended value was used. Machol et al. suggests using an even higher factor of 0.13 $/kWh for Minnesota based on data from Fann et al. The benefit from avoiding indirect pollutants increased by 723% when the Machol value was used. In Phoenix, D_{elec} increased to 0.005 $/kWh, resulting in a 455% increase in the benefit from avoiding indirect pollutant emissions. Machol et al. provide a higher factor of 0.1 $/kWh for Arizona. The benefit from avoiding indirect pollutants increases by 11011% when the Machol value was used.

4.3.3 Alternative Scenario

Appendix A4 describes a model run using data from an alternative scenario proposed by the Lawrence Berkeley National Laboratory research group in November of 2014, which uses the fuel cell model described in Wei et al. (2014). The updated model run uses three alternative and more conservative assumptions: (1) the size of the fuel cell system in large hospitals is 250 kW and not 1 MW; (2) the fuel cell does not provide space heating to buildings; (3) all emissions from the fuel cell system except for CO_2 are increased by 9% (Table A2). One less-conservative assumption is that the building heating equipment is 100% efficient, rather than 80% efficient, meaning less fuel is used to generate the same quantity of heat.

In the alternative scenario, FCS would not provide carbon savings to large hospitals in Phoenix, NYC, Houston, or San Diego or to small hotels in Phoenix (Figure A2). Like the primary scenario presented in this dissertation, the largest monetary benefit associated with the deployment of FCS in large hospitals and small hotels occurred in New York City and Chicago. City-wide deployed could result in savings of $10 million and $1.9 million in Chicago and New York City, respectively. The primary scenario had benefits valued at $31.8 million and $29.2 million, respectively. Results were also evaluated using a kWh-e functional unit, representing the annual power supplied by the FCS. Minneapolis and Chicago would achieve the greatest benefits per kWh-e in both scenarios, at $0.07/kWh-e in Chicago and $0.06/kWh-e in Minneapolis in the alternative case. The primary scenario estimated values of $0.08/kWh-e and $0.09/kWh-e for Minneapolis and Chicago. The value for Phoenix (-$0.003/kWh-e) and for San Diego (-0.002/kWh-e) went from positive to negative when the alternative assumptions were applied.

4.4 Discussion

4.4.1 Fuel Cell Case Study

This dissertation introduces a consequential life cycle impact assessment (LCIA) model to assess the marginal change in environmental and human health impacts associated with fuel cell system (FCS) operation. This study estimates the potential monetary value that a FCS could provide if credits were awarded to commercial buildings for avoiding externalities from GHG and CAP emissions. The amount of power and heat provided by four 250kW FCS to large hospitals and one 50kW FCS to small hotels were determined based on city-specific load shapes and markets as discussed in Wei et al. Environmental and human health impacts of the adoption of FCS varied widely between locations due to differences in regional energy supply systems, building and fuel cell operation, nearby populations, and regional conditions affecting the transport and transformation of pollutants.

All six cities could realize a positive net benefit from adopting FCS in small hotels and large hospitals. Certain cities did not, however, realize a positive climate benefit from FCS adoption; this includes Phoenix and San Diego. The primary contributor to benefits varied by building and location, with indirect CAP emissions dominating benefits in places like Chicago and San Diego, and direct CAP emissions dominating in places like New York City. Greenhouse gas emissions and indirect CAP emissions had comparable contributions in Minneapolis and Houston. The largest annual benefit from city-wide deployment occurred in New York City and Chicago, valued at $31.8 million and $29.2 million, respectively. In the scenario where FCS only provided heat for water heating, FCS would not provide carbon savings to large hospitals in Phoenix, NYC, Houston, or San Diego or to small hotels in Phoenix (Figure A2). FCS could provide the greatest monetary benefit from avoided health damages in regions where there are poorly controled NOx and SOx emissions from energy sources like fuel-oil-powered boilers and power plants.

Many states are adopting future carbon and renewable energy penetration goals; as a result, cleaner energy systems will likely make fuel cell systems obsolete as environmental technologies unless the fuel cell itself achieves lower emissions. In the case of Minneapolis, a 43% reduction in CO_2 emissions from the electricity grid will negate the carbon savings from the FCS modeled in this study; a carbon reduction of 41% is the state goal for Minnesota in 2030 under the EPA Clean Power Plan. Given this timeline, FCS should be evaluated for their ability to act as temporary “drop in” technologies. Conversely, reformate equipt PEM FCS already emit more carbon per kWh than the WECCS electricity grid, where Phoenix and San Diego reside, so these systems would only achieve carbon savings in subareas where the local utility has higher emissions than the region. Even so, savings in Phoenix may be short-term given the ambitious goals of the Clean Power Plan to reduce Arizona 2012 carbon emissions by 53% by 2030.

The model developed in this dissertation was run using first national and then city-specific data to understand the significance of using location-specific emission factors, building fuel consumption, and marginal-benefit-of abatement (MBA) factors. National data included averages for electricity generation emissions, stack- and ground-level MBA factors, and building fuel use. A pollutant emitted in an urban environment is likely to result in higher damages than if it was emitted in a rural environment. Thus, the monetized value of mitigating pollution

emissions is typically higher when city-specific data is used as opposed to national average data. However, results were not solely dependent on the marginal benefit of abatement factor, and spatial heterogeneity in electric grid emission factors and building fuel consumption led to some cities having lower avoided damages than then national average, mainly San Diego and Phoenix.

Based on the results of this study, it is not possible to conclude that PEM fuel cell systems that use a natural gas reformer for onsite hydrogen production are a sustainable technology for distributed generation throughout the entire nation. For example, the small reduction in CAP emissions expected in cities like Phoenix and San Diego is likely to be lost as emissions standards for heating equipment and electricity generators become more stringent. Efforts should be made to reduce emissions from the fuel cell system, particularly CO_2 emissions, and to focus efforts on identifying buildings that have power and heating load shapes suitable for fuel cell operation and that are located in regions where dirtier heating fuels and electric grids are used. Large hospitals and small hotels in Chicago, New York City, and Minneapolis were identified as fitting this criteria, and represent sites where PEM FCS are a sustainable option for CHP.

Capturing spatial heterogeneity was essential for reaching these conclusions, making spatially resolved approaches, like the one presented in this dissertation, all the more critical for the assessment and advancement of emerging technologies.

4.4.2 Extension to other Technologies

The model is designed to assess fuel cell systems, but a few adjustments will allow the user to apply to model to studies of other distributed generation technologies.

The following adjustments are needed to adapt the model:

1. The emission factors (t/kWh) for the distributed generation technology under study. The model currently converts the following pollutants into global warming potential, reduced visibility, crop and timber yields changes, and morbidity and mortality: CO_2, CH_4, N_2O, NO_X, SO_2, $PM_{2.5}$, PM_{10}.
2. The power and heat supplied (kWh) by the distributed generation technology over the period of time specified by the user.

A user could follow the approach outlined in this dissertation to add new locations. The user could also follow the approach to add new building types and sizes, as long as they are included in the CBECS database. CBECS currently includes the following building type categories: office, food sales, education, service, public assembly, non-refrigerated warehouse, lodging, public order assembly, outpatient health care, food service, retail other than mall, nursing home, religious worship, hospital, strip mall shopping, enclosed mall, other. The definition for "other", provided by CBECS is:

> "Buildings that are industrial or agricultural with some retail space; buildings having several different commercial activities that, together, comprise 50 percent or more of the floorspace, but whose largest single activity is

agricultural, industrial/ manufacturing, or residential; and all other miscellaneous buildings that do not fit into any other category."

Examples of the category "other" include: airplane hangar, crematorium, laboratory, telephone switching, agricultural with some retail space, manufacturing or industrial with some retail space, data center or server farm. These building types would most likely have very different building load shapes for heat and power demand, but this detail is lost in the aggregation. Details on fuel consumption queried using CBECS for building types that fall under the category "other" should be crosschecked through an alternative data source before proceeding.

Another concern is that the CBECS database only contains information for buildings built in 2003 or earlier. A future user should look for the most recent database (2012) to be published by the Energy Information Administration (EIA).

4.4.3 Future Work

The model is flexible enough to be updated as electricity grids and buildings change, and the model is coordinated with an approach that uses data from databases updated every few years by agencies like the EIA. Scenarios run in this dissertation case study use building fuel consumption data from 2003 and electric grid emission factors from 2010. Using current data in any future scenario analysis introduces uncertainty since the technology under study may not be deployed for many years. This limitation could be addressed by strengthening the study's temporal sensitivity. One way this could be achieved is by simulating plausible conditions in the years that the FCS is expected to operate, such as integrating scenarios of electricity system evolution (e.g. retirement of coal plants, mandates for greater fractions of renewable energy such as wind and solar) and building evolution (e.g. emissions standard regulations for heating equipment).

While developing the impact model, it became clear that integrating data specific to the targeted buildings and regions identified by fuel cell developers was a challenge. Variable methods for calculating marginal benefit of abatement factors and emission factors make comparison of impact assessment results difficult unless a meta-analysis is performed. Future work is needed to determine best practices for the field, instead of simply including a range of values in a sensitivity analysis. This study would indicate that government support of fuel cells in areas like San Diego may not provide the highest return on investment since the monetized benefit of operating fuel cells in San Diego is small. However, additional work is needed to understand how factors excluded in this study, like building physics and VOC emissions, affect results.

4.5 References

Lipman, T. E.; Edwards, J. L.; Kammen, D. M. Fuel Cell System Economics: Comparing the Costs of Generating Power with Stationary and Motor Vehicle PEM Fuel Cell Systems. *Energy Policy*. **2004**. *32* (1), 101-125.

Feroldi, D.; Basualdo, M. Description of PEM Fuel Cells System. In *PEM Fuel Cells with Bio-Ethanol Processor Systems, Green Energy and Technology;* Springer-Verlag London Ltd 2012; pp 49-72. DOI: 10.1007/978-1-84996-184-4_2.

Mehta, V.; Cooper, J.S. Review and analysis of PEM fuel cell design and manufacturing. *Journal of Power Sources*. **2004**. *114,* 32-53

Baratto F.; Diwekar U.M. Life cycle assessment of fuel cell-based APUs. *Journal of Power Sources*. **2005**. *139*, 188–196.

Life-cycle analysis of criteria pollutant emissions from stationary fuel cell systems with the GREET model. Annual Progress Report. Elgowainy, A.; Wang, M.; Han, J.. Argonne National Laboratory: 2010; 1217-1222.

A Total Cost of Ownership Model for Low Temperature PEM Fuel Cells in Combined Heat and Power and Backup Power Applications; LBNL-6772E; Wei, M.; Lipman, T.; Mayyas, A.; Chien, J.; Chan S. H.; Breunig, H.; Stadler, M.; McKone, T.; Beattie, P.; Chong, P.; Collela, W.; James, B.. Lawrence Berkeley National Laboratory Report: Berkeley, CA, 2014.

Siler-Evans, K.; Lima Azevedo, I.; Morgan, M.G. Marginal Emissions Factors for the U.S. Electricity System. *Environ. Sci. Technol*. **2012**. *46*, 4742-4748.

Siler-Evans, Kyle; Azevedo, Ines Lima, Morgan, M. Granger, Apt, Jay. Regional variations in the health, environmental, and climate benefits of wind and solar generation. *PNAS*. **2013**. *110*, 11768-11773.

Muller, N. Z.; Mendelsohn, R.; Nordhaus, W. Environmental accounting for pollution in the United States economy. *Am. Econ. Rev.* **2011**. *101* (5):1649–75. http://dx.doi.org10.1257/aer.101.5.1649

Brown, K.E.; Henze, D.K.; Milford, J.B. Accounting for climate and air quality damages in future U.S. electricity generation scenarios. *Environ. Sci. Technol*. **2013**; *47*: 3065-3072.

Fann, N.; Fulcher, C. M.; Hubbell, B. J. The influence of location, source, and emission type in estimates of the human health benefits of reducing a ton of air pollution. *Air Qual Atmos Health.* **2009**, *2*, 169-176.

Machol, B.; Rizk, S. Economic value of U.S. fossil fuel electricity health impacts. *Environment International*. **2013**, *52*, 75-80.

Hidden costs of energy: unpriced consequences of energy production and use. National Research Council, Committee on Health, Environmental, Other External Costs and Benefits of Energy Production and Consumption. Washington, DC: The National Academies Press; 2010. http://www.nap.edu/catalog/12794.html.

Laden F.; Schwartz J.; Speizer F. E.; Dockery D. W. Reduction in fine particulate air pollution and mortality: Extended follow-up of the Harvard Six Cities study. *Am. J. Respir. Crit. Care Med.* **2006**, *173*, 667-672.

Pope, C. A.; Burnett, R. T.; Thun, M. J.; Calle, E. E.; Krewski, D.; Ito K.; Thurston, G. D.: Lung cancer, cardiopulmonary mortality, and long-term exposure to fine particulate air pollution. *JAMA* **2002**, *287*, 1132-1141.

The Cost of Air Pollution: Health Impacts of Road Transport. OECD Publishing. 2014. *http://dx.doi.org/10.1787/9789264210448-en*

Fulcher, Charlie. Environmental Protection Agency contact for Ben-Map website. Personal correspondence March 5, 2014. http://www.epa.gov/air/benmap/bpt.html

The Air Pollution Emission and Policy Analysis Model (APEEP): Technical Appendix. Muller, N.Z.; Mendelsohn, R.O. Yale University, New Haven, CT. December 2006. Available at: https://segueuser131les.middlebury.edu/nmuller/APEEP_Tech_Appendix.pdf

Jaramillo, P.; Griffin, W. M.; Matthews, H. S. Comparative life-cycle air emissions of coal, domestic natural gas, LNG, and SNG for electricity generation. *Environ. Sci. Technol*. **2007**. *41*, 6290-6296.

Burnham, A.; Jeongwoo, H.; Clark, C. E.; Wang, M., Dunn, J. B.; Palou-Rivera, I. Life-cycle greenhouse gas emissions of shale gas, natural gas, coal, and petroleum. *Environ. Sci. Technol*. **2012**. *46*, 619-627.

CBECS Database; http://www.eia.gov/consumption/commercial/index.cfm

Energy System and Thermo-economic Analysis of Combined Heat and Power Fuel Cell Systems; Proceedings of the ASME 6th International Conference on Energy Sustainability July 23-25, 2012 ESFuelCell2012-91481. Colella, W. G.; Pilli, S.P. San Diego, CA 2012.

O'Hayre, R. Cha, S.W., Colella, W. Prinz, F. *Fuel cell fundamentals. 2nd Edition.* John Wiley & Sons, Inc. 2009.

U.S. Energy Information Agency (EIA). Voluntary Reporting of Greenhouse Gases Program. Emission Factors and Global Warming Potentials. Accessed August 2013. http://www.eia.gov/survey/form/eia_1605/emission_factors.html, Revised April 28, 2011.

U.S. Energy Information Agency (EIA). Total District Heat Consumption and Expenditures. Table C25. Table 1.3-1 and 1.3-4. Accessed September 2013. http://www.eia.gov/

U.S. Department of Energy Commercial Reference Building Models of the National Building Stock; NREL/TP-550046861; Deru, M.; Field, K.; Studer, D.; Benne, K.; Griffith, B.t; Torcellini, P.; et al. National Renewable Energy Laboratory; 2011.

US Census Bureau. 2010 Census Data. Accessed August 8, 2013. http://www.census.gov/2010census/popmap/.

Climate Change 2007: The Physical Science Basis; Contribution of Working Group I to the Fourth Assessment Report; Intergovernmental Panel on Climate Change; 2007. Accessed 02/13/2012. http://www.ipcc.ch

Technical Support Document:-Technical Update of the Social Cost of Carbon for Regulatory Impact Analysis- Under Executive Order 12866; Interagency Working Group on Social Cost of Carbon, United States Government; 2013. http://www.whitehouse.gov/sites/default/files/omb/inforeg/social_cost_of_carbon_for_ria_2013_update.pdf.

eGRID2012 Version 1.0 Year 2009 GHG Annual Output Emission Rates. Accessed October 2013. www.epa.gov/egrid

Environmental Protection Agency. Carbon Pollution Standards; Where Your Live GIS Database. Accessed July 15, 2014. http://www2.epa.gov/carbon-pollution-standards/where-you-live

Ventyx, 2012. Velocity Suite Mapping Module. Ventyx Ed., Atlanta.

Salt River Project Power and Water. Facts about SRP: Power Source Ownership. Accessed November 10, 2013. http://www.srpnet.com/about/facts.aspx#ownership

Arizona Public Service. Our company: Generation & transmission: generation. Accessed November 10, 2013. http://www.aps.com/en/ourcompany/generationtransmission/generation/Pages/home.aspx

Appendices

A1 Supporting Information for Chapter 2
"Regional Evaluation of Brine Management for Geologic Carbon Sequestration"

S1. Candidate Saline Aquifers and Regions

The three saline aquifers included in this study are: the Vedder Formation (Vedder) in the San Joaquin Basin, California (CA); the Jasper Formation (Jasper) in the Eastern Texas Gulf Basin, Texas (TX); and the southern Mt. Simon Sandstone Formation (Mt. Simon) in the Illinois Basin, Illinois (IL); (Table 1). We were able to capture spatial heterogeneity in brine characterization, regional climate, and geography by using these three aquifers as case studies.

Brine found at the representative depth in the Vedder has total dissolved solids (TDS) less than 50 g/L and temperatures between 90 and 150 °C (Table S1) (Fisher, 1990). Climate in the San Joaquin Valley is arid and dry year round. Transportation of brine and wastes to the Pacific Ocean may be cost prohibitive due to the mountainous topography separating the valley from the ocean. The Salton Sea, located 400 km (250 miles) south of the Vedder, is a large salt water body with TDS higher than Vedder brine (Weghorst, 2004).

Brine found at the representative depth of the Jasper has TDS between 50 and 100 g/L and temperatures less than 90 °C (Department of Energy, 2012; Gulf Coast Carbon Center, 2003). Climate along the eastern Texas shoreline is characterized by heavy precipitation year round. The Jasper is located on the Gulf of Mexico. Unlike Illinois and California, Texas has an established infrastructure and industry dedicated to high salinity waste disposal; the most common practices include surface disposal and injection (Clark and Veil, 2009; Puder and Veil, 2006).

Brine found at the representative depth of the Mt. Simon has TDS greater than 100 g/L and temperatures around 90 °C (Table S1) (Department of Energy, 2012; Gulf Coast Carbon Center, 2003; Zhou, et al. 2010). Climate in Illinois is characterized by humid warm months (183 days) and cold winter months.
The Mt. Simon is located inland, far from any saline water bodies.

Most saline aquifers found within the targeted depth range for geologic carbon sequestration (GCS) have similar temperature profiles and temperature ranges in the Vedder, Jasper, and Mt. Simon are characteristic of aquifers found between 800 and 3000m (Gulf Coast Carbon Center, 2003; Kharaka and Hanor, 2003). Brine chemistry is high variable in most saline aquifers, but tends to average above 100 g/L in the Midwest, below 50 g/L in the West, and between 10 and 100g/L in the Southern regions of the United States (US) (Department of Energy, 2012; Gulf Coast Carbon Center, 2003; Harto and Veil, 2011). Little data is available for saline aquifers in

the Northeast. Average TDS in the Vedder, Jasper, and Mt. Simon fall within their observed regional categories (Table S1).

Site selection for GCS projects is largely based on the location of CO_2 sources and the suitability of the formation to trap large volumes of CO_2 (Department of Energy, 2012). The costs, benefits, and environmental impacts of brine management may be additional metrics used in site selection for GCS projects that require brine extraction.

Table S1: Region and Aquifer-Specific Inputs. Temperature and total dissolved solids vary significantly between regions and within aquifers (Fisher, 1990; Gulf Coast Carbon Center, 2003; US EIA, 2012; USGS, 2002).

Aquifer Inputs			
Hydro-geologic Basin	San Joaquin Basin	Eastern Texas Basin	Illinois Basin
Formation	**Vedder Formation**	**Jasper Interval**	**Mt. Simon**
Primary Site of Climate Data	Bakersfield	Houston	Springfield
Brine Temperature (low, high) [°C]	(30, 150)	(30, 80)	(50, 150)
Representative Top Depth [m]	2750	1200	1000
Assumed Specific Heat Capacity [kJ/(kg*K)]	4.18	4.18	4.18
Total Dissolved Solids (low, high) [mg/L]	(1700, 40900)	(1200, 92700)	(1600, 261000)
Density Water [kg/L]	1.03	1.03	1.04

S2. Environmental Impacts

Environmental assessments were found for several brine management options. Based on a literature review, we evaluated significant environmental impacts for individual options and generated a list of potential benefits and concerns that could result from merging options through a brine use sequence (BUS). Currently, staged brine management has not been explored from an environmental perspective.

Several indirect environmental impacts are functions of spatial variables. Indirect impacts attributed to electricity generation vary regionally due to heterogeneity in state electricity mixes. State electricity mixes dominated by coal and fossil fuels generally have higher operation emissions of greenhouse gases (GHG) (CO_2, CH_4, N_2O), acidifying gases (SOx), and particulate matter (PM) than states with a greater percentage of renewable energy sources (Stokes and Horvath 2009). Transportation distances and the mode of transportation for materials, chemicals, and specialized workers are likely to vary regionally across the US depending on available routes, topography, location of manufacturers and climate; this may change the intensity and nature of environmental impacts related to brine management. Whether these changes are significant between GCS locations has yet to be determined. Climate will affect the duration of construction and decommissioning, and the hours of operation for brine management options. For example, climate will greatly affect the feasibility and days of operation of evaporation ponds in Illinois.

S2.1. Geothermal Energy System:

Geothermal energy systems have lower associated GHG emissions than natural gas or coal combustion (Evans et al., 2009; Frick et al., 2010). The majority of CO_2-equivalent emissions related to geothermal energy result from the construction of wells and downhole pumps at a geothermal energy plant;(Frick et al., 2010) these emissions would be allocated to CO_2 injection and brine extraction stages of GCS brine management in a life cycle assessment (LCA). Another primary source of GHG emissions could be avoided by choosing a binary system over a flash steam system; direct CO_2 and H_2S gas emissions occur at geothermal plants using systems that vent vapors from the brine to the environment, not at plants that use binary cycle systems (DiPippo, 1991). Releases of binary cycle working fluid isobutane and waste heat can degrade local ecosystems and should be controlled.

Unlike traditional enhanced geothermal systems, where water is injected into heat reservoirs to maintain production, CO_2 would be used to maintain reservoir pressures at a GCS site. Water consumption will only be observed in the cooling system (Mishra et al., 2011). This water may be partially or fully supplied by a sequential brine desalination stage. We predict that coupling geothermal energy capture with GCS will result in reduced air emissions and water consumption. Geothermal energy harvesting would not decrease the volume of brine waste needing disposal but it could provide a source of renewable energy for sequential BUS stages.

S2.2. Desalination System:

Desalination is energy intensive; electrical generation contributes over 80% of the GHG emissions, (Stokes and Horvath, 2009) and between 40-100% of SOx, volatile organic compounds (VOC), and NOx emissions attributed to the life cycle of desalination (Munoz and Fernandez-Alba, 2008; Stokes and Horvath, 2009; Zhou et al., 2011). The study by Stokes and Horvath (Stokes and Horvath, 2009) assumed electricity was generated using California's average electricity mix of fossil fuels and renewables. Emissions will be higher in states that use a lower proportion of renewable energy in electricity production. Desalination supplied with geothermal sourced electricity would have much lower emissions. The production and transportation of chemicals used in pre- and post-desalination treatment consume large amounts of energy and result in NOx and PM emissions (Fritzmann et al., 2007). Nanofiltration and/or reverse osmosis (RO) membrane treatment would significantly lower concentrations of salts, minerals, and heavy metals (Fu and Wang, 2011) in the desalinated brine and would concentrate them in a waste stream. Concentration of the brine would improve the efficiency of a mineral harvesting stage, potentially reducing related environmental impacts, but the increased toxicity of the waste stream could limit local surface disposal options (Voutchkov, 2011). Desalination would decrease the volume of brine waste requiring disposal.

S2.3. Mineral Harvesting:

The mineral harvesting option is likely to have significant environmental impacts. Evaporation ponds require large land surface areas (SA) and they compete with other land uses. Local freshwater reservoirs can become contaminated if evaporation ponds are not properly lined and monitored. Open water attracts birds and other wildlife that could be exposed to toxic levels of heavy metals and salts (Kharaka et al., 1996). Subsequent electrolysis and mineral extraction stages are energy and chemical intensive; they require large amounts of electricity and corrosive compounds like hydrochloric acid (Ahmed et al., 2001; Jeppesen et al., 2009; Thayer and Neelameggham, 2001). Mineral extraction would reduce the volume of brine requiring disposal. Substitution of compounds produced from traditional mining and thermal extraction methods with compounds produced from GCS sourced brine could lead to mitigation of local and global environmental impacts. For example, China produces over 70% of the world's magnesium. China's primary method for producing magnesium ingots involves mining and transporting ores to plants where the ore undergoes an energy- and chemical-intensive process called pidgeoning (Cherubini et al., 2008; Gao et al., 2009). Extraction processes like pidgeoning cause large emissions of GHGs, acidifying compounds, toxic compounds and depletion and degradation of natural resources (Norgate and Haque, 2010). It is likely that brine mineral harvesting will result in local and global environmental impacts. Whether these impacts are lower than traditional production methods or could be mitigated through the BUS brine management method has yet to be determined.

S2.4. Algae Ponds:

Algae cultivation and harvesting is water-, chemical-, and energy intensive, but coupling algae production with GCS brine management could provide opportunities to lower water, chemical, and energy consumption. Halophilic algae like Dunaliella salina thrive in nutrient supplemented, high salinity water and are competitive in open pond systems (Singh and Olsen, 2011). CO_2 is a typical carbon source for algae, and could be supplied by the CO_2 capture system at the CO_2 source. Heat and electricity are required to strain, dry and extract bio-oils from algae biomass. Part of this energy could be met by sending residual biomass to anaerobic digesters (AD) to produce methane (Collet et al., 2011). Fertilizer consumption by the algae is a primary contributor to the eutrophication associated with algae production. Fertilizers mineralized in AD waste streams have been successfully recycled back to algae ponds.

Algae ponds produce more biomass per unit area than terrestrial plants used to make biofuels and algae feedstock harvesting is unlikely to compete with food crops for fertile land (Clarens et al., 2010). Algae productivity is proportional to pond SA. Individual ponds average between 1-2 hectares, and additional land is required to house the digesters, drying machinery, roads and storage units (Borowitzka and Moheimani, 2010; Campbell et al., 2011). We assumed that an algae pond stage would not significantly decrease the volume of brine requiring disposal, and that waste brine would have organic contaminants. The presence of organics could increase eutrophication and other environmental impacts in surface water bodies used for brine discharge.

S2.5. Aquaculture:

Inland aquaculture is water-, energy-, chemical-, and land intensive and generates substantial organic waste streams (Bosma and Verdegem, 2011). The production and transportation of fish meal and antibiotics to aquaculture ponds generates GHG emissions. Increased demand for fish oil and fish meal can stress marine ecosystems if feed is not farmed onsite (Aubin et al., 2009). Aquaculture requires expert farming to ensure productivity, and these experts could be required to make long commutes that result in additional GHG emissions. Ponds open to the environment are susceptible to contamination and diseases. Compounds found in untreated brines can bioaccumulate in marine species and affect the productivity or value of cultivated species (Fu and Wang, 2011). Ponds with inadequate lining or cracks could contaminate nearby freshwater resources (Ayer and Tyedmers, 2008). Without maintenance, this brine management option may degrade local environments and fail due to economics.

Aquaculture ponds coupled with GCS brine management may have lower net water and energy requirements if desalinated brine and geothermal energy can be supplied to the ponds (Boyd and Lund, 2003). The organic waste from fish ponds could be converted to energy using AD along with algae biomass waste. This brine management option will not decrease the volume of brine waste requiring disposal.

S2.6. Disposal:

Many environmental assessments were found for ocean discharge of brine; desalination plants are commonly cited near a source of seawater and the ocean presents a simple, economic sink for the waste brine (Kim, 2011; Mickley, 2006; Puder and Veil, 2006; Van Der Bruggen et al., 2003; Voutchkov, 2011). Desalination plants generally discharge concentrated brine into nearby saline water bodies. Sometimes the brine must be diluted using low salinity water and mechanical mixing to prevent the loss of local benthic communities. Few environmental impacts have been quantified for alternative disposal methods like sewers, evaporation ponds and landfills (Khan et al., 2009; Zhou et al., 2011). Studies predict that evaporation ponds and brine reinjection can degrade local soils and freshwater resources if evaporation ponds and injection wells are not properly sealed.

High salinity run-off from roads de-iced with rock salt or brine during the winter can degrade local soils and freshwater resources. Brine may have heavy metal and mineral concentrations that degrade local environments (Ohno, 1990). The life cycle of rock salt road de-icing typically includes salt mining, salt processing, transportation and freshwater consumption at application (Donahey and Burkheimer, 1996; ND Department of Health, 2009; Ripley, 2011). The substitution of mined rock salt with extracted brines treated and approved for road application could avoid environmental impacts from upstream salt mining processes.

S3. Regional Land Surface Area Requirement

S3.1. Evaporation Ponds:

A simple material balance was set so that the annual volume of water entering the evaporation pond (precipitation (P) and a constant flow rate of extracted brine) was equal to the annual volume of water exiting the pond (evaporation (E)). We assumed residual minerals were harvested or disposed of in a sequential BUS stage.

We compiled parameter estimates of monthly average E and P from a variety of climate data sources; they are summarized in Table S1 and in Table 1 of the report (Ahmed et al., 2003; Illinois State Water Survey, 2011; Texas Water Development Board, 2010; Weghorst, 2004). The SA of the evaporation pond system was calculated using:

$$SA = \frac{\frac{(100-\%\text{Recovery})*(\mathbf{M_{CO2}})}{\rho_{CO2}}}{(E-P)} \qquad (1)$$

where $\mathbf{M_{CO2}}$ is the annual mass of CO_2 injected into an aquifer [mt-CO_2], %Recovery is the RO recovery factor realized in a prior desalination stage, listed in Table 1 of the report, and $\boldsymbol{\rho_{CO2}}$ is the density of supercritical CO_2 in the reservoir [mt-CO_2/m^3]. We assumed additional land requirements for roads and storage were equivalent to 20% of pond SA.

As seen in Fig. S1, different maximum RO recovery factors can be achieved for the three brines due to differences in salinity. The SA required for evaporation ponds in southern California is relatively small due to high annual evaporation rates, moderate in Illinois due to precipitation during summer months and large in eastern Texas due to the high annual precipitation.

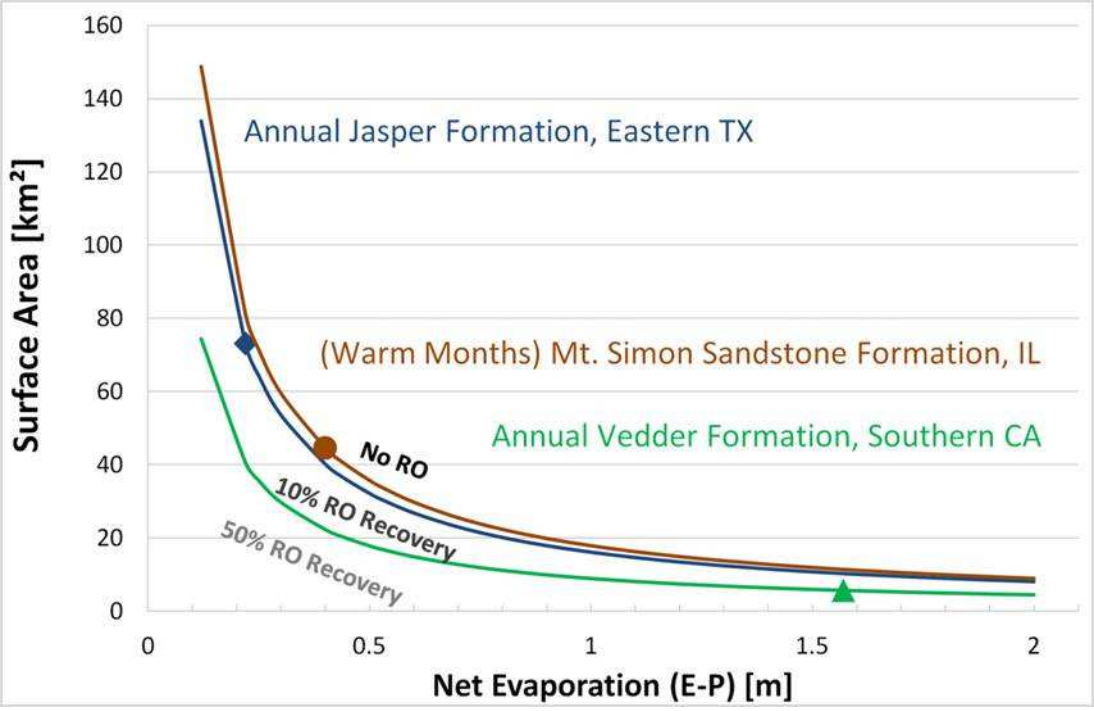


Figure S1: Surface area of evaporation ponds as a function of average net evaporation (evaporation E – precipitation P) rates and reverse osmosis (RO) freshwater recovery fraction. Solid symbols show the SA required to hold the brine from one carbon dioxide capture and sequestration (CCS) project in three saline aquifers: Mt. Simon (orange circle), Vedder (green triangle), and Jasper (blue diamond).

S3.2. Algae Ponds:

Pond SA was calculated using a material balance assuming: (1) an annual volumetric flow rate of brine, (2) a complete purge of pond water every two months,(Collet et al., 2011) (3) the algae would be harvested every 4 days,(Sander and Murthy, 2010) (4) a pond height of 30 cm, which is optimal for algae ponds, (5) annual regional E and P, and (6) 99% of the water could be captured and recycled from the harvesting stage back to the ponds. This led to SA requirements of 6, 8, and 5 km^2 for the Mt. Simon, Jasper, and Vedder respectively. Pond SA increased to 80 km^2 when ponds were not purged and when evaporated water was replaced with freshwater for dilution. Such a large SA resulted in enormous production volumes of bio-oils, but freshwater recharge was calculated to be more than 100 m^3/mt-CO_2; we assumed this was not feasible. Land requirements for roads and buildings were assumed to be equivalent to 30% of pond SA.

S3.3. Aquaculture Ponds:

Average US aquaculture systems have pond SA much less than 0.1 km^2 (Boyd and Lund, 2003). For scenarios where geothermal heat was sent to aquaculture ponds, we calculated the aquaculture pond SA using a material balance assuming: (1) a stock density of 50 kg-fish/m^3 pond and harvesting cycle of 6 months,(Boyd and Gross, 2000; Roque d'Orbcastel et al., 2009) (2) a pond height of 70 cm, and (3) 365 days of activity for the Vedder and Jasper and 183 days of activity for the Mt. Simon. This resulted in average pond SA of 110, 46, and 90 m2 for the Vedder, Jasper, and Mt. Simon respectively. Additional land requirements for roads and buildings were assumed to be 30% of pond SA. We calculated fish production using Equation 6 from the report.

We calculated SA for scenarios where all of the desalinated brine from the Vedder or Jasper was sent to fish ponds assuming: (1) a constant volumetric flow rate of desalinated brine, and (2) replacement of evaporated water with a freshwater source. This resulted in pond SA of 6 and 8 km^2 for the Vedder and Jasper respectively. Theoretically, 3,000-4,000 mt-fish could be cultivated from ponds this size assuming an average production rate of ~500 mt-fish/km^2 (Boyd and Gross, 2000). We assumed this option, at full scale, was not feasible given that this production rate of fish was roughly a third of US domestic production in 2007. More practically, desalinated brine could be used to supply ponds of 0.1 km^2 that generated 50 mt-fish when operated year round.

If all of the extracted brine was sent to the fish ponds, SA was calculated: (1) assuming a volumetric flow rate of brine, (2) replacement of evaporated water with a freshwater source, and (3) a pond height of 70 cm (Campbell et al., 2011). This resulted in pond SA of 11, 80, and 20 km2 for the Vedder, Jasper, and Mt. Simon respectively. We assumed aquaculture systems this size were not feasible due to high energy demands, high organic waste production, and low US demand for tilapia (Bosma and Verdegem, 2011; Roque d'Orbcastel et al., 2009).

S4. Pipeline Construction and Operation

The construction and operation of pipelines for brine disposal is costly. We determined the net present value (NPV) of pipeline transportation using data from the construction and operation of a 100 km pipeline for water and biomass transportation (Deutz, 2012). Our calculation assumed an 8% discount rate, 30 year lifespan, $2,000,000 operation and maintenance cost, and $60,000,000 capital cost. This resulted in a NPV of -$9/mt-$CO_2$ (-$0.1/mt-$CO_2$-mile). Another source calculated that brine pipeline operation cost $0.08-0.1/mt-$CO_2$-mile (Harto and Veil, 2011). We assumed pipeline NPV could range from -$0.1 to -$0.2/mt-CO_2-mile.
Methods for reducing costs include paying to use local pipelines or constructing pipelines that are less than 50 miles, do not cross state borders, and avoid steep topography.

S5. Data Quality

The quality of data used in this research was evaluated using a data quality matrix method introduced in (Lindfors et al., 1995). Results of the assessment are listed in Table S2. The quality of data varied for the different brine treatment, utilization, and disposal options. Technical, cost, and market value data received lower scores (3-4) if they did not represent technology applications that were managing geologic-sourced saline water (aquaculture, algae ponds). Data also received low scores if they were not representative of the scale that would be required to manage the brine from one large GCS project (49 million liters per day). Although our research is forward-looking, and thus relies on a large number of assumptions, we strived to use "good" quality data, data that ranked at least a 2.

Table S2: Data Quality Assessment. Data was ranked based on 6 parameters (column headings) on a scale of 1-5, with 1 represented the highest quality.

Data Quality Table	Acquisition method	Independence of data supplier	Representa-tiveness	Data age	Geographical correlation	Technological correlation
Aquifer Data	1	1	2	1	1	NA
Geothermal						
Technical	3	2	2	1	2	2
Capital, O&M Costs	3	1	2	1	2	NA
Market Value	1	1	1	1	1	NA
Desalination						
Technical	2	2	2	1	2	1
Capital, O&M Costs	2	2	2	1	3	NA
Market Value	1	1	1	3	1	NA
Algae						
Technical	3	1	3	1	2	3
Capital, O&M Costs	3	1	3	1	NA	NA
Market Value	2	1	3	1	2	NA
Mineral						
Technical	2	1	3	2	2	3
Capital, O&M Costs	2	1	3	2	2	NA
Market Value	2	1	2	1	2	NA
Aquaculture						
Technical	2	1	4	2	2	3
Capital, O&M Costs	2	1	4	1	2	NA
Market Value	1	1	1	1	2	NA
Evaporation						
Technical	2	1	1	1	1	1
Capital, O&M Costs	2	1	1	1	2	NA
Market Value	NA	NA	NA	NA	NA	NA
Discharge						
Technical	2	1	1	1	2	1
Capital, O&M Costs	2	1	2	1	1	NA
Market Value	NA	NA	NA	NA	NA	NA
Road Salt						
Technical	3	1	3	1	2	3
Capital, O&M Costs	3	1	3	1	2	NA
Market Value	2	1	2	1	1	NA
Pipeline Transportation						
Technical	3	1	3	1	2	2
Capital, O&M Costs	3	1	3	1	2	3
Market Value	NA	NA	NA	NA	NA	NA

S6. References

Ahmed, M.; Arakel, A.; Hoey, D.; Coleman, M., Integrated power, water and salt generation: a discussion paper. Desalination **2001**, 134, 37-45.

Ahmed, M.; Arakel, A.; Hoey, D.; Thumarukudy, M. R.; Goosen, M. F. A.; Al-Haddabi, M.; Al-Belushi, A., Feasibility of salt production from inland RO desalination plant reject brine: a case study. Desalination **2003**, 109-117.

Aubin, J.; Papatryphon, E.; Van der Werf, H. M. G.; Chatzifotis, S., Assessment of the environemental impact of carnivorous finfish production systems using life cycle assessment. Journal of Cleaner Production **2009**, 17, 354-361.

Ayer, N. W.; Tyedmers, P. H., Assessing alternative aquaculture technologies: life cycle assessment of salmonid culture systems in Canada. Journal of Cleaner Production **2008**, 17, 362-373.

Borowitzka, M. A.; Moheimani, N. R., Sustainable biofuels from algae. Mitigation and Adaptation Strategy for Global Change **2010**.

Bosma, R. H.; Verdegem, M. C. J., Sustainable aquaculture in ponds: Principles, practices and limits. Livestock Science **2011**, 139, 58-68.

Boyd, C. E.; Gross, A., Water use and conservation for inland aquaculture ponds. Fisheries Management and Ecology **2000**, 7, 55-63.

Boyd, T. L.; Lund, J. W., Geothermal heating of greenhouses and aquaculture facilities. In International Geothermal Conference, Reykjavik, Iceland, **2003**.

Campbell, P. K.; Beer, T.; Batten, D., Life cycle assessment of biodiesel production from microalgae in ponds. Bioresource Technology **2011**, 50-56.

Cherubini, F.; Raugei, M.; Ulgiati, S., LCA of magnesium production: Technological overview and worldwide estimation of environmental burdens. Resources, Conservation and Recycling **2008**, 52, 1093-1100.

Clarens, A. F.; Resurreccion, E. P.; White, M. A.; Colosi, L. A., Environmental Life Cycle Comparison of Algae to Other Bioenergy Feedstocks. Environmental Science & Technology **2010**, 44, 1813-1819.

Clark, C. E.; Veil, J. A. Produced Water Volumes and Management Practices in the United States; National Energy Technology Laboratory: Argonne National Laboratory for the U.S. Department of Energy, Office of Fossil Energy, **2009**.

Collet, P.; Helias, A.; Lardon, L.; Ras, M.; Steyer, J.-P., Life-cycle assessment of microalgae culture coupled to biogas production. Biosource Technology **2011**, 102, 207-214.

Department of Energy, National Carbon Sequestration Database and Geographic Information System In Technologies: Carbon Sequestration, NETL: **2012**.

Deutz, P., A Class-Based Analysis of Sustainable Development: Developing a Radical Perspective on Environmental Justice. Sustainable Development **2012**.

DiPippo, R. Geothermal Energy: Electricity generation and environmental impact; **1991**; pp 798-807.

Donahey, T. J.; Burkheimer, D. In Prewetting with Salt Brine, Semisequicentennial Transportation Conference, Ames, Iowa State University: Ames, **1996**.

Evans, A.; Strezov, V.; Evans, T. J., Assessment of sustainability indicators for renewable energy technologies. Renewable and Sustainable Energy Reviews **2009**, 13, 1082-1088.

Fisher, J. B. B., J. R., Water-rock interaction in Tertiary sandstones, San Joaquin basin, California, U.S.A." Diagenetic controls on water composition. Chemical Geology **1990**, 83-101.

Frick, S.; Kaltschmitt, M.; Schroder, G., Life cycle assessment of geothermal binary power plants using enhanced low-temperature reservoirs. Energy **2010**, 35, 2281-2294.

Fritzmann, C.; Lowenberg, J.; Wintgens, T.; Melin, T., State-of-the-art of reverse osmosis desalination. Desalination **2007**, 216, 1-76.

Fu, F.; Wang, Q., Removal of heavy metal ions from wastewaters: A review. Journal of Environmental Management **2011**, 92, 407-418.

Gao, F.; Nie, Z.; Wang, Z.; Gong, X.; Zuo, T., Life cycle assessment of primary magnesium production using the Pidgeon process in China. International Journal of Life Cycle Assessment **2009**, 14, 480-489.

Gulf Coast Carbon Center, Brine-Formation Database. Horvorka, S. D., Ed. Bureau of Economic Geology and Jackson School of Geosciences: **2003**.

Harto, C. B.; Veil, J. A. Management of Water Extracted from Carbon Sequestration Projects; **2011**.

Illinois State Water Survey, Pan Evaporation Across Illinois. In Illinois State Water Survey: Prairie Research Institute, **2011**.

Jeppesen, T.; Shu, L.; Keir, G.; Jegatheesan, V., Metal recovery from reverse osmosis concentrate. Journal of Cleaner Production **2009**, 703-707.

Khan, S. J.; Murchland, D.; Rhodes, M.; Waite, T. D., Management of Concentrated Waste Streams from High-Pressure Membrane Water Treatment Systems. Environmental Science and Technology **2009**, 39, 367-415.

Kharaka, Y. K.; Ambats, G.; Presser, T. S.; Davis, R., Removal of selenium from contaminated agricultural drainage water by nanofiltration membranes. Applied Geochemistry **1996**, 11, 797-802.

Kharaka, Y. K.; Hanor, J. S. Deep Fluids in the Continents: I. Sedimentary Basins; **2003**; pp 499-540.

Kim, D. H., A review of desalting process techniques and economic analysis of the recovery of salts from retentates. Desalination **2011**, 1-8.

Lindfors, L.-G.; Christiansen, K.; Hoffman, L.; Virtanen, Y.; Juntilla, V.; Hanssen, O.-J.; Ronning, A.; Ekvall, T.; Finnveden, G. Nordic Guidelines on Life-Cycle Assessment; Nordic Council of Ministers: Copenhagen, Denmark, **1995**.

Mickley, M. C. Membrane Concentrate Disposal: Practices and Regulation (Second Edition); U.S. Department of the Interior, Bureau of Reclamation: **2006**.

Mishra, G. S.; Glassley, W. E.; Yeh, S., Realizing the geothermal electricity potential- water use and consequences. Environmental Research Letters **2011**, 6, 8pp.

Munoz, I.; Fernandez-Alba, A. R., Reducing the environmental impacts of reverse osmosis desalination by using brackish groundwater resources. Water Research 2008, 42, 801-811.

ND Department of Health Guidelines for the Use of Oilfield Salt Brines for Dust and Ice Control; North Dakota Department of Health: **2009**.

Norgate, T.; Haque, N., Energy and greenhouse gas impacts of mining and mineral processing operations. Journal of Cleaner Production **2010**, 18, 266-274.

Ohno, T., Levels of total cyanide and NaCl in surface water adjacent to road salt storage facilities. Environmental Pollution **1990**, 67 (123-132).

Puder, M. G.; Veil, J. A. Offsite commercial disposal of oil and gas exploration and production waste: availability, options, and costs; Argonne National Laboratory, **2006**.

Ripley, K. Smooth road ahead: A rise in local funding and a new bill will lead to steady growth; Report 23411b; IBISWorld: **2011**; pp 1-34.

Roque d'Orbcastel, E.; Blancheton, J.-P.; Aubin, J., Towards environmental sustainable aquaculture: Comparison between two trout farming systems using Life Cycle Assessment. Aquaculture Engineering **2009**, 40, 113-119.

Sander, K.; Murthy, G. S., Life cycle analysis of algae biodiesel. International Journal of Life Cycle Assessment **2010**, 704-714.

Singh, A.; Olsen, S. I., A critical review of biochemical conversion, sustainability and life cycle assessment of algal biofuels. Applied Energy **2011**, 88, 3548-3555.

Stokes, J. R.; Horvath, A., Energy and Air Emission Effects of Water Supply. Environmental Science and Technology **2009**, 43, 2680-2687.

Texas Water Development Board, Quadrangle:912 Evaporation and Precipitation. Service;, N. W., Ed. **2010**.

Thayer, R. I.; Neelameggham, R., Improving the Electrolytic Process for magnesium Production. Journal of Management **2001**, 15-17.

U.S. Energy Information Administration State Electricity Profiles; Data for **2010**. http://www.eia.gov/electricity/.

U.S.G.S., Produced Waters Database. Management, C. E. D., Ed. **2002**.

Van Der Bruggen, B.; Lejon, L.; Vandecasteele, C., Reuse, Treatment, and Discharge of the Concentrate of Pressure-Driven Membrane Processes. Environmental Science & Technology **2003**, 3733-3738.

Voutchkov, N., Overview of seawater concentrate disposal alternatives. Desalination **2011**, 205-219.

Weghorst, P. A. Salton Sea Salinity Control Research Project; U.S. Department of the Interior & Salton Sea Authority: **2004**.

Zhou, J.; Chang, V. W.-C.; Fane, A. G., Environmental life cycle assessment of brackish water reverse osmosis desalination for different electricity production models. Energy & Environmental Science **2011**, 4, 2267-2278.

Zhou, Q.; Birkholzer, J. T.; Mehnert, E.; Lin, Y.-F.; Zhang, K., Modeling Basin- and Plume-Scale Processes of CO_2 Storage for Full-Scale Deployment. Ground Water **2010**, 494-514.

A2. Supplimental materials for Chapter 3 "Assessment of Carbon Dioxide Utilization as a Carbon Management Strategy for Coal-Fired Power Plants"

1. **Supplementary Life Cycle Methods**

Results for the six large-scale CO_2 utilization options are shown in Figure 2 of the paper for a functional unit of one million tonnes (Mt) of captured CO_2. The marginal change in GHG emissions from BAU for each CO_2 utilization pathway represents the change from a scenario where power plants do not adopt CCS and industries do not replace their current processes with captured CO_2 utilization processes. Details on the life cycle methodology for each option are included in this section.

The annual greenhouse gas (GHG) emissions from life cycle stages for each CO_2 utilization option were modeled using a consequential life cycle approach. Consequential life cycle assessment (C-LCA) uses system expansion to account for the environmental changes that result from the product- or process-life cycle under assessment. In C-LCA, life cycle stages that are identical to those in the business as usual (BAU) scenario are not included because they do not contribute a change in environmental impacts. For example, if the process for making dry ice is the same regardless of the source of CO_2, then the emissions associated with producing the dry ice manufacturing equipment would be excluded because their existence is not scenario-dependent.

The GHG emissions associated with the production of captured CO_2 were modeled using the method described in Sathre & Masanet for coal fired power plants (CFPP) retrofitted with amine-based CCS technology, and for new CCS-capable CFPP.[1] Life cycle stages associated with producing CO_2 include: coal mining and transport, plant infrastructure production, non-fuel consumables production, and CO_2 transport and geologic sequestration in saline aquifers (Figure S1). Life cycle stages for geologic sequestration were not included for CO_2 utilization options that did not require CO_2 recompression and injection. We modeled CFPP in the business as usual scenario (BAU) by interpolating annual values from five year GHG emissions data, provided in Table S6 in Sathre and Masanet.[1]

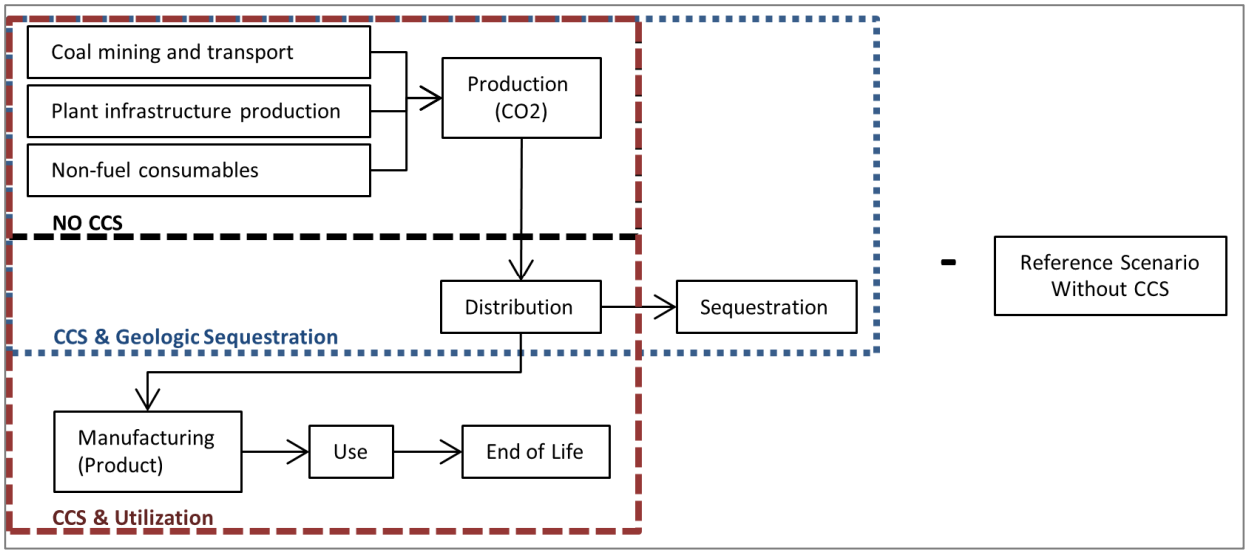


Figure S1. System Boundaries for the life cycle assessments of three scenarios.

Our estimates for the annual demand for captured CO_2 by CO_2 utilization markets were bound by the maximum rate of captured CO_2 supply from CCS deployment through retrofits and fleet turnover, detailed in Sathre & Masanet. We assumed that retrofitted power plants would supply CO_2 to utilization markets and that future CCS-ready power plants would have access to saline aquifer storage sites. The mass of captured CO_2 at power plants is not equivalent to the mass of avoided CO_2 emissions (Figure S2). Carbon dioxide capture requires energy, which leads to an increase in coal consumption. The efficiency of CO_2 capture technology is expected to improve over time at bituminous and sub-bituminous CFPP. We interpolated the CO_2 capture energy penalty (EP) for each year from 2020 to 2065 using the medium EP data provided for bituminous and sub-bituminous coal power plants in Sathre and Masanet in Table S1. We found that EP will decrease from 32 to 21% for scenario A1 (CFPP are retrofitted and new CFPP perform CCS) and from 28 to 21% for scenario A2 (only new CFPP perform CCS).

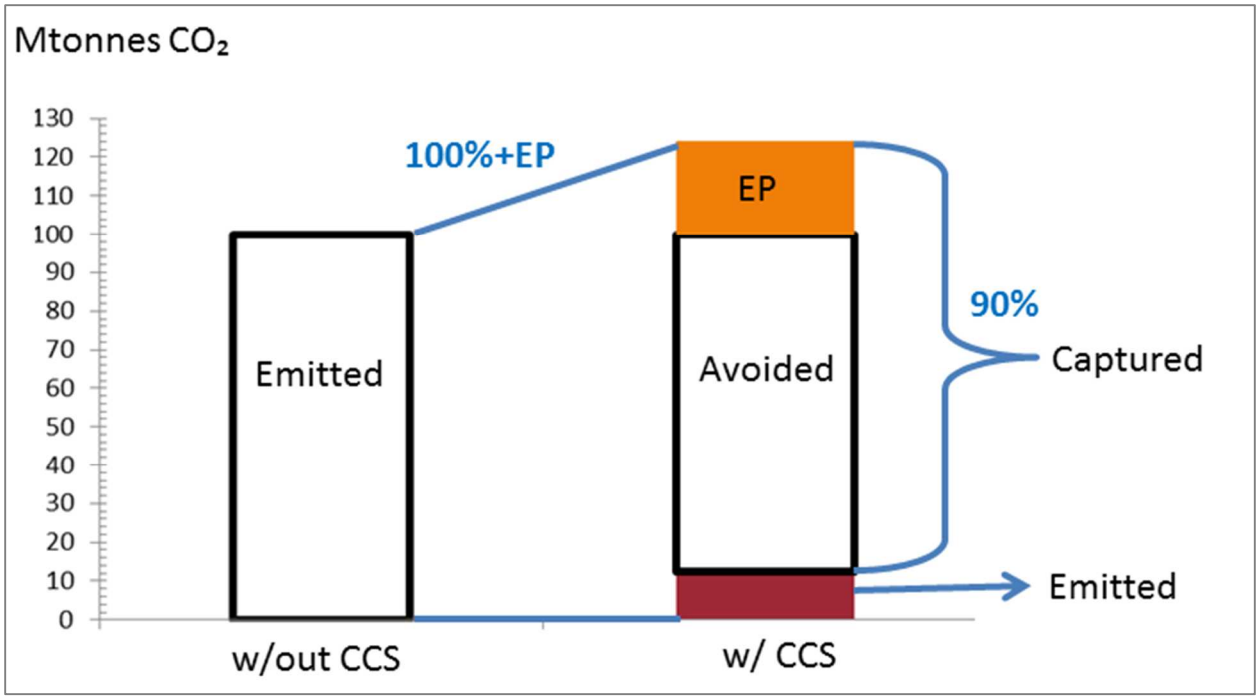


Figure S2. Conceptual diagram showing how CO_2 emissions change with CCS adoption and are accounted for. The example shown is for a hypothetical power plant that initially emits 100 Mt of CO_2 and installs CO_2 capture equipment with 90% capture efficiency. The energy penalty (EP) is a function of time, but is shown as 24%.

The GHG emissions from 155 miles of pipeline transportation from CFPP to saline aquifers were used to represent the emissions from pipeline transportation from power plants to oil, gas, or coalbed fields. We assumed that methanol and urea production facilities were co-located with power plants. This may not be the case, but the specific placement of future utilization facilities was outside the scope of this paper. The technology needed to purify the CO_2 stream was also considered outside the scope of this paper.

1.1 Conversion Factors

To simplify the study, a representative utilization process was selected for each application based on data availability and sustainability indicators such as lowest net energy use. We hen developed CO_2-to-product conversion factors (CF) for these manufacturing processes. These CFs allowed us to determine low, base case, and high estimates for the mass of CO_2 needed to produce a given unit of product (ex: X tonnes of CO_2 to produce Y tonnes of methanol). Table S1 lists relevant assumptions, including the percentage of CO_2 that is captured in the product and the percentage of CO_2 that is emitted during the use of the product. Conversion factors were developed to convert annual production volumes of products to annual demand for captured CO_2 (*Equation S1*).

$$CO2_i = V_i(t) * CF_i \qquad S1$$

where CO_{2i} is the mass of CO_2 needed to make product i (tCO_2), i represents the product that uses CO_2 as a material input, V_i is the volume of the product produced over a time step t (one year for this analysis), and CF_i is the conversion factor for product I, with units of (tCO_2/unit_product). These CFs are also useful for estimating the mass of product that one power plant could produce (Figure S3).

Table S1. CO_2-to-product conversion factors and CO_2 material balance data. Conversion factors include efficiency adjustments. Sources of CO_2 include industrial CO_2 (Ind CO2) and geologic CO_2 (geo CO2). Details are included in Section 1 for large-scale uses and Section 2 for small-scale uses.

CCUS Options	Conversion Factor LOW	Conversion Factor MED	Conversion Factor HIGH	Units of Conversion Factor (mt CO2 per)	Chemical Avoided:	% Demand Sequestered During Manufacturing	% Demand Emitted During Product Use	Retention Time [yr]
Enhanced Oil Recovery	8.2E-02	1.1E-01	1.4E-01	bbl oil	Water; Ind/Geo CO2	90	0	1000+
Enhanced Gas Recovery	1.5E-02	3.3E-02	5.1E-02	cf natural gas	Ind/Geo CO2	90	0	1000+
Enhanced Coalbed Methane Recovery	4.4E-02	6.0E-02	7.6E-02	cf CH4	Ind/Geo CO2	90	0	1000+
PM-Compressed Air Energy Storage	8.0E-01	1.2E+00	1.6E+00	project	Ind/Geo CO2	100	0	1000+
Dry Ice	1.8E+00	1.9E+00	2.0E+00	m^3 dry ice	Ind CO2	80 to 100	100	0
Decaffeination	4.9E-02	7.6E-01	1.5E+00	mt decaf coffee	Ind CO2	90	0	0
Carbonated beverage	1.1E-05	1.2E-05	1.3E-05	gal water	Ind CO2	90	100	0.5
15 lb-Net Fire Extinguisher	2.3E-03	2.4E-03	2.5E-03	extinguisher	Ind CO2	90 to 100	100	5
DME (bireforming)	5.3E-02	1.0E-01	1.5E-01	bbl DME	Reformed Methane	50 to 75	100	0.5
Methanol (cat hydrolysis)	1.9E+00	3.1E+00	4.4E+00	mt MeOH	Reformed Methane	20 to 50	100	1
Ethylene (methanol cat)	4.6E-04	1.0E-03	1.6E-03	bbl CH2CH2	Reformed Methane	15 to 46	0	1000+
Propylene (methanol cat)	7.0E-04	1.6E-03	2.4E-03	bbl CH2CHCH3	Reformed Methane	15 to 46	0	1000+
Urea	8.9E-01	1.1E+00	1.3E+00	mt urea	Reformed Methane	50 to 75	100	0.5
Ethylene Carbonate (EC)	7.1E-01	8.5E-01	9.9E-01	mt EC	Ind CO2	50 to 70	100	0.5 to 1000+
Propylene Carbonate (PC)	6.5E-01	7.5E-01	8.6E-01	mt PC	Ind CO2	50 to 66	100	0.5 to 1000+
Algae Biofuel	4.8E-02	6.7E-02	8.5E-02	gal biodiesel		40 to 60	100	1
Mineral Carbonates	3.7E-01	4.7E-01	5.6E-01	mt carbonate	Ind CO2	50 to 75	0	1000+

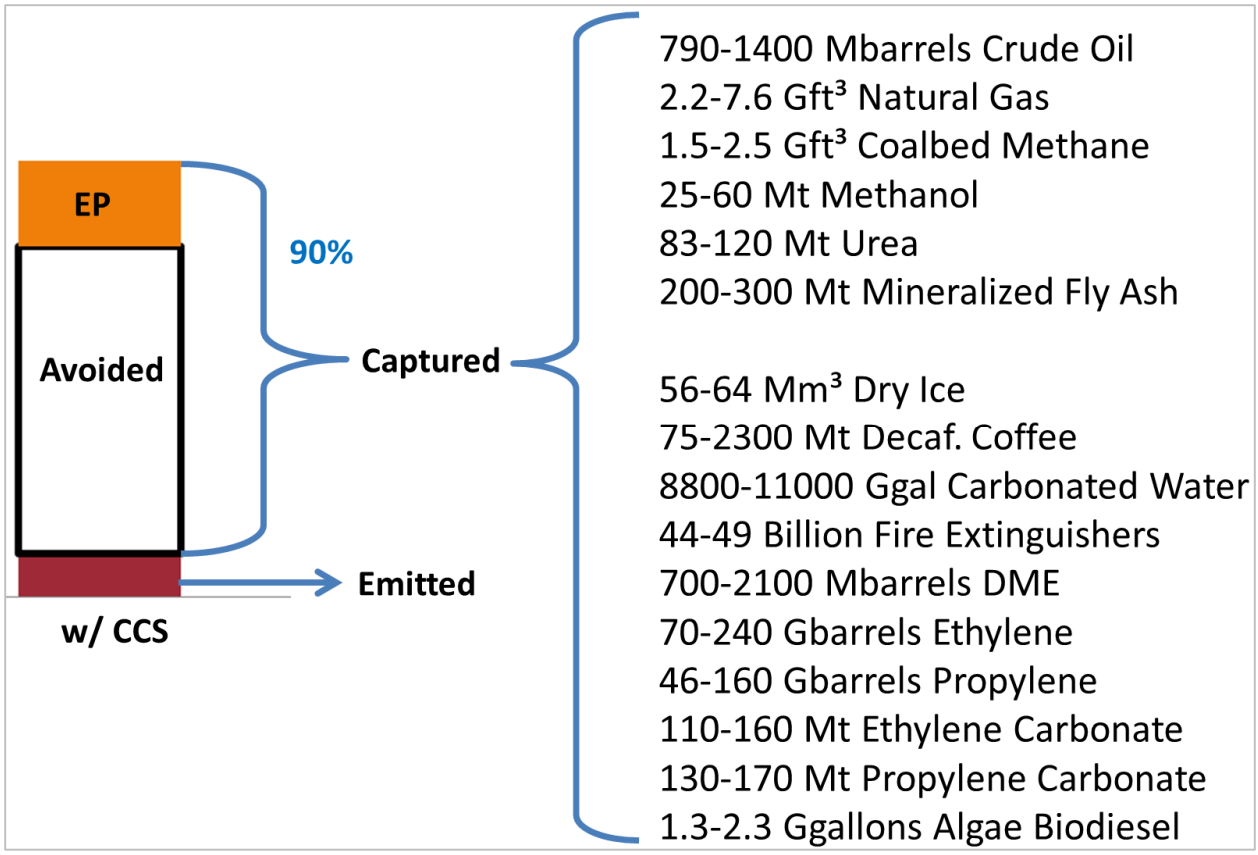


Figure S3. Conceptual diagram showing the amount of each product from CO_2 utilization that could be produced from 111.6 Mt of captured CO_2 (as described in Figure S2). These values assume that the power plant directs all of its captured CO_2 to one of 16 product options and does not incur an energy penalty for CO_2 utilization.

1.2 Enhanced Oil Recovery

Depleted oil reservoirs can be used for geologic sequestration without enhanced oil recovery (EOR). In this analysis, we modeled CO_2 stored during the years of active EOR to distinguish between utilization processes and sequestration-only processes. We assumed that 100% of CO_2 supplied to current EOR projects comes from geologic CO_2 reservoirs and active oil and gas projects;[2] this assumption was assessed in our sensitivity analysis. In this study, geologically sourced CO_2 is replaced with CCS captured CO_2. Therefore the emissions from the extraction and transportation of CO_2 from geologic sources were counted as avoided greenhouse gas emissions. The GHG emissions for CO_2 recompression, and the construction and operation of wells were not included in our system boundary for the same reason. We assumed CO_2 is recovered from the extracted oil and recycled back for further EOR with a 90% capture efficiency (Figure S4). This loss would already occur at EOR projects using geologically sourced CO_2. Although the plume of CO_2 may take years to appear at the oil production wells for new EOR sites, we assumed the CO_2 appeared within one year of injection.

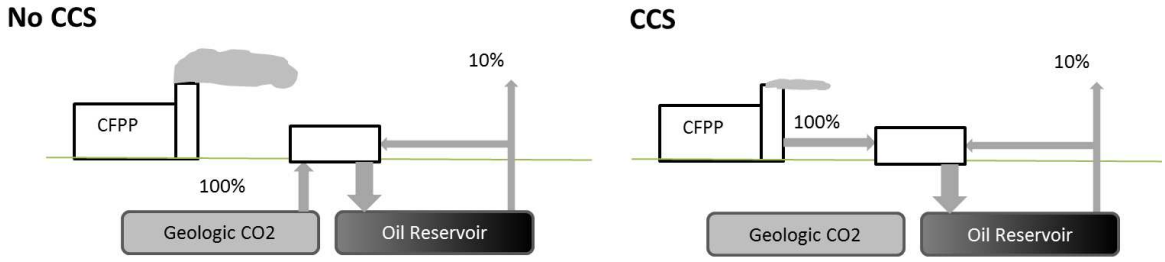


Figure S4. Conceptual diagram of CO_2 supply to EOR, with and without CCS.

CO_2 remains in a supercritical state (density of 467 kg/m^3) at 73.8 bar, the pressure found at depths near 800m. Typical CO_2 densities range from 467 to 800 kg/m^3 at depths between 800 and 3000m. We assumed the density of crude oil is 873 kg/m^3 (density of oil in Texas at 60°C). Assuming a 1:1 volume displacement of CO_2 to oil, we found 0.54 to 0.92 kg CO_2 is required to displace 1 kg of oil. This is equivalent to 0.07 to 0.13 tCO_2/barrel oil. The IPCC report found that 0.26 to 0.32 tCO_2/barrel oil could be sequestered through EOR.[3] This higher ratio may be due to the fact that EOR is performed in reservoirs that are mostly depleted, so CO_2 must be injected for much longer in order to reach the oil bank. We found that 0.08 to 0.14 tCO_2/barrel-oil are required during the EOR process when we assumed a 90% CO_2 recovery at the oil production well.

1.3 Enhanced Gas Recovery

We assumed that enhanced gas recovery (EGR) from depleted gas seams would displace other methods of natural gas extraction. We modeled BAU natural gas extraction using the life cycle assessment from Spath and Mann.[4] CO_2 transportation, recompression, and injection well construction and operation were calculated using the method described in Sathre & Masanet. Typical densities of natural gas range from 162 to 320 kg/m^3 at depths ranging from 800 to 3000 meters. Assuming a 1:1 volume displacement of CO_2 to methane, we estimated that 2.5 to 2.9 tCO_2 will displace one tonne of natural gas.[5] As much as 6.25 to 10 tCO_2 may be sequestered per

tonne natural gas in mature gas fields.[6] The energy requirements for CO_2 injection and for natural gas extraction were estimated from Khoo and Tan 2006 as 5-6 kWh/tCO_2 injected and 38 kWh/t natural gas produced.[7] Emissions from the transmission, storage, and processing of the natural gas were assumed to be the same as traditional natural gas extraction. Fugitive emissions, and emissions from pneumatic control devices, engines, and turbines associated with extraction and pipeline transportation were also assumed to be the same.[4]

1.4 Enhanced Coalbed Methane Recovery

Enhanced coalbed methane recovery (ECBM) is an emerging technology that involves the injection of CO_2 into depleted or unmineable coalbeds to stimulate the production of methane. CO_2 transportation, recompression, and injection well construction and operation were calculated using the method described in Sathre & Masanet. Energy requirements were calculated using the method described for EGR. At least a 3:1 volume displacement of CO_2 to methane is expected to occur because CO_2 preferentially adsorbs to coal over methane. Given this displacement ratio, 8.6 to 14.8 t CO_2 will displace one t methane.[5] We assumed a 90% capture efficiency of the CO_2 from the natural gas stream.

1.5 Feedstock Applications

Natural gas is commonly used in industry as a source of carbon. Natural gas is scrubbed to remove sulfur and then sent through a steam-reforming step to produce syngas. This syngas is reacted with air to produce H_2 and CO_2.[8-10] In theory, captured CO_2 could replace natural gas-sourced CO_2 in the production of: urea, olefin, methanol, ethylene carbonate, propylene carbonate, and dimethyl ether (DME). We assumed solar-powered water-splitting hydrogen systems were built to supply the hydrogen in chemical production, previously supplied from natural gas.

We used the life cycle of steam-reformed natural gas-sourced hydrogen from Spath and Mann to model the GHG emissions associated with life cycle stages in the BAU scenario. The life cycle includes the production and transportation of natural gas, electricity generation, and the production of the hydrogen facility. In Spath and Mann, net GHG emissions were 11.9 $kgCO_2e/kgH_2$, with 10.6 $kgCO_2e/kgH_2$ attributed to the natural gas production stage.[4] We chose an emission factor of 2 $kgCO_2e/kgH_2$ for solar-powered water splitting, and 4 $kgCO_2e/kgH_2$ for water splitting powered by electricity from the average national grid.[11] The effect of varying these emission factors was explored in our sensitivity analysis.

1.6 Urea

Urea (NH_2CONH_2) is used as a source of nitrogen in agriculture and as a raw material for resin and yeast production. Nitrogen gas from air and hydrogen are reacted on an iron catalyst to produce ammonia (NH_3) – this is called the Haber process (Equation S2). CO_2 and water are removed prior to ammonia synthesis. The CO_2 and NH_3 are then sold to industries and urea plants. The excess CO_2 from this process is a significant source of CO_2 emissions in the US. These emissions would be significantly reduced if renewably-sourced hydrogen was supplied to the ammonia production process. However, with the adoption of hydrogen, the urea industry would require an alternative source of CO_2, which we assume would be supplied by power plants with CCS capabilities.

The upstream and operation life cycle phases of ammonia production were modeled using the method in Wood and Cowie (1.5 $kgCO_2e/kgNH_3$).[12] Greenhouse gas emissions associated with the life-cycle of solar-sourced hydrogen production and the air reformer were included. We assumed the following process for urea synthesis is the same regardless of the source of CO_2. Therefore, life cycle stages associated with the production, granulation, and shipment of urea were not included.

Urea synthesis is produced through a two-step process (Equation S3-S4). Ammonia and CO_2 are fed into a reactor at a high temperature and pressure. The urea concentration is increased by recycling the degradation products of unreacted ammonium carbamate, NH_3, and CO_2. Concentrations up to 99.6 percent can be achieved prior to granulation.[13]

$N2 + 3H2 \rightarrow 2NH3$	Haber process	S2
$2NH3 + CO2 \rightarrow NH2COONH4$	ammonium carbamate synthesis	S3
$NH2COONH4 \rightarrow H2O + NH2CONH2$	urea synthesis	S4

Theoretically, for every gram of urea produced, 0.67 grams of CO_2 are consumed. A yield range of 50 to 75% was assumed for this study.

When urea is applied to moist ground, it is hydrolyzed into ammonia and CO_2. Nitrosomonas use the energy gained from oxidizing ammonia to nitrite to sequester CO_2 as biomass. Since urea is likely to be applied to crops used for food or fuel, the captured CO_2 will eventually enter the atmosphere as CO_2 (and some CH_4 and CO) via combustion, exhalation, or volatilization. We assumed a 6 month retention time for capture CO_2 in the product.

1.7 Methanol

Methanol can be used as a feedstock in the production of chemicals, as a transportation fuel, and as a hydrogen carrier. The process of synthesizing methanol from natural gas consumes roughly 10 GJ of energy per tonne of methanol, and has CO_2 emissions range from 1.15 to 1.6 tCO_2/t methanol.[14-16]

In this study, methanol is produced when CO_2 is hydrogenated in a one step process using a copper- or zinc-based catalyst with pure H_2 gas (Equation S5). In this process, 1.38 grams of CO_2 are consumed for every gram of methanol produced. With an efficiency ranging from 20 to 50%, we estimate that the process requires ~1.9 to 4.4 tCO_2/t methanol.

$$CO2 + 3H2 \rightarrow CH3OH + H2O \qquad \text{catalytic hydrogenation} \qquad \text{S5}$$

Cifre and Badr estimated that the production of methanol from captured CO_2 and renewably sourced H_2 would have life-cycle emissions of 0.8tCO_2/t methanol.[14] The authors note that 50% of the emissions are attributed to the upstream carbon capture process. In theory, 0.2 tonnes of H_2 are needed for each tonne of methanol. We find that 0.8 tCO_2e/t methanol would be associated with the solar production of hydrogen alone. We assumed that methanol would be produced regardless of CCS adoption, so the emissions from the combustion of methanol were not included. We assumed the residence time of CO_2 in the product was approximately 6 months if methanol was used as a transportation fuel, or as a feedstock in the production of DME or olefins.

1.8 Mineralization of Fly Ash

Silicate weathering is a natural process that sequesters CO_2 over geologic time scales. The hydrolysis of metal oxide containing minerals occurs when CO_2 dissolved in water comes in contact with the mineral. Equation S6 demonstrates how CO_2 is involved in the hydrolysis of olivine.

$$Mg2SiO4 + 4CO2 + 4H2O \rightarrow 2Mg^{2+} + 4HCO_3^- + H4SiO4 \quad \text{silicate weathering} \quad \text{S6}$$

Mineral carbonation is an emerging technology whereby captured CO_2 is reacted with divalent-metal-oxide containing minerals on shorter time scales to form insoluble inorganic carbonates.[17] The chemistry for magnesium oxide and calcium oxide are shown in Equations S7-S10 and Equations S11-S12, respectively. In wet-carbonation, the process is designed so that the metal

ions react with carbonic acid, precipitate, and are filtered out of solution so that unreacted metal ions may be recovered.

$Mg2SiO4 \rightarrow 2MgO + SiO2$	step 1	S7
$2MgO + 2H2O \rightarrow 2Mg(OH)2$	step 2	S8
$2Mg(OH)2 + 2CO2 \rightarrow 2MgCO3 + 2H2O$	step 3	S9
$Mg2SiO4 + 2CO2 \rightarrow 2MgCO3 + SiO2$	net reaction	S10

Calcium, magnesium, or iron containing silicates, and alkaline wastes from the power and industrial sectors, are the most commonly proposed mineral feedstocks. Calcium silicate can be found in high concentrations in CFPP fly ash and bottom ash, in waste cement, and in stainless steel slag. Fly ash is comprised of CaO (25-35 wt%), SiO_2 (20-40 wt%), MgO (0.5-8 wt%) and other residuals of coal combustion.[18]

$CaO + H2O \rightarrow Ca(OH)2$	step 2	S11
$Ca(OH)2 + CO2 \rightarrow CaCO3 + H2O$	step 3	S12

We assumed that fly ash has a 30% CaO and 4.3% MgO composition. In theory, when this fly ash reacts with water and CO_2 to produce carbonates it consumes 0.28 tCO_2/t fly ash and produces 0.63 tonnes of solid carbonates (0.54 $tCaCO_3$, 0.089 $tMgCO_3$). We assumed a 50 to 75% CO_2 conversion efficiency.

There is a small international market for inorganic carbonates (~8 Mt/y).[3] Therefore, inorganic carbonate products from CO_2 utilization and sequestration may need to be sent to storage sites, mines, or landfills if market demand is low in a given year.[3] The avoided GHG emissions attributed to the extraction of mined inorganic carbonates were calculated using the EIO-LCA tool for lime and gypsum product manufacturing (Sector 3274A0) and by selecting the GHG contributions from "other nonmetallic mineral mining" (Sector 212390). We assumed a tonne of lime costs $100 and that it takes 1.8 tonnes of calcium carbonate to produce a tonne of lime. We assumed that the energy required during the mineralization of fly ash was supplied by the power plant and the solid waste was transported 10 miles by diesel fueled trucks. The energy demand for processing the fly ash, 140 kWh/tCO_2, was calculated by adjusting the values provided by the IPCC for olivine mineralization. The energy associated with mining and pretreating olivine was subtracted from the life cycle energy input assuming a 90% carbonation conversion and 10% losses in the clarifier. For every tonne of fly ash originally sent from a power plant to a landfill, 2.6 tonnes of inorganic carbonate would require transportation. The emissions from the transportation phase were calculated using the method developed in Facanha et al.[19]

Although the reaction is spontaneous at low temperatures and pressures, the rate is slow due to the limited diffusion of CO_2. Emerging catalysts may help to achieve carbonation on a reasonable time scale.[17] For example, a peptoid catalyst that mimic proteins used in bio-carbonation may improve the reaction rate of calcium carbonation.[20] We assumed that mineralization is not time-constrained by the year of deployment and varied the year of deployment from 2020 to 2035 in our sensitivity analysis.

2. Small Scale Processes

Small-scale CO_2 utilization processes include compressed air energy storage CO_2 buffering and the production of carbonated beverages, dry ice, CO_2 fire extinguishers, olefins, organic carbonates, dimethyl ether, algae biodiesel, and CO_2 supercritical caffeine extraction. Details on the technical, market, and life cycle analysis for each process are included in the following sections. Assumptions regarding technology diffusion rates are listed in Table S2.

Table S2. Percent of product markets met by CO_2 utilization technologies, increasing from 2020 to 2065, in the conservative, moderate, and upper-bound scenarios. *Fractions represent annual growth in technology in reference to the upper-bound scenario. **Fraction represents the number of project sites brought online in the study period, where one project is brought online every ten years.

CO2 utilization application	conservative	moderate	upper-bound
consumer products	0 to 25%	1 to 50%	100%
dry ice	0 to 25%	1 to 50%	100%
organic carbonates	0 to 25%	1 to 50%	100%
olefins: ethylene and propylene	1% to 5%	1% to 20%	100%
dimethyl ether*	50% slower	25% slower	100%
algae biodiesel*	50% slower	25% slower	100%
PM-CAES**	none	begin in 2030	30%

Unfortunately, we found little or no data for several consumer products and chemicals beyond 2015. For these products we made a simple assumption that the main driver for annual growth is population growth.

Current CO_2 Demand

The production of carbonated beverages, CO_2 fire extinguishers, and the use of CO_2 for supercritical fluid extraction of caffeine from coffee beans were assessed. We assumed that 90% of the CO_2 supplied to current CO_2 demand applications comes from natural gas refining facilities, and 5% comes from ammonia production facilities. These CO_2 flows would be emitted to the atmosphere regardless of whether captured CO_2 was supplied to the current CO_2 demand applications (Figure S5). The remaining 5% of CO_2 supply was assumed to come from geologic CO_2 reservoirs. These fractions were estimated based on the CO_2 supplied to EOR and industries in 2006.[2] The deconstruction of current CO_2 supply pipelines was not included in this study. We did not include CO_2 cleaning stages due to data limitations. We believe this would not have a significant effect on the results since the treatment processes necessary to get captured CO_2 from power plants and industry to food-grade quality are likely to be similar. In practice, captured CO_2 may be scrubbed of impurities like water to avoid corrosion and meet pipeline standards.[54]

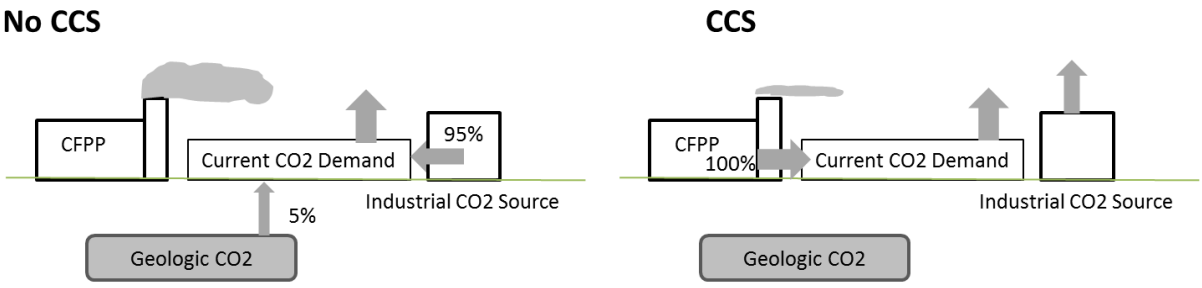


Figure S5. Conceptual diagram of CO_2 supply to current CO_2 demand technologies, excluding EOR, with and without carbon dioxide capture and sequestration (CCS).

2.1 Supercritical Fluid Extraction: Decaffeination

Supercritical Fluid Extraction (SFE) is the process whereby an extract is separated from a matrix using a supercritical fluid. This process is used to remove unwanted components, separate a component for experimental purposes, or extract marketable products like essential oils, flavors, and fragrances. The largest demand for CO_2 as an extraction agent is coffee decaffeination. Manufacturers in the US define decaffeinated roasted coffee beans as having 97% less caffeine. Supercritical extraction is commercially feasible at large scale; in 1999, this meant product at an annual capacity of at least 3000 tons per year.[22] We used coffee decaffeination to represent the SFE application due to the availability of market and technical data.

A regular cup (16 oz or 473.18 mL) of coffee may have between 190 – 270 mg of caffeine per ounce ($C_8H_{10}N_4O_2$).[23] The most commonly used bean, *Coffea arabica*, has a 1.2% caffeine composition.[22] The solubility of caffeine in liquid CO_2 improves if the CO_2 is saturated with water or blended with a polar co-solvent like ethanol.[24] The caffeine composition of *C. arabica* beans can be reduced to 0.08% using a water-saturated CO_2 stream. We estimated that a green coffee bean weighing 0.171 g has 2 mg of caffeine. Based on the range of solubility given in Figure 2 of Kopcak & Mohamed, we determined that extracting 1.99 mg (0.01mmol) of caffeine per bean would require between 0.3 and 9 grams of CO_2.[24] Twenty-one to 630 grams of CO_2 are required to produce one cup of decaffeinated coffee assuming ~70 beans are used (16 oz water is 473.18g). We calculate that 0.05 to 1.4 tonnes of CO_2 per tonne of decaffeinated liquid coffee is required when we assumed a 90% efficiency.

We assumed decaffeination would occur regardless of CCS. Therefore, we did not include life cycle phases associated with the transportation of the decaffeinated beans, with the consumption of coffee, or with the production of necessary materials and machinery. The residence time of CO_2 in the product is zero. The avoided GHG emissions attributed to the extraction and transportation of geologic-sourced-CO_2 were calculated using the EIO-LCA tool for coffee decaffeination (Sector 311920), assuming decaffeinated coffee cost $15/lb.[25]

The US Food and Drug Administration estimated that in 2009 the US population consumed 184.5 mg of coffee-sourced caffeine per day.[26] Using the median 1.65% caffeine content for coffee beans, we estimated an annual consumption of 3.8 kg caffeinated-coffee per capita. We

assumed that 75% of coffee consumed in the US was also processed in the US and that 5% of all coffee consumption was decaffeinated.

2.2 Dry Ice

Dry ice, or solid CO_2, has roughly twice the cooling power of regular ice per pound. It is used to cool products, especially in shipping containers where it replaces electric refrigeration. Commercial dry ice has a density between 1.4 and 1.6 g/cm^3. The avoided greenhouse gas emissions attributed to the current extraction and transportation of CO_2 for dry ice production were calculated using the EIO-LCA tool for soft drink and ice manufacturing (Sector 32110) assuming dry ice cost $70/lb. We assumed that dry ice would be produced regardless of whether CO_2 was captured at power plants. Therefore, we did not include life cycle phases associated with the transportation of dry ice. Dry ice is typically made with food-grade CO_2, but we did not include the process for scrubbing the CO_2 of impurities. We assumed the residence time of CO_2 in dry ice is zero since dry ice sublimates rapidly. Finally, we assumed the conversion efficiency varied from 80 to 100%. Approximately 72490 tonnes of dry ice were sold in 2007.[27]

2.3 Carbonated Beverages

Carbonated beverages are fluids that have been injected with pressurized CO_2. All the CO_2 escapes to the atmosphere shortly after the beverage is opened and consumed. No data was found on the mass of CO_2 required for various beverages, so we used the solubility of CO_2 in water at 10°C (2.5 g CO_2 per kg water) as a low estimate and 3 g CO_2 per kg water as a high estimate. The residence time of CO_2 in beverage containers is on the order of six months. We assumed that carbonated beverages would be produced regardless of carbon capture. Therefore, we did not include life cycle phases associated with the transportation of the carbonated beverages, or with the production of the materials in the container. The avoided GHG emissions attributed to the extraction and transportation of geologic-sourced-CO_2 were calculated using the EIO-LCA tool for soft drink and ice manufacturing (Sector 32110), assuming a 12 oz carbonated beverage cost one dollar.

Per capita soft drink consumption is expected to decline from 38.6 gallons in 2013 to 36.7 gallons in 2018.[28] This decline reflects the projected increase in the price of corn and sugar products and increasing consumer demand for health-conscious purchases. We assumed that consumption would continue to decline by 1% per year. We held per-capita consumption of non-soft drinks constant. According to the United States Census Bureau, in 2009, 48.1 gallons of carbonated beverages were consumed per capita; this number includes carbonated water, soft drinks, enhanced waters, and energy drinks.[29]

2.4 Fire Extinguishers

Fire extinguishers are pressurized containers filled with an inert agent like CO_2. A typical 15 lbs extinguisher has about 5 lbs of liquid CO_2. At 850 psi and room temperature, the CO_2 has a density of 781.4 kg/m^3 (1.72 lb/L). The CO_2 is released into the atmosphere when the container is used to control a fire or when the extinguisher is emptied and tested during routine

maintenance. We assumed that all fire extinguishers not used to fight fires are properly maintained and emptied every five years with a 75% compliance.

The avoided GHG emissions attributed to the extraction and transportation of geologic-sourced-CO_2 were calculated using the EIO-LCA tool for whole sale trade (Sector 420000), which includes fire extinguishers (Sector 4239905), assuming a 15 lb fire extinguisher costs $320. We assumed that fire extinguishers would be produced regardless of CCS. Therefore we did not include life cycle phases associated with the production of materials in the container, or with the transportation of the fire extinguishers.

Fire extinguisher production is driven by the number of fires and by the growth and decline of the construction sector; production is expected to increase 3.1% by 2017.[30] The US Fire Administration (USFA) published fire statistics showing that the number of residential-building cooking fires rose 3% from 2007 to 2011, while residential-building electrical malfunction fires, heating fires, and smoking fires dropped 3%, 5%, and 3%, respectively.[31] There were a total of 244,900 residential fires in 2011. Residential outnumber non-residential fires 3:1 according to the USFA. Outdoor and vehicle fires were not included. There were 132,452,405 housing units in 2012 according to the US census bureau; we assumed that housing units would grow with population.

2.5 Methanol-Sourced Organic Carbonates

Organic carbonates are heavily oxidized cyclic and linear molecules.[33] Organic carbonates can be used as solvents in lithium ion batteries, as substitutes for toluene as a solvent in painting processes, and as fuel additives to improve the octane value of gasoline and to reduce particulate emissions from light oils. Ethylene carbonate (EC), propylene carbonate (PC), dimethyl carbonate (DMC), and diphenyl carbonate (DPC) are marketable organic carbonates that can be produced using CO_2.[34] DMC, the simplest organic carbonate, was classified by the EPA as VOC-exempt in 2009, and it has become popular as a substitute for VOC classified solvents like butanone. Also, it has replaced several toxic reagents like dimethyl sulfate and methyl chloroformate. Ethylene carbonate, DMC, and DPC can replace the toxic compound phosgene ($COCl_2$) in the production of polycarbonates and polyurethanes.

There are a number of alternative reaction pathways for forming organic carbonates, but most start with either epoxides or phosphine as a substrate and require the presence of a catalyst to achieve significant yields. Progress has been made toward replacing these toxic substrates with more benign compounds like CO_2, and to develop catalysts with higher activity.

CO_2 and methanol will react in the presence of metal complexes to form linear carbonates like DMC (Equation S13). In addition, the process using CO_2 does not generate hydrogen chloride, but water. Yields as high as 88% have been achieved in the presence of a tin catalyst and acetals. Theoretically, this process would consume 0.49 grams of CO_2 per gram of DMC.

$$CO2 + 2CH3OH \rightarrow OC(OCH3)2 + H2O \qquad \text{DMC synthesis} \qquad \text{S1}$$

CO_2 and the epoxide ethylene oxide are reactants in the synthesis of cyclical EC (Equation S14). Yields have been measured around 70%.[34,35] This would require 0.71 g CO_2 to produce 1 gram of EC, as opposed to the theoretical yield of 1 gram of EC per 0.5 grams of CO_2. Ethylene carbonate can be reacted further with methanol to produce DMC, as can cyclic PC (Equation S15). Propylene oxide and CO_2 react to form PC in the presence of a catalyst like zinc halide or aluminum-salen (Equation S16). The synthesis of PC using an aluminum-salen catalyst converted 66% of the waste CO_2 to carbonate. The theoretical yield for this process is 1 gram of PC per 0.43 grams of CO_2.

$C2H4O + CO2 \rightarrow C2H4CO3$	EC synthesis	S2
$C2H4CO3 + 2CH3OH \rightarrow OC(OCH3)2 + HOC2H4OH$		
EC transesterification for DMC synthesis		S15
$C3H6O + CO2 \rightarrow C4H6O3$	PC synthesis	S3

Ethylene carbonate and propylene carbonate are currently produced using industry-sourced CO_2. The avoided GHG emissions attributed to the extraction and transportation of geologic-sourced-CO_2 were calculated using the EIO-LCA tool for "other basic organic chemical manufacturing (Sector 325190).

Annual world production of organic carbonates is estimated to be 2.6 Mt, with EC and PC comprising approximately 90% of production.[3,36] However, DMC and DPC are not widely produced in the United States. We assumed that 10% of EC and PC production occurs in the US and that the domestic market experiences the same strong 3% annual growth as the global market.

2.6 Olefins

Steam cracking of naphtha and ethane is used to synthesis light olefins like ethylene and propylene. The synthesis of olefins from methanol is an emerging technology that has been demonstrated at pilot plants. Methanol is converted to DME, which is then converted to olefins using a catalyst. Life cycle emission ranges for producing high value chemicals (HVC), which includes both light olefins and non-olefins, were calculated by Ren et al.[16] Light olefin yields range from 15% to 46%. The energy for producing ethylene from natural-gas sourced methanol is approximately 150% higher than the state-of-the-art process using naphtha steam cracking. However, most of this energy is attributed to the production of methanol. The authors calculated the following emission factors: 1.4 tCO_2/tHVC for naphtha, 1.05tCO_2/tHVC for ethane, 1.5-1.7 tCO_2/tHVC for methanol. Between 0.35 to 0.45 tCO_2 were attributed to the production of HVC, while the rest was allocated to the production of methanol. The GHG emissions calculated for the production of methanol from captured CO_2 and solar-sourced hydrogen were used in our analysis. We assumed that HVC would be produced regardless of CCS adoption, so the emissions from the combustion of HVC were not included. We assumed that the residence time of CO_2 in the product is 6 months.

In 2012, 1.8 million barrels of ethylene and 101.3 million barrels of propylene were produced.[39] Demand for petrochemicals like ethylene and propylene is expected to rise by 2.8% through 2018 as demand for rubber and plastics rise. The volatility of raw materials will limit the

construction of production facilities to areas near oil fields and petroleum hubs. Little information could be found regarding future projections due to the volatile nature of the petroleum industry. Since olefin production is driven by demand for building products, we modeled a conservative growth trend that used the B2 population growth model.[64]

2.7 Dimethyl Ether

Dimethyl ether (DME) is an emerging low-carbon and low-particulate-matter diesel alternative. Although DME is expected to be manufactured from natural gas feedstocks, it is theoretically possible to produce DME from CO_2-sourced methanol. When methanol is converted into olefins, it is first converted into DME. This process emits 0.35 to 0.45 tonnes of CO_2 per tonne of high value chemical.[16] We used the lower value to approximate the GHG emissions associated with converting methanol to DME (0.68 tCO_2/tDME). DME can be produced through three different production pathways: a two-step, a one-step, and a liquid-one-step process called bireforming. DME is typically produced through a two-step process where syngas is converted to methanol, which is then converted to DME. The most common processed used in Japan, Korea, and China is a single step process. This DME synthesis step merges the methanol formation, dehydration and water-gas shift reaction. If methane is used instead of syngas, methane is converted to syngas through a methane-dry-reforming step prior to DME synthesis. We assumed the conversion efficiency ranged from 40 to 75 percent. An emerging third process for DME production is called bireforming. Metgas is a syn-gas with a 2:1 H_2:CO mix, designed to optimize methanol production. Metgas is produced through a methane-steam-reforming and methane-dry-reforming step. These steps are followed by methanol formation and methanol dehydration. The water from methanol dehydration is used to supply the methane-steam-reforming step. For every one gram of DME produced, 0.48 grams of CO_2 are consumed. Since no CO_2 is emitted during bireforming, theoretically, we chose this process for our analysis.

While gasoline is expected to decrease out to 2040, diesel is expected to increase. In 2015 an estimated 0.1 million barrels per day of non-petroleum diesel will be produced. We took 1 million barrels per year as the starting point for DME production in 2020 and followed the projected trend for advanced renewable fuels in California from 2000-2040.[29] California is currently in the process of approving DME as a transportation fuel. We assumed a 2.3% annual growth rate out to 2065, using the average advanced renewable fuels growth in California from 2030 to 2040.

2.8 Algae Biodiesel

Lipid-rich algae can be harvested to produce biomass and biodiesel that can offset hydrocarbon consumption.[40] Algae are grown in bioreactors or ponds, so algae fuel does not compete with crops for fertile land. Some lipid-rich species of algae can be grown in wastewater or saline water and most algae species can take advantage of highly concentrated CO_2 as a source of carbon. Carbon dioxide is introduced into the ponds from the air and from concentrated injections of carbon dioxide.[41] The combustion of fossil fuels releases carbon that was stored underground. The combustion of algae fuels releases CCS-captured carbon and carbon from the air that was sequestered through photosynthesis.

The mass of CO_2 captured by the algae will depend on the design of the pond, the alkalinity of the water, and the species of algae. Benemann estimated that algae with 5 to 10% solar energy conversion efficiencies would capture 66 to 131 tC/ha/y.[42] Campbell et al. estimated between 170 and 200 tCO_2/ha/y (46 to 55 tC/ha/y) should be supplied to algae with 30 g/m^2/d dry-weight productivity.[43] Using these values, we estimate that two grams of CO_2 should be supplied for every one gram of expected biomass. Yields equivalent or greater than 30 g/m^2/d have only been achieved under laboratory conditions. Pate et al. calculated similar productivity yields for large-scale production scenarios in the Southwest (31 g/m^2/d), Midwest (19-21 g/m^2/d), and Southeast (21-25 g/m^2/d) of the US.[44] Even under optimal conditions, CO_2 would not be captured during the night or in regions with cold winters.

Algae biodiesel and biomass production requires electricity and heat. Shirvani et al. assessed the sensitivity of CO_2 emissions associated with the well to wheel (WTW) life cycle of algae biodiesel to the carbon intensity of electricity and heat sources.[45] The WTW emissions are roughly 100 gCO_2eq/MJ fuel if the electricity for biodiesel refining is supplied by a CFPP without CCS and if the heat is supplied by natural gas. For comparison, the WTW emissions for diesel are 88 gCO_2eq/MJ fuel. Coal-sourced electricity has an average carbon intensity of 280 g CO_2/MJ. We estimated the LCA carbon intesity of a CFPP with CCS to be between 50 and 70 g/MJ.[1,46] A simple calculation for a 1000MW CFPP with a 64% capacity, 34% CCS energy penalty, and 90% CO_2 capture capacity gives a carbon intensity of 53 gCO_2/MJ. We assumed a carbon intesity of 70g/MJ for electricity generated from a CFPP with CCS. Using the sensitivity analysis from Shirvani et al., we determined the WTW of algae fuel to be 95 g/MJ. If heat was provided by a renewable source, this value would drop to 50 g/MJ.

Our study modeled algae oil as having a density of 0.87 g/l and energy density of 1000 MJ per 24 kg biodiesel. We assumed 5.93 kg dry of biomass gives 1 kg of diesel.[47]

A 2009 study by the national renewable energy laboratory (NREL) placed algae diesel as a long-term fuel opportunity due to very high production barriers associated with the process technology.[48] US domestic production of biodiesel was 132 million gallons in October of 2013, however the US could have an annual capacity of 2.2 billion gallons.[49] Projections estimate that 1.15 billion gallons of biomass-based advanced diesel could be produced annually.[60] We assumed 1 million gallons of algae biodiesel were produced using captured CO_2, starting in 2022. We used the advanced renewable fuels trends in California from 2022 to 2040 to model market growth. Annual growth out to 2065 was approximated by calculating the average growth from 2030 to 2040, 2.3%.[38]

2.9 Compressed Air Energy Storage

Compressed air energy storage (CAES) is a novel emerging energy storage technology whereby renewable energy is used to compress and inject air into salt deposit caverns during off-peak hours when energy prices are cheap.[50] The air is released to power turbines to generate electricity during peak periods or during periods when wind and solar power are not available.

Simulations of porous media CAES (PM-CAES) show that a large fraction of the gas volume injected into the formation is never recovered. This gas is referred to as the cushion air. It is

possible that CO_2 could be injected prior to air injection and CAES operation as a form of carbon sequestration.[51] The opportunities and constraints for using CO_2 as a cushion gas are discussed in Oldenburg et al.
We assumed that there would be no leakage of CO_2 out of the formation and that CO_2 could be used in salt caverns shaped to reduce air-CO_2 mixing. The transportation and storage of captured CO_2 were modeled following the method used in Sathre and Masanet. We assumed 1.2 Mt of CO_2 would be injected per project, prior to operation. In the upper-bound scenario, 10 project sites (a third of the 31 identified sites) were utilized by 2065, with an addition of one project every five years, starting in 2030.

In this analysis, the air compressors are powered by solar and wind-sourced electricity and do not contribute CO_2 emissions. The compressed air powers a 100MW system of natural gas turbines for 3 hours each day with an efficiency of 60%. This high efficiency was chosen because the compressor and the turbine are separate in a CAES system. We assumed the energy content of natural gas is 1030 Btu/ft^3 and that 100% of the carbon in natural gas is converted to CO_2.[52] These assumptions were used to calculated an emission factor for CAES electricity. We estimated that CAES electricity emits 0.42 kg CO_2/kWh. This is lower than the average emission factor for electricity from a natural gas power plant (0.635 kgCO_2/kWh).[53] We assumed that CAES-sourced electricity replaced grid-electricity. Weber et al. used data from the Energy Information Agency (EIA) Egrid database from 2005 to calculate a US average of 0.69 kgCO_2/kWh.[11]

3. Supplementary Market Projection Methods

Market projections were developed for: oil extracted using CO_2-enhanced recovery, natural gas from gas wells, coalbed methane, urea, and methanol. Current domestic production values and projected annual growth rates were acquired from market and government databases, and from literature.

In 2010, an estimated 281,269 barrels of oil per day (BOD) were extracted using EOR.[54] We used the Energy Information Administration's (EIA) projected annual growth for CO_2-EOR from 2012 to 2040, and extended the growth expected from 2035 to 2040 out to 2065.[55] It is important to note that the EIA is known for reporting conservative estimates on future demand.

Currently, only a few pilot projects use CO_2 for enhanced gas recovery in the United States. There were 12,736,678 million cubic feet (MCF) of gross withdrawals from gas wells (not tight plays or oil wells) in 2012.[56] We used the projected trend from the EIA Annual Energy Outlook 2013 to model the natural gas market out to 2040, then extended the data to 2065 assuming a 1.3% annual growth rate. This is the average rate of growth of dry natural gas production from 2011 to 2040.[58] The United States produced 1,539,395 MCF of methane from coalbeds in 2012. We assumed the same annual growth rates as natural gas production out to 2065.

Values for methanol production in the US vary from 712,000 tonnes to 7.8 Mt in 2006.[59-60] All forecasts show methanol production increasing, with expected production ranging from 4 to 16 Mt in 2020. This growth is based on proposed projects for methanol production facility development and on an average drop in natural gas prices. We took the lower value as the starting point in 2015 and modeled annual growth out to 2065 using the growth rate from our natural gas projections. Natural gas is the primary cost component of ammonia production (75-90% of total cost).[61] Between 90 and 107 Mt of urea are produced annually in the world, and approximately 12 million nutrient tons of nitrogenous fertilizer were used in the US in 2008.[3,9,61] Assuming this fertilizer is supplied as urea, and urea is 45% N, this equates to ~24 Mt of urea consumption. The market is expected to grow by as much as 3.2% annually as the price of natural gas decreases and the demand for food and crop biofuels increases.[62]

We found little data on the total US market for inorganic carbonates. As an upper bound, we assumed that 57% of fly ash from CFPP was available for CO_2 utilization; this is the fraction currently sent to landfills. The mass of fly ash available for mineralization was determined by multiplying the mass of fly ash in year zero (2020) by the percent change in coal consumption for CCS adoption scenarios.[1] This method captured the increase in fly ash that would occur with increased coal consumption due to CCS and the decrease in fly ash that would occur as CFPP retired.

In our conservative and moderate scenarios, 1% of this fly ash was converted to inorganic carbonates in the first year. This resulted in 1.6 Mt of calcium and magnesium carbonate production, which is roughly 20% of the estimated global inorganic carbonate market in 2005. In our upper-bound scenario, we assumed that 100% of the available fly ash was converted to inorganic carbonates. This assumption resulted in a production volume that exceeded current market demand; in this scenario we assumed excess carbonate products were transported to

storage sites for later use. The assumption that the carbonate products were not utilized immediately did not have a significant effect on the results of this study. This is because the GHG emissions that would be offset from calcium carbonate mining were negligible compared to other life cycle contributions, such as the energy-related emissions that occurred at the CFPP for mineralization.

4. Supplementary Technology Diffusion Methods

In the upper-bound scenario, enhanced oil recovery, urea synthesis, methanol synthesis, and fly ash mineralization were modeled to reflect a future where 100% of annual product demand is met by manufacturing processes that use captured CO_2. Market demand for captured CO_2 was calculated by determining the mass of CO_2 needed to meet the projected annual product demand. However, we assumed competition with hydraulic-fracking would prevent 100% market penetration of CO_2 utilization in gas recovery. For this reason, we modeled diffusion for enhanced gas recovery and ECBM as linear growth from 1 to 10% from 2020 to 2065.

Several factors were involved in constructing technology diffusion scenarios that we believe are in the 50^{th} or 90^{th} percentile of what is possible. For example, when we evaluated enhanced oil recovery, we determined that it is a mature technology, it has little competition with other manufacturing processes, and it generates a product that has steady or growing demand. Based on these factors, we believe that a future where 15% of domestic oil is produced using captured CO_2 for EOR is in the 50^{th} percentile of what is plausible.

The fraction of projected annual domestic demand for captured CO_2 met by different applications is shown in Figure S6a,c,e for all three scenarios. In our moderate scenario, over 65% of the total CO_2 demand is met by EGR, despite the fact that only 3% of the natural gas market is met using captured CO_2 EGR techniques. Urea synthesis and EOR consume more CO_2 over time as the markets for urea and oil grow with population growth and as CO_2 utilization technologies realize a greater market penetration. The CO_2eq sequestered each year as a result of CO_2 utilization is lower than the demand for CO_2 due to manufacturing inefficiencies, and losses or emissions associated with each technology's life cycle (Figure S6b,d,f). The values decrease in 2065 for the upper-bound scenario because the mass of CO_2 supplied from CFPP is restricted by the rate of power plant retirements and carbon capture efficiency improvements.

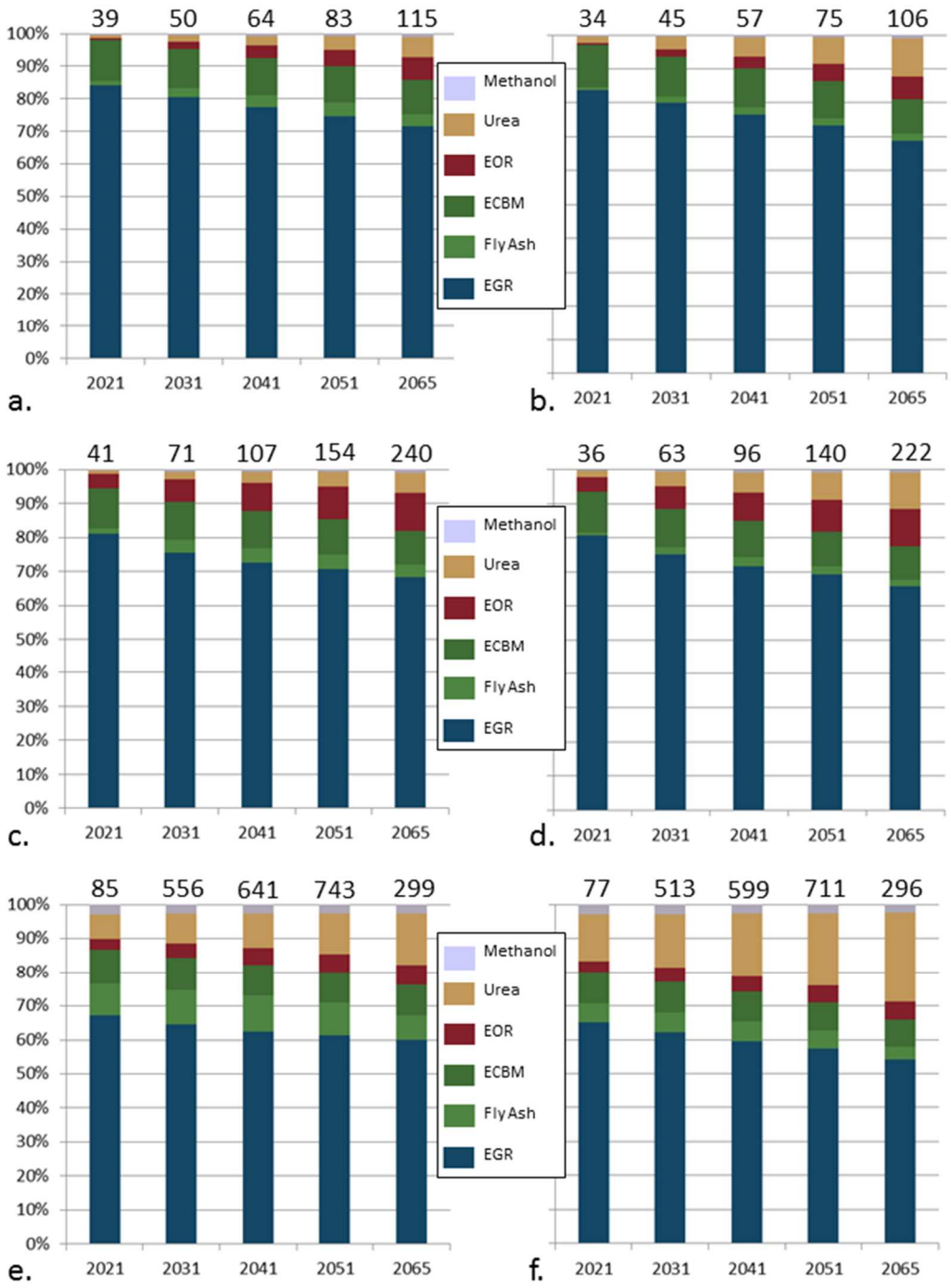


Figure S6. (a, c, e) Market demand for captured CO_2 and (b, d, f) the annual CO_2eq sequestered for technologies at different time steps of their life cycle for the conservative, moderate, and upper-bound scenarios, respectively, using base case conversion factors. Contributions are presented as a fraction of the total for that year. Totals are given in MtCO_2eq above bar graphs.

5. Radiative Forcing Model

Reducing GHG emissions and increasing permanent CO_2 storage are needed to reduce global warming. Near term, temporary storage is also important because it delays CO_2 releases, thus decreasing the length of time that CO_2 molecules reside in the atmosphere and absorb radiation over a finite time-period. Conversely, substantial GHG emissions released early in a time-period could cause irreversible sea-level rise and damage to ecosystems that are vulnerable to global warming. The difference in the cumulative radiative forcing (CRF) of the BAU scenario and the CO_2 utilization scenarios is a valuable indicator of what climate change mitigation can be achieved over a span of time.

The annual GHG emissions time profiles for CO_2 utilization life cycle scenarios were converted into CO_2 equivalents (CO_2e) emissions. We modeled the emissions from each year as pulse and used an atmospheric decay function to determine the mass of CO_2 remaining in the atmosphere over time (*Equation S17*).

$$CO2_t = CO2_0 * [0.217 + 0.259e^{\frac{-t}{172.9}} + 0.338e^{\frac{-t}{18.51}} + 0.186e^{\frac{-t}{1.186}}] \quad S17$$

where t is the number of years since the pulse emission, CO_{2t} is the mass of CO_2 remaining in the atmosphere in year t, and CO_{20} is the mass of CO_2 emitted in year zero. The parameters in *Equation S17* are a function of the global atmospheric concentration of CO_2, but we have kept them constant in this study.

These mass time profiles were converted to concentration time profiles assuming the molecular mass of air is 28.95 $gmol^{-1}$ and the mass of the atmosphere is 5.148 x 10^{21} g.[14] Concentration profiles were then converted to radiative forcing (*Equation S18*).

$$F_{CO2} = \frac{3.7}{\ln(2)} * ln\left\{1 + \frac{\Delta CO2}{CO2_{ref}}\right\} \quad S18$$

where F_{CO2} is the instantaneous radiative forcing [W/m^2], ΔCO_2 is the change in the atmospheric concentration of CO_2 [ppmv], and CO_{2ref} is the atmospheric concentration of CO_2 in the year 2015, assumed to be 400ppmv. CO_{2ref} will vary with the global atmospheric concentration changes, but it is often kept constant. The CRF that occurred over each year was estimated by integrating the time-dependent radiative forcing (F_{CO2}) over the time step in seconds.

6. Supplementary Results for Spatial Analysis

The locations and CO_2 storage potential of oil and gas formations and coalbeds were mapped using data from the NATCARB GIS database.[63] Only formations that were listed as suitable for CCS were included in the study.

Power plant specific time profiles for CCS retrofitting were developed for two scenarios. The first scenario assumes that coal fired power plants with the largest name plate (NP) capacities, built before 2020, would be retrofitted first. Power plants were retrofitted, starting with the largest NP capacity (>1400MW), according to the year CO_2 utilization built up enough demand to utilize 100% of the power plant's captured CO_2. Figure S7 shows time profiles for the conservative and moderate CO_2 utilization scenarios, where 10 and 26 power plants were retrofitted by 2065, respectively.

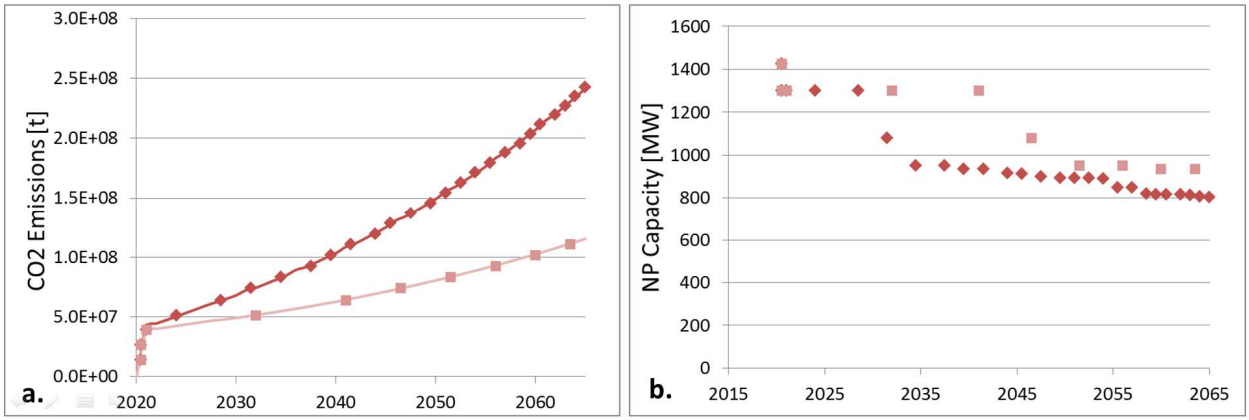


Figure S7. Timeline of power plants retrofitted where the power plants with the largest NP capacity before 2020 are retrofitted first. Rate of CCS-retrofitting that would match CO_2 demand from the moderate (red) and conservative (pink) scenarios.

In our second scenario, power plants built before 2020, and with NP capacities greater than 15MW, were retrofitted by age, where new plants were retrofitted before older plants. This scenario was used in Sathre and Masanet. Figure S8 shows time profiles for the conservative and moderate CO_2 utilization scenarios. For these scenarios 108 and 169 power plants were retrofitted by 2065.

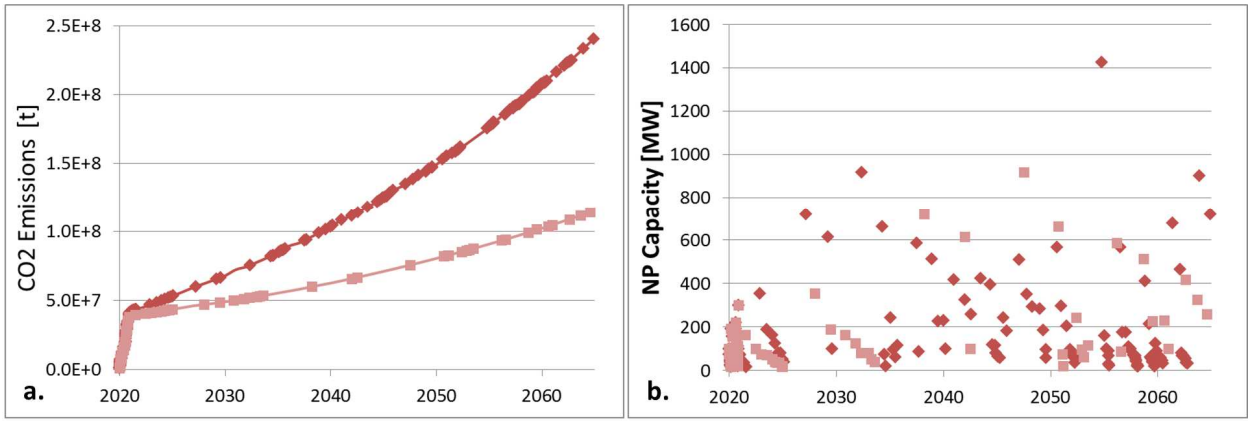


Figure S8. NP Capacity of power plants retrofitted under assumption where newest power plants, built before 2020, are retrofitted first. Rate of CCS-retrofitting that would match CO_2 demand from the moderate (red) and conservative (pink) scenarios.

We mapped the locations of retrofitted power plants, by deployment year, in ArcGIS using the first scenario. We assumed that larger power plants would have the economies of scale to build the first pipelines and oil and gas extraction sites. The captured CO_2 was directed to nearby CO_2 utilization options until 75% of the storage capacity was reached (Figure 6).

7. Supplementary Sensitivity Analysis

Nine variations were made to our three base case CO_2 utilization scenarios to assess the sensitivity of cumulative CO_2 demand, cumulative CO_2 sequestration, and avoided cumulative radiative forcing (CRF) to variable uncertainty (Table S3).

1. The addition of small-scale CO_2 utilization applications had a negligible effect on the results. For most applications, this was due to the limited size of product markets and the negligible residence time of CO_2 in products. In some cases, like dimethyl ether and algae biodiesel, the product market had the potential to grow, but the life-cycle net carbon savings were negligible.
2. Replacing base case conversion factors with low or high factors (Table S1) had a significant effect on all three metrics.
3. The projected rate at which coal fired power-plants are retrofitted significantly constrained the upper-bound scenario. Ignoring this constraint resulted in a 6% increase in avoided CRF. This would be possible if other sources of CO_2, such as natural gas power plants, captured CO_2 in the future.
4. Delaying the deployment of EGR and ECBM by 15 years decreased cumulative CO_2 demand by 15% and decreased avoided CRF by 28% for the moderate scenario.
5. Delaying the adoption of fly ash mineralization by 15 years had a negligible effect on the three metrics.
6. In this study, we used the three county-level population projection scenarios developed by the U.S. Department of Agriculture Forest Service for the 2010 RPS Assessment, with the A1 scenario as our base case. We used linear interpolation to determine annual growth from the 5 year interval data. Substituting the A2 and B2 population growth models for our base case A1 model had a negligible effect.[31]
7. Carbon dioxide is currently supplied to markets by limekilns, fermentation, ammonia production facilities, natural gas reforming facilities, geologic formations, and industrial gas providers. We did not find adequate data on the allocation of CO_2 from these suppliers to various markets. However, we found that the majority of CO_2 for enhanced oil recovery currently comes from geologic sources; a small fraction of EOR sites are supplied by ammonia and natural gas processing plants. The majority of CO_2 for markets applications comes from industrial sources. We assumed that 90% of CO_2 currently consumed by dry ice, supercritical fluid extraction, carbonated beverage, fire extinguisher, ethylene carbonate, and propylene carbonate production is supplied by industry. Varying this fraction from 50 to 100 percent had a negligible effect on the cumulative radiative forcing of the moderate scenario.
8. A source of hydrogen is required if captured CO_2 is used to produce methanol, ethylene, propylene and urea. Presently, steam-reformed natural gas processing supplies both hydrogen and carbon to these industries and emits 12 $kgCO_2/kgH_2$. In this analysis, we assumed that a co-located facility would provide hydrogen via solar-powered electrolysis (2 $kgCO_2/kgH_2$). If hydrogen facilities used grid electricity instead of solar power, then 4 kg of CO_2 would be emitted per kg of H_2.[11] This change resulted in a 2% decrease in the CRF of the upper-bound scenario.
9. Changing the CO_2 leakage rate from saline aquifers from zero to one percent had a significant effect (27%) on the CRF of geologic CO_2 sequestration. This compares well with the sensitivity analysis performed in Sathre & Masanet.

Table S3. Sensitivity analysis of key assumptions.

Base Case	Variation	Cumulative CO_2 Demand [Mt CO_2]	Cumulative Sequestration [Mtonnes CO_2e]	Cumulative Radiative Forcing [MW s/m^2]
Upper-bound base case		**25,403**	**-17,336**	**-13.1**
without small-scale uses	with small-scale uses	0%	0%	0%
medium conversion factor	low conversion factor	-46%	-33%	-38%
medium conversion factor	high conversion factor	78%	28%	28%
constrained by CO2 supply	unconstrained by CO2 supply	19%	14%	6%
EGR amd ECBM deployed in 2020	EGR and ECBM deployed in 2035	-19%	-17%	-26%
mineralization deployed 2020	Mineralization deployed in 2035	-2%	0%	0%
100% of CO2 currently supplied to EOR is extracted	50% supplied from oil and gas production (would be emitted in BAU)	0%	-4%	-3%
Population Growth follows A1 Scenario from RES 2010 study	A2, B2	0%,0%	0%,0%	0%,0%
Hydrogen is produced from renewably-sourced electricity	H2 produced from average grid electricity	0%	-5%	-5%
Moderate base case		**5,594**	**-3,662**	**-2.0**
without small-scale uses	with small-scale uses	1%	0%	0%
medium conversion factor	low conversion factor	-57%	-53%	-52%
medium conversion factor	high conversion factor	78%	72%	69%
constrained by CO2 supply	unconstrained by CO2 supply	0%	0%	0%
EGR amd ECBM deployed in 2020	EGR and ECBM deployed in 2050	-15%	-14%	-28%
mineralization deployed 2020	Mineralization deployed in 2035	-1%	0%	0%
100% of CO2 currently supplied to EOR is extracted	50% supplied from oil and gas production (would be emitted in BAU)	0%	-7%	-6%
Population Growth follows A1 Scenario from RES 2010 study	A2, B2	0%,0%	0%,0%	0%,0%
Hydrogen is produced from renewably-sourced electricity	H2 produced from average grid electricity	0%	-2%	-2%
Conservative base case		**3,179**	**-2,067**	**-1.2**
without small-scale uses	with small-scale uses	1%	0%	0%
medium conversion factor	low conversion factor	-59%	-55%	-55%
medium conversion factor	high conversion factor	87%	76%	100%
constrained by CO2 supply	unconstrained by CO2 supply	0%	0%	0%
EGR amd ECBM deployed in 2020	EGR and ECBM deployed in 2050	-21%	-19%	-36%
mineralization deployed 2020	Mineralization deployed in 2035	-1%	0%	0%
100% of CO2 currently supplied to EOR is extracted	50% supplied from oil and gas production (would be emitted in BAU)	0%	-3%	-3%
Population Growth follows A1 Scenario from RES 2010 study	A2, B2	0%,0%	0%,0%	0%,0%
Hydrogen is produced from renewably-sourced electricity	H2 produced from average grid electricity	0%	-2%	-2%

8. References

(1) Sathre, R.; Masanet, E. Long-Term Energy and Climate Implications of Carbon Capture and Storage Deployment Strategies in the US Coal-Fired Electricity Fleet. *Environ. Sci. Technol*. **2012**, *46*, 9768–9776.

(2) *Inventory of U.S. Greenhouse Gas Emissions and Sinks: 1990-2011.* EPA 430-R-13-001; U.S. Environmental Protection Agency: Washington, DC, **2013**; www.epa.gov/climatechange/downloads /ghgemissions/us-ghg-inventory-2013-main-text.pdf.

(3) *Chapter 7: Mineral carbonation and industrial uses of carbon dioxide*, by Marco Mazzotti; IPCC special report on carbon dioxide capture and storage; Intergovernmental Panel on Climate Change, **2005**; https://www.ipcc.ch/pdf/special-reports/srccs/srccs_chapter7.pdf.

(4) *Life Cycle Assessment of Hydrogen Production via Natural Gas Steam Reforming,* by Pamela L. Spath and Margaret K. Mann; DOE/NREL/TP-570-27637; National Renewable Energy Laboratory: Golden, CO, **2001**.

(5) *Geology and Coal Resources of the Livingston Coal Field, Gallatin and Park Counties, Montana*, by Albert E. Robert; Professional Paper 526-A; U.S. Geological Survey: Washington, DC, **1966**.

(6) Oldenburg, C.; Stevens, S.; Benson, S. Economic feasibility of carbon sequestration with enhanced gas recovery (CSEGR). *Energy* **2004**, *29*, 1413–1422.

(7) Khoo, H.H.; Tan, R.B.H. Life cycle investigation of CO_2 recovery and sequestration. *Environ. Sci. Technol*. **2006**, *40*, 4016-4024.

(8) Centi, G.; Iaquaniello, G.; Perathoner, S. Can We Afford to Waste Carbon Dioxide? Carbon Dioxide as a Valuable Source of Carbon for the Production of Light Olefins. ChemSusChem. **2011**, *4*, 1265–1273.

(9) Markewitz, P.; Kuckshinrichs, W.; Leitner, W.; Linssen, J.; Zapp, P. et al. Worldwide innovations in the development of carbon capture technologies and the utilization of CO_2. Energy Environ. Sci. **2012**, *5*, 7281-7305.

(10) Olah, G.A.; Prakash, G.K.S.; Goeppert, A. Anthropogenic Chemical Carbon Cycle for a Sustainable Future. *J. Am. Chem. Soc.* **2011**, *133*, 12881–12898.

(11) Weber, C.L.; Jaramillo, P.; Marriott, J.; Samaras, C. Life cycle assessment and grid electricity: what do we know and what can we know? *Environ. Sci. Technol.* **2010**, *44*, 1895–1901.

(12) *A Review of Greenhouse Gas Emission Factors for Fertiliser Production* by Sam W. Wood and Annette Cowie; International Energy Agency (IEA) Bioenergy Task 38, **2004**. www.ieabioenergy.com.

(13) Copplestone, J.C.; Kirk, C.M. Ammonia and Urea Production. In *Chemical Processes in New Zealand*; New Zealand Institute of Chemistry: Christchurch, New Zealand **1998**; http://www.nzic.org.nz/ChemProcesses/production/index.html.

(14) Galindo Cifre, P.; Badr, O. Renewable hydrogen utilisation for the production of methanol. *Energy Convers. Manag.* **2007**, *48*, 519–527.

(15) Olah, G.A.; Goeppert, A.; Prakash, G.K.S. *Beyond Oil and Gas: The Methanol Economy*; John Wiley & Sons, Inc. **2009**.

(16) Ren, T.; Patel, M.K.; Blok, K. Steam cracking and methane to olefins: Energy use, CO_2 emissions and production costs. Energy. **2008**, *33*, 817–833.

(17) Khoo, H.H.; Bu, J.; Wong, R.L.; Kuan, S.Y.; Sharratt, P.N. Carbon capture and utilization: Preliminary life cycle CO_2, energy, and cost results of potential mineral carbonation. *Energy Procedia*. **2011**, *4*, 2494–2501.
(18) Styron, R.W. (Mineral Resource Technologies, Llc). Fly ash composition. US Patent 6,251,178 B1, 2001.
(19) Facanha, C.; Horvath, A. Environmental Assessment of Freight Transportation in the U.S. *Int. J. Life Cycle Assess*. **2006**, *11*, 229–239.
(20) Chen, C.-L.; Qi, J.; Zuckermann, R.N.; DeYoreo, J.J. Engineered Biomimetic Polymers as Tunable Agents for Controlling CaCO3 Mineralization. *J. Am. Chem. Soc*. **2011**, *133*, 5214–5217.
(21) Choi, Y.-S.; Nesic, S.; Young, D. Effect of Impurities on the Corrosion Behavior of CO_2 Transmission Pipeline Steel in Supercritical CO_2−Water Environments. *Environ. Sci. Technol*. **2010**, *44*, 9233–9238.
(22) Ramalakshmi, K.; Raghavan, B. Caffeine in Coffee: Its Removal. Why and How? *Crit. Rev. Food Sci. Nutr.* **1999**, *39*, 441–456.
(23) McCusker, R.R.; Goldberger, B.A.; Cone, E.J. Caffeine content of specialty coffees. *J. Anal. Toxicol.* **2003**, *27*, 520–522.
(24) Kopcak, U.; Mohamed, R.S. Caffeine solubility in supercritical carbon dioxide/co-solvent mixtures. *J. Supercrit. Fluids.* **2005**, *34*, 209–214.
(25) Carnegie Mellon University Green Design Institute. (**2013**) Economic Input-Output Life Cycle Assessment (EIO-LCA) US 2002 (428) model [Internet], Available from: www.eiolca.net. [Accessed 7 Aug, 2013].
(26) *Caffeine Intake by the U.S. Population; Subcontract# 70000073494* by Somogyi, L.P.; The Food and Drug Administration; Oakridge National Laboratory; **2010**.
(27) Gas World Website; www.gasworld.com
(28) *Per Capita Soft Drink Consumption;* IBIS*World* Business Environmental Profiles; IBIS*World*, 2013.
(29) Andreyeva, T; Chaloupka, F.J.; Brownell, K.D. Estimating the potential of taxes on sugar-sweetened beverages to reduce consumption and generate revenue. *Prev. Med*. **2011**, *6*, 413-416.
(30) *Fire Extinguisher Manufacturing;* IBIS*World* Industry Report OD5062; IBIS*World*, **2012**.
(31) U.S. Fire Administration (FEMA) Website; Fire Statistics; Residential Fire Trends. www.usfa.fema.gov/statistics.
(32) U.S. Census Bureau Website. www.census.gov (accessed January 2014).
(33) Shaikh, A.-A.G.; Sivaram, S. Organic carbonates. *Chem. Rev*. **1996**, *96*, 951–976.
(34) Sakakura, T.; Kohno, K. The synthesis of organic carbonates from carbon dioxide. *Chem. Commun.* **2009**, (11), 1312-1330.
(35) Schäffner, B.; Schäffner, F.; Verevkin, S.P.; Börner, A. Organic Carbonates as Solvents in Synthesis and Catalysis. *Chem. Rev*. **2010**, *110*, 4554–4581.
(36) Pacheco, M.; Marshall, C.L. Review of dimethyl carbonate (DMC) manufacture and its characteristics as a fuel additive. *Energy Fuels*, **1997**, *11*, 2-29.
(37) *Annual Energy Outlook 2013; Figure 102. U.S. motor gasoline and diesel fuel consumption, 2000-2040; DOE/EIA-0383*. U.S. Energy Information Administration: Washington, DC, **2013**; www.eia.gov/forecasts/aeo.

(38) *Annual Energy Outlook 2013; Figure 101. Consumption of advanced renewable fuels, 2011-2040; DOE/EIA-0383*. U.S. Energy Information Administration: Washington, DC, **2013**; www.eia.gov/forecasts/aeo.
(39) *Short-term energy outlook; U.S. Petroleum and other liquids*; U.S. Energy Information Administration, Washington, DC; http://www.eia.gov/forecasts/steo/report/us_oil (accessed August 2013).
(40) Sander, K.; Murthy, G.S. Life cycle analysis of algae biodiesel. *Int. J. Life Cycle Assess*. **2010**, *15*, 704–714.
(41) Singh, A.; Olsen, S.I. A critical review of biochemical conversion, sustainability and life cycle assessment of algal biofuels. *Appl. Energy*. **2011**, *88*, 3548–3555.
(42) Benemann, J.R. Utilization of carbon dioxide from fossil fuel-burning power plants with biological systems. *Energy Convers. Mgmt*. **1993**, *34*, 999-1004.
(43) Campbell, P.K.; Beer, T.; Batten, D. Life cycle assessment of biodiesel production from microalgae in ponds. *Bioresour. Technol.* **2011**, *102*, 50–56.
(44) Pate, R.; Klise, G.; Wu, B. Resource demand implications for US algae biofuels production scale-up. *Appl. Energy*. **2011**, *88*, 3377–3388.
(45) Shirvani, T.; Yan, X.; Inderwildi, O.R.; Edwards, P.P.; King, D.A. Life cycle energy and greenhouse gas analysis for algae-derived biodiesel. *Energy Environ. Sci.* **2011**, *4*, 3773–3778.
(46) Odeh, N.A.; Cockerill, T.T. Life cycle GHG assessment of fossil fuel power plants with carbon capture and storage. *Energy Policy*. **2008**, *36*, 367–380.
(47) Lardon, L.; Hélias, A.; Sialve, B.; Steyer, J.-P.; Bernard, O. Life-cycle assessment of biodiesel production from microalgae. *Environ. Sci. Technol.* **2009**, *43*, 6475–6481.
(48) Humbird, D. Cellulosic ethanol and advanced biofuels overview. EIA 2009 Energy Conference, April 7, 2009; www.eia.gov/conference/2009/session5/humbird.pdf.
(49) *Short-term energy outlook; Table 4a. U.S. crude oil and liquid fuels supply, consumption, and inventories*; U.S. Energy Information Administration: Washington, DC, January 2014; www.eia.gov/forecasts/steo/tables/?tableNumber=9# (accessed February 11, 2014).
(50) *Compressed air energy storage: Theory, resources, and applications for wind power* by Samir Succar and Robert H. Williams; Princeton University Energy Systems Analysis Group: Princeton, NJ, **2008**.
(51) Oldenburg, C. M.; Pan, L. Utilization of CO_2 as cushion gas for porous media compressed air energy storage. *Greenhouse Gas Sci. Technol.* **2013**, *3*, 124–135.
(52) *Emission Factor Documentation for AP-42 Section 1.4—Natural Gas Combustion*, Technical
Support Division, Office of Air Quality Planning and Standards, U. S. Environmental Protection Agency: Research Triangle Park, NC, **1997**.
(53) Jaramillo, P.; Griffin, W.M.; Matthews, H.S. Comparative Life-Cycle Air Emissions of Coal, Domestic Natural Gas, LNG, and SNG for Electricity Generation. *Environ. Sci. Technol*. **2007**, *41*, 6290–6296.
(54) Moritis, G. Special Report: EOR/Heavy Oil Survey: CO_2 Miscible, Steam Dominate Enhanced Oil Recovery Processes. *Oil and Gas Journal*. **2010,** *108*.
(55) *Annual Energy Outlook 2014; Table A14. Oil and Gas Supply, Reference Case; DOE/EIA-0383ER(2014)*. U.S. Energy Information Administration: Washington, DC, 2013; www.eia.gov/forecasts/aeo/data.

(56) *Natural Gas Gross Withdrawals and Production.* U.S. Energy Information Administration, Washington, DC, **2013**; www.eia.gov (accessed January 2014).
(57) *Annual Energy Outlook 2013 with Projections to 2040; DOE/EIA-0383.* U.S. Energy Information Administration: Washington, DC, **2013**; www.eia.gov/forecasts/aeo.
(58) *Annual Energy Outlook 2013; Table 13. Natural Gas Supply, Disposition, and Prices, Reference Case; DOE/EIA-0383*. U.S. Energy Information Administration: Washington, DC, **2013**; www.eia.gov/forecasts/aeo/data.
(59) *2013 Methanol Industry in Focus*; Methanol Institute: Alexandria, VA, **2013**; www.methanol.org/getattachment/cbafe847-88c6-4736-8823-82ac55dc9d45/2013-mile stones-final.pdf
(60) *Analysis: Cheap gas fuels North American methanol expansion* by Mukhopadhyay, B. and Krishnamurthy, K.; Reuters, **2013**. www.reuters.com
(61) *Fertilizer Manufacturing in the US*; IBIS*World* Industry Report 32531; IBIS*World*, **2013**.
(62) *Market Study: Urea; UC-3805*. Ceresana: Konstanz, Germany, **2012**. http://www.ceresana.com/en/market-studies/agriculture/urea.
(63) Carbon Storage NATCARB; www.netl.doe.gov (accessed July 2013).
(64) *Projecting County-Level Populations Under Three Future Scenarios: A Technical Document Supporting the Forest Service 2010 RPA Assessment* by Zarnoch SJ, Cordell HK, Betz CJ, Langner L.; Technical Report SRS–128. U.S. Department of Agriculture Forest Service, Southern Research Station: Asheville, NC, **2010**.

A3. Supplemental materials for Chapter 4 "Spatially-explicit life-cycle impact assessment approach for stationary proton exchange membrane fuel cell systems in the United States."

1. Heating fuels for five building types in different cities in the United States.

Table A1. Representative fraction of building heat load provided by electricity (elec), natural gas (ng), fuel oil (o), propane (p), and district heating (dh) in large hospitals and small hotels. In this analysis the same fraction is used for both water heating and space heating. Variable codes used in the excel file are listed in the top row.

Location	Lelec_s	Lng_s	Lo_s	Lp_s	Ldh_s
Minneapolis					
Large Hospitals	0%	65%	4%	0%	30%
Small Offices	19%	74%	8%	0%	0%
Small Hotels	18%	52%	4%	0%	26%
Large Offices	1%	0%	0%	80%	19%
Large Hotels	8%	91%	1%	0%	1%
Phoenix					
Large Hospitals	2%	88%	3%	0%	8%
Small Offices	16%	84%	0%	0%	0%
Small Hotels	13%	75%	12%	0%	0%
Large Offices	38%	0%	1%	0%	61%
Large Hotels	0%	100%	0%	0%	0%
Chicago					
Large Hospitals	26%	58%	1%	0%	15%
Small Offices	12%	88%	0%	0%	0%
Small Hotels	22%	66%	4%	0%	8%
Large Offices	74%	16%	0%	0%	9%
Large Hotels	5%	95%	0%	0%	0%
Miami					
Large Hospitals	31%	55%	7%	0%	8%
Small Offices	36%	58%	6%	0%	0%
Small Hotels	32%	60%	2%	0%	7%
Large Offices	79%	9%	1%	0%	11%
Large Hotels	19%	64%	1%	0%	16%
San Diego					
Large Hospitals	23%	47%	1%	0%	29%
Small Offices	16%	84%	0%	0%	0%
Small Hotels	13%	75%	12%	0%	0%
Large Offices	38%	0%	1%	0%	61%
Large Hotels	0%	100%	0%	0%	0%
New York City					
Large Hospitals	11%	57%	7%	0%	25%
Small Offices	8%	60%	32%	0%	0%
Small Hotels	24%	60%	7%	0%	9%
Large Offices	0%	67%	6%	0%	26%
Large Hotels	0%	35%	57%	0%	8%
Houston					
Large Hospitals	0%	86%	1%	0%	13%
Small Offices	23%	77%	0%	0%	0%
Small Hotels	18%	74%	0%	0%	8%
Large Offices	15%	74%	1%	0%	11%
Large Hotels	17%	81%	2%	0%	0%
National					
Large Hospitals	0%	71%	4%	0%	25%
Small Offices	0%	81%	11%	0%	8%
Small Hotels	25%	75%	0%	0%	0%
Large Offices	3%	34%	2%	0%	62%
Large Hotels	0%	89%	5%	0%	6%

2. Electricity Profiles for Local Companies

The ArcGIS geographical information system (GIS) program was used to link sources of power with the assumed installation location of fuel cell systems. Companies were identified in electrical service areas provided by Ventyx. As of 2014, Phoenix is served by two primary companies: Arizona Public Service Co. and the Salt River Project. Minneapolis is served by the Northern States Power Co (Minnesota) which recently became a subsidiary of Xcel Energy. An example of a city-specific power service area completed for Phoenix Arizona is shown in Figure A1. The city is supplied by two companies; company ownership of generators and transmission lines inside and outside the state of Arizona are color coordinated.

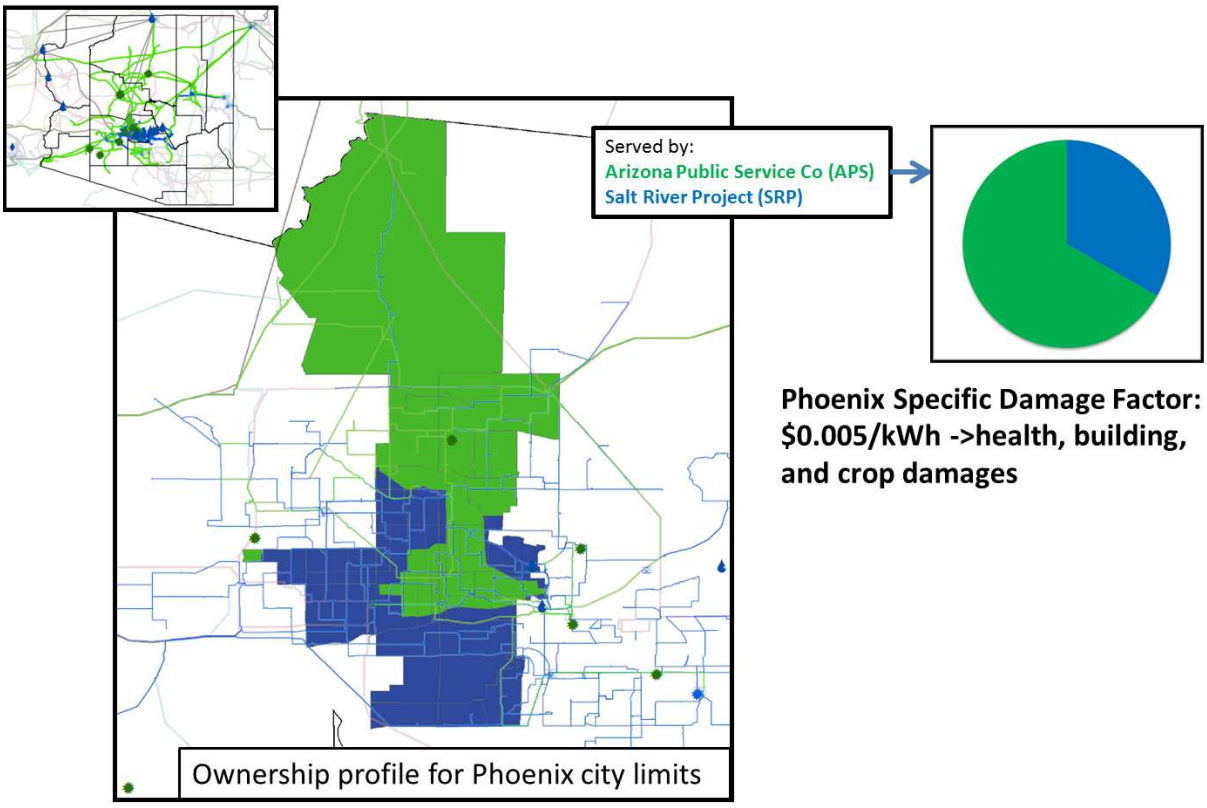


Figure A1. Power Service Area for Phoenix Arizona. Lines represent distribution and transmission lines, with blue representing capital owned by the Salt River Project and green representing capital owned by the Arizona Public Service Co. Points represent power generators (sun icons represent solar farms and drops represent hydroelectric generators). The inset shows the geospatial footprint of the two company's capital. For example, the Four Corners is the coal fired power plant in New Mexico in the upper right-hand corner of the inset. Data was gathered from Ventyx 2012, srpnet.com, and aps.com. Tear-drops indicate hydro-power and circles indicate solar power. Pie chart shows percent of annual generation provided by each company.

Census data at the county-subdivision-scale from 2010 was used to estimate the population distribution near power plants and within service areas. Power plants were linked to companies

using data from Ventyx. This information was cross-referenced and improved using data from online company profiles. Valuable information gathered includes: ownership, baseline or peak power generation, and nameplate capacity per power plant. Utility ownership and power purchases between utilities were used to allocate a generator's annual emissions to a city or locality. Annual emissions data was collected from eGRID, and from APEEP. These emissions were converted to average emission factors (L-AEF) by dividing the annual emissions by the annual generation attributed to the company (Table A2). Emissions were converted to damages using APEEP, and by assuming a social cost of carbon of $44. In principle, this approach is a general attribution method that could be scaled up nationally to generate a first approximation of a power plant's customer base.

Table A2. Damage factors and localized average emission factors for electricity use in Phoenix AZ and Minneapolis MN.

City	Average Damage Factor	Average Damage Factor for Peaker Plants	L-AEF SO2	L-AEF NOx	L-AEF PM10	L-AEF PM2.5	L-AEF CO2
	$/kWh	$/kWh	gSO2/kWh	gNOX/kWh	gPM10/kWh	gPM2.5/kWh	gCO2e/kWh
Phoenix	0.03	0.04	0.64	1.21	0.13	0.16	693.21
Minneapolis	0.05	0.05	1.86	1.70	0.05	0.09	600.10

Localized average emissions factors were compared to the average emission factors (AEF) calculated using two alternative approaches and the marginal emission factors (MEF) calculated in Siler-Evans et al and used in this dissertation (Table A3). Factors developed using the 2009 eGRID database (aggregation at the state level) were calculated by dividing total annual emissions by the total annual generation for a specific state. The L-AEF for CO_2 in Minneapolis was 25% and 19% less than those determined using Siler-Evans et al and eGRID, respectively, while the L-AEFs for CO_2 in Phoenix was 50% and 28% greater, respectively. For SO_2, the L-AEF in Minneapolis was 28% and 2% less than those determined using Siler-Evans et al and eGRID, respectively, while the L-AEFs in Phoenix was 21% and 129% greater, respectively. Finally, the L-AEF for NOx in Minneapolis was 22% and 61% greater than, while the L-AEF in Phoenix was 78% and 75% greater than the Siler-Evans et al. and eGRID approaches, respectively. It is difficult to know whether these discrepancies are due to spatial heterogeneity at the city-level that is lost when data is aggregated at the state-level or NERC-level since each approach uses a different database and set of assumptions. Siler-Evans et al., for example, uses CEMS data and did not include imports and exports of electricity in their analysis. They estimate in their supporting information that 2.7 and 2.8 percent of total generation in the MRO and WECCS region is attributed to EGUs (coal, gas, oil, biomass) not included in the CEMS database but that are included in eGRID.

Localized-AEFs were higher than the Siler-Evans et al MEF used in this dissertation. Assuming the L-AEFs are accurate, this means the avoided emissions from fuel cell adoption is underestimated in this study if the fuel cell is run near-continuously and displaces local electricity. Siler-Evans et al. also found AEFs to be greater than MEFs in these regions and cautions the use of AEFs for technologies that are run on the margin since avoided emissions would be overestimated.

Table A3. Marginal emission factors (MEF) and average emission factors (AEF) for electricity grids aggregated across spatial areas that include Phoenix and Minneapolis for CO_2, SO_2, and NOx.

		CO2 [g/kWh]			SO2 [g/kWh]			NOx [g/kWh]		
Source	Aggregation	MEF	AEF	% diff	MEF	AEF	% diff	MEF	AEF	% diff
Siler-Evans et al 2012	MRO	786	799	2	2.13	2.57	21	1.15	1.39	20
	WECC	464	462	0	0.14	0.53	280	0.26	0.68	161
L-AEF 2010	Minneapolis		600	-24		1.86	-13		1.69	47
	Phoenix		693	49		0.64	357		1.21	365
eGRID 2009	Minnesota		739	-5.9		1.89	-11		1.05	-8.7
	Arizona		540	16		0.28	100		0.69	165

Since each power plant was identified, the exact contribution of impacts from CAP emissions to the monetized damages could be determined using the APEEP model (FIGURE A2-a, A3-a). Human health impacts dominated damages, at 99% in Phoenix, and 97% in Minneapolis. Upon investigation, it was determined that the majority of damages caused by electricity consumption in both cities can be attributed to particulate matter, with minor contributions from ozone in Phoenix, and ozone and NOx in Minneapolis (FIGURE A2-b, A3-b). Much of the PM and the ozone that cause damages are secondary air pollutants that derive from direct emissions of SO_2, NOx, and PM (FIGURE A2-c, A3-c). In both cities, the social cost of carbon was the primary contributor to the total damages assessed in this study. This occurred despite the fact that a relatively conservative value of $44/tC was used in the study.

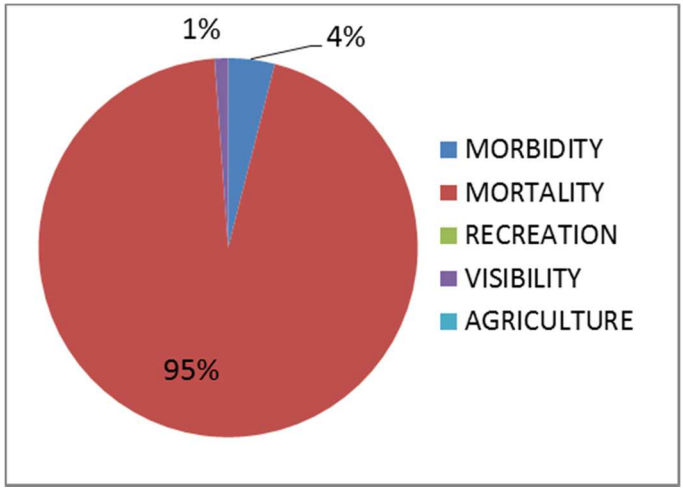


Figure A2-a. Contribution of end impact to total damages from the consumption of electricity in Phoenix Arizona.

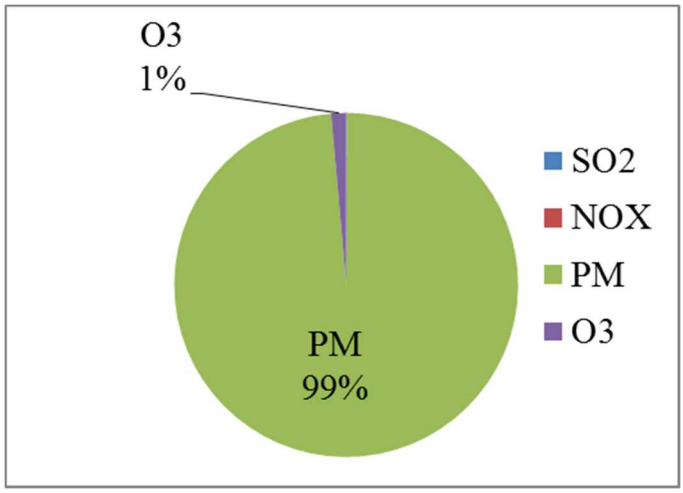


Figure A2-b. Contribution of disparate CAP emissions to damages from the consumption of electricity in Phoenix Arizona.

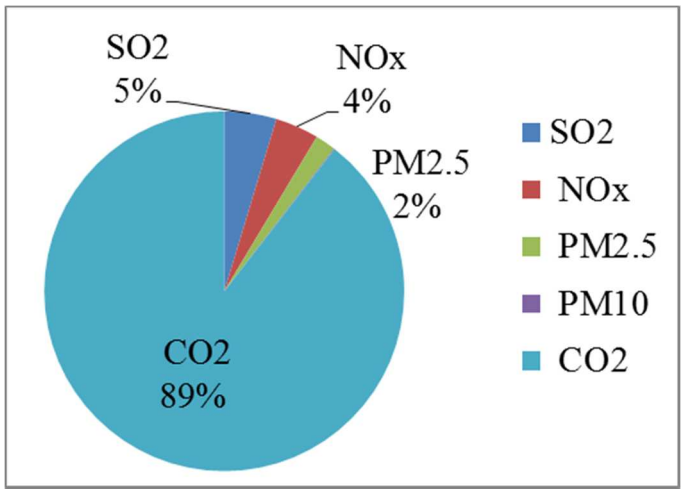


Figure A2-c. Contribution of disparate direct emissions to damages from the consumption of electricity in Phoenix Arizona.

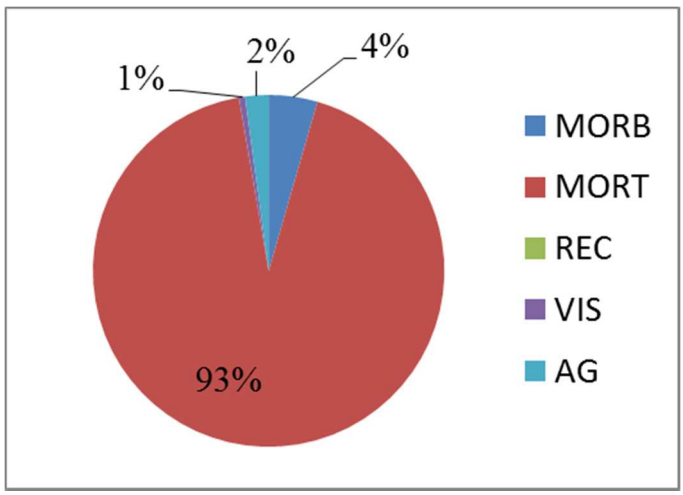


Figure A3-a. Contribution of end impact to total damages from the consumption of electricity in Minneapolis Minnesota.

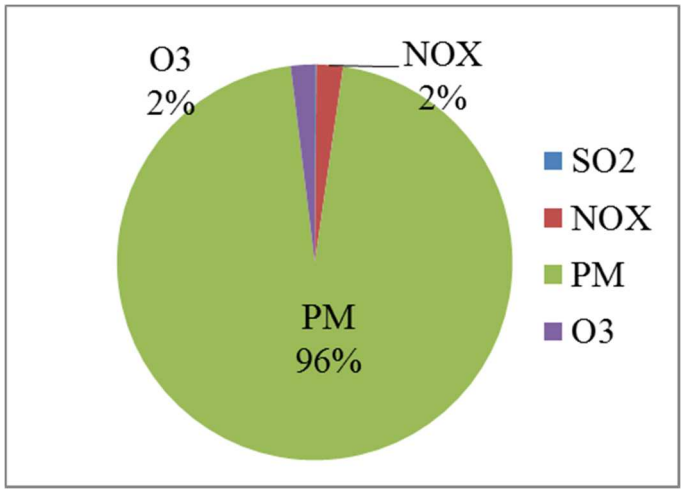


Figure A3-b. Contribution of disparate CAP emissions to damages from the consumption of electricity in Minneapolis Minnesota.

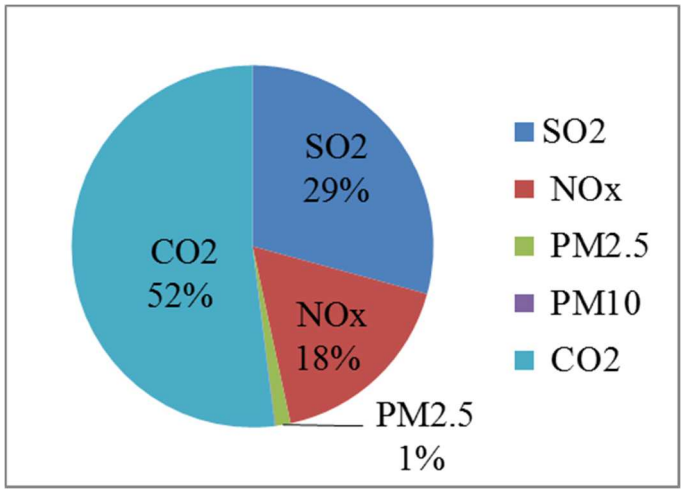


Figure A3-c. Contribution of disparate direct emissions to damages from the consumption of electricity in Minneapolis Minnesota.

3. Equations in Excel Model

Emissions from fuel cells, heating fuels, and electricity were calculated using Equations A1-A17. These equations were developed to support the model developed in Wei et al. (Figure A4). The subscript "elec" indicates the emissions are associated with grid electricity. The subscript "fuel" indicates the emissions are associated with building heating fuels and the subscript "fcell" indicate the emissions are associated with the fuel cell. P is the electricity provided by the fuel cell [kWh] over a designated period of time. Emissions factors (EF) for fuel cells are labeled with a subscript "f", while EF for natural gas, fuel oil, propane, district heating, and electricity are noted with a subscript "ng", "o", "p", "dh", and "e", respectively. Emission factors for CO_2, CH_4, N_2O, NOx, SOx, PM10, and PM2.5 are labeled with subscripts "1", "2", "3", "4", "5", "6", and "7", respectively. H is the heat provided by the fuel cell [kWh], with "s" indicating space heating and "w" indicating water heating. The variable L is the fraction of building heating load supplied by a specific heating fuel, where the fuels are labeled as "elec" for electricity, "ng" for natural gas, "o" for fuel oil, "p" for propane, and "dh" for district heating. The efficiency of the heating fuel equipment ε is included in the equation to adjust for the actual consumption of fuels in the building.

$$CO2_{fuel} = H_s*(L_{ng_s}*EF_{ng1}/\varepsilon_{ng_s} + L_{o_s}*EF_{o1}/\varepsilon_{o_s} + L_{p_s}*EF_{p1}/\varepsilon_{p_s} + L_{dh_s}*EF_{dh1}/\varepsilon_{dh_s}) + H_w*(L_{ng_w}*EF_{ng1}/\varepsilon_{ng_w} + L_{o_w}*EF_{o1}/\varepsilon_{o_w} + L_{p_w}*EF_{p1}/\varepsilon_{p_w} + L_{dh_w}*EF_{dh1}/\varepsilon_{dh_w})$$

Equation A1

$$CH4_{fuel} = H_s*(L_{ng_s}*EF_{ng2}/\varepsilon_{ng_s} + L_{o_s}*EF_{o2}/\varepsilon_{o_s} + L_{p_s}*EF_{p2}/\varepsilon_{p_s} + L_{dh_s}*EF_{dh2}/\varepsilon_{dh_s}) + H_w*(L_{ng_w}*EF_{ng2}/\varepsilon_{ng_w} + L_{o_w}*EF_{o2}/\varepsilon_{o_w} + L_{p_w}*EF_{p2}/\varepsilon_{p_w} + L_{dh_w}*EF_{dh2}/\varepsilon_{dh_w})$$

Equation A2

$$N2O_{fuel} = H_s*(L_{ng_s}*EF_{ng3}/\varepsilon_{ng_s} + L_{o_s}*EF_{o3}/\varepsilon_{o_s} + L_{p_s}*EF_{p3}/\varepsilon_{p_s} + L_{dh_s}*EF_{dh3}/\varepsilon_{dh_s}) + H_w*(L_{ng_w}*EF_{ng3}/\varepsilon_{ng_w} + L_{o_w}*EF_{o3}/\varepsilon_{o_w} + L_{p_w}*EF_{p3}/\varepsilon_{p_w} + L_{dh_w}*EF_{dh3}/\varepsilon_{dh_w})$$

Equation A3

$$NOx_{fuel} = H_s*(L_{ng_s}*EF_{ng4}/\varepsilon_{ng_s} + L_{o_s}*EF_{o4}/\varepsilon_{o_s} + L_{p_s}*EF_{p4}/\varepsilon_{p_s} + L_{dh_s}*EF_{dh4}/\varepsilon_{dh_s}) + H_w*(L_{ng_w}*EF_{ng4}/\varepsilon_{ng_w} + L_{o_w}*EF_{o4}/\varepsilon_{o_w} + L_{p_w}*EF_{p4}/\varepsilon_{p_w} + L_{dh_w}*EF_{dh4}/\varepsilon_{dh_w})$$

Equation A4

$$SOx_{fuel} = H_s*(L_{ng_s}*EF_{ng5}/\varepsilon_{ng_s} + L_{o_s}*EF_{o5}/\varepsilon_{o_s} + L_{p_s}*EF_{p5}/\varepsilon_{p_s} + L_{dh_s}*EF_{dh5}/\varepsilon_{dh_s}) + H_w*(L_{ng_w}*EF_{ng5}/\varepsilon_{ng_w} + L_{o_w}*EF_{o5}/\varepsilon_{o_w} + L_{p_w}*EF_{p5}/\varepsilon_{p_w} + L_{dh_w}*EF_{dh5}/\varepsilon_{dh_w})$$

Equation A5

$$PM10_{fuel} = H_s*(L_{ng_s}*EF_{ng6}/\varepsilon_{ng_s} + L_{o_s}*EF_{o6}/\varepsilon_{o_s} + L_{p_s}*EF_{p6}/\varepsilon_{p_s} + L_{dh_s}*EF_{dh6}/\varepsilon_{dh_s}) + H_w*(L_{ng_w}*EF_{ng6}/\varepsilon_{ng_w} + L_{o_w}*EF_{o6}/\varepsilon_{o_w} + L_{p_w}*EF_{p6}/\varepsilon_{p_w} + L_{dh_w}*EF_{dh6}/\varepsilon_{dh_w})$$

Equation A6

$$PM2.5_{fuel} = H_s*(L_{ng_s}*EF_{ng7} + L_{o_s}*EF_{o7}/\varepsilon_{o_s} + L_{p_s}*EF_{p7}/\varepsilon_{p_s} + L_{dh_s}*EF_{dh7}/\varepsilon_{dh_s}) + H_w*(L_{ng_w}*EF_{ng7}/\varepsilon_{ng_w} + L_{o_w}*EF_{o7}/\varepsilon_{o_w} + L_{p_w}*EF_{p7}/\varepsilon_{p_w} + L_{dh_w}*EF_{dh7}/\varepsilon_{dh_w})$$

Equation A7

$$CO2_{fcell} = P*EF_f$$

Equation A8

$CH4_{fcell} = P*EF_{f2}$ *Equation A9*

$N2O_{fcell} = P*EF_{f3}$ *Equation A10*

$CO2_{elec} = (P + H_s*L_{elec_s} + H_w*L_{elec_w})*EF_{e1}$ *Equation A11*

$CH4_{elec} = (P + H_s*L_{elec_s} + H_w*L_{elec_w})*EF_{e2}$ *Equation A12*

$N2O_{elec} = (P + H_s*L_{elec_s} + H_w*L_{elec_w})*EF_{e3}$ *Equation A13*

$NOx_{elec} = (P + H_s*L_{elec_s} + H_w*L_{elec_w})*EF_{e4}$ *Equation A14*

$SOx_{elec} = (P + H_s*L_{elec_s} + H_w*L_{elec_w})*EF_{e5}$ *Equation A15*

$PM10_{elec} = (P + H_s*L_{elec_s} + H_w*L_{elec_w})*EF_{e6}$ *Equation A16*

$PM2.5_{elec} = (P + H_s*L_{elec_s} + H_w*L_{elec_w})*EF_{e7}$ *Equation A17*

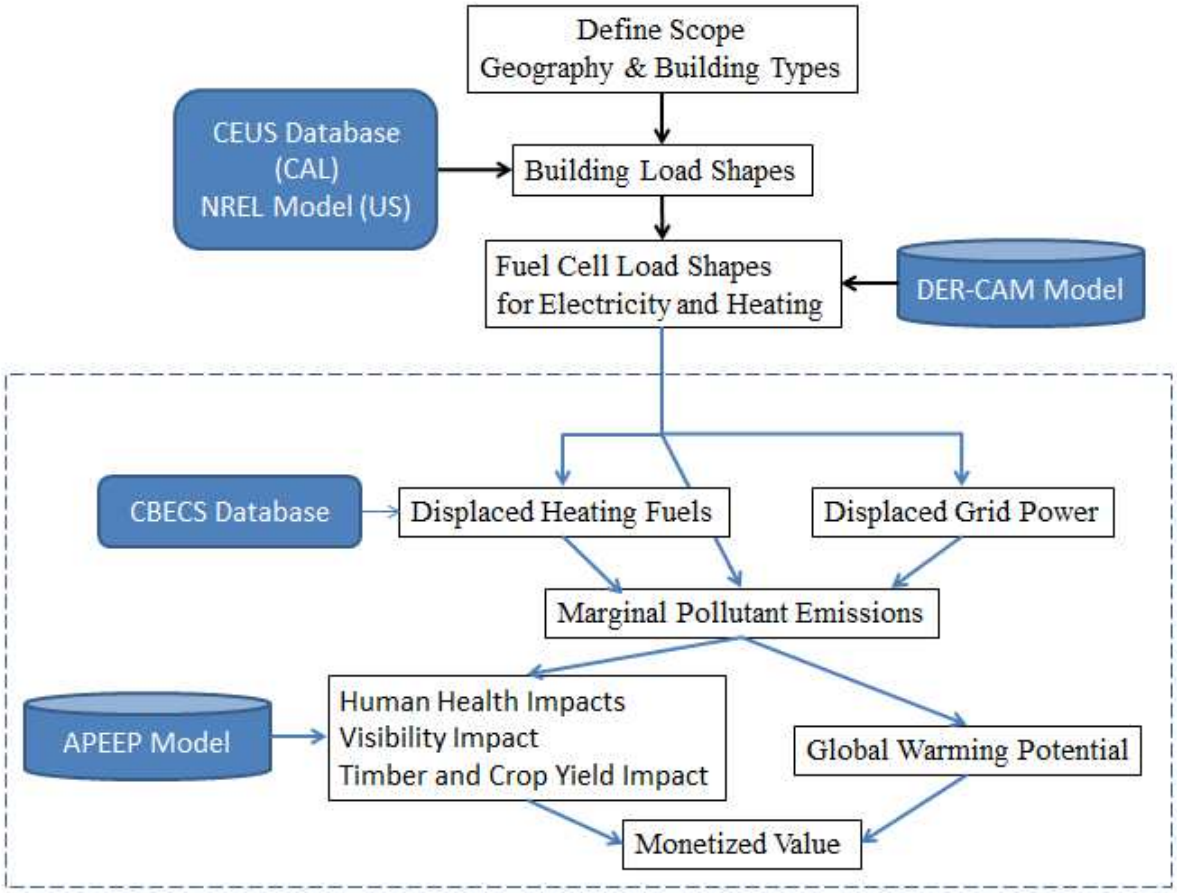


Figure A4. Flow diagram showing how steps in the model presented in this dissertation (dashed box) supports the model developed in Wei et al. External databases and models are shown. New acronyms: California Commercial End-Use Survey (CEUS); National Renewable Energy Laboratory (NREL); Distributed Energy Resources Customer Adoption Model (DER-CAM).

4. Alternative Scenario

This section describes a model run using updated data from an alternative scenario proposed by the Lawrence Berkeley National Laboratory research group in November of 2014, which uses the fuel cell model described in Wei et al. The updated model run uses four alternative assumptions. Three conservative assumptions are: (1) the size of the fuel cell system in large hospitals is 250 kW and not 1 MW; (2) the fuel cell does not provide space heating to buildings; (3) all emissions from fuel cell except for CO_2 are increased by 9% (Table A2). One less conservative assumption is that the building heating equipment is 100% efficient, rather than 80% efficient, meaning less fuel is used to generate the same quantity of heat.

Table A4. Fuel cell emission factors in metric ton per kWh.

Emission in g/kWh	Value
CO_2	543
NO_x	0.0075
SO_x	neglible
PM_{10}	neglible
VOC	neglible
CH_4	0.555
CO	0.019
N_2O	0.065

Table A5. Power and heat provision scenarios for large hospitals in seven cities.

		250 kW FC system- Hospital					
	Phx	Mnpls	Chicago	NYC	Miami	San Diego	Houston
P	2102000	2102000	2102000	2102000	NA	1964700	2102000
Hs	0	0	0	0	0	0	0
Hw	139579	229907	215320	209529	NA	75516	150698

Table A6. Power and heat provision scenarios for small hotels in seven cities.

		50 kW FC system- Small Hotel					
	Phx	Mnpls	Chicago	NYC	Miami	San Diego	Houston
P	382253	345368	345791	314930	0	0	362000
Hs	0	0	0	0	0	0	0
Hw	76954	127112	118971	116075	NA	NA	83071

4.1 Results

Table A7. Monetized marginal environmental and human health impacts of FCS operation scenarios.

City	Building Type	Estimated # Buildings	Electricity [kWh/y]	Space Heating [kWh/y]	Water Heating [kWh/y]	GWP Damages ($44/tCO2) [$/building]	Direct Avoided CAP Damages [$/building]	Indirect Avoided CAP Damages [$/building]	Total Avoided Damages [$/city]
Minneapolis									
	Hospital	9	2102000	0	229907	$ 25,297	$ 535	$ 33,212	$ 531,397
	Small Hotels	96	345368	0	127112	5381.18	294.18	5826.70	$ 1,104,198
Phoenix									
	Hospital	23	2102000	0	139579	$ (7,142)	$ 72	$ 1,894	$ (119,041)
	Small Hotels	206	382253	0	76954	$ (718)	$ 164	353	$ (41,384)
New York City									
	Hospital	325	2102000	0	209529	$ (6,333)	$ 1,397	$ 8,973	$ 1,312,155
	Small Hotels	249	314930	0	116075	$ 62	$ 841	$ 1,449	$ 585,519
Chicago									
	Hospital	90	2102000	0	215321	17261.61	$ 89	$ 53,745	$ 6,398,582
	Small Hotels	266	345791	0	118971	$ 3,896	$ 203	$ 9,259	$ 3,553,244
San Diego									
	Hospital	22	1964700	0	75516	$ (7,011)	$ 105	$ 2,719	$ (92,102)
	Small Hotels		NA	NA	NA				
Houston									
	Hospital	69	2102000	0	150698	$ (3,420)	$ 92	$ 3,445	$ 8,049
	Small Hotels	163	362000	0	83071	64.28	$ 44	$ 618	$ 118,412

Environmental and human health impacts of the adoption of FCS varied widely between locations due to differences in building and fuel cell operation, nearby population, and regional conditions affecting the transport and transformation of pollutants. The amount of power and heat provided by 250kW FCS to large hospitals and 50kW FCS to small hotels were determined based on city-specific load shapes and markets as discussed in the previous sections.

In the scenario where FCS only provide heat for water heating, FCS would not provide carbon savings to large hospitals in Phoenix, NYC, Houston, or San Diego or to small hotels in Phoenix (Figure A5). Conversely, large carbon savings could be achieved if FCS were deployed in Minneapolis or Chicago. Avoided greenhouse gas emissions were lower for all scenarios except Minneapolis and Chicago when spatial data, as opposed to national-average data, was used in the model. This indicates that most of the regional grids studied had lower greenhouse gas emissions than the average US grid. The adoption of FCS resulted in reduced direct criteria air pollutants (CAP) damages in all six cities, with noticeable benefits in Minneapolis and New York City (Figure A6). Avoided damages for hospitals in New York City and Minneapolis were much higher when spatial data was used due to high ground-level MBA factors.

Both MBA and avoided building fuel emissions significantly influenced results. For example, the average small hotel in Chicago uses heating oil while the average small hotel in the nation does not. In Chicago, avoided damages from direct SOx emissions were 100x higher when spatial data was used in the small hotel scenario due to higher SO_2 emission from heating oil and a higher city-specific MBA factor for SO_2. On the other hand, direct SO_2 emissions from large hospitals

were lower when modeled with Chicago data, but the higher city-specific MBA factor for SO_2 led to comparable model results of $89 and $114 for city and national.

Avoided damages due to indirect CAP emissions (from avoided grid electricity generation) were lower for all scenarios except Minneapolis and Chicago when spatial data was used in the model (Figure A7). Surprisingly, the avoided damages associated with FCS adoption in NYC scenario were low. This can be explained by the fact that the marginal emission factors in the NPCC NERC region for NOx and SO_2 are lower than the national average, and the MBA factors for NOx and SO_2 were lower and higher than the national average, respectively. This resulted in a lower damage factor ($/kWh) for NYC than for the national average.

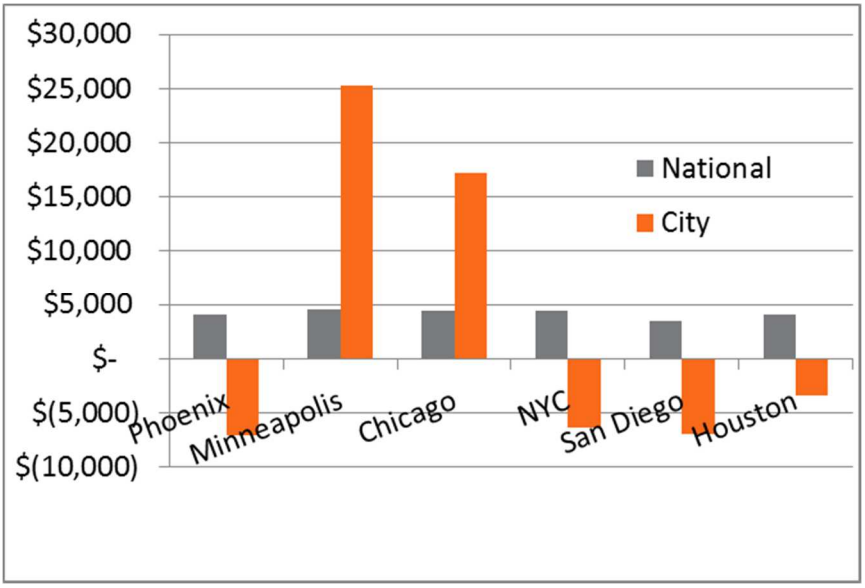


Figure A5a. Comparison of GWP damages results for large hospitals using spatial or US average data.

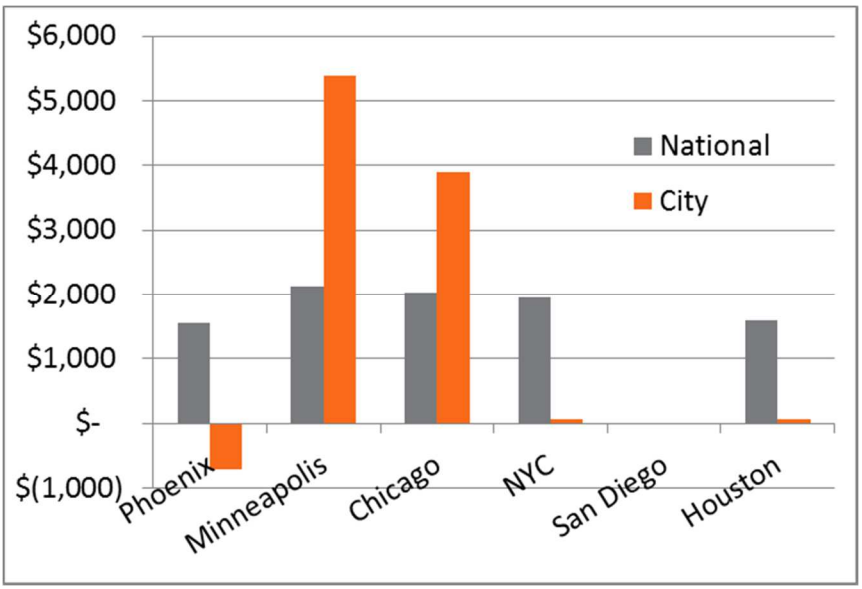


Figure A5b. Comparison of GWP damages results for small hotel using spatial or US average data.

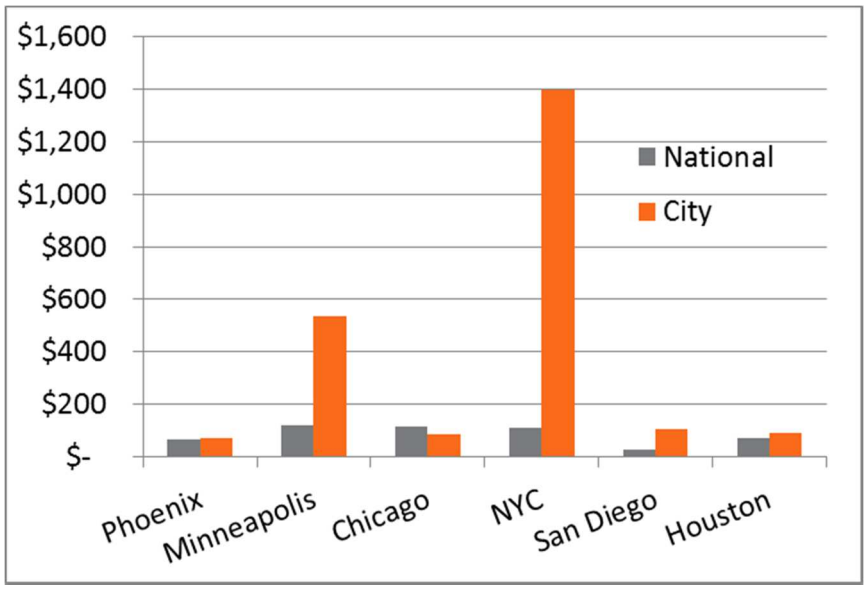


Figure A6a. Comparison of direct CAP damages results for large hospitals using spatial or US average data.

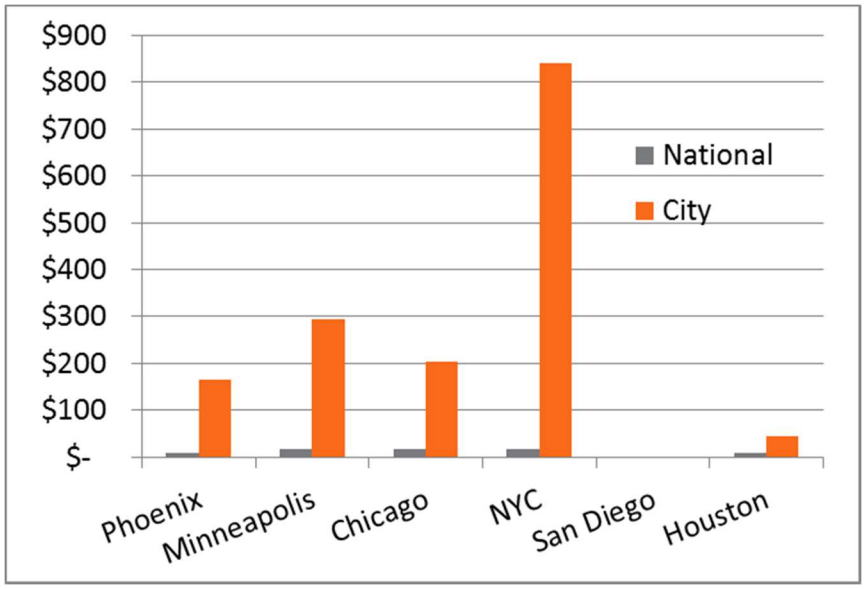


Figure A6b. Comparison of direct CAP damages results for small hotels using spatial or US average data.

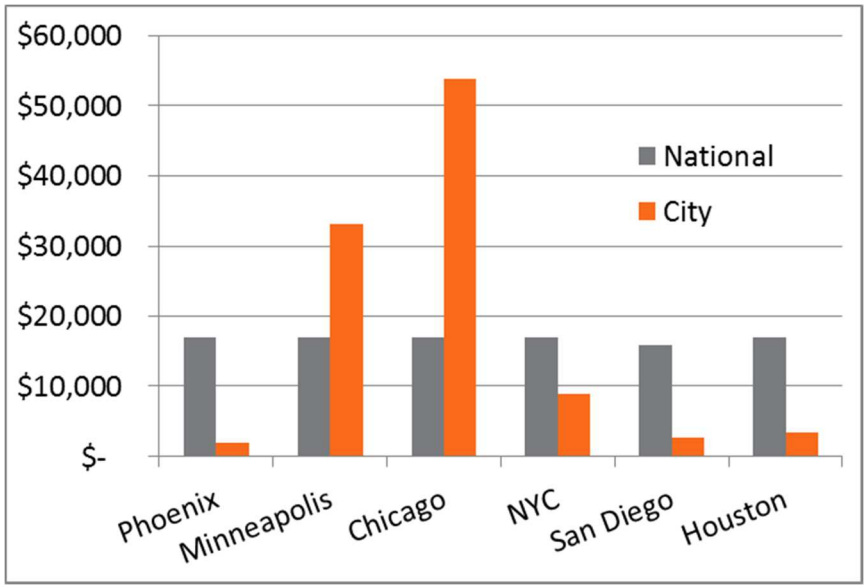


Figure A7a. Comparison of indirect CAP damages results for large hospitals using spatial or US average data.

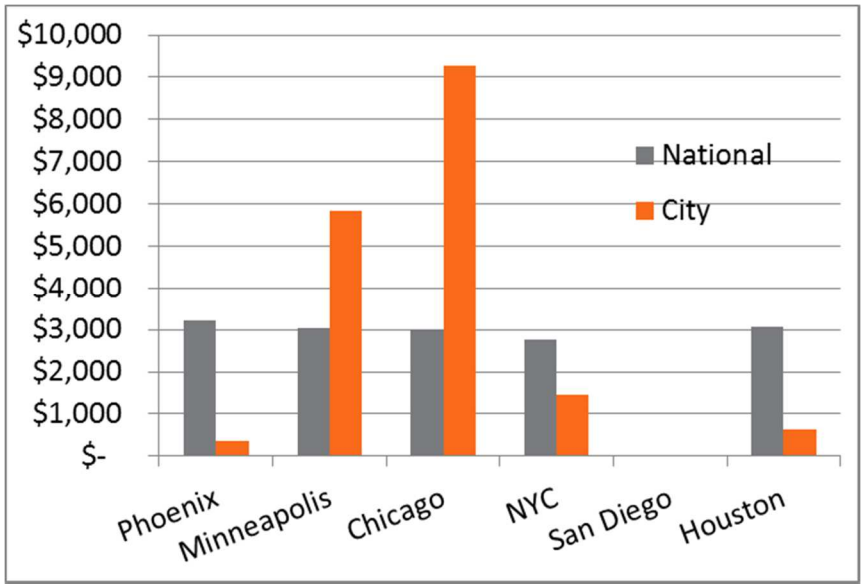
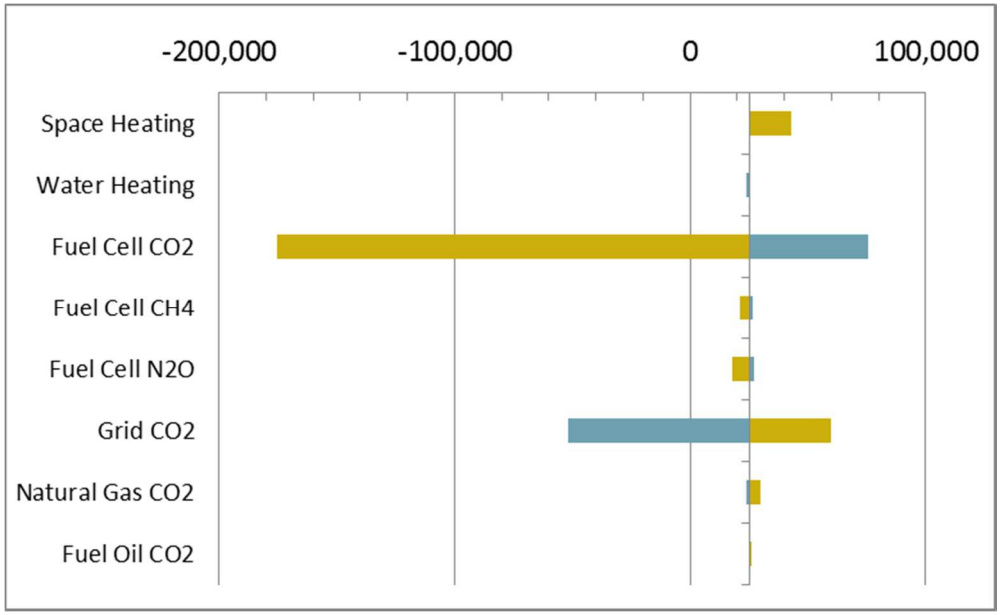


Figure A7b. Comparison of indirect CAP damages results for small hotels using spatial or US average data.

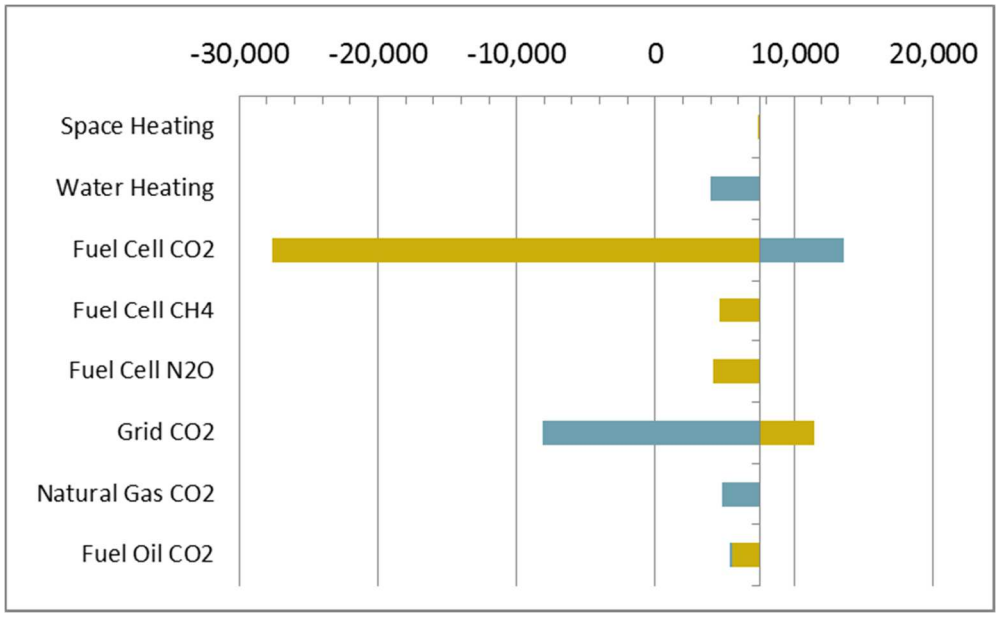
5. Sensitivity Analysis for LCIA

The monetized value from marginal greenhouse gas emission in Minneapolis and Phoenix was most sensitive to the CO_2 emission from fuel cells and regional electricity grids (Figure A8 a-d). In Minneapolis, the monetized value in our large hospital scenario was zero when the electricity grid CO_{2eq} emission factor dropped to 561 g/kWh, a value 33% less than the 2011 marginal emission factor. In Phoenix, the value became negative when the electricity grid CO_{2eq} emission factor dropped below 563 g/kWh. This value is 16% higher than the 2011 marginal emission factor used in our analysis, explaining why FCS deployed in Phoenix would not receive carbon credits.

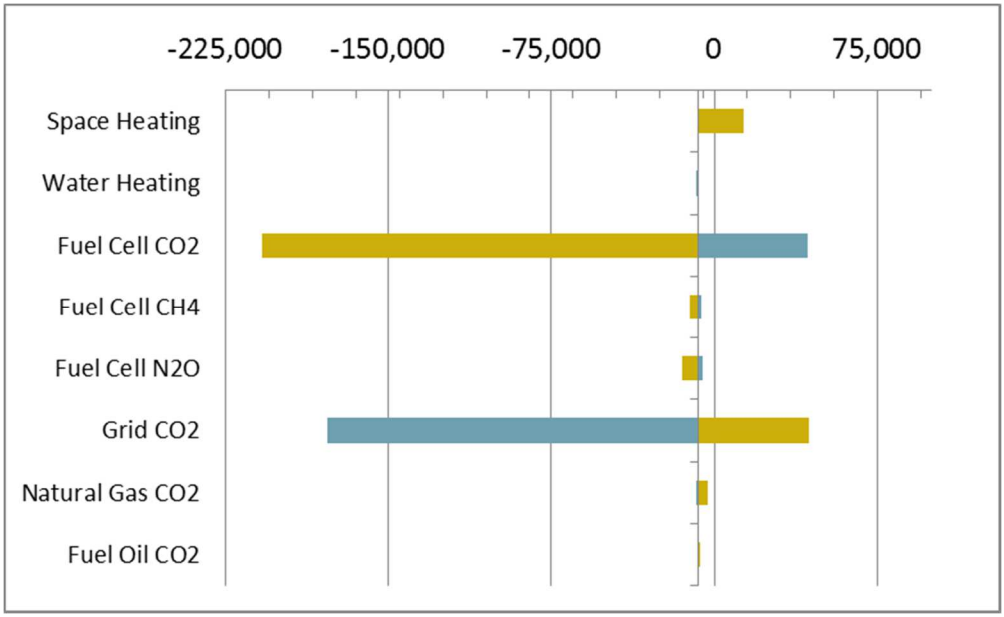
The monetized value from direct marginal CAP emission in large hospitals in Minneapolis and Phoenix was most sensitive to: (1) whether the fuel cell provided space heating to the building, (2) the SO_2 emissions from fuel oil powered heating equipment, (3) the ground-level MBA of NOx, and (4) the NOx emissions from natural gas powered heating equipment (Figure A9 a, c). The monetized value from direct marginal CAP emission in small hotels in Minneapolis was most sensitive to: (1) the ground-level MBA of NOx, (2) the SO_2 emissions from fuel oil powered heating equipment, (3) the NOx emissions from natural gas powered heating equipment, and (4) whether the fuel cell provided space heating to the building (Figure 10 b). Finally, the value from direct marginal CAP emission in small hotels in Phoenix was most sensitive to: (1) whether the fuel cell provided water heating to the building, (2) the ground-level MBA of NOx, (3) the SO_2 emissions from fuel oil powered heating equipment, and (4) the ground-level MBA of SO_2 (Figure A9 b,d). FCS will provide the greatest monetary benefit from avoided health damages in regions where there are poorly controled NOx emissions from natural gas and SO_2 emissions from heating oils. Furthermore, FCS must achieve lower emissions in counties where population is growing to maintain health benefits.



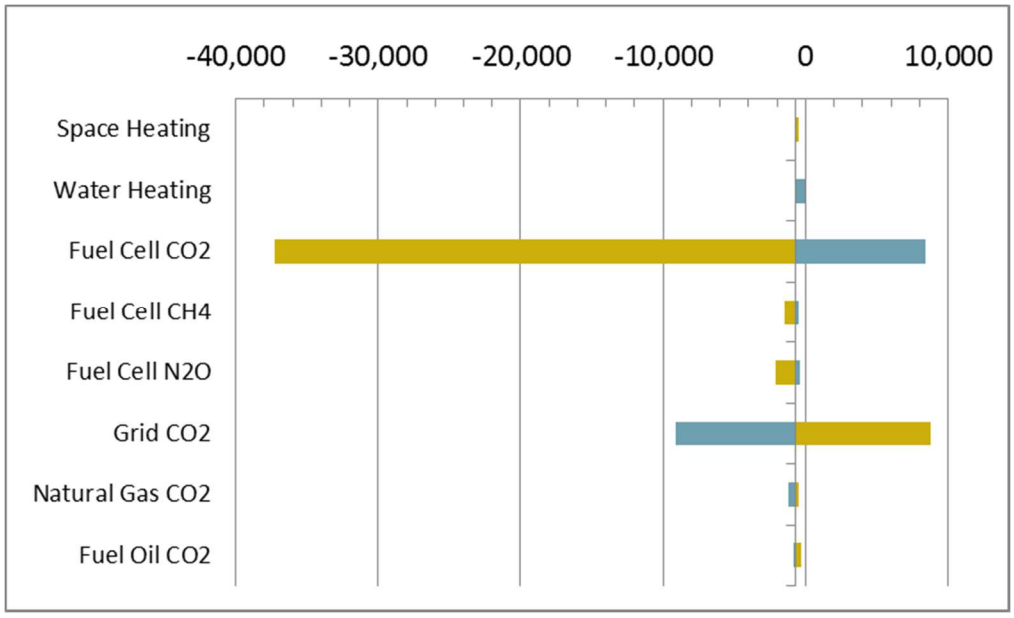
a. Monetized value of marginal GHG emissions from large hospitals in Minneapolis.



b. Monetized value of marginal GHG emissions from small hotels in Minneapolis.

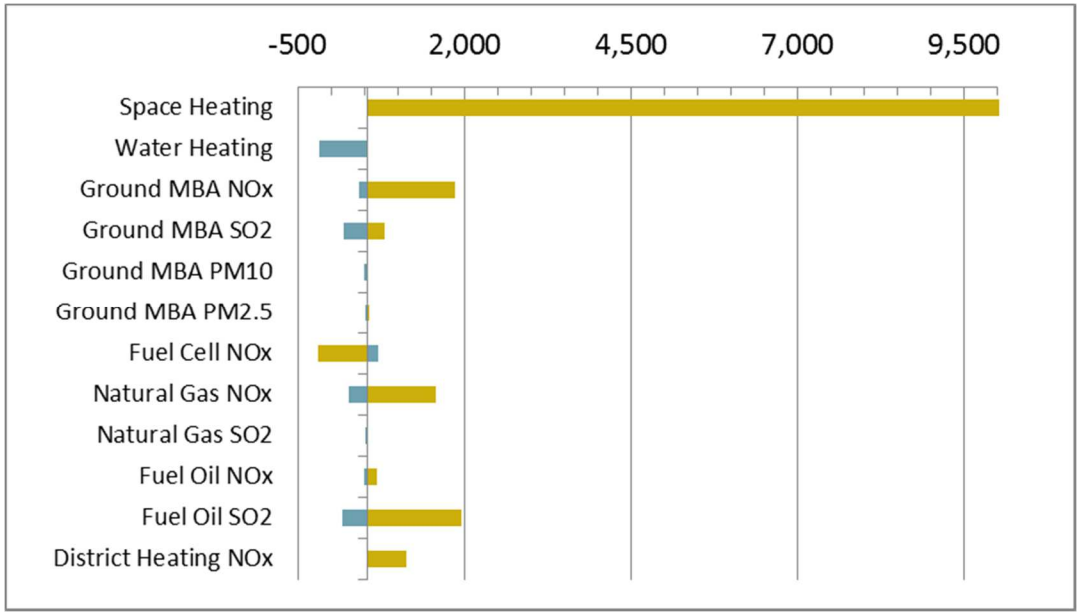


c. **Monetized value of marginal GHG emissions from large hospitals in Phoenix.**

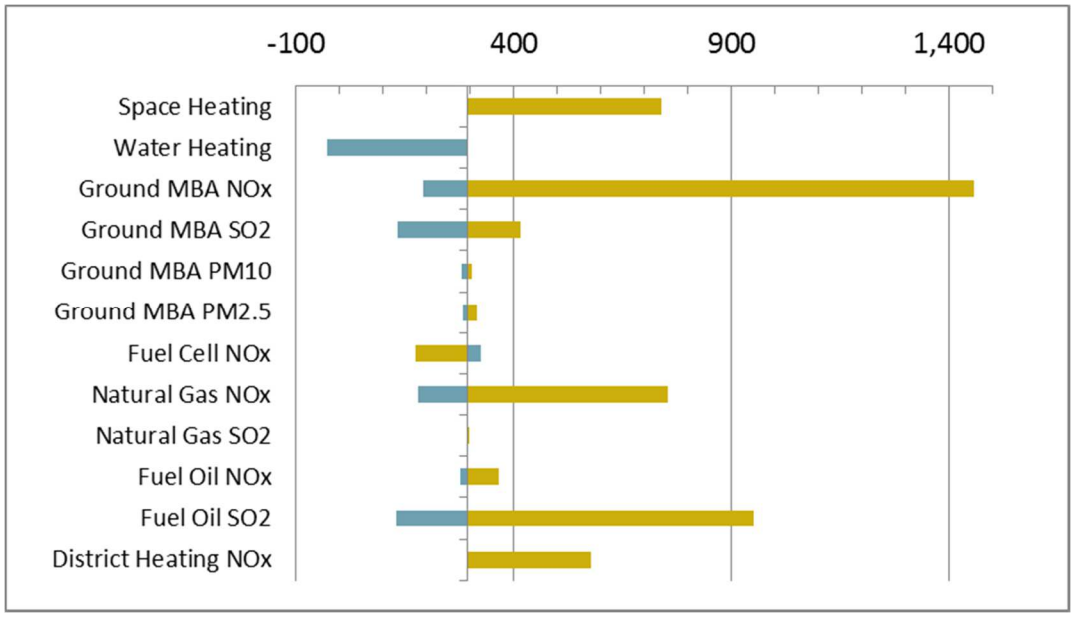


d. Monetized value of marginal GHG emissions from small hotels in Phoenix.

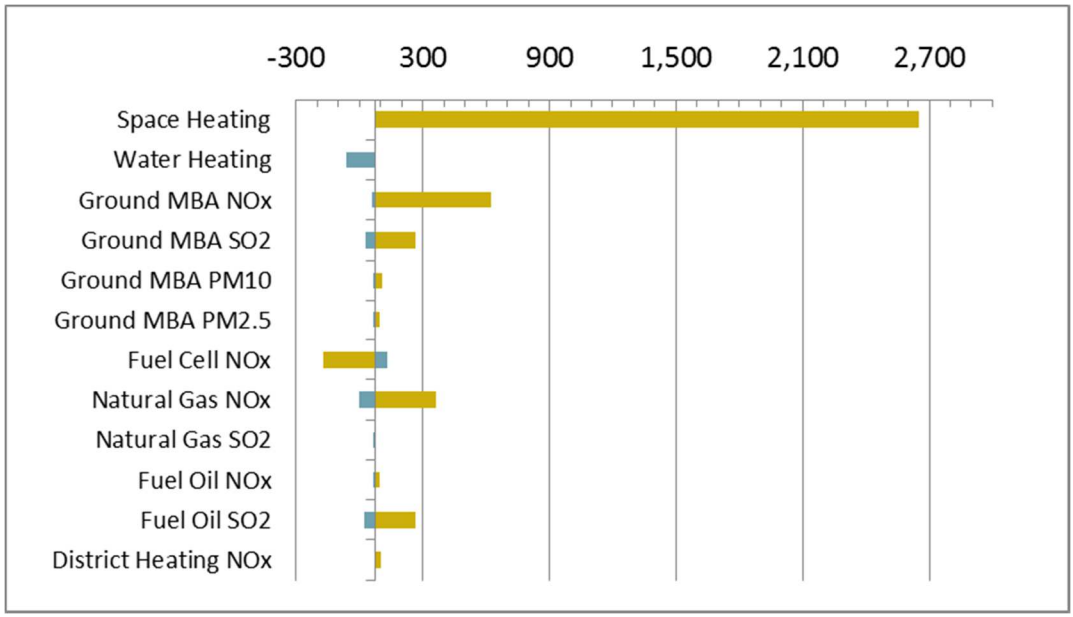
Figure A8. A-D. Tornado plots showing sensitivities of monetized value of marginal GHG emissions from scenarios run in Minneapolis and Phoenix. Blue and yellow bars represent variations caused by low and high parameter values, respectively.



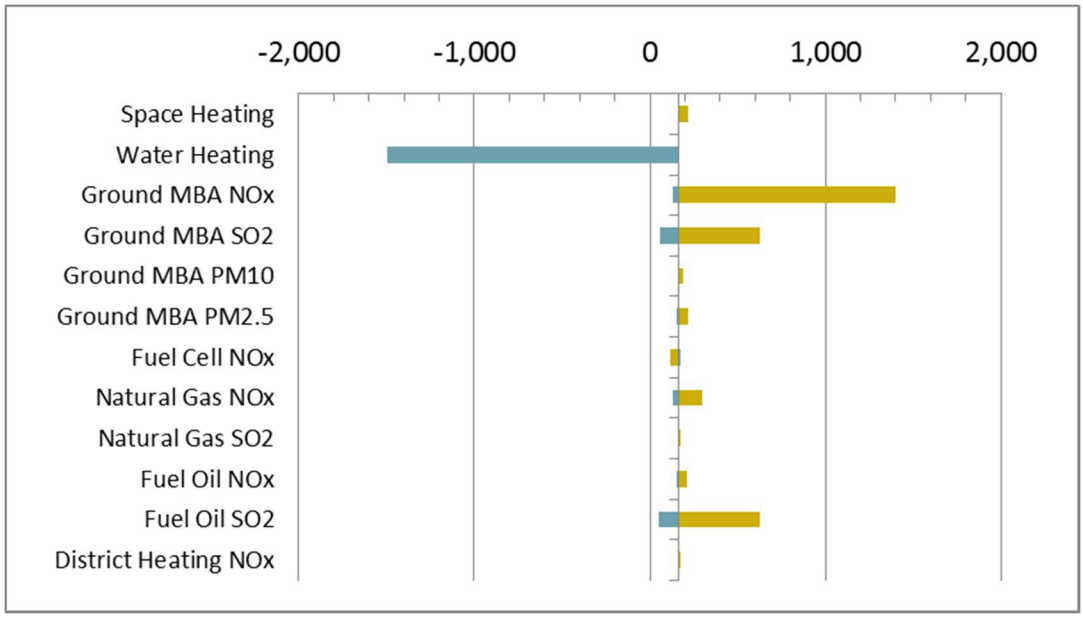
a. Monetized value of marginal direct CAP emissions from large hospitals in Minneapolis.



b. Monetized value of marginal direct CAP emissions from small hotels in Minneapolis.



c. **Monetized value of marginal direct CAP emissions from large hospitals in Phoenix.**



d. Monetized value of marginal direct CAP emissions from small hotels in Phoenix.

Figure A9. A-D. Tornado plots showing sensitivities of monetized value of marginal direct CAP emissions from scenarios run in Minneapolis and Phoenix. Blue and yellow bars represent variations caused by low and high parameter values, respectively.

Dynamic Electricity Grid

Carbon emissions for electricity generators in the Midwest Reliability Organization (MRO) NERC region range from 0 - 1208 gCO_2/kWh, 0 – 0.51 gCH_4/kWh, and 0 – 0.07 gN_2O/kWh (Cai et al.). The upper bound value for CO_2 emissions resulted in a 59% and 53% increase in the total benefit (value from GHG, direct, and indirect emissions avoidances) that was calculated for large hospitals and small hotels when we used 2011 marginal CO_2 emission factors from Siler-Evans et al. Emission factors for the electricity generators in the Western Electricity Coordinating Council (WECC) NERC region range from 0 - 1035 gCO_2/kWh, 0 – 0.55 gCH_4/kWh, and 0 – 0.074 gN_2O/kWh. The upper bound value caused the net benefit for large hospitals to increase from -$5176 to $45,645 and the benefit for small hotels to increase from $201 to $9270.

Groundlevel damage factors for NOx, SOx, PM_{10} and $PM_{2.5}$ vary from 68 - 141,038 $\$/tNO_X$, 743 – 36,669 $\$/tSO_X$, 203 – 22,116 $\$/tPM_{10}$, and 844 - 141,038 $\$/tPM_{2.5}$ in the United States according to Muller and Mendelson (given in $2014 for a VSL of 6 million). For NOx emissions, the benefit was 99% to 102% of the baseline value in Minneapolis large hospitals, and 99% to 110% in Minneapolis small hotels. The cost in Phoenix was 99% to 105% of the base line value in large hospitals. A benefit occurred in small hotels in Phoenix, where the baseline net value of -$201 went to -$190 to 120. These results indicate that FCS must further reduce emissions in counties where population is growing to maintain health benefits.

Fuel Cell Technology Improvement

There is a great deal of discrepancy in the literature regarding fuel cell emission factors; to account for this uncertainty, fuel cell emission factors were varied from 0 to 500% of baseline values. The GWP benefit of FCS in large Minneapolis hospitals became negative when fuel cell CO_2 emission factors were greater than 816 g/kWh, respectively. The benefit was negative for FCS in hospitals in Phoenix when the fuel cell CO_2 emission factor was greater than 465g/kWh, respectively.

Changing the fuel cell NOx emission factor from 0 to 500% of the base case value 0.0069 g/kWh caused the benefit in Minneapolis large hospitals and small hotels to change from 99% to 100. 4% of its base value, and from 99% to 105% and from 94% to 122% in Phoenix large hospitals and small hotels, respectively. Space heating was set to zero in our baseline scenario. The energy provided to space heating was increased to 2,689,000 kWh and 3,102,093 kWh in large hospitals in Phoenix and Minneapolis and to 23,000 and 174,743 kWh in small hotels in Phoenix and Minneapolis in our sensitivity analysis.

Dynamic Building Emissions

Changing the NOx emission factors for natural gas and heating oil from 0 to 500% produced a benefit in Minneapolis large hospitals that was 99.5% to 102% and 99.9 to 100.2% of the baseline value, respectively. Changing the SO_2 emission factor for heating oil over the same range resulted in the same change in the benefit. Varying the emission factors for other pollutants resulted in <20% change in the benefit. When the emissions of district heating were modeled using 100 to 500% of natural gas's emission factor for NOx, the benefit changed from 100.2 to 101% of the base value. For large hospitals in Phoenix, the cost decreased by 5% when NOx emissions from natural gas were increased by 500%, but only increased by 1% when natural gas NOx emissions were set to 0. The same changes occurred when the SO_2 emissions from fuil oil were varied. Large variations were seen for small hotels in Phoenix. Increasing NOx emissions from natural gas and fuil oil reduced the cost by 68% and 24%. Increasing SO_2 emissions from fuil oil resulted a net benefit of $265.

6. EPA Value of a Statistical Life Adjustments

Table A8. Comparison of two methods used by the Environmental Protection Agency for determining the VSL to use in their impact assessment studies. Highlighted value under "Endorsed Method" is the base VSL estimate currently used. Highlighted value under "OAR Interim Methodology (2004-2009)" is the value used in Fann et al. Data acquired from a personal correspondence with Charlie Fulcher of the EPA, March 5, 2014.

	Endorsed Methodology			OAR Interim methodology (2004-2009)		
Currency Year	Base VSL Estimate	With Income Growth to 2015	With Income Growth to 2020	Base VSL Estimate	With Income Growth to 2015	With Income Growth to 2020
1990	**$4.8**	$5.5	$5.8	$4.2	$4.6	$4.8
1999	$6.1	$7.1	$7.3	$5.3	$5.9	$6.2
2000	$6.3	$7.3	$7.6	**$5.5**	$6.1	$6.4
2001	$6.5	$7.5	$7.8	$5.7	$6.3	$6.5
2002	$6.6	$7.6	$7.9	$5.7	$6.4	$6.6
2003	$6.8	$7.8	$8.1	$5.9	$6.5	$6.8
2004	$6.9	$8.0	$8.3	$6.0	$6.7	$7.0
2005	$7.2	$8.3	$8.6	$6.2	$6.9	$7.2
2006	$7.4	$8.5	$8.9	$6.4	$7.2	$7.4
2007	$7.6	$8.8	$9.1	$6.6	$7.4	$7.7
2008	$7.9	$9.1	$9.5	$6.9	$7.6	$8.0
2009	$7.9	$9.1	$9.5	$6.9	$7.6	$7.9
2010	$8.0	$9.2	$9.6	$7.0	$7.7	$8.1